2011-01-01

Implications Of Surface Runoff Recharge In Semi-Arid Regions On Groundwater Sustainability

Omar M. Al-Qudah
University of Texas at El Paso, omal@miners.utep.edu

IMPLICATIONS OF SURFACE RUNOFF RECHARGE IN SEMI-ARID REGIONS ON GROUNDWATER SUSTAINABILITY

OMAR MOHAMMAD AL-QUDAH

Environmental Science and Engineering Program

APPROVED:

John C. Walton, Ph.D., Chair

David Borrok, Ph.D.

Lin Ma, Ph.D.

Zhuping Sheng, Ph.D.

Benjamin C. Flores, Ph.D.
Acting Dean of the Graduate School

Dedication

To my beloved parents; to my loving wife; to my precious kids: Yahia, Ihssan, Yamen, Faisal, and the new baby girl Farah; to all members of my family. Without your inspiration, encouragement, support and prayers, this work would not be.

IMPLICATIONS OF SURFACE RUNOFF RECHARGE IN SEMI-ARID REGIONS ON GROUNDWATER SUSTAINABILITY

by

OMAR MOHAMMAD AL-QUDAH, B.S., M.S

DISSERTATION

Presented to the Faculty of the Graduate School of

The University of Texas at El Paso

in Partial Fulfillment

of the Requirements

for the Degree of

DOCTOR OF PHILOSOPHY

Environmental Science and Engineering Program

THE UNIVERSITY OF TEXAS AT EL PASO

August 2011

Acknowledgements

At the beginning, I wish to thank ALLAH (God) the most merciful the compassionate the lord of the world.

I would like to express my sincere appreciation, deepest gratitude, and respect to my mentor, Dr. John Walton, for his valuable guidance, continued help, support, and encouragement, and for having confidence in me. He pushed me as hard as he did to do as much as I did.

I would like to thank my committee members, Dr. David Borrok and Dr. Zhuping Sheng, and their research groups for their help, support and guidance, with the samples chemical analysis, in addition to Dr. Lin Ma for accepting the heavy task of going through my dissertation. Also, it is of my pleasure to thank to Dr. Arturo Woocay, for his help and support during the years of my study. I am grateful to all faculty and staff of the Environmental Science and Engineering Ph.D. program and Civil Engineering Department especially: Dr. Barry Benedict, Dr. William Walker, Cindy Conroy, Gwen Pratt, Joseph Gonzales, Noe Ortega-Corral, and Hans Boenisch, for their help and support.

My thanks and appreciation is to my brothers: Dr. Ali, Abdel-Hammed, Ahmad, Faries, and my sister Khloud and their families for their support, help, and encouragement; I am blessed to have such a supportive and loving family. Also I would like to thank and appreciate all of my friends for their help and support.

I would also like to thank John Klenke, Roger McRae, and the rest of the Nye County Nuclear Waste Repository Project Office (NWRPO) Staff for assistance with sampler

construction, installation, and sampling; Dr. Dale Hammermeister for initiating chloride profile sampling at Nye County.

Finally, funding for this research was provided by Nye County NWRPO, NV through a grant from the US Department of Energy office of Civilian Radioactive Waste Management. Financial support was also provided by the Center for Environmental Resource Management of The University of Texas at El Paso. Funds that allowed me to present my results at conferences were also provided by the College of Engineering, College of Science, the Graduate School, and the Student Government Association at The University of Texas at El Paso. I would like to thank all these organizations for their financial support.

Abstract

Amargosa Desert, Nevada regional groundwater studies show that the surface runoff infiltration occurring in the arroyos following runoff producing storms, and this infiltration is considered to be a major source of groundwater recharge. Groundwater infiltration through alluvium was investigated in the Amargosa Desert using borehole drill cuttings, groundwater chemistry, and applying a novel method for collecting runoff water. The sampling process included sediment, precipitation, and runoff water. In total, 176 runoff, 182 sediment, and 45 precipitation samples were collected between January, 2009 and January, 2011.Water chemistry, chloride concentrations, and stable isotopes of water collected from specially designed runoff samplers, placed in the main ephemeral arroyo and its tributaries in the Amargosa Desert, closely match the chemistry of underlying groundwater where a plume of low chloride water underlies the arroyos until it connects with the Amargosa River. This evidence indicates that current and past infiltration of surface runoff (stormwater) is the primary source of the underlying groundwater plume. The results suggest that infiltration of surface runoff from large storm events in this region is a source of recharge more important that previously realized. Furthermore, the analyses of results indicate that the dominant processes and reactions responsible for the hydrochemical evolution in the Amargosa Desert water system are (1) evaporative concentration prior to infiltration, (2) carbonate equilibrium, (3) silicate weathering reactions, (4) limited mixing with saline water, (5) dissolution/precipitation of calcite, dolomite and fluorite, and (6) ion exchange. The results also indicate that the northern west face of Yucca Mountain groundwater is fresh water, Fortymile Wash groundwater is dilute, and the carbonate signature is shown in the Ash Meadows and Death Valley waters. Moreover, the results show three main groundwater signatures indicating groundwater evolution, potential flowpaths, and recharge areas. The flowpaths are the trace of the Amargosa River, the trace of Fortymile Wash, and its convergence with the Amargosa River. This appears to represent not just a groundwater flow path, but traces of surface runoff infiltration as well.

Table of Contents

List of Tables

List of Figures

Chapter 1

1. General Introduction

Natural tributaries in arid regions are generally ephemeral and the flow occurs intermittently during short, isolated flow periods separated by longer periods of low or zero flow; sustained flow is rare and baseflow is essentially absent (Sharma and Murthy, 1996). Peak flow rates occur within a few hours of the start of a rise. The steep rise results from the nature of arid zone rainfall, i.e. afternoon and evening thunderstorms in the south-western U.S.A. (Osborn and Renard, 1970), low pressure monsoon depressions in the Indian arid zone (Sharma and Vangani, 1982), large scale convective winter storms in Middle East (Jones, 1981) and tropical cyclones/troughs in Australia (Pilgrim et al., 1988), and sometimes from the steepness of the channels draining the well-defined runoff generating zones. Normally, large volumes of surface runoff water move into the ephemeral channel in a short period causing the flash flooding characteristic of arid zone drainage basins. Flash floods are usual hydrologic features of desert drainage. Drainage basins with high relief, a large percentage of land bedrock, sparse vegetation and shallow soils are particularly susceptible to flash flooding (Fisher and Minckley, 1978). Regularly, peak flow rates are reached almost immediately because the ephemeral flood wave forms a steep wave front, or the wall of water of legends, in its travel downstream (Jones, 1981; Pilgrim et al., 1988). Two mechanisms contribute to the formation of the wall of water of legends. First, rate of infiltration into the permeable dry streambed is highest at the wave front and decreases in the upstream direction, with the effect that the leading edge of the wave steepens as it moves downstream. Second, the deeper portion of the flood wave near the peak travels faster than the leading edge of the wave, with the result that the wave peak approaches the

front until the peak and front almost coincide and a shock front is formed (Sharma and Murthy, 1996).

Net infiltration is the penetration of water through the ground surface to a depth where it can no longer be withdrawn readily by evaporation or transpiration by plants (DOE-OCRWM, 2006). Net infiltration in arid and semi-arid regions is usually estimated based on other variables rather than determined from direct measurement. While infiltration in arid and semi-arid climates is temporally and spatially variable due to intermittent precipitation that is sensitive to topography, long-term average net infiltration rates effectively measure the steady-state flow of water through the unsaturated zone (the zone of soil or rock below the ground surface and above the water table) (DOE-OCRWM, 2006).

Run-off in desert environments is ephemeral and at Amargosa Desert occurs only as a transient response to precipitation events. When enough water falls to create run-off, it can be sudden and intense. The Great Basin desert is known for flash floods that start and end abruptly, carrying objects as large as boulders and cars when they do strike. During these events, large amounts of water can move rapidly away from upland areas. Run-on occurs when water from higher areas accumulates in lower areas, which creates the potential for localized increases in infiltration (DOE-OCRWM, 2006).

Because nearly all water infiltrating into deep soils and thick alluvium (sedimentary material deposited by a stream or running water) in vegetated arid and semi-arid areas is retained, in such areas net infiltration below the root zone is thought to be generally negligible (DOE-OCRWM, 2006). Thick alluvium effectively redistributes water and encourages the establishment of deep root zones. The combined effect of redistribution and water uptake by deep-rooted plants prevents water from becoming net infiltration (DOE-OCRWM, 2006).

Evapotranspiration consists of the water returned to the atmosphere by direct evaporation and transpiration (e.g., the water used by plants). It is a complex process and depends on factors such as solar radiation, air and soil temperatures, soil moisture content, air turbulence (e.g., wind), and the types and density of vegetation (e.g., amount of canopy cover, rooting depths, and leaf structure) (DOE-OCRWM, 2006). Important aspects of the water cycle processes at Amargosa Desert include the temporal and spatial distribution of precipitation, run-off and run-on, redistribution, and evapotranspiration. Water movement through the unsaturated zone at Amargosa Desert is thought to be mainly vertical, and evaporative losses below the root zone are insignificant (DOE-OCRWM, 2006).

In the period (2001-2005), the U.S. Department of the Interior and U.S. Geological Survey (SNL, 2008) estimated the total annual precipitation in the Amargosa Desert area in the range 3.5-178 mm/yr and by an average of 130 mm/yr; changes in soil moisture were recorded in early August 2005 to a depth of at least 2.75 m at the devegetated native soil site and 1.25 m at the vegetated native soil site and this is the deepest downward percolation of soil moisture documented at Amargosa Desert since 1983 (SNL, 2008; Johnson et al., 2007); recorded annual evapotranspiration was in the range of 48-233 mm/yr by an average of 157 mm/yr (SNL, 2008; Johnson et al., 2007). Woolhiser (2006) estimated the runoff rate in the vicinity of Amargosa Desert in the range of 0.38-3.59 mm/yr. Furthermore, SNL (2008) estimated the alluvium thickness in the Amargosa Desert vicinity in the range of 0.3 m in the mountains and greater than 20 m in the valley.

Many literature accounts of desert flash floods confirm that suspended alluvial concentrations in this kind of environment are amongst the highest recorded, despite human settlements that induced changes in land use and cover (Stewart and LaMarche, 1967; Inbar,

1992). Furthermore, redistribution and mobilization of such large amounts of alluvial materials the majority sediments amount of it fine-grained, helps explain the importance of mudstones in ancient desert rock sequences (Alexandrov Y., et. al., 2007). In addition to the high sediment yield, flash floods in arid regions ensure a short half-life for reservoirs that are fed in part or in total by ephemeral channels (Alexandrov Y., et. al., 2007), enhancement wind-blown dust in endorheic basins through raising sediment loads in these areas, provides a relation between suspended sediment concentration and water discharge (Forstick et al., 1983), and decrease in the soil layer thickness on mountains and hills to increase its thickness down-gradient through the runoff process which considered a type of mechanical weathering and a sedimentary carrier, and then it could affect the infiltration process.

Fisher and Minckley 1978 described the change in selected chemical parameters during a single flash flooding event on Sycamore Creek, Arizona. Although floods are often viewed as dilution phenomena in terms of dissolved substances, in which low conductivity rainwater dilutes groundwater or spring water that are nearer chemical equilibrium with substrates, and thus rich in dissolved salts. They observed that the dilution effects are partially offset by increased leaching and dissolution of solutes from newly exposed rock and soil minerals as well as from suspended particles. However, they noted that the major anion, bicarbonate, and conductivity, followed a dilution pattern. In the other hand, nitrate, phosphate and iron varied widely through the cycle, and generally increased over levels recorded at base flow. They attributed the increased concentrations of nitrate as discharged increased to leaching from the ephemeral stream beds and surrounding lands, and suggested that surface runoff contributed few nitrates to streams but yielded significant amounts of phosphate shifted to release from high concentrations of particles in the water.

The chemistry of precipitation evolves as it falls from the sky, contacts the earth's surface, and makes its way into the groundwater. Sampling of surface runoff in a desert environment from ephemeral arroyos is complicated by a number of practical concerns. Surface runoff events are uncommon, sometimes separated by gaps of more than a year, and difficult to forecast in advance. One is forced either to place potentially expensive equipment in the field for extensive time periods or to have a large supply of workers ready to be called into the field for each potential storm. In the absence of very large sources of funding, any desert arroyo surface runoff system requires compromises.

Accurate estimates of groundwater recharge are necessary to understanding the long-term sustainability of groundwater resources and predictions of groundwater flow rates and directions. Therefore, as an arid region, the surface runoff water could be a major source of groundwater recharge and then the powerful transporter of the contaminants to the vadose zone (unsaturated zone). The present study attempts to provide a new insight into the chemical evolution of southern Nevada's groundwater and its potential flow paths and rates during the infiltration and surface runoff processes, through initiating a surface runoff sampling network to track the chemical footprint of the surface runoff water on the groundwater recharging and infiltration chemistry, by collecting a baseline data on a comprehensive suite of chemical parameters, which included the major ion chemistry, nutrients, trace elements, as well as the stable isotope ratios and the resources available at Nye County Nuclear Waste Repository Project Office (NWRPO). Multiple analytical methods were created to analyses these data to development a defensible groundwater chemistry monitoring network, in the Amargosa Desert, suitable for long-term performance confirmation monitoring, which is the overall goal of this study.

Water flux densities are often measured indirectly (for example with water balance methods, water content-water storage change methods, tracer methods, etc.) and are often predicted with notable uncertainties. Exact information about the soil water balance is needed to quantify solute transfer within the vadose (unsaturated) zone. Different methods exist for measuring water and solute flux in and below the root zone and have been critically reviewed (Fuehr et. al., 1998; Meissner et. al., 2000). In the last several years, researchers are diligently developing a device for collecting water from the pore spaces of soils and for determining the soluble constituents removed in the drainage. A lysimeter (Figure 1.1) is a device for measuring water percolation through soil, something like a "flower pot" that is buried and filled with soil, measuring water and solute balance, measuring movement of water and chemicals in the unsaturated and saturated zone of the soil, and aiding clarification of differences and similarities between experimental results obtained in the laboratory and the field and for combining data systematically.

Many researchers (Migliaccio et al., 2009; Takamatsu et al., 2007; Meissner et al., 2000, 2002, 2004) designed different types of lysimeters for soil water sampling to investigate the behavior of solutes in soil, measure water and solute balance, and investigate of water, gas, and solute transport in soils. The limitations and the problems of using different types of lysimeters are: (1) the fluids could only be gathered under saturated gravity flow; (2) samplers materials could interfere with the super sensitive chemical analyses; (3) it is generally expensive; (4) and may not be practical for unusual soil types and unusual research objectives such as capturing total leached volumes, hydraulic discontinuity, and sometimes artificial sidewall flow.

Figure 1.1: Polyethylene (PE-HD) lysimeter station with four lysimeters in a clover leaf arrangement with an entering hatch (center position) during the installation process. Source: Meissner et al. (2004).

To our knowledge, no information is available on using lysimeters in arid regions to measure water percolation through soil, measure water and solute balance, measure movement of water and chemicals in the unsaturated and saturated zone of the soil, and investigate the behavior of solutes in soil.

This study presents a modification to the lysimeter "we call it here surface runoff sampler (SRS)", was designed to provide a stronger collection surface, more efficient connections for sample collection, and to measure particularly the first flush of runoff. But in the absent of runoff, the runoff sampler acts as lysimeter. The runoff sampler designed has the following advantages and limitations, advantages: easy to assemble, requires minimum maintenance once installed, and total cost is relatively low; limitations: manual pumping is required, the runoff sampler must be checked on a regular schedule and pumped when full (depending on rain frequency and intensity), and doesn't clearly delineate between runoff and infiltration.

This study included precipitation, runoff, soil chemistry, and groundwater chemistry in the Amargosa Desert. The field and experimental work collected the required chemical data for precipitation, runoff, and sediment analysis. The groundwater chemistry and isotope data administered by the Independent Scientific Investigation Program (ISIP) that contains data from more than 200 wells that encompass the entire region. New methods were developed to control the construction and emplacement of surface runoff samplers in addition to the collection, field testing, and handling of precipitation, runoff, and sediment samples from the time the samples are gathered at the location until they are ready to be sent to the laboratory for chemical analysis. Different analytical methods, mapping, and modeling techniques were performed on these four sections to proof the hypothesis of this research, which has been proofed, "The long term monitoring of the chemical analysis of surface runoff can provide a unique insight into the processes controlling the groundwater recharge and the sustainable yield of groundwater in the Amargosa Desert Region". The water ion chemistry, stable isotopic composition and statistical analyses of these various kinds of water samples from the Amargosa Desert show similarity between the surface water and underlying groundwater. This provides an important evidence for that current and past infiltration of surface runoff (stormwater) is the primary source of the underlying groundwater reservoir and that infiltration of surface runoff from large storm events in this region is a source of recharge more important that previously realized.

This study covers groundwater recharge from the surface runoff and infiltration in arid environments. The dissertation presented noval methods and results in identifying interaction of surface runoffs and infiltration with groundwater, groundwater flow patterns, groundwater recharge and geochemical evolution around Fortymile Wash near Yucca Mountain. Chapters 2 through 6 were covered specific issues: identification of probable groundwater paths in the

Amargosa Desert Vicinity, groundwater recharge in the Amargosa Desert using surface-runoff chemistry, and groundwater recharge in southern Nevada.

REFERENCES

Alexandrov, Y., J.B. Laronne, and I. Reid (2007), Intra-Event and Inter-Seasonal Behavior of Suspended Sediment in Flash Floods of the Semi-Arid Northern Negev, Israel, Geomorphology, 85:85-97.

DOE-OCRWM (U.S. Department of Energy-Office of Civilian Radioactive Waste Management) (2006), Evaluation of Technical Impact on the Yucca Mountain Project Technical Basis Resulting From Issues Raised by E-Mails of Former Project Participants, DOE/RW-0583, 144 p.

Fisher, S.G., and W.L. Minckley (1978), Chemical Characteristics of a Desert Stream in Flash Flood, Journal of Arid Environments, 1:25-33.

Frostick, L.E., I. Reid, J.T. Layman (1983), Changing Size Distribution of Suspended Sediment in Arid-Zone Flash Floods: Special Publication of the International Association Sedimentologists, 6:97-106.

Fuehr, F, R.J. Hance, J.R. Plimmer, J.O. Nelson (1998), the Lysimeter Concept: ACS Symposium Series 699, Washington, DC.

Inbar, M. (1992), Rates of Fluvial Erosion in Basins with a Mediterranean Type Climate: Catena, 19:393-409.

Johnson, M.J., C.J. Mayers, C.A. Garcia, B.J. Andraski (2007), Selected Micrometeorological, soil Moisture, and Evapotranspiration Data at Amargosa Desert Research Site in Nye County near Beatty, Nevada, 2001-2005, U.S. Department of the Interior, U.S. Geological Survey.

Jones, K.R. (1981), Food and Agricultural Organisation of the United Nations: Arid Zone Hydrology, 271 pp.

Meissner, R., and M. Seyfarth (2004), Measuring Water and Solute Balance with New Lysimeter Techniques, SuperSoil, 3rd Australian New Zealand Soils Conference, University of Sydney, Australia.

Meissner, R., H. Rupp, and M. Schubert (2000), Novel Lysimeter Techniques-a Basis for Improved Investigation of Water, Gas and Solute Transport in Soils, Journal of Plant Nutrition and Soil Science, 163:603-607.

Meissner, R., J. Seeger, and H. Rupp (2002), Effects of Agricultural Land Use Changes on Diffuse Pollution of Water Resources, Irrigation and Drainage, 51:119-127.

Migliaccio, K.W., Y.C. Li., H. Trafford, and E.A. Evans (2009), A Simple Lysimeter for Soil Water Sampling in South Florida, ABE361, Agricultural and Biological Engineering Department, Florida Cooperative Extension Service, IFAS, URL: http://edis.ifas.ufl.edu/AE387, 3 pgs.

Osborn, N.B., and K.G. Renard (1970), Thunderstorm Runoff on the Walnut Gulch Experimental Watershed, Arizona, USA, Results of Research on Representative and Experimental Basins, pp. 455-464. Paris, IAHS-Unesco.

Pilgrim, D.H., T.C. Chapman, and D.G. Doran 1(988), Problems of Rainfall-Runoff modeling in arid and semi-arid regions, Hydrological Sciences Journal, 1988, 33: 379-400.

Sharma, K.D., and J.S.R. Murthy (1996), Ephemeral Flow Modeling in Arid Regions, Journal of Arid Environments, 33:161-178.

Sharma, K.D., and N.S. Vangani 1(982), Flash Flood of July 1979 in the Luni Basin: a Rare Event in the Indian Desert, Hydrological Sciences Journal, 27:365-377.

SNL (Sandia National Laboratories) (2008), Total System Performance Assessment for the Yucca Mountain Site, DOC. 20080312.0001/ MDL-WIS-PA-000005 REV00.

Stewart, J.H., and V.C. Lamarche (1967), Erosion and Deposition Produced by the Flood of December 1964 on Coffee Creek, Trinity County, California, U.S. Geological Survey, 19:827-831.

Takamatsu, T., M.K. Koshikawa, M. Watanabe, H. Hou, and T. Murata (2007), Design of a Meso-Scale Indoor Lysimeter for Undisturbed Soil to Investigate the Behavior of Solutes in Soil, European Journal of soil Science, 58:329-334.

Woolhiser, D.A., R.W. Fedors, R.E. Smith, and S.A. Stothoff (2006), Estimating Infiltration in the Uper Split Wash Watershed, Yucca Mountain, Nevada, Journal of hydrologic Engineering, 11(2), pp. 123-133. DOI: 10.1061/ ASCE 1084-0699 2006 11:2 123

Chapter 2

Yucca Mountain Region Groundwater Geochemical Data Analysis

The material of this chapter was published in the International High-Level Radioactive Waste Management Conference (IHLRWMC), Las Vegas, Nevada. La Grange Park, Illinois: American Nuclear Society, September 7-11, 2008, p. 87-94.

ISBN: 978-0-89448-062-1

2. Yucca Mountain Region Groundwater Geochemical Data Analysis

Omar Al-Qudah [a,*], Arturo Woocay [a, b], and John C. Walton [a]

[a] *Civil Engineering Department-Environmental Science and Engineering Program , The University of Texas at El Paso, 500 W University Ave, El Paso, TX 79968, USA.*

[b] *División de Estudios de Posgrado e Investigación, Instituto Tecnológico de Ciudad Juárez, Ave. Tecnológico 1340, Ciudad Juárez, CHIH 32500, MX.*

[*] *Corresponding author: Tel.:+1 915 422 4260; fax: +1 915 747 8037; omal@miners.utep.edu*

ABSTRACT

Groundwater geochemical data from the Amargosa Desert region were analyzed to better understand the general flow system, geochemical evolution and recharge patterns around Fortymile Wash near Yucca Mountain, Nevada. Major ion chemistry, silica, fluoride and associated saturation indices, determined with PHREEQC, were examined sequentially using the multivariate statistical methods of principal component factor analysis and *k*-means cluster analysis. Analysis of both major ion data concentrations and their saturation indices allows simultaneous consideration of arithmetic (raw concentrations) and logarithmic (saturation indices) variables that describe the hydrochemical system and therefore can provide further insight into the system's behavior. The factor analysis of the major ion and saturation indices transforms the variables into a tractable number of descriptive factors that are rotated to summarize the chemical groundwater system and better interpret system variation. Cluster analysis of the reduced hydrochemical system establishes distinct hydrochemical facies independently of the lithological data, but in good agreement with it. These analyses showed

several groundwater signatures or hydrochemical processes indicating groundwater evolution, potential flowpaths, and recharge areas such as the important one along Fortymile Wash.

2.1 INTRODUCTION

Geochemistry has contributed significantly to the understanding of groundwater systems over the last 50 years. Historic advances include development of the hydrochemical facies concept, application of equilibrium theory, investigation of redox processes, and radiocarbon dating (Glynn and Plummer, 2005). Other hydrochemical concepts, tools, and techniques have helped elucidate mechanisms of flow and transport in groundwater systems, and have helped unlock an archive of paleoenvironmental information. Hydro-chemical and isotopic information can be used to interpret the origin and mode of groundwater recharge, refine estimates of time scales of recharge and groundwater flow, decipher reactive processes, provide paleohydro-logical information, and calibrate groundwater flow models (Glynn and Plummer, 2005). A thermodynamic perspective is offered that could facilitate the comparison and understanding of the multiple physical, chemical, and biological processes affecting groundwater systems. The chemical species of an element is important regarding its environmental chemistry. The species also give information on the mobility and therefore availability of the metal to living things and their potential toxicity (Fergusson, 1990).

The conceptual hydrological model of the Yucca Mountain region has evolved as more data are gathered and understanding of the region increases (Flint et al., 2001). Several researchers (Eddebbarh et al., 2003; Winterle et al., 2003; Kelkar et al., 2003; Liu et al., 1995) have conducted mathematical modeling of the Yucca Mountain conceptual model at the site and/or regional scale, and base their confidence in modeling results by comparing calculated to observed hydraulic heads, estimated to measured infiltration rates, and comparing their results to

results obtained by other mathematical models. They present groundwater flow in the Amargosa Desert region, generally from areas of higher hydraulic head under the mountains to the north to the low hydraulic head regions in the south.

Groundwater flow paths in the vicinity of Yucca Mountain were estimated from compositional variations in the aerial distribution of relatively nonreactive, naturally occurring tracers (Cl, SO_4, and $\delta^{18}O$) in the volcanic and alluvial aquifers by Kwicklis et al. (2003). The flow paths estimated from this analysis were then used to develop inverse models that attempted to explain the chemical and isotopic composition of groundwater at selected down-gradient wells in terms of groundwater mixing and water/rock interactions.

The work presented herein adds to the understanding of the general groundwater flow system, geochemical evolution and recharge patterns around Fortymile Wash near Yucca Mountain. Groundwater chemistry data used herein were obtained from the Nye County Nuclear Waste Repository Project Office (NWRPO) (NWRPO, 2003) and a Los Alamos National Laboratory report (LANL, 2003).

2.2 DESCRIPTION OF THE STUDY AREA

Yucca Mountain, north of the Amargosa Desert, Nevada, (Figure 2.1) is a group of north-trending block-faulted ridges of volcanic rocks (ash-flow and ash-fall tuffs) (Kelkar et al., 2003). Amargosa Desert is located in the southern portion of Nye County within the Great Basin, and is part of the Death Valley groundwater basin. Fortymile Wash, an ephemeral drainage, originates in the uplands north of Yucca Mountain, flows southward along the east side of the mountain, and terminates in the northern part of the Amargosa Desert. Yucca Mountain has been chosen as the site of a high-level nuclear waste repository and is expected to hold approximately 77,000 metric tons of radioactive waste.

The present climate in the Amargosa Desert region is considered arid to semiarid, with average annual precipitation ranging from less than 130 millimeters (mm) at lower elevations to more than 280 mm at higher elevations (Flint et al., 2001).

Since groundwater beneath Yucca Mountain is directly upgradient from populated areas in the Amargosa Desert (Figure 2.1), an analysis of groundwater geochemical data in this region is important. Furthermore, better understanding the general flow system around Yucca Mountain may provide further insight into its behavior.

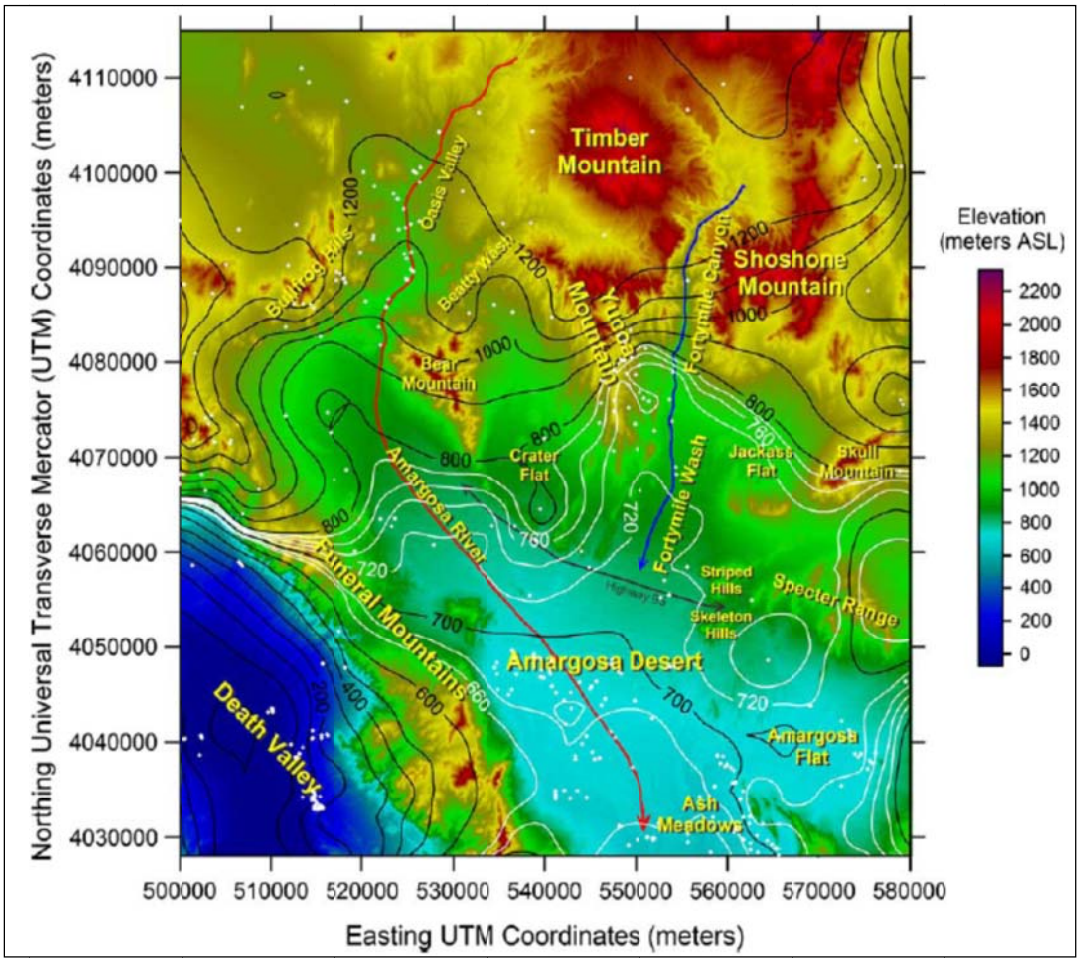

Figure 2.1: Static groundwater elevation contours based on 210 wells within the area shown, overlaid on a digital elevation model (DEM) of the Amargosa region. For illustration purposes, contour intervals are reduced from 100 to 20 m, between the 800 and 660 m levels, and presented in white (modified from Woocay and Walton, 2006).

2.3 METHODOLOGY

2.3.1 Hydrochemical modeling

The computer program PHREEQC is capable of describing a variety of geochemical processes in groundwater systems. The program was used to conduct simulations using a chosen set of dissolved species and mineral phases to describe oxidation-reduction (redox) reaction and thermodynamic equilibrium, including ion exchange, dissolution, and precipitation. PHREEQC was used to calculate thermodynamic equilibrium saturation indices for mineral species, based on major ions, temperature, pH, F^- and SiO_2. The saturation index (SI) is defined as the logarithm of the ratio of the ion activity product (IAP) of the component ions of the solid in solution to the solubility product (K) for the solid [SI=log IAP/K]. If the SI is zero, the water composition reflects the solubility equilibrium with respect to the mineral phase. A negative value indicates undersaturation and a positive value indicates supersaturation.

When redox reactions occur between the atoms to form molecules or ions with polar covalent bonds, certain assumptions are required in order to maintain a consistent concept. Knowledge of valence and bonding theory serves as the key to correct the formulas of chemical species. In general, knowledge of electrostatics is applied to write formulas with elements and radicals that have a fixed valence (or oxidation state) like oxygen. The difficulty stems from elements that can assume several oxidation states like sulfur (most common oxidation numbers are +6, +4, +2, 0, and -2), from which a variety of ions, molecules, and radicals can result. Here the redox couple H_2O/O_2 is used for calculating initial pE values.

Groundwater chemistry data for 210 sampling locations in the vicinity of Yucca Mountain were obtained from NWRPO and Los Alamos National Laboratory and compiled into a single database covering the Amargosa Desert region. These data were then input into

PHREEQC. The data included the major ions (Ca^{2+}, Mg^{2+}, Na^{+}, K^{+}, Cl^{-}, SO_4^{2-}, SiO_2, F^{-}, and total alkalinity), in addition to pH, temperature and redox.

2.3.2 Multivariate statistical methods

The multivariate statistical methods applied herein are principal component factor analysis (PCFA) and k-means cluster analysis (CA). PCFA is a dimension reduction method and CA is a classification method.

Factor analysis methods allow a reduction in the number of variables that describe system behavior and the identification of new, homogeneous subgroups that are easier to identify (Lawrence and Upchurch, 1982). PCFA uses linear combinations of the variables to form the factors. The linear combinations permit PCFA to retain as much as possible of the original data variation and spatial distribution in factor-space, and allows for the use of rotation schemes that better reveal similarities within variables or cases. The most common rotation is the normalized varimax rotation, which attempts to find the rotation that will maximize variability on the rotated axes while minimizing it everywhere else (Mellinger, 1987). A *k*-means CA attempts to minimize the variability within each cluster while maximizing the variability between clusters. The mean of a cluster, or centroid, has its components specified by the average of each variable in the analysis. The algorithm uses one initial observation per cluster as the mean for that cluster, and then evaluates each of the remaining observations for inclusion into a particular cluster.

Using STATISTICA^{TM}8, a PCFA was performed on TDS and Cl^{-} data along with the species near saturation data, obtained by applying PHREEQC to the major ion data, to reduce the number of variables to four. In addition, a rotation of the first four factors was conducted to find relationships among the original variables. From the rotated factors of the ion chemistry, factor scores were generated for each of the 210 sampling locations, thus producing a loading table

indicating the decomposition of each of the samples into the four rotated factors. Using the same statistical software, the factor scores from the rotated PCFA results were then evaluated with the *k*-means CA to cluster wells with a similar composition into eight separate sample groups, or chemical facies. The *k*-means CA variables evaluated are the four factor scores, and the observations are the factor scores for each sampling location.

Rotated factor loadings for major ions and factor scores for each sampling location, grouped into hydrochemical facies, are presented on biplots. Biplots are simultaneous bivariate (factor loadings and factor scores) scatter plots that provide a visual picture of the relationships between and among different variables and observations. The biplots presented herein have two scales: one for factor scores of sampling locations (i.e., bottom and left) and the other for factor loadings of ions (i.e., top and right). Sampling locations are shown as symbols, and ions are shown as vectors with their end (i.e., arrow) located at the factor loading values for that ion. For illustration purposes, the scale for ions is arbitrarily selected since only their direction is of relevance to the factor scores, but the same scale is used for all ions. Each ion vector indicates the direction of increasing ion content in the samples, and their projection onto the factor axis is their contribution and correlation to that factor.

Contour plots of the first resulting factor were overlaid on a DEM of the region to reveal groundwater signatures and potential flowpath (Figure 2.1). A contour plot of a factor would be equivalent to a contour plot of a hydrochemical process delineating its areas of influence (Lawrence and Upchurch, 1982) and indicating the direction of evolution of that process (perpendicular to the contour).

2.4 RESULTS AND DISCUSSION

2.4.1 Ionic strength

The groundwater's ionic strength ranges between 2.26E-03and 1.44E-02 (mean 5.3E-03) (Table 2.1). According to Appelo and Postma (1999), the ionic strength for freshwater is normally less than 0.02 while seawater has ionic strength of about 0.7. Also Deutsch (1997) reported that the ionic strength of most dilute groundwater is in the range of 10^{-2} to 10^{-3}. The values of the ionic strength here show that the groundwater samples from Yucca Mountain area are fresh.

Table 2.1: Ionic Strength for the Chemical Species in Yucca Mountain Region.

	Ionic Strength
Minimum Value	0.0023
Maximum Value	0.0144
Mean	0.0053
St.dev	0.0028

In addition, it has been noted (Deutsch, 1997) that the higher the ionic strength, the greater the solubility of the mineral in contact. Thus, the ionic strength results herein indicate that dissolved species in the Yucca Mountain region are very soluble and mobile.

2.4.2 Chemical speciation and saturation indices

Carbon (IV): the major ionic species of C (IV) in the Yucca Mountain ground water is HCO_3^-, representing between 82 to 97% of all C (IV) species, by mean concentration of 2.74E-03 molal. The ions CO_2, $CaHCO_3^+$ and CO_3^{2-}, represent between 1 and 18, 0.2 to 1.4 and 0.07 to 0.6 %.

Calcium: the dominant dissolved Ca species in the area is Ca^{2+}, comprising between 72 and 97% of all the species with mean concentration of 2.95E-04 molal; whereas the species $CaSO_4$, $CaHCO_3^+$ and $CaCO_3$ are in the ranges 1.8 to 23, 1.2 to 4 and 0 to 3.4%.

Chloride: chloride is of primary concern in any geochemical analysis because it is a highly nonreactive tracer, nonvolatile, and hydrologically mobile. There are no expected sources or sinks of chloride ions which is an advantage for understanding the flow system. 100% of Cl is in the ionic form of Cl^- with mean concentration of 5.56E-04 molal.

Fluoride: The ionic form F^- by mean concentration of 1.51E-04 molal represents more than 97% of F, but less than 2.5, 0.8 and 0.4% of MgF^+, CaF^+ and NaF, exist.

Potassium: K^+ is the main ionic species constituting 78% of the total K in the area by mean concentration of 1.01E-04 molal. The KSO_4^- species represent less than 0.8%.

Magnesium: the Mg species in the groundwater are Mg^{2+} from 78 to 96% with mean concentration of 7.18E-05 molal, $MgSO_4$ from 2 to 15%, $MgHCO_3^+$ from 1 to 4%, $MgCO_3$ from 0.2 to 3%, MgF^+ from 0.05 to 2 and $MgOH^+$ from 0 to 0.4%.

Sodium: in all the groundwater data, Na^+ constitutes the major ionic species ranging between 99 and 100% with mean concentration of 3.46E-03 molal. The minor species include $NaSO_4^-$ from 0.06 to 0.6%, $NaHCO_3$ from 0.06 to 0.2 % and $NaCO_3^-$ from 0 to 0.1%.

Sulfur: the major ionic species of S^{6+} is in the form SO_4^{2-} ranging from 86 to 99% by mean concentration of 4.11E-04 molal, $CaSO_4$ from 0.9 to 8%, $NaSO_4^-$ from 0.06 to 5% and $MgSO_4$ from 0 to 2%.

Silicate: the Si species in the groundwater are H_4SiO_4 from 71 to 99% with mean concentration of 7.77E-04 molal and $MgSO_4$ from 0 to 0.1%.

The speciation calculation indicates that the elements Ca, Cl, F, K, Mg and Na are distributed more than 90% as free ion species in all the analyzed groundwater samples. And for the elements C^{4+}, S^{6+} and Si the dominant species were HCO_3^-, SO_4^{2-} and H_4SiO_4 by more than 90%.

The Na–Cl relationship has often been used to identify the mechanisms for acquiring salinity and saline intrusions in semi-arid regions. The low concentration of Na^+ and Cl^- in groundwater suggests that the dissolution of halite is not important in regulating the concentration of Na^+ in groundwater and that there are other sources of Na^+ and Cl^-.

Table 2.2 indicates that the groundwater in the area is near saturation with respect to aragonite ($CaCO_3$), calcite ($CaCO_3$), chalcedony (SiO_2), dolomite ($CaMg(CO_3)_2$), fluorite (CaF_2), sepiolite (d) ($Mg_2Si_3O_7(OH)5.3H_2O$) and amorphous silicate (SiO_2). Of the wells, 58, 4, 7, 27 and 4%, were oversaturated with respect to talc ($Mg_3Si_4O_{10}(OH)_2$), Chrysotile ($Mg_3Si_2O_5(OH)_4$), dolomite, quartz (SiO_2), and sepiolite (d).

Table 2.2: Chemical Species Saturation Indices in Yucca Mountain Region.

Species	Minimum value	Maximum value	Mean	Near saturation (%)	Over saturation (%)
Anhydrite	-5.12	-1.68	-2.7	0	0
Aragonite	-1.99	0.94	-0.17	76	0
Calcite	-1.85	1.08	-0.03	78	0.5
Chalcedony	-0.55	1.03	0.43	61	0.5
Chrysotile	-11.6	5.83	-3.2	8	4
Dolomite	-4.18	2.31	-0.6	40	7
Fluorite	-3.45	0.19	-1.1	16	0
Gypsum	-4.93	-1.46	-2.5	0	0
Halite	-8.33	-6.44	-7.5	0	0
Quartz	-0.16	1.47	0.85	6	27
Sepiolite	-7.25	3.73	-1.75	15	4
Sepiolite(d)	-10.1	0.66	-4.7	1	0
SiO_2(a)	-1.35	0.19	-0.39	78	0
Talc	-7.11	9.97	1.33	12	58

Reactions among aqueous species that occur within the same oxidation state of the elements involved (e.g. $CO_2/HCO_3^-/CO_3^{2-}$; SO_4^{2-}/HSO_4^-) are rapid and equilibrium can be assumed; in contrast, equilibrium is usually not attained between aqueous species with differing oxidation states (e.g., SO_4^{2-}/HS^-, HCO_3^-/CH_4). A small number of minerals, usually of relatively high solubility, appear to behave reversibly in natural systems (e.g., calcite, gypsum, halite, and fluorite); most other minerals (primary silicates) do not react completely to equilibrium but can still have an important effect on natural-water chemistry. Some weathering products of primary silicates tend to react to equilibrium, but kinetic processes are important in the formation of complex siliceous clay minerals (Glynn and Plummer, 2005).

Groundwater systems were recognized early on as partial equilibrium systems (Lawrence and Upchurch, 1982); that is, where some reactions respond reversibly while driven by one or more irreversible reactions (e.g., oxidation of organic carbon driving sulfate reduction, and/or carbonate mineral reactions; dissolution of anyhydrite driving dedolo-mitization; dissolution of primary silicates driving the formation of clays and cementation with calcite and silica). These reactions are important in understanding geochemical evolution of groundwater systems, and can affect the hydrologic properties of aquifer systems. Some natural waters that appear to be at or near equilibrium with a given mineral phase, according to speciation calculations, may in fact be undergoing significant dissolution/precipitation of the mineral as a result of other irreversible reactions.

2.4.3 Multivariate statistical methods

Rotated factor loading distributions for each variable are presented in Table 2.3, along with the amount of total proportional variation explained by each rotated factor; high loading indicates a high degree of correlation. Factor 1 explains 25.6% of the variation and is dominated

by anhydrate, gypsum and fluorite, whereas Factor 2 explains 35.6% of the variation and is primarily composed of chrysotile, talc, sepiolite, dolomite and calcite. The first two rotated factors represented about 61% of the variation, whereas the remaining two explain nearly 40% of the variation with dominant species of amorphous silicate in the third factor and chloride in the fourth factor. In total, the first four factors explain 93.0% of the system's variations, implying a loss of only slightly more than 4%.

Table 2.3: Rotated Factor Loadings for TDS, Cl^- and SI

Parameter	Factor1	Factor2	Factor3	Factor4
Chloride	0.276	0.017	0.040	**0.912**
TDS	0.437	0.215	0.002	**0.784**
Anhydrite	**0.910**	0.147	0.075	0.304
Calcite	0.486	**0.785**	-0.172	0.165
Chrysotile	-0.013	**0.994**	-0.002	0.041
Dolomite	0.493	**0.814**	-0.117	0.239
Fluorite	**0.768**	0.013	-0.006	0.293
Gypsum	**0.908**	0.152	0.087	0.306
Halite	0.269	0.097	-0.055	**0.939**
Sepiolite	0.043	**0.964**	0.233	0.061
SiO_2(a)	0.079	0.112	**0.987**	-0.007
Talc	-0.005	**0.984**	0.147	0.035
Variation	3.070	4.278	1.111	2.69
Percentage	25.6%	35.6%	9.3%	22.4%

High factor loadings on variables are presented in red bold.

The factor scores from the rotated PCFA results were evaluated with *k*-means CA to group sampling locations with a similar genesis into eight groups, or hydrochemical facies; results are presented in biplot Figures 2.2, 2.3, 2.4, 2.5 and 2.6.

Figure 2.2 can roughly be interpreted as the separation of samples into Ca^{2+} on one end by 26% and Mg^{2+} on the other by 36%. Figures 2.3 and 2.4 can be interpreted as the separation of samples into Ca^{2+} on one end by 26% and SiO_2 (a) and Cl^- on the other by 9% and 22%,

respectively. Figures 2.5 and 2.6 can be interpreted as the separation of samples into Mg^{2+} on one end by 26% and SiO_2 (a) and Cl^- on the other by 9% and 22%.

In Figure 2.1, static ground water level contours demonstrate a sharp hydraulic gradient under the Funeral Mountains toward Death Valley, and a strong gradient under Yucca Mountain with a southeast direction broadly toward Fortymile Wash. Refined contours next to Yucca Mountain demonstrate a trough surrounding Fortymile Wash, indicating ground water flow toward the wash. In general, hydraulic gradients north of the Amargosa Desert follow a northwest to southeast trend, followed by gradients in the Amargosa Desert that portray a leveling out and then a gradual turn southwest toward Death Valley. Water levels are less than 850 m above sea level (asl) in most of the western side of the Amargosa Desert, Jackass Flats, and Amargosa Flat and decrease to 660 m at the foothills of the Funeral Mountains. In contrast, topography in the same area changes from 1,050 m asl in the west and northeast to 700 m in the southeastern end of the desert near Ash Meadows.

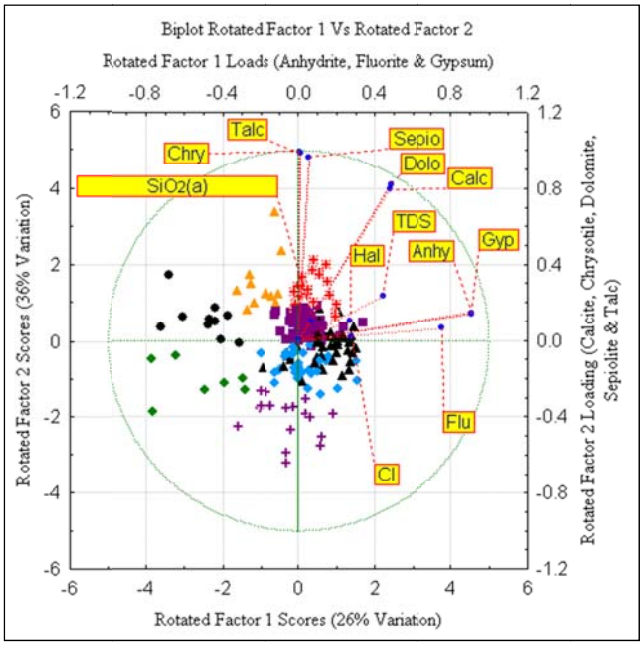

Figure 2.2: Biplot-Rotated Factor 1 Vs Rotated Factor 2.

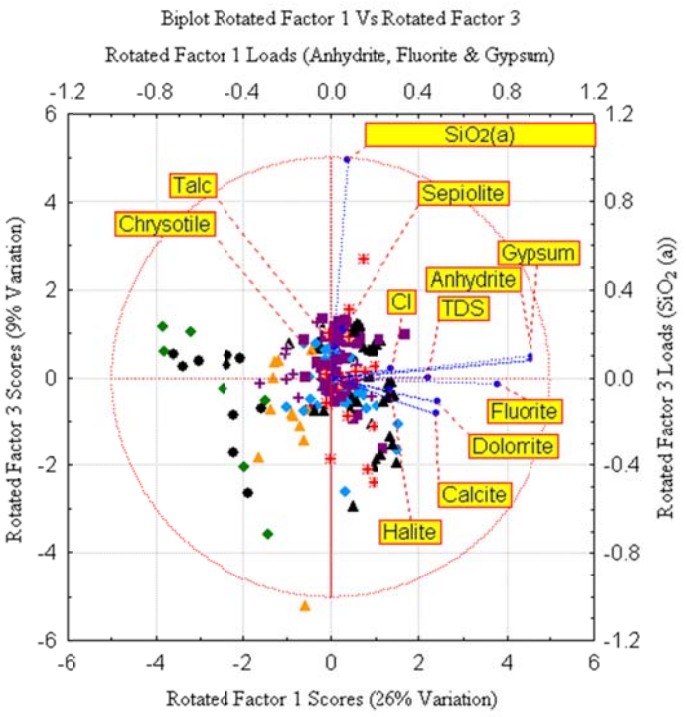

Figure 2.3: Biplot-Rotated Factor 1 Vs Rotated Factor 3.

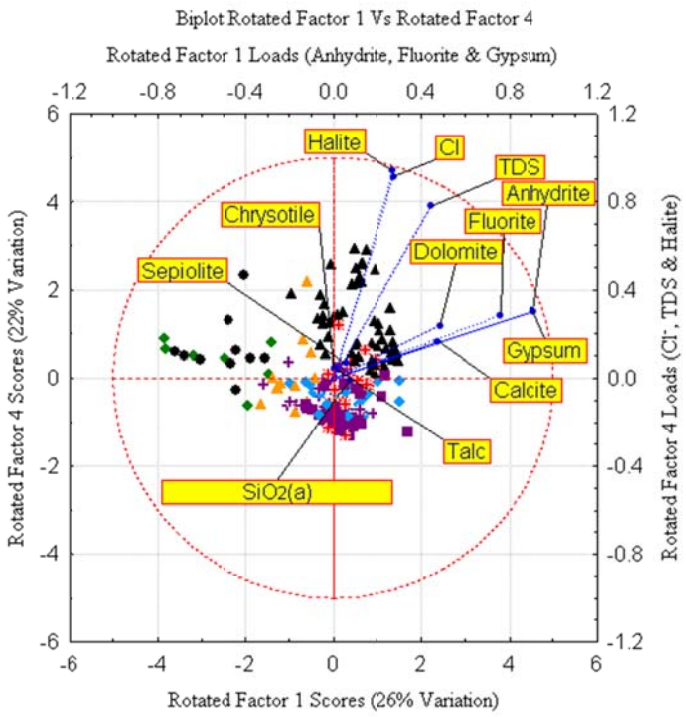

Figure 2.4: Biplot-Rotated Factor 1 Vs Rotated Factor 4.

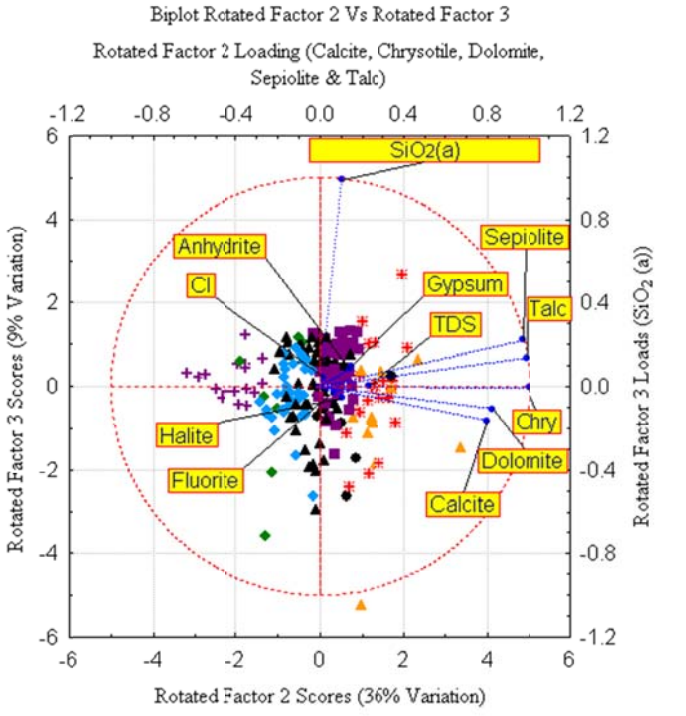

Figure 2.5: Biplot-Rotated Factor 2 Vs Rotated Factor 3.

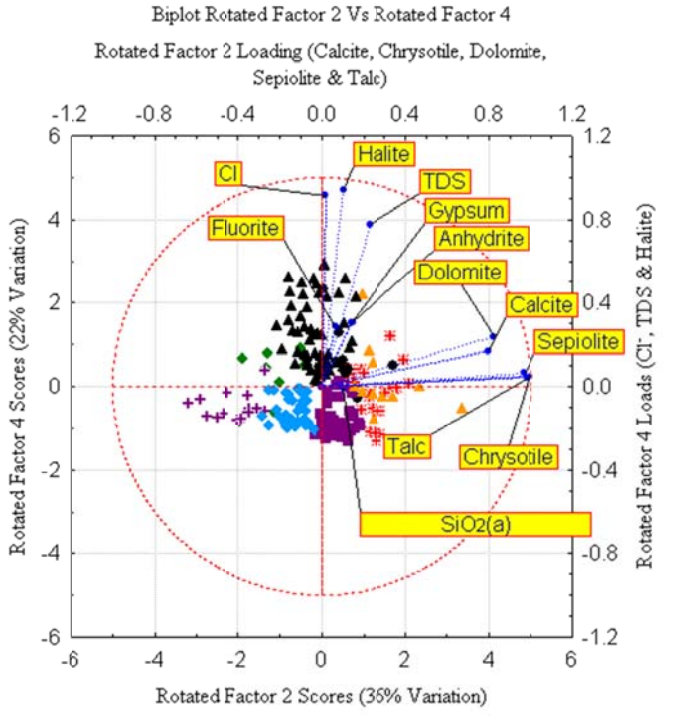

Figure 2.6: Biplot-Rotated Factor 2 Vs Rotated Factor 4.

2.5 CONCLUSIONS

Groundwater ionic strength results of the Amargosa desert region indicate greater solubility and mobility of the dissolved species, in addition to the good water quality. Where elements Ca, Cl, F, K, Mg and Na are distributed as free ion species and HCO_3^-, SO_4^{2-} and H_4SiO_4 are the dominant species of the elements C^{4+}, S^{6+} and Si by more than 90%, in all the analyzed samples.

The low concentration of Na^+ and Cl^- in groundwater suggests that the dissolution of halite is not important in regulating the concentration of Na^+ in groundwater and that there are other sources of Na^+ and Cl^-.

Groundwater saturation indices indicate that the area is near saturation with respect to aragonite, calcite, chalcedony, dolomite, fluorite, sepiolite and amorphous silicate. Of the sampling locations, 58, 4, 7, 27 and 4% were oversaturated with respect to talc, chrysotile, dolomite, quartz and sepiolite, respectively.

In the factor analysis, the variance of Factor 1 is dominated by anhydrate, gypsum and fluorite by 26%, whereas factor 2 explains 35.6% of the variance and is primarily composed of calcite, chrysotile, dolomite, sepiolite and talc. The first two rotated factors represented about 61% of the variation, whereas the remaining two explain nearly 40% of the variation with dominant species of amorphous silicate in the third factor and chloride in the fourth factor. The *k*-means CA produced eight groups, which are presented on biplot to separate the samples into four basic factors of which the factor containing Ca^{2+}, Mg^{2+}, $SiO_2(a)$, Cl^-; Mg^{2+} is the most dominant factor. The previous analyses indicate that the dominant processes and reactions responsible for hydrochemical evolution of the system differ by location and include: carbonate

equilibrium, silicate weathering reactions, evaporative concentration, and dissolution of calcite, dolomite, and fluorite.

The biplots are diagram customized to the dominant hydrochemical processes (i.e., the factors), showing the hydrochemical facies and demonstrating the chemical composition of the processes and facies of the system. The spatial plots of factor-score contours delineate areas influenced by a hydrochemical process and indicate the direction of evolution of that process (perpendicular to the contour); they allow the exposition of hydrochemical signatures indicating ground water flowpaths and their interaction with the geologic context. Together, factor-score contours and hydrochemical facies indicate the five potential ground water flowpaths or signatures presented in Figure 2.1.

ACKNOWLEDGMENTS

The Nye County NWRPO funded this work through U.S. Department of Energy Office of Civilian Radioactive Waste Management cooperative research grant DE-FC28-02RW12163. We also thank the Center for Environmental Resource Management of The University of Texas at El Paso for their funding and support.

REFERENCES

Appelo, C.A.J., D. Postma (1999), Geochemistry, Groundwater and Pollution, AA Balkema Rotterdam 536 pp.

Deutsch, W.J. (1997), Groundwater Geochemistry, Fundamentals and Applications to Contamination, Lewis, New York, 221 pp.

Eddebbarh, A.A., G.A. Zyvoloski, B.A. Robinson, E.M. Kwicklis, P.W. Reimus, B.W. Arnold, T. Corbet, S.P. Kuzio, C. Faunt (2003), The Saturated Zone at Yucca Mountain: an Overview of the Characterization and Assessment of the Saturated Zone as a Barrier to Potential Radionuclide Migration, J. Contam. Hydrol., 62–63, 477-493.

Fergusson, J.E. (1990), The Heavy Elements: Chemistry, Environmental Impacts and Health Effect, Pergamon Press, Oxford, 613 pp.

Flint, A. L., L. E. Flint, G. S. Bodvarsson, E. M. Kwicklis, and J. T. Fabryka-Martin (2001), Evolution of the Conceptual Model of Unsaturated Zone Hydrology at Yucca Mountain, Nevada, J. Hydrology, 247(2001), 1-30, pii: S0022-1694(01)00358-4.

Glynn, P.D., and L. N. Plummer (2005), Geochemistry and the Understanding of Groundwater Systems, Hydrogeology Journal, 13(1), 263-287.

Kelkar, S., P. Tseng, T. Miller, R. Pawar, A. Meijer, B. Robinson, G. Zyvoloski, E. Kwicklis, A.A. Eddebbarh, B. Arnold (2003), Site/Subsite Scale Saturated-Zone Flow-Transport Models for Yucca Mountain, International High- Level Radioactive Waste Management Conference, Las Vegas, Nevada. La Grange Park, Illinois: American Nuclear Society.

Kwicklis, E., A. Meijer, J.T. Fabryka-Martin (2003), Geochemical Inverse Model of Groundwater Mixing and Chemical Evolution in the Yucca Mountain Area, International High- Level Radioactive Waste Management Conference, Las Vegas, Nevada. La Grange Park, Illinois: American Nuclear Society.

LANL (Los Alamos National Laboratory) (2003), Regional groundwater hydrochemical data in the Yucca Mountain area used as direct input to ANLNBS-00021. LA0309RR831233.001.

Lawrence, F.W., S.B. Upchurch (1982), Identification of Recharge Areas Using Geochemical Factor Analysis. Groundwater 20 (6), 680-687.

Liu, B., F. Phillips, S. Hoines, A.R. Campbell, P. Sharma (1995), Water Movement in Desert Soil Traced by Hydrogen and Oxygen Isotopes, Chloride, and Chlorine-36, Southern Arizona, J. Hydrol., 168, 91-110.

Mellinger, M. (1987), Multivariate Data Analysis: its Methods, Chemom. Intell. Lab., Syst. 2, 29-36.

NWRPO (Nuclear Waste Repository Project Office) (2003), Geochemistry data files, Nye County, Nevada. < http://www.nyecounty.com> (accessed April 30, 2004).

Winterle, J.R., A. Claisse, H.D. Arlt (2003), An Independent Site-Scale Ground water Flow Model for Yucca Mountain, International High-Level Radioactive Waste Management Conference, Las Vegas, Nevada. La Grange Park, Illinois: American Nuclear Society.

Woocay, A., and J.C. Walton (2006), Climate Change Effects on Yucca Mountain Region Groundwater Recharge, International High-Level Radioactive Waste Management Conference, Las Vegas, Nevada. La Grange Park, Illinois: American Nuclear Society.

Chapter 3

Identification of Probable Groundwater Paths in the Amargosa Desert Vicinity

The material of this chapter is published in the Journal of Applied Geochemistry, Volume 26, issue 4, p. 565-574, April 2011

doi:10.1016/j.apgeochem.2011.01.014; ISSN 0883-2927

3. Identification of Probable Groundwater Paths in the Amargosa Desert Vicinity

Omar Al-Qudah [a,*], Arturo Woocay [b, c], and John Walton [c]

[a] *Environmental Science and Engineering, The University of Texas at El Paso, 500 W University Ave, El Paso, TX 79968, USA.*

[b] *División de Estudios de Posgrado e Investigación, Instituto Tecnológico de Ciudad Juárez, Ave. Tecnológico 1340, Ciudad Juárez, CHIH 32500, MX.*

[c] *Environmental Science and Engineering, Civil Engineering Department, The University of Texas at El Paso, 500 W University Ave, El Paso, TX 79968, USA.*

[*] *Corresponding author: Tel.:+1 915 422 4260; fax: +1 915 747 8037, omal@miners.utep.edu.*

ABSTRACT

In this study, the hydrogeochemical program PHREEQC was used to determine the chemical speciation and mineral saturation indices (SIs) of groundwater in the vicinity of the proposed high-level nuclear waste repository at Yucca Mountain, Nevada (USA). In turn, these data were used to interpret the origin and recharge mode of groundwater, to elucidate the mechanisms of flow and transport, and to determine potential sources of groundwater contamination. PHREEQC was run to determine aqueous dissolved species and minerals that would be in equilibrium with the study area's groundwater. Selected major ions, associated SI, F^- and Ca/Na ion exchange were then examined using the multivariate statistical methods of principal component factor analysis and *k*-means cluster analysis. Analysis of dissolved ion concentrations, SIs, and Ca/Na ion exchange allows simultaneous consideration of arithmetic

(raw concentrations) and logarithmic (SI, ion exchange) variables that describe the hydrochemical system and, therefore, can provide further insight into the system's behavior. The analysis indicates that the dominant processes and reactions responsible for the hydrochemical evolution in the system are (1) evaporative concentration prior to infiltration, (2) carbonate equilibrium, (3) silicate weathering reactions, (4) limited mixing with saline water, (5) dissolution/precipitation of calcite, dolomite and fluorite, and (6) ion exchange. Principal component factor analysis and k-means cluster analysis of factor scores allow the reduction of dimensions describing the system and the identification of hydrogeochemical facies and the processes that defined and govern their evolution.

Statistical analysis results indicate that the northern west face and southern Yucca Mountain groundwater is fresh water with low concentrations of Ca^{2+}, Mg^{2+}, Cl^{-}, $Ca^{2+}/(Na^{+})^{2}$, and CaF_2. The Fortymile Wash groundwater is dilute. The carbonate signature is shown in the Ash Meadows and Death Valley waters with high fluorite SI. Finally, the Crater Flat, Stripped Hills, and Skeleton Hills are dominated by Ca/Na ion exchange, Mg and Ca. The hydrochemical and statistical analyses showed three main groundwater signatures or hydrochemical processes indicating groundwater evolution, potential flowpaths, and recharge areas. The flowpaths are the trace of the Amargosa River, the trace of Fortymile Wash, and its convergence with the Amargosa River. This appears to represent not just a groundwater flow path, but traces of surface runoff infiltration as well.

3.1 INTRODUCTION

The proposed nuclear repository inside Yucca Mountain, Nevada (USA), was to be built between 201 and 427 m below the mountain's surface and between 174 and 366 m above the water table, and would hold around 70,000 tons of spent nuclear fuel and high-level radioactive

waste (OSTI, 2000). To protect people and the environment, the design of the repository depends on natural and engineered barriers to isolate the nuclear waste and keep it dry as long as possible. Since groundwater beneath Yucca Mountain is directly upgradient from populated areas in the Amargosa Desert, an analysis of groundwater geochemical data in this region is important. Furthermore, better understanding the general flow system around Yucca Mountain may provide further insight into its behavior. Improved understanding of groundwater recharge and movement, with or without the repository, is essential for management of groundwater resources in southern Nevada. Variations in groundwater mineral speciation chemistry in the Yucca Mountain region could affect the processes associated with the potential transport of radionuclides (such as ^{229}Th; ^{240}Pu; ^{239}Pu; ^{238}Pu; ^{232}U; ^{233}U; ^{241}Am; ^{243}Am; ^{237}Np; ^{210}Pb; ^{206}Pb; ^{208}Pb; ^{227}Ac; ^{99}Tc; ^{40}K; and ^{14}C) from the proposed repository to the accessible environment.

The conceptual hydrological model of the Yucca Mountain region has evolved as more data have been gathered and understanding of the region has increased (Flint et al., 2001). The conceptual model of Yucca Mountain groundwater flow paths relies upon the argument that, in the absence of downgradient recharge or groundwater mixing, the composition of nonreactive species in the groundwater should remain constant along a flow path. Therefore, groundwater in an area with a given nonreactive species composition does not flow toward an area where the nonreactive species composition is different, whereas groundwater flow between areas with similar nonreactive species compositions is possible (Kwicklis et al., 2003). Several researchers (e.g., Eddebbarh et al., 2003; Winterle et al., 2003; Kelkar et al., 2003; Liu et al., 1995) have developed mathematical models of the Yucca Mountain conceptual model at the site and/or regional scale. Confidence in modeling results is based on comparisons of calculated and observed hydraulic heads, estimated and measured infiltration rates, and similarity to results

obtained by other mathematical models. Groundwater flow in the Amargosa Desert region is generally from areas of higher hydraulic head under the mountains to the north to the low hydraulic head regions in the south.

Groundwater flow paths in the vicinity of Yucca Mountain were estimated from compositional variations in the areal distribution of relatively nonreactive, naturally occurring tracers (Cl, SO_4, and $\delta^{18}O$) in the volcanic and alluvial aquifers by Kwicklis et al. (2003). The identification of these pathways is important for understanding the extent to which the saturated zone can delay human exposure to any radionuclides that might someday be mobilized from the Yucca Mountain repository. The flow paths estimated from this analysis were then used to develop inverse models that attempted to explain the chemical and isotopic composition of groundwater at selected downgradient wells in terms of groundwater mixing and water/rock interaction. Bushman et al. (2010) studied groundwater sources at Ash Meadows, a site of major groundwater discharge in the Mojave Desert. Those authors applied cluster analysis techniques to characterize and sort similar waters to determine the potential groundwater flow paths. Bushman et al. (2010) concluded from isotopic tracers and solute balances that waters at Ash Meadows are derived from southward flow through volcanic terrains, parallel to the preferred permeability structure induced by active regional east–west extension. The authors suggested that carbonate aquifer systems in extensional terrains are more compartmentalized than previously appreciated and that anisotropy in fracture permeability is a key to compartmentalization and the control of flow directions. Woocay and Walton (2006, 2008) examined the region with multivariate statistical methods using major ion concentrations. They found flowpaths along fracture traces in some regions mixed with flow directly down the hydraulic gradient in alluvial areas.

In this paper, multivariate statistical methods of principal component factor analysis and *k*-means cluster analysis were used to examine major ion chemistry and saturation indices. Analysis of dissolved ion concentrations, saturation index (SI) values, and Ca/Na ion exchange allows simultaneous consideration of arithmetic variables (raw concentrations) and logarithmic variables (SIs) that describe the hydrochemical system and, therefore, can provide further insight into the system's behavior. The factor analysis of the major ions and saturation indices transforms the variables into a tractable number of descriptive factors that are rotated to summarize the chemical groundwater system and better interpret system variation. Cluster analysis of the reduced hydrochemical system establishes distinct hydrochemical facies independently of the lithological data, but in good agreement with them. Results are presented as contours overlaid on a digital elevation model of the region, which provide an image of potential flowpaths, and on bivariate plots (biplots) that allow the simultaneous observation of variable and sample relationships based on established hydrochemical processes and facies. These analyses indicate that the dominant processes and reactions responsible for hydrochemical evolution of the system differ by location and include carbonate equilibrium, silicate weathering reactions, evaporative concentration, and dissolution of calcite, dolomite and fluorite.

3.2 DESCRIPTION OF THE STUDY AREA

The Amargosa Desert (Figure 3.1) is located in southern Nye County, Nevada, approximately 160 km northwest of Las Vegas, within the unique closed-basin, hydrologic regime known as the Great Basin. The Amargosa Desert is part of the Death Valley groundwater basin. The Funeral Mountains separate the Amargosa Desert from Death Valley to the southwest, and a series of mountain ranges bound the northern and eastern extents of the desert. The present climate in the Amargosa Desert region is arid to semi-arid, with average annual precipitation

ranging from less than 130 mm at lower elevations to more than 280 mm at higher elevations (Flint et al., 2001).

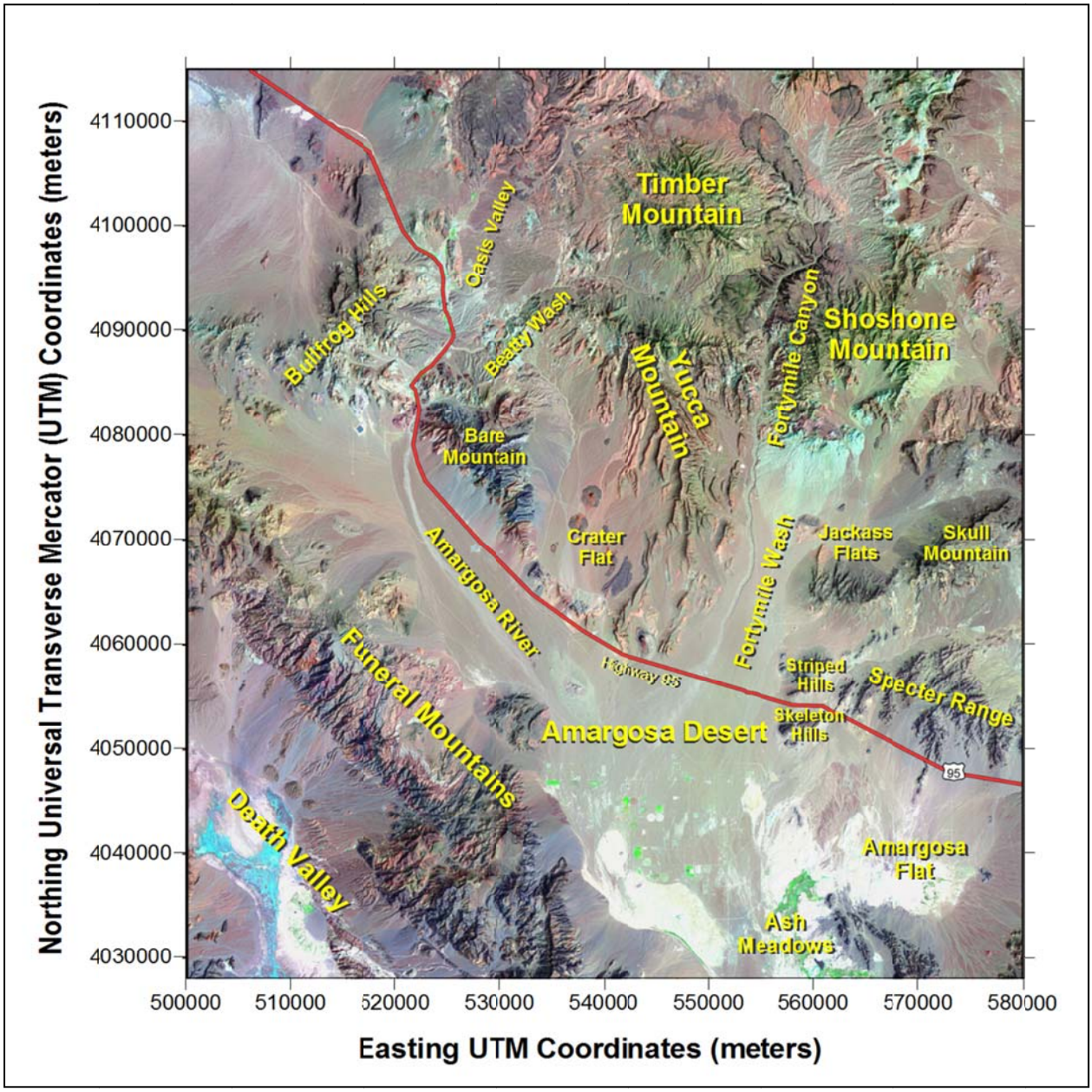

Figure 3.1: Locations of Amargosa Desert, Amargosa River, Yucca Mountain, and Fortymile Wash, Nye County, Nevada (modified from Woocay and Walton, 2008).

The Amargosa River is a major drainage component (over 12,950 km^2) of the Great Basin. This river system begins in the Oasis Valley, turns southeast to run through the Amargosa

Desert, continues until it turns northwest, and terminates in Death Valley from its southeast extension. As a result of the semi-arid to arid continental climate, the Amargosa River and its tributaries are ephemeral streams that are dry most of the time except in a few relatively short reaches where springs maintain small, perennial base flows. Fortymile Wash and Beatty Wash (in addition to the washes in Crater Flat and Rock Valley) are the major tributaries of the upper Amargosa River, which drains through several small, populated areas downstream. Fortymile Wash originates between Timber Mountain and Shoshone Mountain. Fortymile Wash is an ephemeral drainage that flows southward along the east side of Yucca Mountain and fans out in the northern Amargosa Desert just north of U.S. Highway 95. Near Highway 95, the Fortymile Wash channel changes from being moderately confined to several distributary channels that are poorly confined. This distributary drainage pattern persists downstream to its confluence with the Amargosa River.

3.3 METHODOLOGY

Groundwater chemistry data used herein were obtained from the Nye County Nuclear Waste Repository Project Office (NWRPO) (NWRPO, 2008) and a Los Alamos National Laboratory report (LANL, 2007). Data were compiled into a single database consisting of 210 sampling locations covering the Amargosa Desert region. Sampling locations are mainly composed of wells, some with multiple screened depths, while the remainder are fresh springs. These data were then input into PHREEQC (version 2.12.5) and STATISTICA™9 (StatSoft Inc., 1984–2010). The data for hydrochemical modeling included the major ions (Ca^{2+}, Mg^{2+}, Na^{+}, K^{+}, Cl^{-}, SO_4^{2-}, SiO_2, F^{-}, and total alkalinity), in addition to pH, temperature and Eh. Multivariate statistical analyses included the concentrations of Ca^{2+}, Mg^{2+}, Na^{+}, K^{+}, Cl^{-}, SO_4^{2-}, F^{-}, and HCO_3^{-};

the ion-exchange couple $Ca^{2+}/(Na^{+})^2$ using log-transformed concentrations; and the SIs of designated species near saturation (anhydrite [$CaSO_4$], calcite [$CaCO_3$], and fluorite [CaF_2]).

3.3.1 Hydrochemical modeling

The computer program PHREEQC is capable of describing a variety of geochemical processes in groundwater systems. The program was used to conduct simulations using a chosen set of dissolved species and mineral phases to describe oxidation– reduction (redox) reactions and thermodynamic equilibrium, including ion exchange, dissolution, and precipitation. PHREEQC was used to calculate thermodynamic equilibrium SI for mineral species, based on major ions, temperature, pH, F^- and SiO_2. The SI is defined as the logarithm of the ratio of the ion activity product (IAP) of the component ions of the solid in solution to the solubility product (K) for the solid [SI = log (IAP/K)]. If the SI is zero, the water composition reflects the solubility equilibrium with respect to the mineral phase. A negative value indicates undersaturation and a positive value indicates supersaturation.

3.3.2 Multivariate statistical methods

Multivariate statistical methods (MSMs) are powerful tools used to examine large, complex datasets in order to help identify parameters or dimensions that describe data, which may thus provide new insight into their behavior (Mellinger, 1987). MSMs applied herein are principal component factor analysis (PCFA) and k-means cluster analysis. PCFA is a dimension reduction method and cluster analysis is a classification method.

Factor analysis methods allow a reduction in the number ofvariables that describe system behavior and the identification of new, homogeneous subgroups that are easier to identify (Lawrence and Upchurch, 1982). PCFA uses linear combinations of the variables to form the

factors with a mean of zero and standard deviation of one. The linear combinations permit PCFA to retain as much as possible of the original data variation and spatial distribution in factor-space, and allow for the use of rotation schemes that better reveal similarities within variables or cases. The most common rotation is the normalized varimax rotation, which attempts to find the rotation that will maximize variability on the rotated axes while minimizing it everywhere else (Mellinger, 1987). A *k*-means cluster analysis attempts to minimize the variability within each cluster while maximizing the variability between clusters. The mean of a cluster, or centroid, has its components specified by the average of each variable in the analysis. The algorithm uses one initial observation per cluster as the mean for that cluster, and then evaluates each of the remaining observations for inclusion into a particular cluster.

Using STATISTICA™9 (StatSoft Inc., 1984–2010), a PCFA was performed on the concentrations of Ca^{2+}, Mg^{2+}, Na^{+}, K^{+}, Cl^{-}, SO_4^{2-}, F^{-}, and HCO_3^{-}, on the log-transformed ion-exchange couple $Ca^{2+}/ (Na^{+})^2$, and on the SIs of anhydrite, calcite, and fluorite to reduce the number of variables to four. Input data of raw concentrations were not log-transformed as the factor analysis is conducted on the correlation matrix of the data, thus eliminating any normality requirements for variables' distributions. However, the saturation indices and ion-exchange couple are logarithmic. After the factor analysis, a rotation of the first four factors was conducted to find relationships among the original variables. Based on the rotated factors of the ion chemistry, factor scores were generated for each of the 210 sampling locations, thus producing a loading table indicating the decomposition of each of the samples into the four rotated factors. Using the same statistical software, the factor scores from the rotated PCFA results were then evaluated with the *k*-means cluster analysis to cluster wells with a similar composition into six separate sample groups, or hydrochemical facies. The k-means cluster analysis variables

evaluated are the four factor scores, and the observations are the factor scores for each sampling location.

Rotated factor loadings for major ions and factor scores for each sampling location, grouped into clusters, are presented on biplots. Biplots are simultaneous bivariate (factor loadings and factor scores) scatter plots that provide a visual picture of the relationships between and among different variables and observations. The biplots presented herein have two scales: one for factor score of sampling locations (i.e., bottom and left) and the other for factor loadings of ions (i.e., top and right). Note that the positive and negative signs are not significant; only the relative locations along the new dimension are important (normalized and standardized factor scores). Sampling locations are shown as symbols, and ions are shown as purple vectors with their ends (i.e., arrows) located at the factor loading values for each variable. For illustration purposes, the scale for original variables is arbitrarily selected, since only their direction is of relevance to the factor scores, but the same scale is used for all input variables (ion concentration, ratios and SIs). Each variable line indicates the direction of increasing variable content in the samples, and their projection onto the factor axis is their contribution and correlation to that factor.

Contour plots presented herein were developed with Surfer™8 (Golden Software Inc., 2008) using the existing natural neighbor gridding method of the software. Contour plots of the resulting factors were overlaid on a digital elevation map (DEM) of the region to reveal groundwater signatures and potential flowpaths. A contour plot of a factor would be equivalent to a contour plot of a hydrochemical process delineating its areas of influence and indicating the direction of evolution of that process (perpendicular to the contour) (Lawrence and Upchurch, 1982).

3.4 RESULTS

3.4.1 Chemical speciation and saturation indices

The distribution of the Amargosa Desert's groundwater chemical speciation is shown in Table 3.1.

3.4.1.1 Carbon (IV)

The major ionic species of C (IV) in the Yucca Mountain groundwater is HCO_3^-, representing between 82% and 97% of all C (IV) species, with a mean concentration of 2.74×10^{-3} molal. The ion $CaHCO_3^+$ represents 0.2–1.4% of all C (IV) species and CO_3^{2-} represents 0.07–0.6% of all C (IV) species.

3.4.1.2 Calcium

Ca^{2+} comprises 72–97% of all dissolved Ca, with a mean concentration of 2.95×10^{-4} molal. The species $CaSO_4$, $CaHCO_3^+$ and $CaCO_3$ are in the ranges 1.8–23%, 1.2–4% and 0–3.4%, respectively.

3.4.1.3 Chloride

Chloride is of primary concern in any geochemical analysis because it is a highly nonreactive tracer, non-volatile and hydrologically mobile (Glynn and Plummer, 2005; Hem, 1992). There are no expected sources or sinks of Cl^- ions, which is an advantage for understanding the flow system. All of the Cl is in the ionic form of Cl^- with a mean concentration of 5.56×10^{-4} molal.

3.4.1.4 Fluoride

The ionic form F^-, with a mean concentration of 1.51×10^{-4} molal, represents more than 97% of F, while MgF^+, CaF^+, and NaF constitute less than 2.5, 0.8 and 0.4%, respectively.

Table 3.1: Distribution of Species in Yucca Mountain Region Groundwater.

Major Species	Minor Species	Minimum Value (Molal)	Maximum Value (Molal)	Mean	St. dev.	Species percentage %
C (IV)	Total	1.41E-03	5.80E-03	2.91E-03	1.13E-3	100
	HCO_3^-	1.27E-03	5.36E-03	2.74E-03	1.10E-3	82 – 97
	CO_2	3.06E-05	3.74E-04	1.25E-04	0.10E-3	1-18
	$CaHCO_3^+$	2.63E-06	7.41E-05	1.82E-05	1.42E-05	0.2 – 1.4
	$CO3^{2-}$	1.37E-06	2.21E-05	7.77E-06	5.78E-06	0.07– 0.6
	$NaHCO_3$	5.69E-07	2.15E-05	5.75E-06	5.04E-06	0.03 – 0.5
	$MgHCO_3^+$	1.31E-07	2.09E-05	3.82E-06	4.38E-06	0.01 – 0.4
	$CaCO_3$	7.86E-08	1.38E-05	2.12E-06	3.21E-06	0.01 – 0.3
Ca	Total	3.74E-06	1.37E-03	3.28E-04	0.31E-3	100
	Ca^{2+}	3.46E-06	1.15E-03	2.95E-04	0.26E-3	72 – 97
	$CaSO_4$	1.31E-07	1.67E-04	2.05E-05	3.54E-05	1.8 – 23
	$CaHCO_3^+$	7.78E-08	5.13E-05	8.80E-06	1.10E-05	1.2 – 4
	$CaCO_3$	6.46E-08	1.31E-05	3.54E-06	3.80E-06	0.001 – 3.4
Cl	Total	9.03E-05	2.23E-03	5.56E-04	0.61E-3	100
	Cl^-	9.03E-05	2.23E-03	5.56E-04	0.61E-3	100
Na	Total	1.35E-03	7.41E-03	3.48E-03	1.65E-3	100
	Na^+	1.35E-03	7.35E-03	3.46E-03	1.63E-3	99 – 100
	$NaSO_4^-$	8.68E-07	4.01E-05	8.72E-06	1.06E-05	0.06 – 0.6
	$NaHCO_3$	8.42E-07	1.70E-05	4.74E-06	4.48E-06	0.06 – 0.2
	$NaCO_3^-$	3.26E-08	6.02E-06	1.42E-06	1.61E-06	0.01 – 0.1
F	Total	3.16E-05	3.53E-04	1.52E-04	9.47E-05	100
	F^-	3.11E-05	3.52E-04	1.51E-04	9.40E-05	97 – 99.9
	MgF^+	6.29E-08	6.11E-06	8.03E-07	1.48E-06	0.1 – 2.3
	CaF^+	3.92E-09	1.74E-06	2.83E-07	4.19E-07	0 – 0.7
	NaF	1.76E-09	8.15E-07	1.47E-07	2.17E-07	0 – 0.3
K	Total	1.31E-05	3.33E-04	1.01E-04	8.35E-05	100
	K^+	1.30E-05	3.30E-04	1.01E-04	8.29E-05	99 – 100
	KSO_4^-	6.98E-09	2.86E-06	3.47E-07	6.63E-07	0.04 – 0.8
Mg	Total	4.11E-07	6.59E-04	8.44E-05	0.17E-3	100
	Mg^{2+}	3.86E-07	5.28E-04	7.18E-05	0.13E-3	78 – 96
	MgSO4	1.07E-08	1.01E-04	9.14E-06	2.44E-05	2 – 15
	$MgHCO_3^+$	5.89E-09	2.16E-05	2.36E-06	5.32E-06	1 – 4
	$MgCO_3$	2.84E-09	6.11E-06	7.41E-07	1.59E-06	0.2 – 3
	MgF^+	1.76E-09	4.47E-06	4.23E-07	1.02E-06	0.05 – 2
S(6)	Total	7.50E-05	2.14E-03	4.48E-04	0.52E-3	100
	SO_4^{2-}	7.32E-05	1.83E-03	4.11E-04	0.45E-3	86 – 99
	$CaSO_4$	8.22E-07	1.67E-04	2.15E-05	4.00E-05	0.9 – 8
	$NaSO_4^-$	9.08E-08	1.01E-04	1.06E-05	2.36E-05	0.06 – 5
	$MgSO_4$	6.98E-09	4.01E-05	4.58E-06	1.07E-05	0.01 – 2
Si	Total	1.17E-04	1.17E-03	8.00E-04	0.25E-3	100
	H_4SiO_4	1.06E-04	1.16E-03	7.77E-04	0.26E-3	71 – 99
	$H_3SiO_4^-$	1.12E-06	1.56E-04	2.55E-05	3.62E-05	0.1 – 29

3.4.1.5 Potassium

K^+ is the main ionic species, constituting 78% of the total K in the area, with a mean concentration of 1.01×10^{-4} molal. The KSO_4^- species represents less than 0.8%.

3.4.1.6 Sodium

In all the groundwater data, Na^+ constitutes the major ionic species (ranging between 99% and 100% of Na), with a mean concentration of 3.46×10^{-3} molal. The minor species include $NaSO_4^-$ (0.06–0.6%), $NaHCO_3$ (0.06–0.2%), and $NaCO_3^-$ (0–0.1%).

The Na–Cl relationship has often been used to identify the mechanisms for acquiring salinity and saline intrusions in semi-arid regions (Glynn and Plummer, 2005; Hem, 1992). The low concentrations of Na^+ and Cl^- in groundwater suggest that the dissolution of halite is not important in regulating the concentration of Na^+ in groundwater and that there are other sources of Na^+ and Cl^-.

3.4.1.7 Magnesium

Mg^{2+} represents 78–96% of Mg species in the groundwater, with a mean concentration of 7.18×10^{-5} molal; $MgSO_4$ represents 2–15%, $MgHCO_3^+$ 1–4%, $MgCO_3$ 0.2–3%, MgF^+ 0.05–2%, and $MgOH^+$ 0–0.4%.

3.4.1.8 Sulfur

The major ionic species of S (VI) is SO_4^{2-}, ranging from 86% to 99%, with a mean concentration of 4.11×10^{-4} molal; $CaSO_4$ constitutes 0.9–8% and $NaSO_4^-$ constitutes 0.06–5%.

3.4.1.9 Silicon

The Si species in groundwater are H_4SiO_4 (71–99%, with a mean concentration of 7.77×10^{-4} molal) and $H_3SiO_4^-$ (0.1–29%).

The speciation calculations indicate that the elements Ca, Cl, F, K, Mg and Na are distributed more than 90% as free ion species in most of the analyzed groundwater samples. For the elements C, S, and Si, the dominant species (HCO_3^-, SO_4^{2-} and H_4SiO_4, respectively) represented more than 90% of most of the elemental concentration.

Mean saturation indices of different minerals are given in Table 3.2. The groundwater is undersaturated (negative SI) with respect to some minerals (for example: anhydrite, chrysotile, dolomite, fluorite, gypsum, halite, quartz and sepiolite), oversaturated (positive SI) with respect to talc, and near saturation (SI ≈ 0) with respect to some other minerals (for example: amorphous silicate, aragonite, calcite and chalcedony).

Table 3.2: Saturation Indices for Groundwater Samples from Yucca Mountain Region.

Species	Chemical formula	Minimum value	Maximum value	Mean	St. dev.	Wells near saturation (%)	Wells over saturation (%)
Anhydrite	$CaSO_4$	-5.12	-1.68	-2.7	0.69	0	0
Aragonite	$CaCO_3$	-1.99	0.94	-0.17	0.47	76	0
Calcite	$CaCO_3$	-1.85	1.08	-0.03	0.47	78	0.5
Chalcedony	SiO_2	-0.55	1.03	0.43	0.2	61	0.5
Chrysotile	$Mg_3Si_2O_5(OH)_4$	-11.6	5.83	-3.2	2.55	8	4
Dolomite	$CaMg(CO_3)_2$	-4.18	2.31	-0.6	1.1	40	7
Fluorite	CaF_2	-3.45	0.19	-1.1	0.57	16	0
Gypsum	$CaSO_4 \cdot 2H_2O$	-4.93	-1.46	-2.5	0.7	0	0
Halite	NaCl	-8.33	-6.44	-7.5	0.48	0	0
Quartz	SiO_2	-0.16	1.47	0.85	0.21	6	27
Sepiolite	$Mg_2Si_3O_{7.5}OH \cdot 3H_2O$	-7.25	3.73	-1.75	1.8	15	4
SiO_2(a)	SiO_2	-1.35	0.19	-0.39	0.19	78	0
Talc	$Mg_3Si_4O_{10}(OH)_2$	-7.11	9.97	1.33	2.6	12	58

The minerals with positive SI may precipitate, thus reducing aquifer porosity and permeability. Similarly, the minerals with negative SI that are present in aquifer rock will dissolve during groundwater flow, which will increase its porosity and permeability. The minerals with SI near zero refer to a thermodynamic equilibrium between the groundwater and the specified solid phase.

Application of speciation models to low-temperature groundwater environments has led to several important principles and observations. Homogeneous reactions among aqueous species that occur within the same oxidation state of the elements involved (e.g., HCO_3^-/CO_3^{2-}; SO_4^{2-}/HSO_4^-) are rapid and equilibrium can be assumed; in contrast, equilibrium is usually not attained between aqueous species with differing oxidation states (e.g., SO_4^{2-}/HS^-, HCO_3^-/CH_4). A small number of minerals, usually of relatively high solubility, appear to behave reversibly in natural systems (e.g., calcite, halite and fluorite); most other minerals (e.g., primary silicates) do not react completely to equilibrium but can still have an important effect on natural-water chemistry. Some weathering products of primary silicates tend to react to equilibrium, but kinetic processes are important in the formation of complex siliceous clay minerals (Glynn and Plummer, 2005).

Groundwater systems were recognized early on as partial equilibrium systems (Glynn and Plummer, 2005), in which some reactions respond reversibly while driven by one or more irreversible reactions (e.g., oxidation of organic C driving SO_4^{2-} reduction, and/ or carbonate mineral reactions; dissolution of anhydrite driving dedolomitization; dissolution of primary silicates driving the formation of clays and cementation with calcite and silica). These reactions are important in understanding geochemical evolution of groundwater systems, and can affect the hydrologic properties of aquifer systems. Some natural waters that appear to be at or near equilibrium with a given mineral phase, according to speciation calculations, may in fact be undergoing significant dissolution/ precipitation of the mineral as a result of other irreversible reactions.

3.4.2 Multivariate statistical methods

Rotated factor loading distributions for each variable are presented in Table 3.3, along with the amount of total proportional variance explained by each rotated factor; high loading,

shown in bold, indicates a high degree of correlation. Factor 1 explains 29% of the variance and is dominated by Mg^{2+}, HCO_3^- and Ca^{2+}, whereas factor 2 explains 26% of the variance and is primarily composed of Cl^-, Na^+ and SO_4^{2-}.

Table 3.3: Rotated Factor Loadings for Major Ions, Fluoride and SIs.

Parameter	Factor 1	Factor 2	Factor 3	Factor 4
Ca^{2+}	**0.74**	0.42	0.40	-0.01
Mg^{2+}	**0.93**	0.14	0.13	-0.04
Na^+	0.32	**0.75**	-0.47	0.27
K^+	0.49	0.54	0.23	0.12
Cl^-	0.17	**0.91**	-0.01	0.16
SO_4^{2-}	0.57	**0.75**	0.07	0.05
F^-	-0.013	0.08	-0.37	**0.90**
HCO_3^-	**0.83**	0.35	-0.23	0.23
$Ca^{2+}/(Na^+)^2$	0.16	-0.14	**0.95**	-0.16
Anhydrite ($CaSO_4$)	0.54	0.53	0.60	0.04
Calcite ($CaCO_3$)	0.58	0.21	0.26	0.15
Fluorite (CaF_2)	0.29	0.37	0.46	**0.74**
Variation	3.54	3.06	2.18	1.57
Percentage	0.29	0.26	0.18	0.13

High factor loadings on variables are presented in bold.

The first two rotated factors represent about 55% of the variation, whereas the remaining two explain nearly 31% of the variance, with dominant species of (Ca/Na) ion exchange in the third factor and F^- and fluorite SI in the fourth factor. In total, the first 4 factors explain 86% of the system's variations. By matching the chemical compositions of the minerals in each factor, it is noted that the first factor is dominated by ions that are typically associated with the dissolution of carbonate, alkalinity and weathering processes, and/or carbonate aquifer upwelling. The second factor is dominated by ions that are typically associated with concentration of the water by evaporation prior to deep infiltration (Cl^-, Na^+ and SO_4^{2-}). The third factor, dominated by $Ca^{+2}/(Na^+)^2$ and followed by anhydrite, is generally associated with processes involving zeolites from volcanic rocks in the region; it separates Ca- versus Na-dominated waters. The fourth factor aids in the separation of carbonate water groups.

The factor scores from the rotated PCFA results were evaluated with k-means cluster analysis to group sampling locations with a similar genesis into six groups, or hydrochemical facies. Results are presented on the biplots in Figures 3.2 and 3.3, which depict factor 1 versus factor 2 and factor 3 versus factor 4, respectively. Loading and alignment of ions and factors can be observed in Figures 3.2 and 3.3, and Table 3.3. Alignment with a particular factor is indicated by a lack of loading and alignment with other factors. Ions with a high loading and alignment with a factor simplify interpretation of the factors. Figure 3.2 can roughly be interpreted as the separation of samples into Na–Cl and Mg–HCO_3 hydrochemical facies. Further inspection of Figure 3.2 and Table 3.3 demonstrates some factor complexity for Ca, SO_4 and anhydrite, as they do not align with one single factor and instead load with factors 1 and 2. Figure 3.2 indicates two very distinct groundwater chemical signatures: one with carbonate characteristics and the other showing evaporative evolution. Figure 3.3 can roughly be interpreted as the separation of samples into ‘‘ion exchange’’, anhydrite and fluoride with further separation provided by Na and fluorite, both of which present factor complexity. Table 3.4 shows the six groups determined from the *k*-means cluster analysis of the PCFA results and the median of major ion concentrations, Ca/Na ion exchange, and SI, demonstrating the different average compositions between the groups. Description and location of these clusters are shown in Table 3.5.

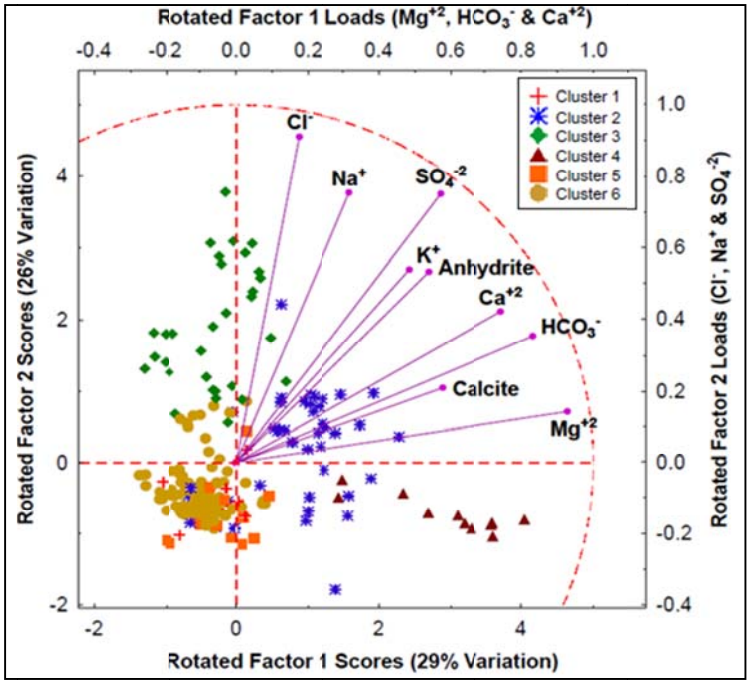

Figure 3.2: Biplot of rotated factor 1 versus rotated factor 2 with sampling-locations clustered into six groups.

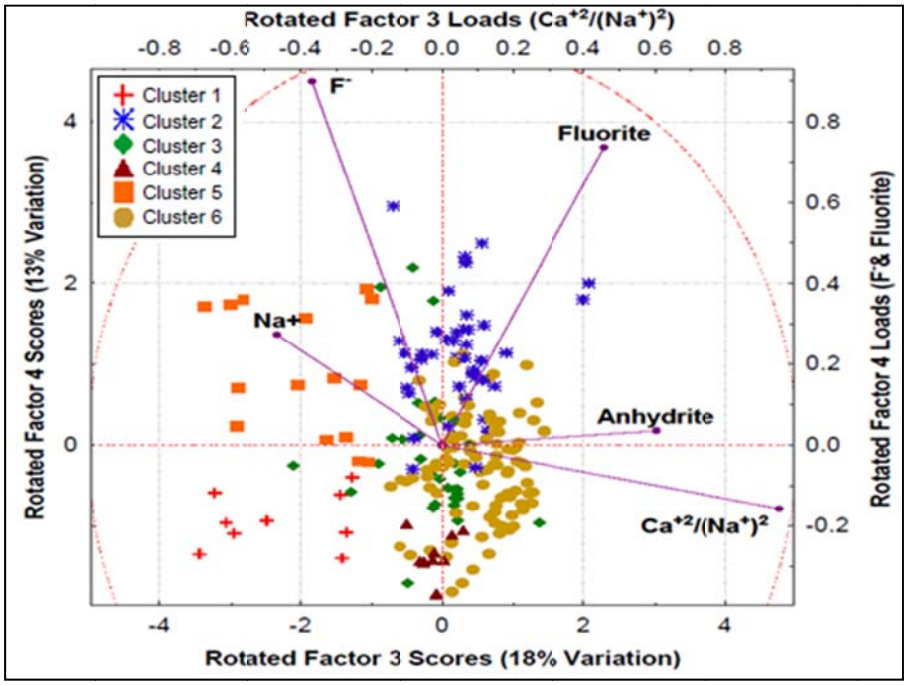

Figure 3.3: Biplot of rotated factor 3 versus rotated factor 4 with sampling-locations clustered into six groups.

Table 3.4: Median Values of Major Ion Composition, Ion Exchange and SI for the PCFA *k*-mean Cluster Analysis for Six Groups.

Parameter	Cluster 1	Cluster 2	Cluster 3	Cluster 4	Cluster 5	Cluster 6	All Samples
Number of wells	10	40	31	11	15	99	206
Ca^{2+} (mg/L)	1.2	42.4	25.7	60.2	2.6	16.8	21.3
Mg^{2+} (mg/L)	0.1	16.0	6.3	31.6	0.1	1.8	4.1
Na^{+} (mg/L)	97.6	101.3	130.0	84.6	90.6	50.2	94.1
K^{+} (mg/L)	2.8	11.8	9.4	8.3	2.0	5.1	6.7
Cl^{-} (mg/L)	6.3	23.9	48.4	16.3	7.8	7.9	12.1
SO_4^{2-} (mg/L)	16.4	99.5	127.5	132.0	28.1	26.9	63.8
F^{-} (mg/L)	2.1	3.3	2.0	0.8	3.9	1.6	2.1
Total alkalinity as CaCO3 (mg/L)	184.2	238.9	193.6	292.2	178.0	112.4	188.9
HCO_3^{-} (mg/L)	178.8	291.4	236.1	356.3	193.0	135.0	214.6
$Ca^{2+}/(Na^{+})^2$	-5.1	-3.6	-3.8	-3.1	-4.7	-3.3	-3.7
SI anhydrite ($CaSO_4$)	-4.3	-2.1	-2.2	-1.9	-3.5	-2.8	-2.5
SI calcite ($CaCO_3$)	-0.4	0.2	0.1	0.6	-0.1	0.0	0.1
SI fluorite (CaF_2)	-2.2	-0.3	-0.9	-1.3	-1.6	-1.2	-1.3
Non carbonate alkalinity fraction (%)	98	37	38	4	96	55	46.5

Table 3.5: Cluster Descriptions and Locations.

Cluster	Description	Location
1	Fresh water diluted, lowest Ca^{2+}, Mg^{2+}, Cl^{-}, $Ca^{2+}/(Na^{+})^2$ and fluorite; non-carbonate alkalinity.	Northern, west face and southern Yucca Mountain
2	Carbonate signature with high fluorite.	Ash Meadows, Death Valley
3	More highly evaporated water. High Na^{+}, Cl^{-}, and SO_4^{2-}.	Funeral Mountains, Ash Meadows, around Oasis Valley, and southeast of Fortymile Wash
4	Highest Ca^{2+}-Mg^{2+}, with high $Ca^{2+}/(Na^{+})^2$, lowest fluoride and highest sulfate. Carbonate waters; supersaturated with calcite and near saturation with anhydrite.	Crater Flat, Striped Hills and Skeleton Hills
5	Waters with highest fluoride. High Na^{+} and low $Ca^{2+}/(Na^{+})^2$ and Mg^{2+} with the lowest K^{+}. Non-carbonate alkalinity	West face of Yucca Mountain
6	Dilute water.	Fortymile Wash

Based on the results in Tables 3.3–3.5 and Figures 3.2 and 3.3, for clusters 1 and 5 the preponderance of the alkalinity appears to be related to silicate weathering rather than dissolution of carbonates. Alkalinity exceeds that which can be accounted for by the Ca^{2+} and Mg^{2+} concentrations in those samples; Na dominates over Ca (ion exchange parameter). Cluster 6 has about 50% non-carbonate alkalinity. The geochemical data support north-south flow along fractures that differs from the hydraulic gradient in the areas of clusters 1, 5, and 6; Ca versus Na preponderance and F^{-} differentiate these three groups (Figure 3.3, factor 4). Clusters 2 and 4 show high Ca^{2+} and Mg^{2+} concentrations, which are more consistent with carbonate waters.

Clusters 2 and 3 have about 1/3 non-carbonate alkalinity, suggesting a combination of dissolution of carbonates and silicate weathering. In the three high carbonate clusters, cluster 4 is predominantly Ca–Mg carbonate alkalinity. Carbonate groups 2 and 4 can also be differentiated on the basis of F^- and fluorite saturation (Figure 3.3, factor 4). Cluster 3 represents highly evaporated shallow groundwater flowing from Oasis Valley through the Amargosa Desert, roughly following the Amargosa River, and then turning towards Ash Meadows. This cluster represents the greatest average evaporative concentration prior to infiltration, as evidenced by Cl^- concentrations, whereas cluster 6 (Fortymile Wash) has the least amount of evaporative concentration. This is consistent with the topography, which is more gentle in the Oasis Valley, leading to less infiltration of storm runoff and less infiltration at high elevations.

Figures 3.4–3.7 present separate contour plots of the first through fourth rotated factor scores overlain on a DEM, along with three inferred potential flow paths. The red arrow shows the trace of the Amargosa River and the solid blue arrow shows the trace of Fortymile Wash and its convergence with the Amargosa River. The dashed pink arrow shows a potential flow path east to west from Rock Valley (east of Skull Mountain) toward Death Valley, along the trace of Gravity Fault (indicative of structural connections between the Yucca Mountain-Crater Flat area and southern Amargosa Desert), or possible upwelling from the underlying carbonate aquifers through fractures and faults. In Figure 3.4, high values of factor 1, which represent Ca^{2+} and Mg^{2+}, are located at Striped Hills, Skeleton Hills, and Crater Flat, which are downgradient of outcrops of the underlying carbonate aquifer. In Figure 3.5, high values of factor 2, which represent Cl^- and Na^+, are found near the Funeral Mountains, around Oasis Valley, and SE of Fortymile Wash. In Figure 3.6, the high values of factor 3 (representing $Ca^{2+}/(Na^+)^2$) are found at Ash Meadows, Crater Flat, Striped Hills, and Skeleton Hills, whereas low values are found at

northern and southern Yucca Mountain and along the west face. Figure 3.7 shows factor 4, with low values corresponding to low concentrations of F^- and fluorite. These are found encompassing Crater Flat, Striped Hills, Skeleton Hills and Fortymile Wash, past the point where it converges with the Amargosa River flowing SE, whereas high values are found at Ash Meadows, Death Valley, and the west face of Yucca Mountain.

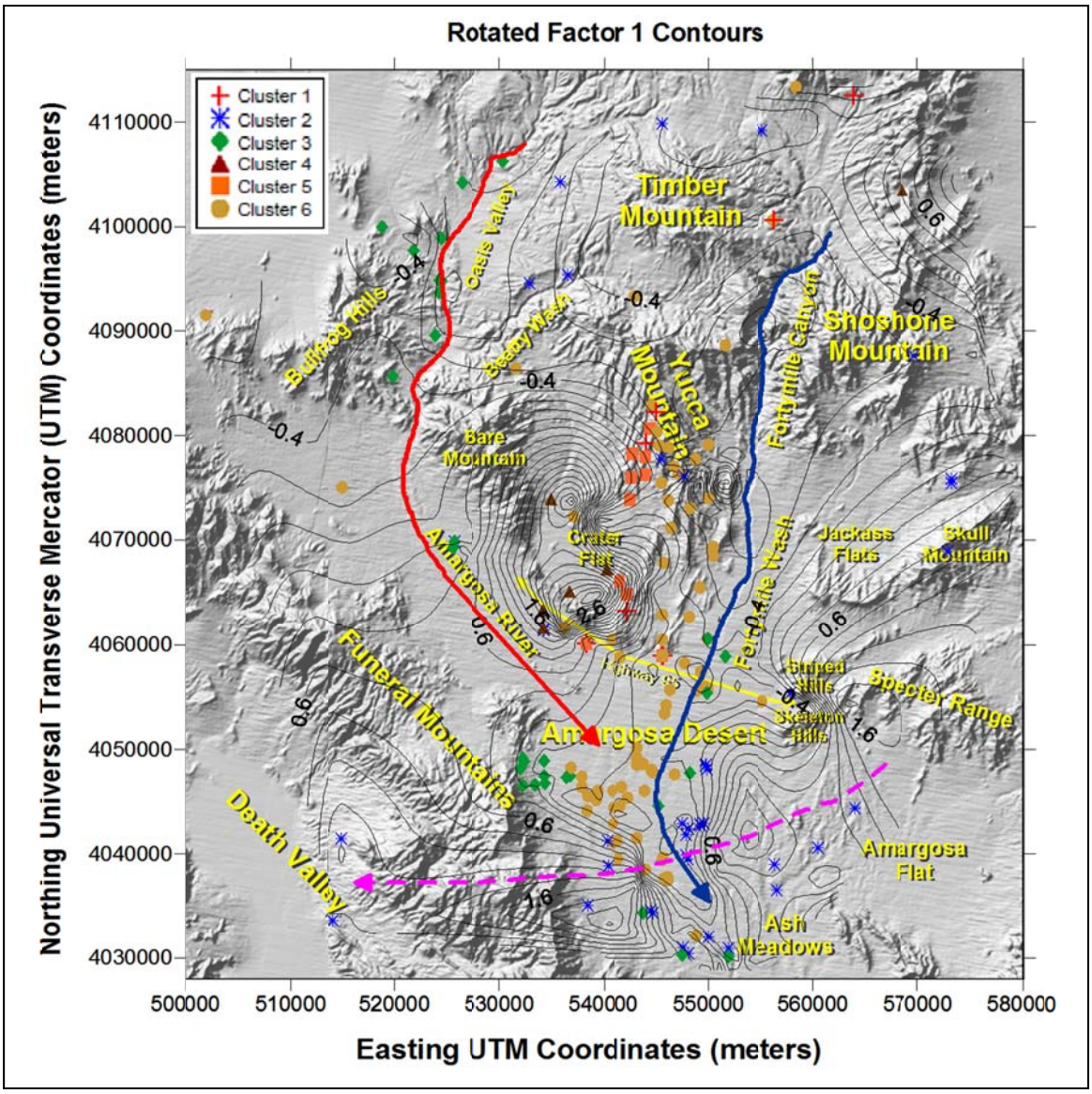

Figure 3.4: Principal component analysis factor 1 contours with sampling locations and sample group, and three suggested flowpaths overlain on a DEM.

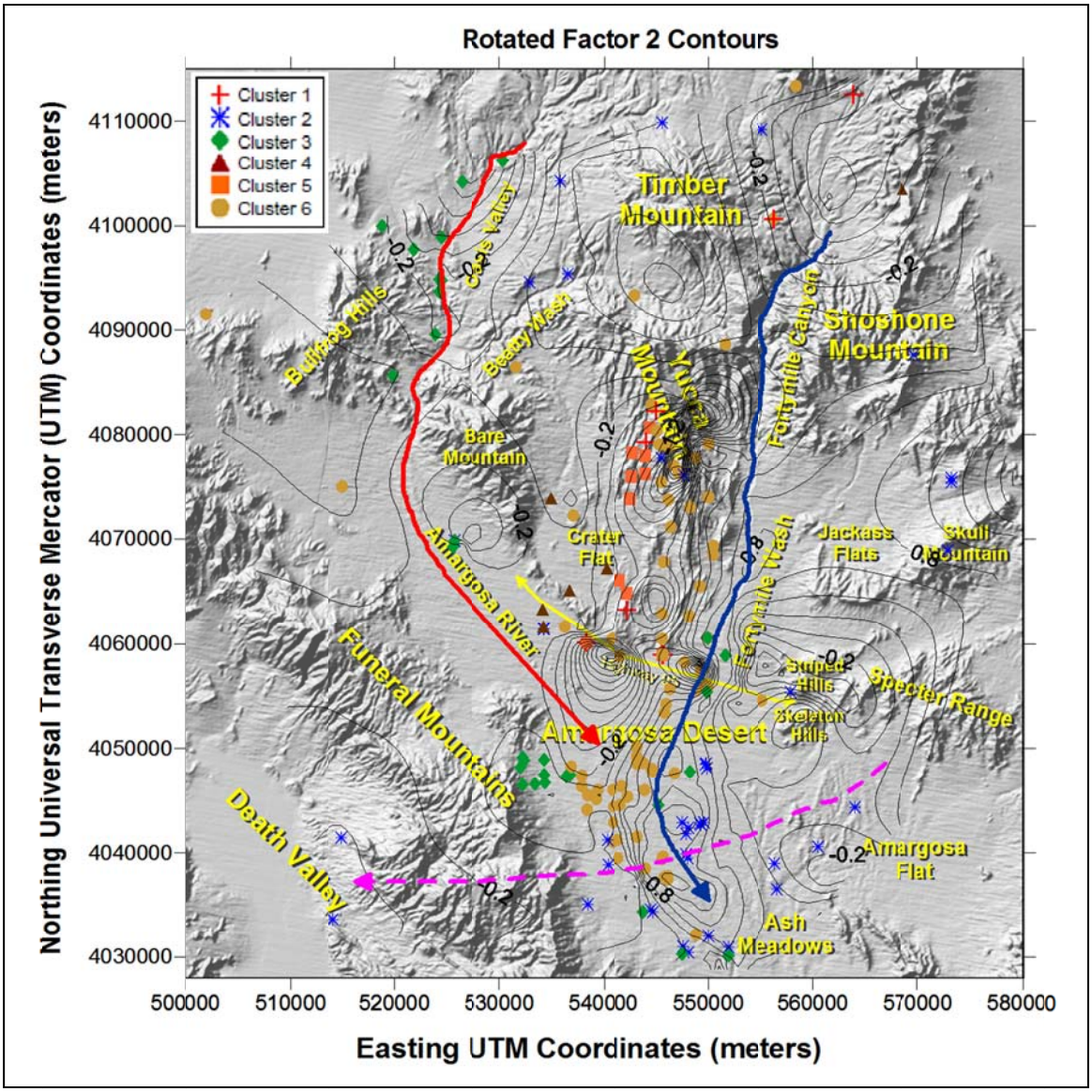

Figure 3.5: Principal component analysis factor 2 contours with sampling locations and sample group, and three suggested flowpaths overlain on a DEM.

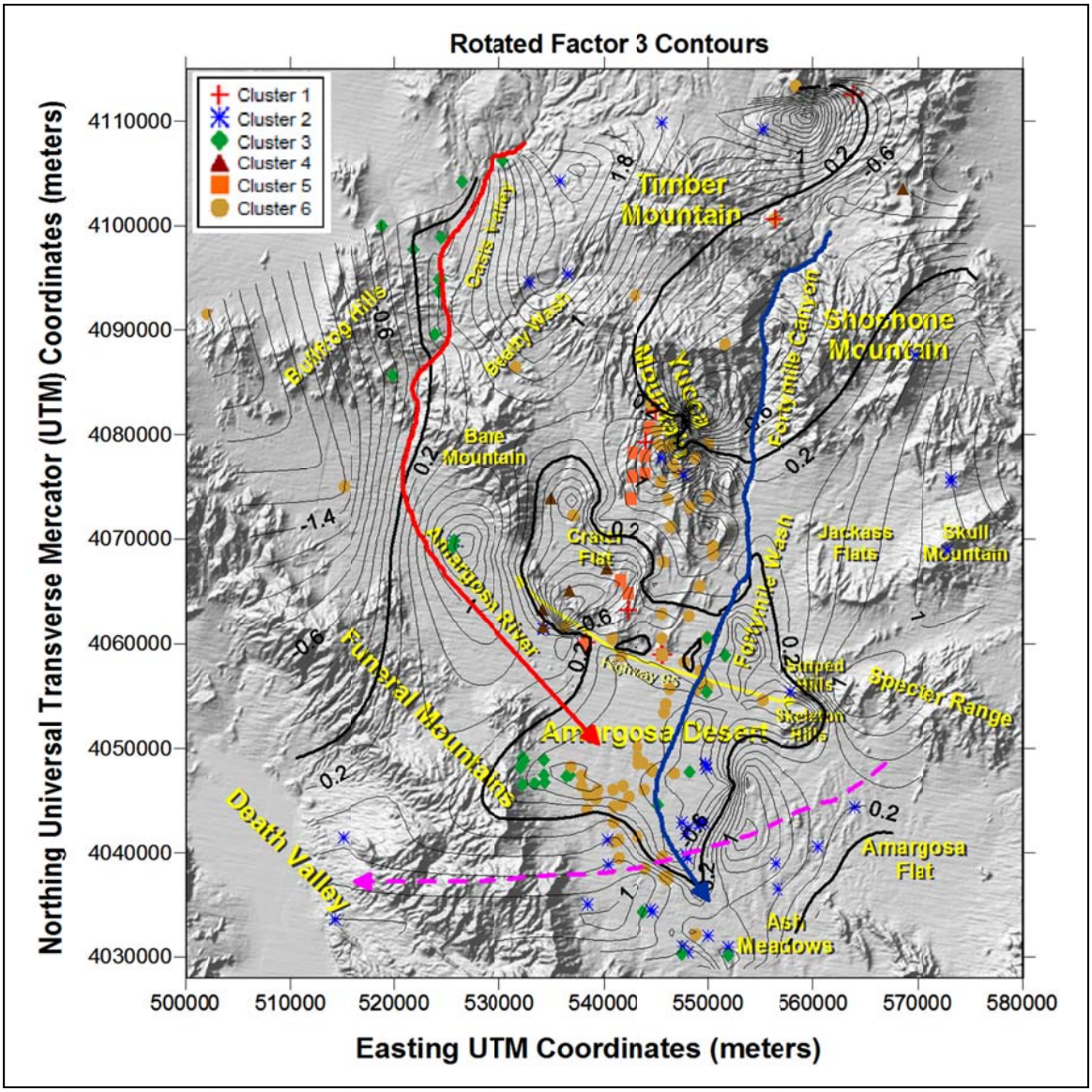

Figure 3.6: Principal component analysis factor 3 contours with sampling locations and sample group, and three suggested flowpaths overlain on a DEM.

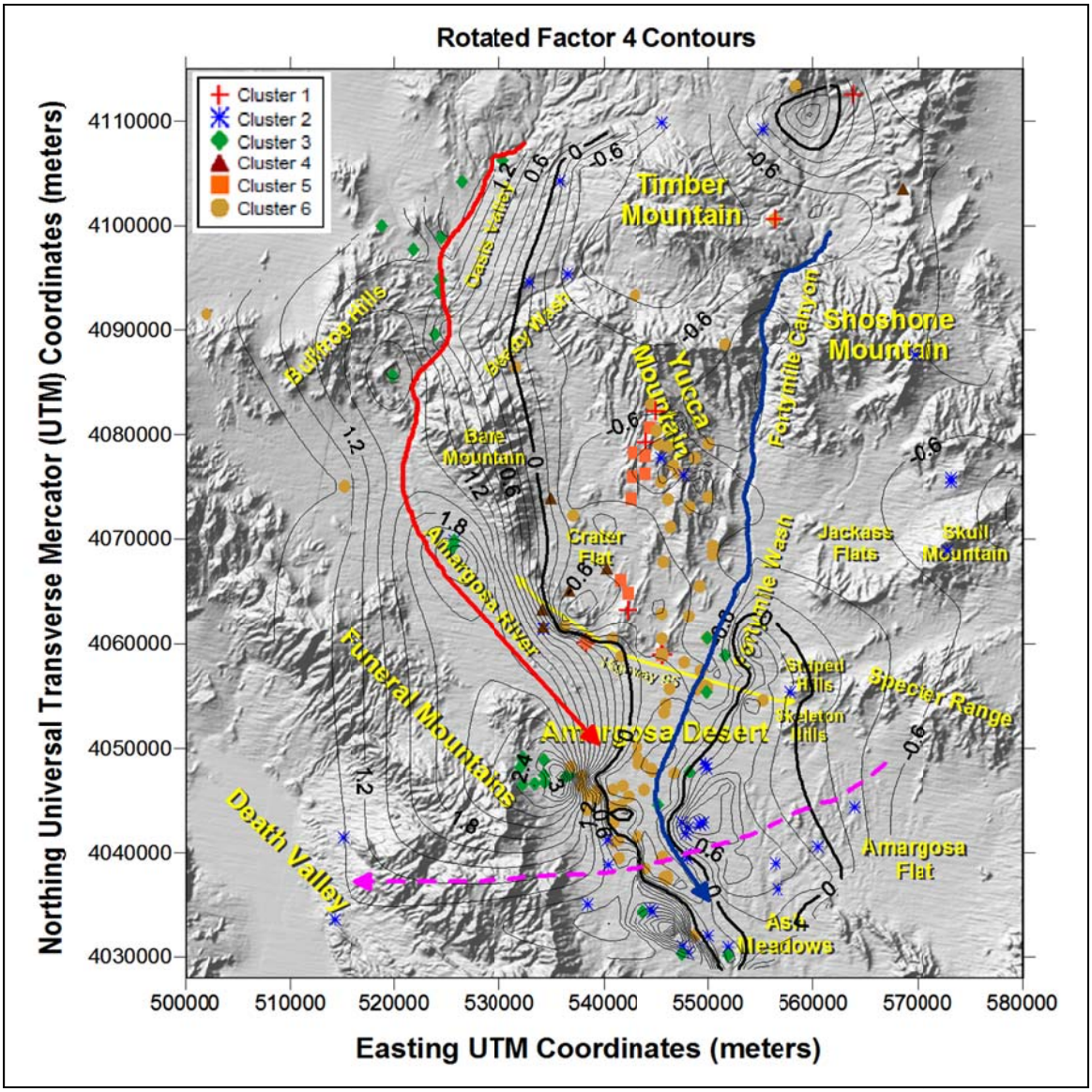

Figure 3.7: Principal component analysis factor 4 contours with sampling locations and sample group, and three suggested flowpaths overlain on a DEM.

3.5 SUMMARY AND CONCLUSIONS

The chemical speciation of the study area's groundwater indicates that free ion species represent more than 90% each of the elements Ca, Cl, F, K, Mg and Na in most of the analyzed groundwater samples. For the elements C, S and Si the dominant species are HCO_3^-; SO_4^{2-} and H_4SiO_4, respectively. Saturation indices indicate that the groundwater in the study area is undersaturated with respect to anhydrite, chrysotile, dolomite, fluorite, gypsum, halite, quartz

and sepiolite, oversaturated with respect to talc, and near saturation with respect to amorphous silicate, aragonite, calcite and chalcedony. The oversaturated minerals may precipitate and adversely affect the aquifer properties. Similarly, the undersaturated minerals, if present, will dissolve from aquifer rock during groundwater flow, which will increase its porosity and permeability. The minerals near saturation reflect thermodynamic equilibrium between the groundwater and the specified solid phase.

Principal component factor analysis and k-means cluster analysis applied to major ions, ion exchange, and SI describe the system through 4 factors, identify six hydrogeochemical facies, and allow the visualization of the processes that govern their evolution. In the factor analysis, factor 1 (29% of the variance) is dominated by Mg, alkalinity and Ca, whereas factor 2 (26% of the variance) is primarily composed of Cl, Na and SO_4. The remaining two factors explain 31% of the variance, dominated by Ca/Na ion exchange in the third factor and F^- in the fourth factor. Factor 1 differentiates clusters 1, 3, and 6 (low Ca–Mg values) from clusters 2 and 4. Factor 2 separates cluster 3 with high Cl–Na values from the other clusters. Factor 3 separates Na-dominated waters (clusters 1 and 5) from the other clusters. Factor 4 differentiates the three Ca–Mg–HCO_3 groups from each other on the basis of F^-. The *k*-means cluster analysis produced six groups, which are presented on biplots to separate the samples into four basic factors.

The spatial plots of factor-score contours delineate areas influenced by particular hydrochemical processes and indicate the direction of change in that process (perpendicular to the contour); they allow the exposition of hydrochemical signatures indicating groundwater flow paths and their interaction with the geologic media. Together, factor-score contours and hydrochemical facies indicate the three potential groundwater flow paths or signatures presented in Figures 3.4–3.7. The hydrochemical and statistical analysis shows that the first major flow

path of the study area's groundwater is beneath the Amargosa River, while the second one follows the trace of Fortymile Wash and its convergence with the Amargosa River. The third flow path is related to the trace of the Gravity Fault, Rock Valley and Death Valley. The signatures of major ion chemistry appear to be obtained near the region of infiltration, with little change along the flow paths. The high values of factor 1, which represent Mg^{2+} and Ca^{2+}, are located at Striped Hills, Skeleton Hills, and Crater Flat, which are downgradient of outcrops of the underlying carbonate aquifer. The high values of factor 2, which represent Cl^- and Na^+, are found near the Funeral Mountains, around Oasis Valley, and SE of Fortymile Wash. The high values of factor 3, representing $Ca^{2+}/(Na^+)^2$, are found at Ash Meadows, Crater Flat, Striped Hills, and Skeleton Hills, whereas low values are found at northern and southern Yucca Mountain and along its west face. Finally, the low values of factor 4, which correspond to low concentrations of F^- and low fluorite SI, are found encompassing Crater Flat, Striped Hills, and Skeleton Hills, whereas the high concentrations are found at Ash Meadows, Death Valley, and the west face of Yucca Mountain. The geochemical data support north-south flow along fractures that differs from the hydraulic gradient in the areas of clusters 1, 5 and 6. In the Ash Meadows area, which is near the edge of the study area, cluster 2 suggests a more east–west flow path. Based on the previous analysis, the study area's groundwater flows from north to south, following the traces of the Amargosa River and Fortymile Wash until they converge, and from east to west from Rock Valley (east of Skull Mountain), along the trace of Gravity Fault toward Death Valley. These results imply that contaminants could migrate from Yucca Mountain toward the Amargosa Valley, where groundwater is widely used for drinking water and crop irrigation.

ACKNOWLEDGEMENTS

Funding for this research was provided by Nye County through a grant from the US Department of Energy office of Civilian Radioactive Waste Management. We also thank the Center for Environmental Resource Management (CERM) of The University of Texas at El Paso for funding and support.

REFERENCES

Bushman, M., S. T. Nelson, D. Tingey, D. Egget (2010), Regional Groundwater Flow in Structurally-Complex Extended Terranes: an Evaluation of the Sources of Discharge at Ash Meadows, Nevada, J. Hydrol., 386, 118-129.

Eddebbarh, A.A., G.A. Zyvoloski, B.A. Robinson, E.M. Kwicklis, P.W. Reimus, B.W. Arnold, T. Corbet, S.P. Kuzio, C. Faunt (2003), The Saturated Zone at Yucca Mountain: an Overview of the Characterization and Assessment of the Saturated Zone as a Barrier to Potential Radionuclide Migration, J. Contam. Hydrol., 62–63, 477-493.

Flint, A. L., L. E. Flint, G. S. Bodvarsson, E. M. Kwicklis, and J. T. Fabryka-Martin (2001), Evolution of the Conceptual Model of Unsaturated Zone Hydrology at Yucca Mountain, Nevada, J. Hydrology, 247(2001), 1-30, pii: S0022-1694(01)00358-4.

Glynn, P.D., and L. N. Plummer (2005), Geochemistry and the Understanding of Groundwater Systems, Hydrogeology Journal, 13(1), 263-287.

Golden Software Inc. (2008), Surfer Version 8.09, Surface Mapping System, Golden, Colorado, <http://www.goldensoftware.com/>, (accessed 2008).

Hem, J. D. (1992), Study and Interpretation of the Chemical Characteristics of Natural Water, USGS Water Supply Paper 2254, < http://pubs.usgs.gov/wsp/wsp2254/> (accessed September, 2010).

Kelkar, S., P. Tseng, T. Miller, R. Pawar, A. Meijer, B. Robinson, G. Zyvoloski, E. Kwicklis, A.A. Eddebbarh, B. Arnold (2003), Site/Subsite Scale Saturated-Zone Flow-Transport Models for Yucca Mountain, International High- Level Radioactive Waste Management Conference, Las Vegas, Nevada. La Grange Park, Illinois: American Nuclear Society.

Kwicklis, E., A. Meijer, J.T. Fabryka-Martin (2003), Geochemical Inverse Model of Groundwater Mixing and Chemical Evolution in the Yucca Mountain Area, International High- Level Radioactive Waste Management Conference, Las Vegas, Nevada. La Grange Park, Illinois: American Nuclear Society.

LANL (Los Alamos National Laboratory) (2003), Regional groundwater hydrochemical data in the Yucca Mountain area used as direct input to ANLNBS-00021. LA0309RR831233.001.

Lawrence, F.W., S.B. Upchurch (1982), Identification of Recharge Areas Using Geochemical Factor Analysis. Groundwater 20 (6), 680-687.

Liu, B., F. Phillips, S. Hoines, A.R. Campbell, P. Sharma (1995), Water Movement in Desert Soil Traced by Hydrogen and Oxygen Isotopes, Chloride, and Chlorine-36, Southern Arizona, J. Hydrol., 168, 91-110.

Mellinger, M. (1987), Multivariate Data Analysis: its Methods, Chemom. Intell. Lab., Syst. 2, 29-36.

NWRPO (Nuclear Waste Repository Project Office) (2003), Geochemistry data files, Nye County, Nevada. < http://www.nyecounty.com> (accessed April 30, 2004).

OSTI (Office of Scientific and Technical Information, U.S. Department of Energy) (2000), Yucca Mountain facts at a glance. <http://www.osti.gov/bridge/purl.cover.jsp;jsessionid=869DF1CD6BF3193F9353D81F9B92D2AA?purl=/860320-0j7JQv/> (accessed February, 2010).

StatSoft Inc. (1984–2010), Statistica computer program manual for windows, Tulsa, Oklahoma, <http://www.statsoft.com/>, (accessed September 22, 2010).

Winterle, J.R., A. Claisse, H.D. Arlt (2003), An Independent Site-Scale Ground water Flow Model for Yucca Mountain, International High-Level Radioactive Waste Management Conference, Las Vegas, Nevada. La Grange Park, Illinois: American Nuclear Society.

Woocay, A., and J.C. Walton (2006), Climate Change Effects on Yucca Mountain Region Groundwater Recharge, International High-Level Radioactive Waste Management Conference, Las Vegas, Nevada. La Grange Park, Illinois: American Nuclear Society.

Woocay, A., and J. Walton (2008), Multivariate Analyses of Water Chemistry: Surface and Groundwater Interactions, Groundwater, 46(3), 437-449, doi:10.1111/j.1745-6584.2007.00404.x.

Chapter 4

Tracking the Chemical Footprint of Surface-Runoff Infiltration on Groundwater Recharge in an Arid Region

The material of this chapter was published in the 36th Annual Radioactive Waste Management Symposium, Phoenix, AZ, March 7-11, 2010, paper number 10454, vol. 5, p. 3621-3637, ISBN: 978-1-61738-797-5

4. Tracking the Chemical Footprint of Surface-Runoff Infiltration on Groundwater Recharge in an Arid Region

Omar M. Al-Qudah [a,*], John C. Walton [a], and Arturo Woocay [a, b]

[a] *Civil Engineering Department-Environmental Science and Engineering Program , The University of Texas at El Paso, 500 W University Ave, El Paso, TX 79968, USA.*

[b] *División de Estudios de Posgrado e Investigación, Instituto Tecnológico de Ciudad Juárez, Ave. Tecnológico 1340, Ciudad Juárez, CHIH 32500, MX.*

[*] *Corresponding author: Tel.:+1 915 422 4260; fax: +1 915 747 8037; omal@miners.utep.edu*

ABSTRACT

This research, as part of the Nye County Nuclear Waste Repository Project Office (NWRPO) attempts to provide new insight into the chemical evolution of southern Nevada's groundwater, its potential flow paths, infiltration rates, and surface-runoff processes, through initiating a surface-runoff sampling network. The sampling network tracks the chemical footprint of the surface-runoff water and groundwater recharging infiltration chemistry, by collecting baseline data through a long term study on a comprehensive suite of chemical parameters. These parameters include major ion chemistry, nutrients, trace elements, and stable isotope ratios. Multiple analytical methods are employed to analyze this data to develop a defensible groundwater chemistry monitoring network, down-gradient of Yucca Mountain, suitable for long-term performance confirmation monitoring. This study includes precipitation water chemistry, surface water runoff chemistry, soil chemistry, and groundwater chemistry in the study area. The field sampling and analyses provide the required chemical data for precipitation water, surface water runoff, and sediment analysis. The groundwater chemistry and isotopic data

administered by the NWRPO contain data from more than 200 wells that encompass the entire region. New methods were developed to control the construction and emplacement of the surface-runoff samplers. In addition, improved methods for the collection, field testing, and handling of precipitation water samples, surface-runoff water samples, and sediment samples were employed between the time the samples were gathered and chemical analyses obtained. The design and emplacement of sixty surface-runoff samplers at thirty separate locations is explained and a look at initial data is provided. It is our belief that long term data collection of this type will help us to better understand processes controlling groundwater recharge, and thus the sustainable yield of groundwater in Nye County.

4.1 INTRODUCTION

Natural tributaries in arid regions are generally ephemeral and the flow occurs intermittently during short, isolated periods separated by longer periods of low or zero flow; sustained flow is rare and baseflow is essentially absent (Sharma and Murthy, 1996). Peak flow rates occur within a few hours of the start of a rise (Sharma and Murthy, 1996). Normally, large volumes of surface-runoff water move into the ephemeral channel in a short period causing the flash flood characteristic of arid zone drainage basins, flash floods are usual hydrologic features of desert drainage (Fisher and Minckley, 1978). Drainage basins with high relief, a large percentage of land bedrock, sparse vegetation and shallow soils are particularly susceptible to flash flooding (Fisher and Minckley, 1978). Regularly, peak flow rates are reached almost immediately because the ephemeral flood wave forms a steep wave front, or the wall of water of legends, in its travel downstream (Jones, 1981; Pilgrim et al., 1988). Two mechanisms contribute to the formation of the wall of water of legends. First, rate of infiltration into the permeable dry streambed is highest at the wave front and decreases in the upstream direction, with the effect

that the leading edge of the wave steepens as it moves downstream (Fisher and Minckley, 1978). Second, the deeper portion of the flood wave near the peak travels faster than the leading edge of the wave, with the result that the wave peak approaches the front until the peak and front almost coincide and a shock front is formed (Sharma and Murthy, 1996).

Studies of the Amargosa Desert regional groundwater indicate that the groundwater recharge is occurring from streamflow in Fortymile Wash. Water quality studies have studied precipitation, surface water, and groundwater isotopic and common ion concentrations and concluded recharge water is entering the groundwater system north of Yucca Mountain from streamflow. Computer simulation of the groundwater system has determined that recharge from Fortymile Wash is a significant component of the water budget. Groundwater levels rise after streamflow events in Fortymile Canyon. Channel geomorphic studies indicate water is being lost from streamflow in the Yucca Mountain area. Several water chemistry studies have determined that streamflow in Fortymile Wash is a source of groundwater recharge. Claassen (1985) investigated common ion and isotope ages and concluded groundwater in the west central Amargosa Desert was recharged primarily from overland flow of snowmelt near the present day Fortymile Wash stream channel. White and Chuma (1987), investigated carbon and isotopic mass balances of the Oasis Valley-Fortymile Canyon groundwater basin and concluded groundwater in Fortymile Canyon may be from local origin. Benson and Klieforth (1989), investigated stable isotopes in precipitation and groundwater in the Yucca Mountain area and concluded groundwater recharge occurred by infiltration of cold-season precipitation, probably along the bottom of Fortymile Canyon.

Estimates of net infiltration from both the mean glacial transition and mean modern climates indicate that the largest infiltration rates occur along northwest-trending fault-controlled

washes on the north end of Yucca Mountain (Patterson, 2004; USGS, 2004). Water from the Eastern Yucca Mountain facies appears to be a mixture of water from the Timber Mountain area to the north and local recharge from the northwest-trending washes on the north end of Yucca Mountain (Patterson, 2004; USGS, 2004). Water from the Timber Mountain area does not appear to flow beneath the crest of Yucca Mountain and mix with water from the Western Yucca Mountain facies (Patterson, 2004; USGS, 2004).

This study explores the relationship between rainfall-runoff and groundwater chemistry, during a flash flood event in the Amargosa Desert Region, Nevada, and presents evidence of runoff chemical signature on the infiltration and groundwater recharge.

4.2 STUDY AREA

4.2.1 Description of the study area

The Amargosa Desert (Figure 4.1) is located in the southern portion of Nye County in south central Nevada, within the Great Basin, and is part of the Death Valley groundwater basin. The Funeral Mountains separate the Amargosa Desert from Death Valley to the southwest, and a series of mountain ranges bound the north and east extents of the desert. The Amargosa River is a major drainage component (over 8,047 km^2) of the unique closed-basin, hydrologic regime known as the Great Basin. This river system begins in the Oasis Valley, turns southeast to run through the Amargosa Desert, continues until it turns northwest, and terminates in Death Valley from its southeast extension. As a result of a dry, semi-arid, continental climate, the Amargosa River and its tributaries are ephemeral streams that are dry most of the time except in a few relatively short reaches where discharging springs maintain small, perennial base flows. Fortymile Wash and Beatty Wash (in addition to the Washes in Crater Flat and Rock Valley) are

the major tributaries of the upper Amargosa River, which drains through several small, populated areas downstream (Figure 4.1).

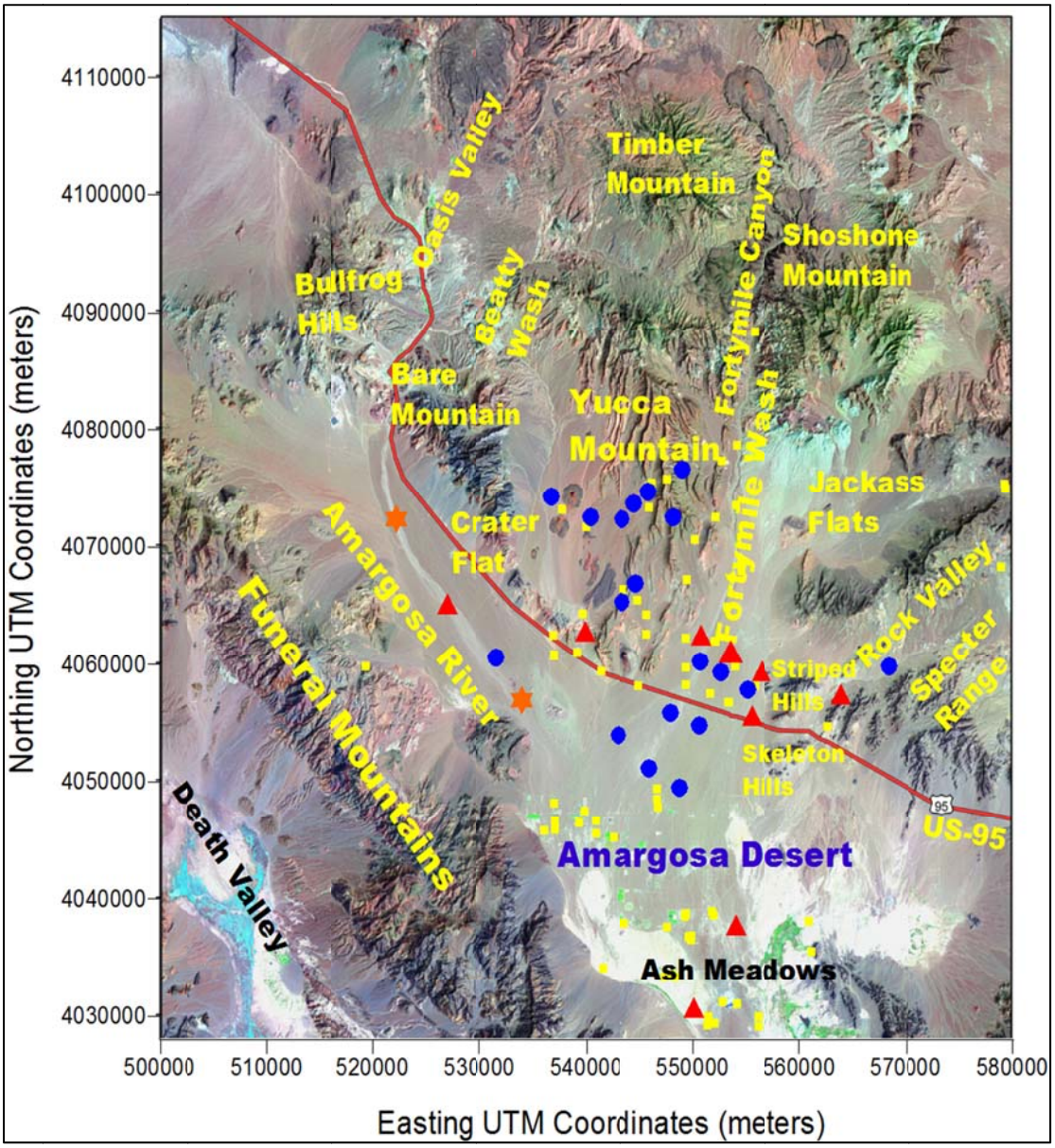

Figure 4.1: DEM map for the study area shows Locations of Amargosa Desert Region, Amargosa River, Yucca Mountain, and Fortymile Wash, Nye County, Nevada. Phase 1 site locations are shown in blue circles, phase 2 site locations are shown in red triangles, phase 3 site locations are shown in orange stars, and groundwater wells are shown in yellow squares.

Fortymile Wash originates between Timber Mountain and Shoshone Mountain. Fortymile Wash is an ephemeral drainage, flows southward along the east side of Yucca Mountain, and

fans out in the northern part of the Amargosa Desert just north of Highway 95. Near U.S. Highway 95, the Fortymile Wash channel changes from being moderately confined to several distributary channels that are poorly confined. This poorly-defined, distributary drainage pattern persists downstream to its confluence with the Amargosa River. Yucca Mountain is located on federal land in southern Nevada, north of the Amargosa Desert, approximately 160 km northwest of Las Vegas, in the Basin and Range province of the western United States, within a zone between the Mojave Desert and the southern boundary of the Great Basin Desert, and it's part of the Amargosa River drainage basin which is the major tributary drainage area to the Death Valley. Yucca Mountain has been chosen by the U.S Department of Energy as a potential site of a geologic repository for long term storage of the Nation's high-level nuclear waste, and it is expected to hold approximately 70,000 metric tons of radioactive waste, and will remain the proposed site to hold this waste until time as congress change the nuclear waste policy act. The present climate in the Amargosa Desert region is considered arid to semiarid, with average annual precipitation ranging from less than 130 millimeters (mm) at lower elevations to more than 280 mm at higher elevations (Flint et al., 2001).

4.2.2 Runoff history in the study area

Precipitation associated with a weather disturbance moving eastward from California has caused the most extensive regional runoff in Fortymile Wash and Amargosa River since February 1969 (Beck and Glancy, 1995). The 1969 flood was the largest known in the Amargosa River system during the previous 25 years. Flow in Fortymile Wash was first documented during site-characterization studies in March 1983. The Wash had flow again three times during July and August 1984 as the result of severe but localized convective storms. The first runoff documented case during site-characterization studies was the runoff of March 9-11, 1995 (Beck

and Glancy, 1995), where Fortymile Wash and Amargosa River flowed, simultaneously throughout their entire Nevada reaches. Preliminary data reported for selected U.S. Geological Survey's (USGS) rain gages around nuclear tests site boundaries and within Amargosa Desert area showed that cumulative precipitation ranged from about 51 to 152 mm during March 9-11, 1995 with the larger amounts falling at the higher-altitude sites (Beck and Glancy, 1995).

4.3 PREVIOUS STUDIES

Fisher and Minckley (1978) described the change in selected chemical parameters during a single flash flooding event on Sycamore Creek, Arizona. Although floods are often viewed as dilution phenomena in terms of dissolved substances, in which low conductivity rainwater dilutes groundwater or spring water that are rich in dissolved salts, they observed that the dilution effects are partially offset by increased leaching and dissolution of solutes from newly exposed rock and soil minerals accumulated salt crusts, and from suspended particles. They noted that the major anions, bicarbonate, and conductivity followed a dilution pattern. Nitrate, phosphate and iron varied widely through the cycle, and generally increased over levels recorded at base flow. They attributed the increased concentrations of nitrate as discharge increased to leaching from the ephemeral stream beds and surrounding lands, and suggested that surface-runoff contributed few nitrates to streams but yielded significant amounts of phosphate from high concentrations of particles in the water.

Savard (1994) and Savard et al. (1994) presented the first hydrologic time series evidence for groundwater recharging in Fortymile Wash watershed, which had been hypothesized by previous water quality and regional groundwater studies, after five separate streamflow event periods happened in the Pah and Fortymile Canyons of Fortymile Wash approximately 10 km from Yucca Mountain during 1992-1993. Savard explained the source of groundwater recharge

as a streamflow infiltrating through the streambed sediments and the under-laying alluvial material. In 1998 Savard estimated the volumes of streamflow, streamflow infiltration loss, and groundwater recharge rate for four reaches of Fortymile Wash near Yucca Mountain (Fortymile Canyon, upper Jackass Flats, lower Jackass Flats, and Amargosa Desert) based on streamflow data from continuous streamflow gauging stations, crest-stage gages, and miscellaneous sites during 1969-1995 and depth-to-water data in boreholes from 1983-1995. He concluded that the Amargosa Desert reach had the highest groundwater recharge rate, 64,300 m^3 per year. The Fortymile Canyon reach had a lower rate, 27,000 m^3 per year, even though it had more frequent steamflow. The lower Jackass Flats reach had the third highest groundwater recharge rate, 16,400 m^3 per year. The upper Jackass Flats reach had the lowest groundwater recharge rate, 1,100 m^3 per year. The greatest depth to the water table, 100 to 350 m, of all the reaches was probably the biggest reason for very little recharge in the upper Jackass Flats reach.

In 2001 USGS developed conceptual and numerical models of net infiltration for Yucca Mountain and the surrounding Death Valley region. The conceptual model describes the effects of precipitation, surface-runoff and runon, evapotranspiration, and redistribution of water in the shallow unsaturated zone on estimated rates of net infiltration (USGS, 2001), The numerical model simulated net infiltration ranging from zero, for a soil thickness greater than 6 meters, to over 350 mm per year for thin soils at high elevations in the Spring Mountains. Estimated average net infiltration over the entire model domain is 7.8 mm per year (USGS, 2001).

Lemoine and others (1995) discussed a proposed methodology for the implementation of a monitoring tool for surface water run-off in (semi-) arid areas, by using integrated remote sensing and GIS techniques in order to develop alternative sources of drinking water and industrial water supplies.

Flint et al. (1996) presented a summary of methods used to estimate the quantity of water percolating below the root zone on Yucca Mountain. Estimates of annual average percolation range from 0 to 6.5 mm per year. It is generally agreed that the greatest amounts of net recharge occur where shallow soils overlie fractured bedrock and that little or no deep percolation occurs in deep colluviums and alluvium (Woolhiser, 2000).

Woocay and Walton (2008) calculated the infiltration dates before present and pore velocities for four boreholes in the unsaturated zone near Yucca Mountain by applying a chloride mass-balance method. They observed, from pore velocities, two distinct slopes corresponding to different infiltration regimes. The first one, near the surface, presents the slowest infiltration rate indicating that, over the recent past, infiltration has been negligible at these locations. The second pore velocity corresponds to a past wetter period (late Pleistocene to early Holocene) with much higher pore velocities. The borehole nearest Fortymile Wash exhibits the highest pore velocities, whereas boreholes farther from the wash demonstrate lower velocities. They considered that the most dilute groundwater is present beneath Fortymile Wash, not beneath the mountains, suggesting that runoff infiltration is the dominant form of recharge in the region. They concluded that the younger and fresher groundwater beneath Fortymile Wash is the result of significant lowland infiltration due to accumulated surface-runoff occurring in localized areas such as the wash.

The present research attempts to provide new insight into the chemical evolution of southern Nevada's groundwater and its potential flow paths and rates during the infiltration and surface-runoff processes, through initiating a surface-runoff sampling network to track the chemical footprint of the surface-runoff water on the groundwater recharging and infiltration chemistry, by collecting a baseline data through a long term study on a comprehensive suite of

chemical parameters. Multiple analytical methods are created to analyze these data to develop a defensible groundwater chemistry monitoring network, down-gradient of Yucca Mountain, suitable for long-term performance confirmation monitoring.

4.4 METHODS

4.4.1 Site locations selection

The site locations were selected to include the major ephemeral streams that are tributaries the Amargosa River, and are surrounded by Nye County wells and boreholes (the yellow squares in Figure 4.1). The study plan is divided into three phases, Phase 1 was in January 2009 and includes 19 site locations (the blue circles in Figure 4.1), Phase 2 was in Feb. 2009 and includes nine site locations (the red triangles in Figure 4.1), where Phase 3 includes two site locations (the orange stars in Figure 4.1) and was in September 2009. In total, 60 surface-runoff samplers were installed in 30 different site locations in the vicinity of the Amargosa Desert Region.

4.4.2 Surface-runoff samplers (SRSs) design and construction

SRSs were designed to collect the soil water to measure the chemical characteristics of runoff water that has leached (infiltrated) through the soil profile. The construction started by threading flexible polyethylene tubing through a hole made about 25 mm below the top edge of the 9.5-liter bucket as shown in Figure 4.2a, to provide an access to the inside of the SRS once it is buried. The inner edge of the tubing was fixed to the bucket bottom with an epoxy adhesive, and the outer end blocked with a plug to prevent clogging the tubing. The completed devices were soaked in tap water for 24 hours before rinsing with distilled water to leach potential contaminants from the materials. In order to wash the silica sand to prevent the sand from

chemically influencing the collected water, an array of holes was drilled in the bottom of one of the 19-liter buckets with a 1.6-mm bit (Figure 4.2b). A volume of 9.5 liter of sand filled in the meshed bucket and 19 liter of deionized water were poured on top of sand. After about 5 minutes, 3.8 liter of distilled was water poured into the sand-filled buckets.

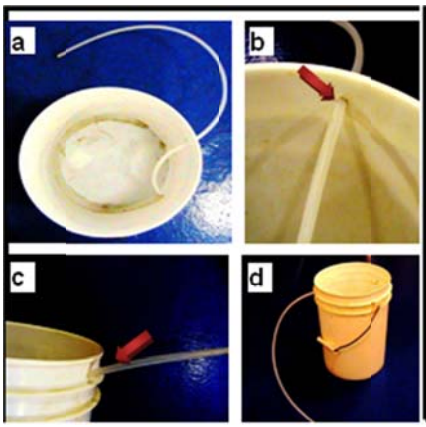

Figure 4.2a **Figure 4.2b**

Figure 4.2a: Photographic sequence of SRS construction: a. shows the 6.35-mm outer diameter polyethylene tubing glued to the bottom of the bucket, b. and c. show the tube exiting the device, and d. shows the finished device.

Figure 4.2b: Photographic sequence of the washing sand protocol: a. Two 19-liter buckets were needed; bucket #2 is graduated to 19 liter; b. Mesh of holes drilled 25.4-mm by 25.4-mm with a 1.6–mm bit; c. The meshed bucket filled with 9.5 liter of the sand; d. Bucket #2 filled with 19 liter of deionized water to rinse bucket #1; e. 3.8 liter of deionized water poured; f. 10 ml collected of the residual rinsed water and the conductivity measured (the conductivity of the last rinse outflow should be <0.1 µS/cm).

4.4.3 Field emplacement of SRSs

Each arroyo that was selected as a sampling location has two samplers a) one filled with washed sand and b) a second sampler filled with alluvial material (sand and silt) from the arroyo. The devices were placed at locations in surface-runoff channels where water is likely to pool and where sufficient depth of sediment facilitates digging a hole for emplacement. The samplers were placed in a low gradient (depositional) portion of the arroyo to the extent possible to

prevent washing out during storms. The emplacement procedure for both washed sand filled samplers and alluvial material filled samplers was the same with a few exceptions detailed in the following:

1. Upon selection of a site for each SRS, approximately 3 liter of alluvial materials was collected in a test bucket after recording the observed sediment moisture. These materials were passed through a No. 4 (4.75 mm) sieve, according to ASTM standards (ASTM D422-63, 1998), and 2 liter of the sieved material was collected in 2-liter sized wide-mouth HDPE bottles. The initial water content of the sediment was determined in the lab according to ASTM standards (ASTM D-2216, 1998). The collected sediment was extracted in the lab according to ASTM standards (ASTM D4542, 1995), by mixing 2 kg of sediment with 3 liter of distilled water and the mixture left over night to settle, after that the leachate was separated, filtered, poured in to 2-liter wide mouth HDPE, and stored in a refrigerator for shipping later to the laboratory for analysis. Latex gloves must be worn during the emplacement process to avoid contaminating the sampler with sweat.

2. A hole was dug at the selected locations within the arroyos, and the excavated dirt placed downstream of each hole.

3. The depth of the hole was tested by using an additional bucket called the test bucket that has the same size as the sampler bucket. The test bucket was placed in the hole and the depth was tested by moving a straight edge laid on the surrounding undisturbed surface over the top of the sampler. For an ideal fit, the top of the sampler was 25-50 mm below the undisturbed surface of the arroyo.

4. When an adequate depth was reached, the test bucket was removed and the earth was leveled beneath it to provide a stable base.

5. 5a below followed for the washed sand samplers and 5b for the alluvial material samplers.

   5a. half of the SRSs were filled with the 8/12 washed sand. The lid was placed on the top of each sampler to check the depth and the level again. The previously removed alluvial material from the hole was used to backfill around the sampler within 25-50 mm of the top, and after removing the lid of the sampler the remaining space to the surface was backfilled with washed sand, and the area brought back up to grade with the undisturbed arroyo surface.

   5b. the second half of the SRSs (alluvial material samplers) were placed about 1.5-2.0 m down gradient of the washed sand samplers. If the arroyo width was 5 m or wider, the washed sand sampler and alluvial sampler was placed cross gradient. Over the sampler tubing intake washed silica sand was layered (filter pack) to further prevent entry and clogging of the hole. After that, the sampler was filled with the alluvial material. The bucket and bucket sides were backfilled with alluvial material and the area was brought back up to grade with the undisturbed arroyo surface.

6. The upper end of the sampling tube was sealed with a cap (ear plug), and the sampling tube was buried underneath the ground level to prevent sun (UV) damage.

7. T-post (fence post) was painted at the top and was pounded on a flank of the wash to prevent it from being washed away during a storm. The T-post will identify the site and serve as the mount for the rain gauge.

8. The rain gauge was mounted about 25 mm above the top of the T-post.

9. The coordinates of the SRS location were recorded by using a Trimble® GeoXH unit that has high accuracy In addition the distance and direction were recorded between the two samplers and from the T-post to the washed sand sampler and the alluvial sampler.

4.4.4 Precipitation monitoring in the study area

Mathematica[7] software is used to monitor the weather data from the Amargosa Desert Region, in order to decide if a storm is strong enough to create surface-runoff in the area or not. Using Mathematica[7], two weather stations (KDRA and KBJN) in the Amargosa Desert Region are monitored daily. These stations provide data for temperature, pressure, humidity, wind speed, and the precipitation rate.

4.5 RESULTS

4.5.1 Surface-runoff sampling and samples chemical analysis results

Two storm events occurred in the study area after the installation of the samplers, the first one was in the period of February 10-12, 2009, and the second one was during February 17-18, 2009. The accumulated water level in the rain gauges was registered as shown in Table 4.1.

In order to decide if the amount of water stored in the samplers after the storm events is enough to analyze all the chemical parameters (the major anions and cations, dissolved metals, nutrients, alkalinity, stable isotope ratio analysis of water, tritium, pH, EC, TDS, temperature, and stable isotope ratio analysis of carbon in total dissolved inorganic carbon) sample volume is compared to ACZ laboratory requirements (Table 4.2). The total amount of water required to analyze all parameters is 2030 ml. A simple model was developed to predict sample volume

based on the hydrological properties of the silica sands and the alluvial sands (i.e. sand porosity, specific yield, and specific retention), sampler dimensions, rainfall rate, and the thickness of the layer that lies above the tubing hole's entrance into the sampler.

Assuming the sediment around samplers is saturated and there is no evapotranspiration, for both types of samplers Equation 4.1 is designed to calculate the water level in the sampler, and Equation 4.2 is designed to calculate the water volume in the sampler:

$$\boldsymbol{H = \frac{R - (Sr \times C)}{n}} \qquad \boldsymbol{Eq.4.1}$$

$$\boldsymbol{V = \pi \times (\frac{D}{2})^2 \times H \times (n - Sr) \times 0.001} \qquad \boldsymbol{Eq.4.2}$$

where,

H: water level in sampler, mm

R: rain gauge reading, mm

Sr: Specific retention, dimensionless

C: layer covers thickness, mm

n: porosity, dimensionless

V: water volume in sampler, liter

D: sampler average diameter, mm

The estimated amount of water accumulated in the washed sand filled buckets is obtained by the substituting values of porosity (Fetter, 2001; Weight, 2008), specific retention (Fetter, 2001; Weight, 2008), rainfall amount, sampler average diameter, sampler depth, and the thickness of the layer that cover the sampler, in the Equations 4.1 and 4.2. Measured and estimated amounts of water obtained from the sampling process are shown in Table 4.1 below.

Table 4.1: The Estimated and the Measured Amount of Water Accumulated in the Washed Sand Filled Buckets and the Rainfall Observations during the Period of 2/10-18/2009.

Bucket filler hydrological properties			Estimated amount of water in the washed sand filled bucket			Measured amount of water in the washed sand filled bucket (Liter)
Specific Retention (Sr)			0.075			
Depth of bucket (mm)			210			
Average diameter of bucket (mm)			216			
Porosity (n)			0.38			
Thickness of the cover layer(mm)			50.4			
SRS Location	Elevation (m)	Cumulative rain gauges precipitation (mm) during the period 02/10-18/2009	Volume (Liter)	% Full	Depth (mm)	Volume (Liter)
SRS-6A	820.68	33	0.86	37%	77	1.45 ± 0.05
SRS-6B	818.81	30	0.77	33%	68	2.00 ± 0.05
SRS-7A	805.35	27	0.68	29%	60	1.55 ± 0.05
SRS-7B	799.05	29	0.75	32%	67	1.82 ± 0.05
SRS-8A1	761.29	27	0.68	29%	60	0.70 ± 0.05
SRS-8A2	763.45	27	0.69	29%	61	0.97 ± 0.05
SRS-8B	765.06	30	0.79	33%	70	1.30 ± 0.05
SRS-9	904.14	37	0.98	41%	87	0.80 ± 0.05
SRS-10	899.23	48	1.31	56%	117	1.01 ± 0.05
SRS-11	1212.12	52	1.43	61%	127	2.24 ± 0.05
SRS-14A	1095.85	46	1.24	53%	110	1.99 ± 0.05
SRS-14B	1115.96	48	1.31	56%	117	1.82 ± 0.05
SRS-14C	1149.69	50	1.35	57%	120	1.50 ± 0.05
SRS-15	815.08	32	0.83	35%	74	2.10 ± 0.05
SRS-17	967.32	41	1.09	46%	97	0.70 ± 0.05
SRS-18	960.61	42	1.13	48%	100	1.35 ± 0.05
SRS-19	1154.89	53	1.46	62%	130	2.10 ± 0.05
SRS-20	782.77	32	0.83	35%	74	1.25 ± 0.05
SRS-21	912.74	23	0.56	24%	50	0.80 ± 0.05

In Figure 4.3, cumulative precipitation was plotted versus the elevation of SRS locations (Table 4.1). It is clear in the figure that precipitation increased with elevation. This agrees with previous literature results that indicate that the rainfall rate in the Yucca Mountain is higher than that in the Amargosa Desert. This will increase the chances of surface- runoff on the mountain sides.

Prior to the sampling process the chemical parameters were ordered based on their importance in this study (Table 4.2). Table 4.2 includes all the required information to deal with the samples during sampling, storage, and shipping based on the standard methods for the examination of water and wastewater (Clescerl et al., 2000). When limited amounts of water are available, samples are allocated according to the priority list.

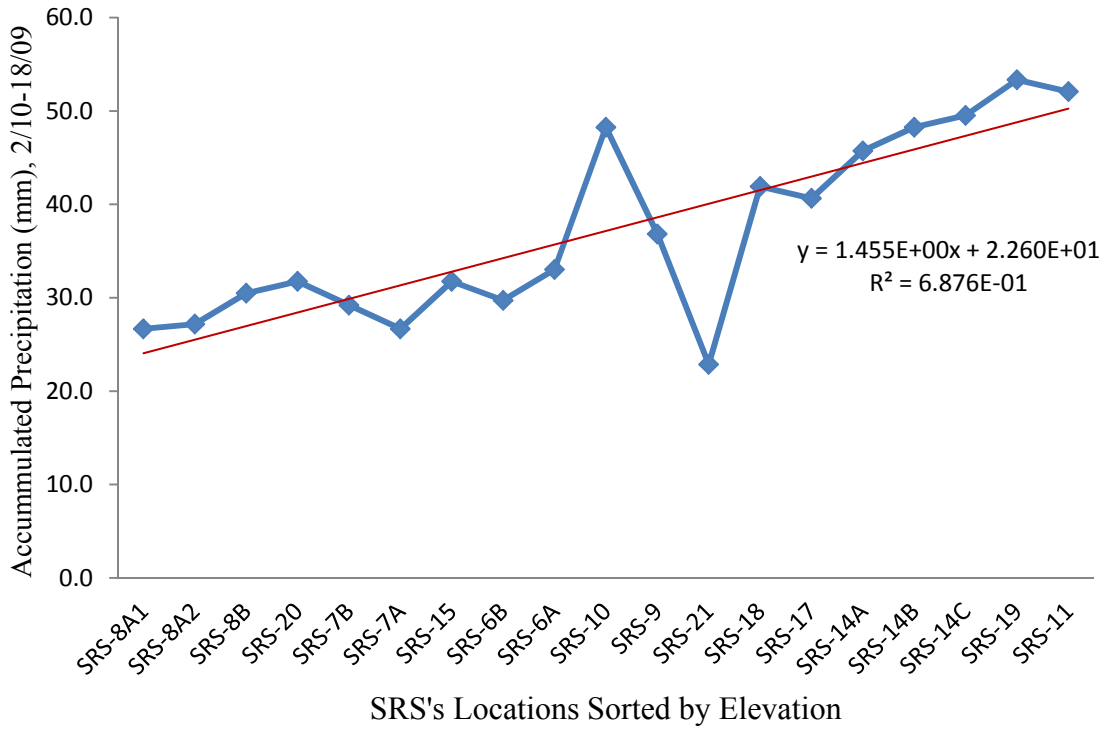

Figure 4.3: The relationship between the cumulated rain gauges precipitation and runoff sampler's elevation.

According to the calculated results (Table 4.1) that were obtained after the February 10-18, 2009 storm events, the estimated water volume in the washed sand samplers was sufficient to analyze the first six priorities in Table 4.2, and very little water could be pumped from the alluvial sand samplers insufficient to do any analysis. We decided to collect the samples during the period of February 24-28, 2009, after sufficient precipitation had occurred to provide adequate sample size for chemical analysis.

The sampling session included all the SRSs that were installed. Samples were collected from each of the devices for the laboratory analyses listed in Table 4.2, in order listed under the priority column. Subsequent to arrival at each location the cap was removed from the tube, and the peristaltic pump was attached where the direction of flow was from bottom to top. The first 25 ml of sample was purged. After purging was complete, the requested water samples were collected in the specified order (Clescerl et al., 2000). Prior to collecting samples requiring filtering from each sampling location, a clean piece of silicone tubing was installed on the peristaltic pump along with a new large-capacity 0.45 micron filter on the discharge end of the tubing based on the standard methods for the examination of water and wastewater (Clescerl et al., 2000). After sampling was completed, the remaining water (if any) from the SRS was purged to provide space for collection during the next runoff event.

Table 4.2: Sample Collection in Order of Priority, Storage, and Shipping Information.

Analyte Priority	Sample Type	Filter (Yes/No)	Fill Level	Preservative	Typical Bottle Size (ml)	Bottle Type[3]	Type of Storage	Shipping Instructions
1	pH, EC,TDS, Temp.	No	30 ml	None	50	HDPE	Analyzed in field	None
2	Alkalinity, Anions	Yes	Fill completely	None	250	HDPE	refrigerate	Ship with Cold Packs
3	Metals, Cations	Yes	Fill completely	HNO_3	250	HDPE	refrigerate	None
4	N-NH3,NO3-NO2,total P	Yes	To the neck	H_2SO_4	250	HDPE	refrigerate	Ship with Cold Packs
5	Stable Isotope Ratio Analysis of Oxygen and Hydrogen in Water	No	To the neck	None	25	HDPE	refrigerate	None
6	Stable Isotope Ratio Analysis of Carbon in Total Dissolved Inorganic Carbon; Radiocarbon (C-14)	No	To the neck	NaOH	1,000	HDPE	refrigerate	Ship with Cold Packs, Tape Seal Around Cap
7	Tritium[1]	No	To the neck	None	250	A. Glass	refrigerate	Wrap in Bubble Wrap
8	Remaining Volume in RSD[2]	No	NA	None	NA	HDPE	refrigerate	Ship with Cold Packs

[1]Tritium analysis requires a detection limit of 1 TU and shall only be collected from the washed sand buckets, [2]If water remains in SRS, the remaining volume shall be collected and analyzed as specified, [3]Sample bottles shall be of the appropriate size/type and contain preservatives as specified by the analytical laboratory.

Table 4.3 summarizes the first priority results that were obtained after the end of the sampling process. All the natural alluvial samplers failed to produce water, all the water in the alluvial samplers is bound by the alluvium and failed to gravity drain. In contrast, all the washed sand samplers had stored water in different amounts, where the maximum amount was in the sampler that installed in site SRS-11, 2.24 liter, and the minimum amount was in the samplers at sites SRS-8A1 and SRS-17, 0.70 liter (Table 4.1). The first priority for all collected samples was done in the field (Table 4.3). During the sampling process we noted that the water in all the rain gauges in site locations had evaporated. Surface-runoff samples were analyzed for the major anions and cations by ACZ Laboratories, Inc.

Table 4.3: First Priority Results of Surface-Runoff Sampling.

	Washed Sand Filled Bucket						
Location	Date	Time 24H	Water Amount (Liter)	pH	Temp. °C	EC (µS/cm)	TDS (ppm)
SRS-6A[1]	2/25/09	1625	1.45 ± 0.05	6.57	19.20	148.9	75.2
SRS-6B[1]	2/25/09	1535	2.00 ± 0.05	6.88	24.40	86.4	43.4
SRS-7A[1]	2/26/09	1010	1.55 ± 0.05	6.54	20.40	136.6	68.8
SRS-7B[1]	2/26/09	1102	1.82 ± 0.05	7.30	20.80	422.0	213.0
SRS-8A1[2]	2/26/09	1209	0.70 ± 0.05	6.54	23.20	141.3	71.10
SRS-8A2[1]	2/26/09	1240	0.97 ± 0.05	6.60	23.20	158.5	79.8
SRS-8B[1]	2/26/09	1136	1.30 ± 0.05	6.77	23.00	178.5	90.5
SRS-9[1]	2/26/09	1520	0.80 ± 0.05	6.70	14.40	173.1	86.3
SRS-10[1]	2/26/09	1459	1.01 ± 0.05	6.62	21.80	146.6	74.1
SRS-11[1]	2/25/09	1425	2.24 ± 0.05	6.55	23.60	68.7	34.7
SRS-14A[1]	2/27/09	1106	1.99 ± 0.05	6.65	14.10	114.4	58.9
SRS-14B[1]	2/27/09	1136	1.82 ± 0.05	6.88	14.60	131.2	65.9
SRS-14C[1]	2/25/09	1320	1.50 ± 0.05	6.77	32.40	77.0	38.9
SRS-15[1]	2/25/09	1012	2.10 ± 0.05	6.47	21.20	75.2	74.1
SRS-17[1]	2/27/09	1002	0.70 ± 0.05	6.71	17.90	118.4	59.3
SRS-18[1]	2/27/09	1035	1.35 ± 0.05	6.86	16.70	131.3	65.6
SRS-19[1]	2/27/09	1207	2.10 ± 0.05	6.63	19.70	113.7	57.8
SRS-20[1]	2/26/09	1353	1.25 ± 0.05	6.65	20.00	174.5	87.9
SRS-21[1]	2/26/09	1640	0.80 ± 0.05	6.36	12.40	172.8	84.7

[1]Silica sand saturated, [2]Silica sand saturated but there was no enough water for tritium analysis.

Figure 4.4 shows an interesting match between the average major anions and cations for groundwater in green line (triangle symbol) and surface-runoff in blue line (circle symbol), where the average precipitation major anions and cations in red line (square symbol) has a different trend. Groundwater chemistry data used herein were obtained from the NWRPO website as of March 2003 (NWRPO, 2008) and a Los Alamos National Laboratory report (LANL, 2007), whereas the precipitation chemistry data were taken from Stetzenbach (1994) and Meijer (2002). Long-term monitoring of these parameters in addition to the multiple analytical methods and infiltration modeling that will be applied may clarify the infiltration and groundwater recharge chemistry in the Amargosa Desert Region.

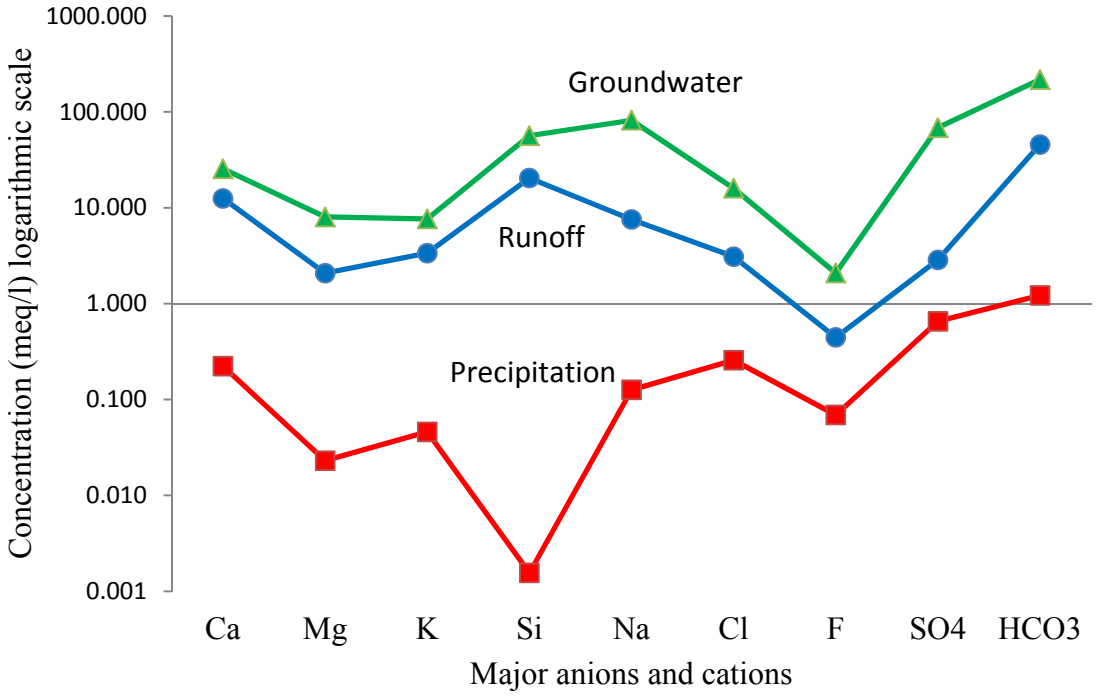

Figure 4.4: Average concentration of major anion and cations of groundwater, surface-runoff, and rainfall.

4.6 CONCLUSIONS

Studies of Amargosa Desert regional groundwater indicate that infiltration of surface-runoff occurs in the valleys subsequent to runoff-producing storms and this infiltration represents a large portion of the groundwater recharge. Sampling of surface-runoff in a desert environment from ephemeral arroyos is complicated by a number of practical concerns. Surface-runoff events are uncommon, sometimes separated by gaps of more than a year, and difficult to forecast in advance.

This study presents a modification to the lysimeter called "Surface-Runoff Sampler (SRS)" designed to provide a stronger collection surface, more efficient connections for sample collection, and to measure particularly the first flush of runoff. In the absent of runoff a SRS acts as lysimeter. SRS design has the advantages of low cost, low maintenance, and being long lived. Disadvantages are that it captures both precipitation and runoff and requires manual pumping. The SRS design proved its ability to resist the arid weather conditions and capture surface-runoff.

The sampling processes included surface-runoff, precipitation, and sediment samples. The sampling results indicate that there is a high similarity between groundwater and surface-runoff chemistry, and this suggests that surface-runoff is a main source of groundwater recharge especially in the ephemeral arroyos. Moreover, the hydrological model that was built and the forecasting program proved their ability in providing an initial estimate of the precipitation rate in the study area and the amount of water accumulated in the SRSs.

Further sample collection, statistical analysis, and infiltration modeling are required to achieve the main goal of this study which is to better understand processes controlling groundwater recharge, and thus the sustainable yield of groundwater in Nye County.

ACKNOWLEDGEMENTS

Funding for this research was provided by Nye County, NV through a grant from the US Department of Energy office of Civilian Radioactive Waste Management. Nye County Staff for assistance with sampler construction, installation, and sampling. Dr. David Borrok (Geology Department, UTEP) and Dr. Zhuping Sheng (Texas Agrilife Research Center) and their research groups for their help and support with chemical analysis. The Center for Environmental Resource Management of The University of Texas at El Paso for their funding and support.

REFERENCES

ASTM D2216 (1998), Standard Test Method for Laboratory Determination of Water (Moisture) Content of Soil and Rock by Mass, ASTM international, west Conshohocken, Pennsylvania.

ASTM D422-63 (1998), Standard Test Method for Particle-Size Analysis of Soils, ASTM international, west Conshohocken, Pennsylvania.

ASTM D4542 (1995), Standard Test Method for Pore Water Extraction and Determination of the Soluble Salt Content of Soils by Refractometer, ASTM international, west Conshohocken, Pennsylvania.

Beck, D.A., and P.A. Glancy (1995), Overview of Runoff of March 11, 1995, in Fortymile Wash and Amargosa River, Southern Nevada, U.S. Geological Survey-95.

Benson, L., and H. Klieforth (1989), Stable Isotopes in Precipitation and Groundwater in the Yucca Mountain Region, Southern Nevada – Paleoclimate Implications, in Peterson, D.H., ed., Aspects of Climate Variability in the Pacific and Western Americas, American Geophysical Union Geophysical Monograph 55, 41-59.

Claassen, H.C. (1985), Sources and Mechanisms of Recharge for Groundwater in the West-Central Amargosa Desert, Nevada-A Geochemical Interpretation, U.S. Geological Survey Professional Paper 712-F, 31 p.

Clescerl, L.S. (Editor), A.E. Greenberg (Editor), A.D. Eaton (Editor) (2000), Standard Methods for the Examination of Water and Wastewater, (20th ed.) American Public Health Association, Washington, DC. ISBN 0-87553-235-7.

Fetter, C.W. (2001), Applied Hydrogeology, Fourth Edition, Prentice-Hall Inc.

Fisher, S.G., and W.L. Minckley (1978), Chemical Characteristics of a Desert Stream in Flash Flood, Journal of Arid Environments, 1, 25-33.

Flint, A.L., J.A. Hevesi, and L.E. Flint (1996), Conceptual and Numerical Model of Infiltration for the Yucca Mountain Area, Nevada, Milestone 3GUI623M. Denver, Colorado: U.S. Geological Survey. ACC: MOL.19970409.0087.

Flint, A.L., L.E. Flint, G.S. Bodvarsson, E.M. Kwicklis, and J.T. Fabryka-Martin (2001), Evolution of the Conceptual Model of Unsaturated Zone Hydrology at Yucca Mountain, Nevada, J. Hydrology, 247(2001), 1-30, pii: S0022-1694(01)00358-4.

Jones, K.R. (1981), Food and Agricultural Organization of the United Nations, Arid Zone Hydrology, 271 pp.

LANL (Los Alamos National Laboratory) (2007), Regional Groundwater Hydrochemical Data in the Yucca Mountain Area Used as Direct Input to ANLNBS-00021, Revision 01. LA0309RR831233.001.

Lemoine, G.G., A. Gitelson, E. Adar, and J.G.M. Bakker (1995), Water Runoff Monitoring in Arid Areas Using Integrated Remote Sensing and GIS Techniques, IEEE, Piscataway, NJ, USA, pp. 2236-2238.

Meijer, A. (2002), Conceptual Model of the Controls on Natural Water Chemistry at Yucca Mountain, Nevada, Applied Geochemistry, 17, pp.793–805.

NWRPO (Nuclear Waste Repository Project Office) (2008), Geochemistry data files. Nye County, Nevada. <http://www.nyecounty.com> (accessed April 30, 2007).

Patterson, G.L. and T.A. Oliver (2004), Trace and Minor Elements in Saturated-Zone Water Near Yucca Mountain, Nevada, Geological Society of America Annual Meeting, 36(5).

Pilgrim, D.H., T.C. Chapman, and D.G. Doran (1988), Problems of Rainfall–Runoff Modeling in Arid and Semi-Arid Regions, Hydrological Sciences Journal, 33: 379–400.

Savard, C.S. (1994), Groundwater Recharge in Fortymile Wash Near Yucca Mountain, Nevada, 1992-93, IHLRWM Proceedings of the Fifth Annual International Conference, Las Vegas, Nevada, May 22-26, 1994. American Nuclear Society and American Society of Civil Engineers, p. 1805-1813.

Savard, C.S., and D.A. Beck (1994), Transmission Losses in Fortymile Wash Near Yucca Mountain, Nevada, Eos, American Geophysical Union Transaction, 75(44), p. 283.

Savard, C.S. (1998), Estimated Groundwater Recharge From Streamflow in Fortymile Wash Near Yucca Mountain, Nevada, U.S. Geological Survey Water Resources Investigation Report 97-7273, pp. 1-30.

Sharma, K.D., and J.S.R. Murthy (1996), Ephemeral Flow Modeling in Arid Regions, Journal of Arid Environments, 33: 161–178.

Stezenbach, K. (1994), Fingerprinting of Groundwater by ICP-MS: Yucca Mountain Precipitation Sample Analysis Result, Progress Report October 1, 1992 to December 31, 1992, Harry Reid Center for Environmental Studies, University of Nevada, Las Vegas, DOE Cooperative Agreement No. DE-FC 08-90NV10872.

USGS, INFIL V2.0 (2001), Validation Test Report: SDN: 10307-VTR-2.0-00. Las Vegas, Nevada: U.S. Department of Energy, Yucca Mountain Site Characterization Office. ACC: MOL.20011023.0171.

USGS, Yucca Mountain Research, Groundwater Chemistry: http://www.usgs.gov/.(2004).

Weight, W.D. (2008), Hydrogeological Field Manual: 2nd Edition, Published by McGraw-Hill Professional, 751 p., ISBN 0071477497, 9780071477499.

White, A.F., and N.J. Chuma (1987), Carbon and Isotopic Mass Balance Models of Oasis Valley-Fortymile Canyon Groundwater Basin, Southern Nevada, Water Resources Research, 23(4), 571-582, paper number 6W4383, doi:0043-1397/87/006W-4383505.00

Woolhiser, D.A., S.A. Stothoff, , and G.W. Wittmeyer (2000), Channel Infiltration in Solitario Canyon, Yucca Mountain, Nevada, Journal of Hydrological Engineering, 5(3),pp. 240-249.

Woocay, A., and J.C. Walton (2008), Infiltration History at Fortymile Wash, IHLRWM 2008, pp. 41-46, Las Vegas, NV.

Chapter 5

Groundwater Recharge in the Amargosa Desert Using Surface-Runoff Chemistry

Part of this chapter was published in the 37th Annual Radioactive Waste Management Symposium, Phoenix, AZ, February 27 – March 3, 2011, paper number 11489; ISBN # 978-0-9836186-0-7. The second part of this chapter was published in the 13th International High-Level Radioactive Waste Management Conference (IHLRWMC), Albuquerque, NM, La Grange Park, Illinois: American Nuclear Society, April 10-14, 2011, paper number 3476; ISBN: 978-0-89448-085-0.

5. Groundwater Recharge in the Amargosa Desert Using Surface-Runoff Chemistry

Omar Al-Qudah [a,*], John Walton [a], Arturo Woocay [a, b], and John Klenke [c]

[a] *Civil Engineering Department-Environmental Science and Engineering Program , The University of Texas at El Paso, 500 W University Ave, El Paso, TX 79968, USA.*

[b] *División de Estudios de Posgrado e Investigación, Instituto Tecnológico de Ciudad Juárez, Ave. Tecnológico 1340, Ciudad Juárez, CHIH 32500, MX.*

[c] *Nye County Nuclear Waste Repository Project Office (NWRPO) 2101 E. Calvada Blvd., Suite 100, Pahrump, NV 89048, USA.*

[*] *Corresponding author: Tel.:+1 915 422 4260; fax: +1 915 747 8037; omal@miners.utep.edu*

ABSTRACT

Accurate estimates of groundwater recharge are necessary components for understanding long-term sustainability of groundwater resources and predictions of groundwater flow rates and flow directions. Amargosa Desert regional groundwater studies show that the surface runoff infiltration occur in the arroyos following runoff producing storms, and this infiltration is considered to be a major source of groundwater recharge. The present study attempts to investigate how water chemistry evolves during the surface runoff and infiltration processes, in the Amargosa Desert region. In this ongoing study, sixty surface runoff samplers (SRS) were installed at thirty different locations in the Amargosa Desert's major arroyos to capture the surface runoff water. The sampling process included sediment, precipitation, and runoff water samples. In total, 176 runoff, 182 sediment, and 45 precipitation samples were collected between

January, 2009 and January, 2011. Analysis of chloride and the stable isotopes of water show substantial overlap of values with underlying groundwater consistent with the concept that infiltration of surface runoff is a major contributor to groundwater recharge in the study area. Groundwater ion concentrations represent a large collection of infiltration events occurring over time, and an exact match with surface runoff samples is unlikely. The SRS design proved its ability to function in arid weather conditions and capture surface-runoff. Further sample collection, statistical analysis, and infiltration modeling will be required to fully describe the evolution of water chemistry between infiltration and old groundwater.

5.1 INTRODUCTION

The climate, geology, hydrology and chemistry of the Amargosa Desert vicinity have been extensively studied by many agencies and researchers. These studies indicate that groundwater recharge occurs from infiltration of stream-flow in the ephemeral arroyos and infiltration of precipitation and runoff on the mountain ranges. Water may infiltrate from melting snowpack in the mountains primarily on volcanic or carbonate rocks or adjacent to the mountains from streams flowing over alluvium (fans and channels) (Faunt et al., 2004). Groundwater moves through permeable zones under the influence of hydraulic gradients from areas of recharge to areas of discharge in the regional system. Water quality studies of precipitation, surface water, and groundwater isotopic and common ion concentrations, in addition to the computer simulation of the groundwater system in the vicinity of the Amargosa Desert (Claassen, 1985; White and Chuma, 1987; Benson and Klieforth, 1989; Patterson and Oliver, 2004; USGS, 2004; Savard, 1998, 1996, 1995, 1994; Savard and Beck, 1994) have concluded recharge water is entering the groundwater system north of Yucca Mountain and have determined that recharges from Fortymile Wash, Oasis Valley, and Amargosa River is a significant source of groundwater.

Groundwater in the Amargosa Desert occurs in several interconnected, complex groundwater flow systems (Faunt et al., 2004), and this flow field is influenced by complex geologic structures created by regional faulting and fracturing that can create conduits in the carbonate rocks or barriers to flow (Faunt et al., 2004). The water moves along relatively shallow and localized flow paths that are superimposed on deeper, regional flow paths (Faunt et al., 2004). The groundwater below Amargosa Desert and in the surrounding region flows generally south toward discharge areas in the southern Amargosa Desert and Death Valley (SNL, 2008; Wilson et al., 2001).

The primary sources of groundwater recharge to the regional system are infiltration on Oasis Valley, and Timber Mountain to the north (high mountain ranges) and infiltration on the ephemeral arroyos (Fortymile Wash, Beaty Wash, and Amargosa River) and its tributaries (Figure 1), this infiltration is the precipitation that is not lost to evapotranspiration, runoff, or change in the amount held in the soil or rock, and makes it into the unsaturated zone flow system. Recharge in the immediate Amargosa Desert vicinity is low, consisting of water reaching Fortymile Wash as well as precipitation that infiltrates into the subsurface (SNL, 2008; Wilson et al., 2001). Direct recharge from precipitation is estimated to be less than five millimeters per year. In the saturated zone, downward flow through the tufts is believed to be of low quantity, less than ten centimeters per year (Montazer and Wilson, 1984; Matuska and Hess, 1989). Water also enters the regional flow system as through flow from adjoining groundwater basins, predominantly from the north, west, and east, but the amount of water coming into the system laterally is estimated to be relatively small (roughly ten percent) in comparison with that coming in as recharge from the surface (EPA, 2001).

Near Yucca Mountain and in areas immediately to the south, vertical gradients are dominantly upward from the carbonate-rock aquifer into the intermediate system and flow is toward discharge areas to the south and southwest. Groundwater in the southern Amargosa Desert may either flow through fractures in the southeastern end of the Funeral Mountains and discharge in the Furnace Creek area or flow southward and discharge at Alkali Flat (Franklin Playa), and Ash Meadows (Faunt et al., 2004).

5.2 PREVIOUS STUDIES

Water samples from the western Yucca Mountain facies contain elevated Na^+, HCO_3^-, SO_4^{2-}, F^-, U, and B as compared to water from either the eastern Yucca Mountain or Fortymile Wash facies (Patterson and Oliver, 2004; USGS, 2004), while Ca^{2+} decreases, relative to the eastern section (Blankennagel and Weir, 1973).This may be due to longer flowpaths in the western section which allow more water/rock interaction and hydrothermal alteration of older volcanic rocks. Secondary mineralization believed to have formed under closed conditions (Matuska and Hess, 1989; Moncure et al., 1981). Water samples from the eastern Yucca Mountain and Fortymile Wash facies are similar except that water from the eastern Yucca Mountain facies contains slightly higher Na^+ and HCO_3^- and water from the Fortymile Wash facies contains higher Mg^{2+} and K^+. Also, water from the Eastern Yucca Mountain facies contains higher $^{234}U/^{238}U$ ratios than that of any other facies (Patterson and Oliver, 2004; USGS, 2004). Water samples from the Bare Mountain and Amargosa River facies are distinguished by higher concentrations of SO_4^{2-}, HCO_3^-, and U (Patterson and Oliver, 2004; USGS, 2004). Water from the Amargosa River facies contains higher concentrations of B, Na^+, and Li than water from the Bare Mountain facies (Patterson and Oliver, 2004; USGS, 2004). The eastern Amargosa River facies and the southern Amargosa Desert are the least distinct because of mixing of water

from Fortymile Wash, and Jackass Flats which are the suspected source areas (Patterson and Oliver, 2004; USGS, 2004).

Winograd and Thordarson (1975) described the groundwater in the southern Amargosa Desert as a mixed type, which graded into a (Na+K) HCO_3-mixed type to the west. They first suggested the flow path from Pahute Mesa to Oasis Valley to Amargosa Desert, and this path shows an increase of K-montmorillonite, K-feldspar and Ca-montmorillonite precipitation along the flow paths. They explained this by either the thermodynamics of the system being most conducive for K^+ and Ca^{2+} ion exchange within the montmorillonites, or an increase in Ca^{2+} to the system through weathering of carbonate detritus or inflow from a carbonate aquifer. For the area of Oasis Valley and Amargosa Desert, both of these are likely to be factors in controlling the dominance of K and Ca minerals.

Claassen (1985) divides the water chemistry in the Amargosa Desert into three groups: volcanic, carbonate and mixed groundwaters. He found that the north-central part of Amargosa Desert has the lowest values of Na^+, Ca^{2+}, HCO_3^- and SO_4^{2-}, with ion concentrations increasing sharply to the east and west. This coincides with the presence of highly permeable sands and gravels within the center of the Amargosa Desert. Amargosa Desert has been modeled as a system that is closed to atmospheric CO_2 (Claassen, 1985; White and Chuma, 1987) because Pco_2 decreases along the flow path. Assuming cooler recharge conditions during Pleistocene time, Claassen (1985) used $\delta^{13}C$, $\delta^{2}H$ and $\delta^{18}O$ to support his hypothesis that water was recharged to the valley fill primarily through runoff infiltration and overland flow from Pleistocene age. Studies of the southern Amargosa Desert (Eberl et al., 1982; Khoury et al., 1982; Papke, 1972) indicate that the mineralogy itself is likely to be a factor in controlling the dominance of K^+, Mg^{2+} and Ca^{2+} minerals, and it appeares to be controlled with respect to

montmorillonites, illites, feldspars, quartz polymorphs, chlorite, and deposits of sepiolite, dolomite, and calcite. Bish (1988) noted that sodium is the dominant alkaline exchangeable cation in the shallow smectites, whereas deeper smectites contain subequal Na^+, K^+ and Ca^{2+}.

White (1979) found that evapotranspiration causes total dissolved solids (TDS) increase, calcium increases due to $CaCO_3$ input from carbonate rocks, and potassium and fluoride. He also found that in water containing moderate amounts of Mg^{2+}, the principal alteration product is montmorillonite, Mg^{2+} is deficient, but Na^+ and K^+ were present, zeolites such as clinoptilolite, mordenite, analcime and chabasite would form.

Kerrisk (1987) described six active processes that may control groundwater chemistry at Amargosa Desert, which are: physical transport of dissolved species with water; rock-water interactions; ion exchange; gas dissolutions; mixing of different water compositions; and evaporation. The ground water in the tufts is primarily a Na/HCO_3-type: Na = 65-95 % of cations and HCO_3 = 80 % of anions with sub-equal Cl and SO_4 (Ogard and Kerrisk, 1984; Matuska and Hess, 1989). Mineralogical studies of the Yucca Mountain groundwater (Matuska and Hess, 1989; Broxton et al., 1986, 1987; Al-Qudah et al., 2011, 2010, 2008) indicate that the Yucca Mountain groundwater is supersaturated with respect to montmorillonites, illites, chlorite, feldspars, albite, and talc. The ground water is undersaturated with respect to analcime, anhydrite, chrysotile, dolomite, fluorite, gypsum, halite, quartz, sepiolite, and calcite. The eastern side of Yucca Mountain is considered a calcic rich suite, and the western side an alkali rich suite, with a potassic rich suite in the northern end.

Potentiometric heads and hydrochemical data (EPA, 2001) indicate that the Alkali Flat (also known as the Franklin Lake Playa), located in the southern end of the Amargosa Desert is a major discharge area for the alluvial aquifer system. Estimated discharge at Alkali Flat is about

12.33E+6 m^3 per year. Discharge at the playa occurs primarily through evapotranspiration, the principal component of which is bare-soil evaporation (EPA, 2001). Some groundwater may flow beneath the mountain at the south end of the playa and continue southward (EPA, 2001). Regional water table maps of the alluvial aquifer (EPA, 2001) also suggest that a portion of the flow in the alluvial aquifer may be moving southwest through the abutting carbonate rocks of the Funeral Mountains, and discharging into Death Valley.

Groundwater in Amargosa Desert is recharged in part by infiltration of precipitation within the tributary drainage area, but the most is supplied by groundwater underflow through the bed rocks (Walker and Eakin, 1963). Using hydrogeologic data and interpretations presented in Winograd and Thordarson (1975), Winograd (1981) calculated potential infiltration rates on the order of 2 mm/yr through alluvium at the Nevada Test Site (NTS) where average annual precipitation is about 120 mm/yr. Scott et al. (1983) estimated net infiltration rates in the Jackass Flats basin on the order of 6 mm/yr with average precipitation rates 200 mm/yr, meaning that net infiltration rates counted 3 percent of the average precipitation. Montazer and Wilson (1984) reviewed various approaches that could be used to obtain estimates of net infiltration, including regional recharge techniques, water-budget studies, and analyses of geothermal heat flux, with estimating the average annual precipitation at Amargosa Desert to be 150 mm/yr; they concluded that 0.5 to 4.5 mm/yr becomes net infiltration. Using chloride mass balance approach (CMB), based on approximately 50 years of measurement, CRWMS M&O (2000) gives a net infiltration rate of 7 to 14 mm/yr plotted against an average precipitation rate of 170 mm/yr.

Flint et al. (2001a, 2001b) presented the processes governing net infiltration in the Amargosa Desert as the distribution and timing of precipitation, the physical properties of the surface soils and bedrock, and the components controlling evapotranspiration. He noted that the

most net infiltration occurs from ridge tops and side slopes where the soils are thinner and the fractured bedrock allows rapid penetration; net infiltration is negligible in deep soils and alluvium, except in large channels that are fed by large volumes of runoff during extreme precipitation events. Flint et al. (2001a, 2001b) reported the average net infiltration rates in the Amargosa Desert as an order of 5-10 mm/yr, with an average precipitation of 170 mm/yr, placing the net infiltration estimate for the Amargosa Desert at 3-6 percent of average precipitation.

In 2002, Flint et al. described the various recharge-estimation methods applied at Amargosa Desert vicinity, identifying the strengths and limitations of each approach. These methods included water-balance techniques, calculations using Darcy's law, a soil physics method applied to neutron-hole water-content data, inverse modeling of thermal profiles, chloride mass balance, atmospheric radionuclides, and empirical approaches. The results of these methods are useful for defining upper boundary conditions, evaluating hydrologic parameter values, and calibrating and testing the models. The complex factors at Amargosa Desert vicinity (i.e., variable precipitation, topography, and soil depth; and a thick, layered, unsaturated zone with highly variable properties, including fractures and faults) result in spatially and temporally variable infiltration and recharge rates ranged from less than 1 to about 12 mm/yr by an average of 5 mm/yr, which would be about 1 percent to 7 percent of average precipitation. However, the authors point out that, under steady-state conditions, net infiltration at the surface becomes recharge at the water table.

Bagtzoglou (2003) estimated the net infiltration rates in the Amargosa Desert to be 8.2 mm/yr, using the perched water chemistry, based on the presence of Carbon-14 found in perched water. Calcite abundance studies of calcite mineral coatings on rock fractures provide an

indication of net infiltration rates, since these coatings form as infiltrating water evaporates. Model analyses indicate a range of net infiltration values from 2 to 20 mm/yr with a mean net infiltration rate of 5.92 mm/yr (Bechtel SAIC Company LLC, 2004).

In addition to the net infiltration rate that forms by the precipitation part, Rush (1970) estimated average annual total recharge (from precipitation and underflow of groundwater) and discharge for the Ash Meadows (southern Amargosa Desert) regional system on the order of 33,000 and 17,000 acre- feet, respectively, and for the Pahute Mesa regional system these estimates are 11,000 and 9,000 acre-feet, respectively. He estimated the precipitation rate from 127 to 508 mm/yr by an average of 279 mm/yr. According to Blankennagel and Weir (1970), the estimated average annual total recharge to Pahute Mesa groundwater system is on the order of 8000 acre-feet. Walker and Eakin (1963) estimated the average annual total recharge to the groundwater of Amargosa Desert and Ash Meadows on the order of 24,000 acre-ft. of this amount 17,000 acre-feet are dicharged by the springes and evaporation, and 7000 acre-feet is potentially available for pumping from groundwater in Amargosa Desert.

Woolhiser et al. (2000) estimated the average annual infiltration into the ephemeral-stream channels of Solitario Canyon attributed to surface runoff under current climate conditions. he measured inflows and outflows of individual channel reaches to estimate the quantity of water infiltrating into channels during runoff, and the results indicate significant runoff and infiltration events in one year with a very low runoff and infiltration rates, where the mean annual runoff rate was in the range 0.38-1.51 mm/yr and the mean annual channel infiltration was in the range 0.8-0.57 mm/yr, whereas in 2006, he found the runoff rate in the range of 0.38-3.59 mm/yr. (USGS, 2001; Liu et al., 2003; SNL, 2008) have estimated the net infiltration rate in the vicinity of Amargosa Desert on the order of 7.8, 0.73-10.57, and 0.4-12

mm/yr, respectively. Moreover, (Savard, 1994; Liu et al., 2003) have estimated the average annual recharge in the Amargosa Desert on the order of 27,200, and 2156-177,323 m^3/yr. Savargd (1996) estimated the groundwater recharge rate for four reaches of Fortymile wash and he found it as 64300, 27000, 16400, and 1100 m^3/yr for Amargosa Desert, Fortymile Canyon, lower Jackass Flats, and upper Jackass Flats, respectively. Lopes and Evetts (2004) estimated the average annual precipitation and the groundwater recharge in different basins at Amargosa Desert and they found it as (30.1; 1.09) for Yucca Flat, (5.2; 0.17) for Rock Valley, (56.0; 2.11) for Forymile Canyon, (34.7; 1.04) for Oasis Valley, (17.5; 0.58) for Crater Flat, and (47.8, 0.80) mm/yr for Amargosa Desert.

This study explores the relationship between rainfall-runoff and groundwater chemistry, during flood events in the Amargosa Desert Region, Nevada, and presents an evidence of runoff's chemical signature on the infiltration and groundwater recharge. Moreover, it gives an estimate of the net infiltration in the Amargosa Desert.

5.3 DESCRIPTION OF THE STUDY AREA

The Amargosa Desert (Figure 5.1) is located in the southern portion of Nye County in south central Nevada, within the Great Basin, and is part of the Death Valley groundwater basin. The Funeral Mountains separate the Amargosa Desert from Death Valley to the southwest, and a series of mountain ranges bound the north and east extents of the desert. The Amargosa River is a major drainage component (over 8,047 km^2) of the unique closed-basin, hydrologic regime known as the Great Basin. This river system begins in the Oasis Valley, turns southeast to run through the Amargosa Desert, continues until it turns northwest, and terminates in Death Valley from its southeast extension. As a result of a dry, semi-arid, continental climate, the Amargosa River and its tributaries are ephemeral streams that are dry most of the time except in a few

relatively short reaches where discharging springs maintain small, perennial base flows. Fortymile Wash and Beatty Wash (in addition to the Washes in Crater Flat and Rock Valley) are the major tributaries of the upper Amargosa River, which drains through several small, populated areas downstream (Figure 5.1).

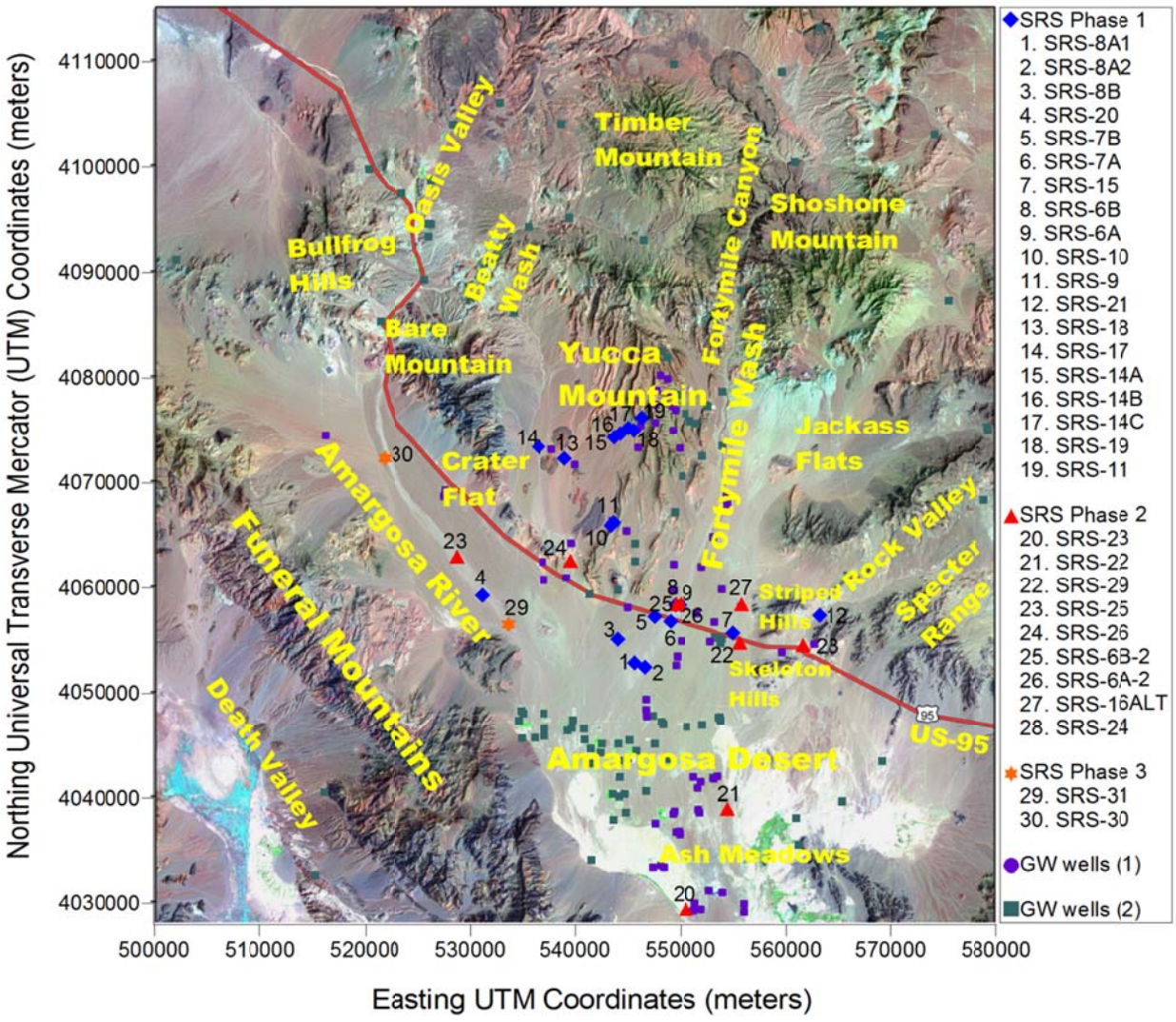

Figure 5.1: UTM coordinates map for the study area shows Locations of Amargosa Desert Region, Amargosa River, Yucca Mountain, and Fortymile Wash, Nye County, Nevada. Phase 1 site locations are shown in blue diamonds, phase 2 site locations are shown in red triangles, phase 3 site locations are shown in orange stars, and selected groundwater wells are shown in purple circle. (SRS refer to surface runoff sampler; GW refer to groundwater). Map created by SurferTM8 (Golden Software Inc., 2008).

Fortymile Wash originates between Timber Mountain and Shoshone Mountain. Fortymile Wash is an ephemeral drainage, flows southward along the east side of Yucca Mountain, and fans out in the northern part of the Amargosa Desert just north of Highway 95. Near U.S. Highway 95, the Fortymile Wash channel changes from being moderately confined to several distributary channels that are poorly confined. This poorly-defined, distributary drainage pattern persists downstream to its confluence with the Amargosa River. Yucca Mountain is located on federal land in southern Nevada, north of the Amargosa Desert, approximately 160 km northwest of Las Vegas, in the Basin and Range province of the western United States, within a zone between the Mojave Desert and the southern boundary of the Great Basin Desert, and it's part of the Amargosa River drainage basin which is the major tributary drainage area to the Death Valley. The present climate in the Amargosa Desert region is considered arid to semiarid, with average annual precipitation ranging from less than 130 millimeters (mm) at lower elevations to more than 280 mm at higher elevations, and the average annual precipitation is considered as 170 mm/yr (DOE-OCRWM, 2006; Flint et al., 2001a, 2001b, 2002). From above, we note that net infiltration at Amargosa Desert is a small fraction of average annual precipitation, representing between about 1 percent and about 14 percent by an average annual of 7 percent, meaning that, on average, between 1 and 20 mm/yr infiltrates into Amargosa Desert, in addition, precipitation estimates for a single area can vary by a factor of 2 and as much as 4; recharge estimates for a single area can vary by as much as a factor of 5.

5.4 METHODS

The methodology of this research included site selection criteria, runoff sampler design construction and field emplacement, and sample analysis criteria as described in the previous

chapter (chapter 4) in detail. This chapter will be focused on the chemical analysis results of precipitation, sediment, surface runoff, and groundwater in the Amargosa Desert Region.

5.4.1 Runoff samplers

In total, sixty surface runoff samplers (SRS) were installed at thirty different locations in the major arroyos in the Amargosa Desert region (Figure5.1) to collect surface runoff water in order to measure the chemical characteristics of runoff water that has contacted and leached some of the top soil, which believed to be an important source of groundwater recharge in the area. The samplers were placed at locations in surface-runoff channels where water is likely to pool and where sufficient depth of sediment facilitates digging a hole for emplacement. To the extent possible, samplers were placed in low gradient (depositional) portions of the arroyo to minimize washing out during storms. Two surface runoff samplers were installed at each location, one was filled with silica sand (WSB), and the other was filled by natural alluvium (NAB) (silt and sand) from the arroyo. The silica sand was washed by deionized water before use to minimize its conductivity to around 0.1 (μS/cm) and to avoid any type of contamination. Table 5.1 below shows the surface runoff sampler locations taken by Trimble Geo XH instrument (latitude, longitude, elevation, and azimuth direction from T-posts), location descriptions, the distance from the T-post to the WSB and NAB, and the distance between the WSB and NAB. The Amargosa Desert region has been divided into five sub-regions based upon elevation as follows: southern Amargosa Desert region around Ash Meadows and Franklin Playa and includes (SRS-23 and SRS-22) within the elevation of 622 to 707 m, and an average of 661 m; Fortymile Wash includes (SRS-6A, 6A-2, 6B, 6B-2, 7A, 7B, 8A1, 8A2, 8B, 15, 16-ALT, and SRS-29) within the elevation of 761 to 840 m, and an average of 801 m; Amargosa River region include (SRS-20, 25, 30, and SRS-31) and the elevation ranged between 763 and 888 m, by an

average of 804 m; Rock Valley region lays between the elevations of 875 and 913 m, by an average of 895 m and includes (SRS-20 and SRS-24); finally the western side of Yucca Mountain includes (SRS-17, 18, 14A, 14B, 14C, 19, 11, 10, 9, and SRS-26), and the elevation ranged between 811 and 1212 m, by an average of 1034 m.

Table 5.1: Surface Runoff Sampler Locations-Trimble Geo XH

Location	Site description	Latitude	Longitude	Elevation (m)	Distance from T-Post (m)	Azimuth from T-Post (degree)	Distance between WSB & NAB (m)
SAD [a]							
SRS-23	Upper Mud and Alkali Flat, 0.6 km upgradient from Ash Meadows Rd.	36.309037319	-116.402756598	621.67	2.77	65	2.06
SRS-24	Rock Valley Wash-upper reaches, 1 km up-gradient of Hwy 95	36.634803151	-116.311495180	874.54	7.71	19	1.80
FMW [b]							
SRS-6A	South of the pole line road, middle channel of FMW	36.669884789	-116.440446042	819.64	7.22	279	1.98
SRS-6A-2	South of the pole line road, western channel of FMW	36.670662204	-116.440473076	821.66	9.08	273	1.95
SRS-6B	South of the pole line road, western channel of FMW	36.669902196	-116.446060897	817.29	6.20	303	1.86
SRS-6B-2	South of the pole line road, middle channel of FMW	36.670385047	-116.445332186	818.32	7.56	10	2.91
SRS-7A	South of Hwy 95, eastern channel of FMW	36.655717428	-116.451272695	802.29	9.36	318	1.97
SRS-7B	South of Hwy 95, western channel of FMW	36.659707845	-116.468407770	797.76	7.65	347	1.97
SRS-8A1	Near well 32P, western branch of eastern channel of FMW	36.620807944	-116.489959924	760.61	4.18	326-328	1.97
SRS-8A2	Near well 32P, eastern branch of eastern channel of FMW	36.617246160	-116.479075702	762.56	4.97	207	2.06
SRS-8B	Near well 32P, western channel of FMW	36.640598904	-116.507470820	764.49	7.41	313	1.97
SRS-15	Topopah Wash 122 m up-gradient from the AVSTP [f]	36.645637040	-116.385009152	814.25	3.96	247	NA
SRS-16ALT	Topopah Wash, 3 km up-gradient from the AVSTP on NTS border	36.669927984	-116.375764967	838.72	3.66	345	1.97
SRS-29	Wash draining the west side of the Striped Hills, 0.43 km down-gradient from Hwy 95	36.636918495	-116.377439493	806.64	6.61	139	1.83
AR [c]							
SRS-20	Amargosa River channel, 5.3 km northwest of Big Dune	36.678956027	-116.651490013	782.29	4.00	256	1.75
SRS-25	Amargosa River channel, 1.14 km northwest of Ashton site	36.712673211	-116.677893541	807.00	8.47	18	1.95
SRS-30	Amargosa River channel, 13.1 km northwest of Ashton site	36.796441044	-116.755968586	886.35	4.21	245	NA
SRS-31	Amargosa River channel, 2.7 km northwest of Big Dune	36.653799795	-116.624380220	763.09	4.08	219	NA
RV [d]							
SRS-21	Rock Valley Wash-upper reaches,	36.660132021	-116.293688407	912.67	3.70	116	1.94
SRS-22	Tributary of Rock Valley Wash (lower reaches), 0.21 km east of Mecca Rd E.	36.520761742	-116.380661262	705.27	3.96	88	2.10
YMW [e]							
SRS-9	Area of increased probability of runoff southeast of well 13P	36.741220594	-116.511189890	903.86	3.46	145	2.13
SRS-10	Area of increased probability of runoff southeast of well 13P	36.738436531	-116.513821958	898.70	5.07	103	1.69
SRS-11	Solitario Canyon	36.830812004	-116.480775917	1210.78	7.32	110	2.04
SRS-14A	Tributary of Windy Wash	36.813775589	-116.510107406	1094.32	5.27	65	1.90
SRS-14B	Tributary of Windy Wash	36.817201763	-116.503903275	1114.50	6.52	133	2.00
SRS-14C	Tributary of Windy Wash	36.821732073	-116.495381817	1148.40	8.23	118	1.91
SRS-17	Tributary to the main drainage off the east side of Bare Mtn, 1.2 km north west of Red Cone.	36.805724488	-116.590881279	966.19	5.49	305	1.97
SRS-18	Tributary of Windy Wash, 0.76 km northeast of Red Cone.	36.796034630	-116.563370966	960.40	4.02	300	1.91
SRS-19	Lower Solitario Canyon off of southwest slope of Yucca Mtn.	36.819590891	-116.489665165	1153.81	13.87	140	1.97
SRS-26 [g]	Crater Flats area, 1.78 km up-gradient from Hwy 95	36.708375582	-116.556875720	810.50	5.76	121	1.81

[a] southern Amargosa Desert; [b] Fortymile Wash; [c] Amargosa River; [d] Rock Valley; [e] western side of Yucca Mountain; [f] Amargosa Valley Science and Technology Park; [g] surface runoff sampler.

The samples collected from these sites included sediment, precipitation, and surface runoff. Sediment samples were collected from each site at the time of the surface runoff samplers

installation, and also shortly after four storm events occurring in February 2009, September 2009, January 2010, and December 2010 (Table 2); following these storms, SRS samples were collected from the WSBs at each location,. Additionally, after the January 2010 precipitation event, samples were collected from rain gauges at each site along with a NAB runoff sample from some locations. In total, 167 SRS-WSB, 9 SRS-NAB, 182 sediment, and 45 precipitation samples were collected during January, 2009 and January, 2011 (Table 2).

5.4.2 Sediment sampling

Sediment samples were separated into two subsamples; the first was oven dried to determine the sample's water percent content by weight, and the second one was used to obtain soil lechates. An extraction dilution of 3.76 of deionized water per 2 kg of soil was used with a correction for the sample's original water content. Additional sediment samples were collected to study the physical properties of the soil based on the ASTM standards (ASTM D2216-98, D422-63-98, D4542-95) (Table 5.3).

5.4.3 Samples chemical analysis

Runoff and precipitation samples were collected, preserved, and shipped based on the standards methods for the examination of water and wastewater (Clescerl, 2000); runoff, precipitation, and soil extracted samples were analyzed based on the same standards (Clescerl, 2000) by using inductively coupled plasma mass spectrometry (ICP-MS) and ion-exchange chromatography (IEC) machines, in addition to the volumetric titration, for major cations and anion (Cl^-, HCO_3^-, SO_4^{2-}, Ca^{2+}, Mg^{2+}, K+, and Na^+), in addition to the trace elements and water stable isotopes.

5.4.4 Nye County groundwater wells

Groundwater chemistry data for 89 groundwater wells around the runoff samplers (Figure 5.1) were obtained from Nye County Nuclear Waste Repository Project Office (NWRPO) (NWRPO, 2008) and Los Alamos National Laboratory (LANL, 2007) and compiled into a single database. The chemical data includes Cl^-, SO_4^{2-}, total alkalinity, Na^+, Ca^{2+}, K^+, Mg^{2+}, TDS, F^-, SiO_2, δ^2H, $\delta^{18}O$, and some of trace elements.

5.4.5 Statistical analysis

Statistica^{TM}9 (StatSoft Inc., 1984-2010) is used to simplify the interpretation of the samples chemical properties by applying the descriptive statistics, box plots, and the analysis of variance test on the chemical constituents for each sample type as follows.

5.4.5.1 Descriptive statistics

Descriptive statistics (Tables 5.5-5.8) (StatSoft Inc., 1984-2010) are calculated separately for each chemical constituent per sample type (precipitation, sediment, runoff, and groundwater) and per all site locations together (i.e., Amargosa Desert area), and they provide such basic information as the mean, median, minimum and maximum values, as well as different measures of variation (the standard deviation, and the standard error). Table 5.A1, in Appendix 5.A, shows the median concentrations of the chemical constituents of each sample type (precipitation, sediment, runoff, and groundwater) normalized by sample chloride for all site locations together (Amargosa Desert Area).

5.4.5.2 Box plots

In box plots (StatSoft Inc., 1984-2010) ranges of values of selected variables (the chemical constituents) are plotted separately for groups of cases defined by values of a

categorical (grouping) variable (precipitation, sediment, runoff, and groundwater) per sample locations (southern Amargosa Desert, Fortymile Wash, Amargosa River, western side of Yucca Mountain, and Rock Valley). The central tendency (median) and range or variation statistics (quartiles) are computed for each group of cases, and the selected values are presented in graphs (Figures 5.4-5.35). In Appendix 5.A, Figures 5.A1-5.A34 show the box plots of the chemical constituents of each sample type (precipitation, sediment, runoff, and groundwater) normalized by sample chloride for all site locations together (Amargosa Desert area).

5.4.5.3 Analysis of variance (ANOVA)

In general, the purpose of analysis of variance (ANOVA) is to test for significant differences between means (StatSoft Inc., 1984-2010). The statistical significance of a result is an estimated measure of the degree to which it is true (StatSoft Inc., 1984-2010). The value of the *p*-level represents a decreasing index of the reliability of a result (StatSoft Inc., 1984-2010). The higher the *p*-level, the less believe that the observed relation between variables in the sample is a reliable indicator of the relation between the respective variables in the population (StatSoft Inc., 1984-2010). Specifically, the *p*-level represents the probability of error that is involved in accepting the observed result as valid (StatSoft Inc., 1984-2010). For example, a *p*-level of .05 (i.e., 1/20) indicates that there is a 5% probability that the relation between the variables found in the observed sample is a stroke of luck. In many areas of research, the *p*-level of 0.05 is customarily treated as a borderline acceptable error level (StatSoft Inc., 1984-2010). Results that are significant at the $p \leq 0.01$ level are commonly considered statistically significant, and $p \leq 0.005$ or $p \leq 0.001$ levels are often called highly significant; whereas the results that yield *p*-level > 0.05 are considered statistically insignificant. Table 5.9 shows ANOVA tests for significant differences between means.

5.4.6 Piper diagram

The Piper diagram allows comparison of a large number of samples on the same figure, shows clustering of samples and water type, used to classify water as hydrochemical facies, and the mixing between water types can be identified on a Piper diagram (Drever, 1997).

The idea of hydrogeochemical facies is the classification of waters according to the relative proportions of major ions (Drever, 1997). Water plotting in the upper half of both the cation and anion triangles would be referred to as magnesium sulfate-type water (Drever, 1997). Water plotting in the lower left hand side of the cation triangle and the lower right hand side of the anion triangle would be calcium chloride-type water (Drever, 1997). If both cation and anion compositions plot in the middle of the two triangles, then the waters would be referred to as mixed cation-mixed anion-types (Drever, 1997). If a water plots near the middle of one of the edges of the triangles, then one might refer to, e.g., magnesium-calcium sulfate water (Drever, 1997).

If waters are the result of mixing of two different end member waters, then the compositions of the waters should plot along a straight line in each of the fields of the diagram. On the other hand, if the compositions do not plot along a straight line on the Piper diagram, then the waters cannot be related by simple mixing between two end members. If the waters do plot along a straight line, this is not definitive proof that mixing did occur, but it is strongly suggestive and other tests can be designed to prove mixing (Drever, 1997).

To represent the water composition on a piper diagram, major cations and anion (calcium, magnesium, sodium, potassium, sulfate, chloride, carbonate, and bicarbonate) are taken for precipitation, sediment, runoff, and groundwater in equivalents per liter unit, and used as an input to the GW-Chart software (version 1.23.4.0) (Winston, 2000). GW-Chart is a

program for creating specialized graphs used in groundwater studies. It incorporates the functionality of two previous programs, Budgeteer and Hydrograph Extractor (Winston, 2000). Figure 5.31 shows Piper diagram for definition of precipitation, sediment, surface runoff, and groundwater chemical types. Figures (5.A35-5.A39), in Appendix 5.A, show the Piper diagram for each site location individually.

5.4.7 Hydrochemical modeling

The computer program PHREEQC (Parkhurst and Appelo, 1999; Parkhurst, 1995; Parkhurst et al., 1982) is capable of describing a variety of geochemical processes in groundwater systems, and simulating a variety of surface runoff and groundwater reactions and processes that can explain the water chemistry's evolution. The program was used to calculate thermodynamic equilibrium saturation indices (SI) for mineral species, based on anion and cation mean concentrations, temperature, pH, fluoride, bromide, phosphate, total nitrogen, aluminum, iron, copper, barium, lithium, strontium, zinc, lead, manganese, boron, and silicate in addition to the ion exchanges couples of precipitation, sediment leached, surface runoff, and groundwater in the Amargosa Desert region.

The SI is defined as the logarithm of the ratio of the ion activity product (IAP) of the component ions of the solid in solution to the solubility product (K) for the solid [SI = log (IAP/K)]. If the SI is zero, the water composition reflects the solubility equilibrium with respect to the mineral phase. A negative value indicates undersaturation and a positive value indicates supersaturation.

The PHREEQC output shows many potential models that explain the evolution, and the best model was chosen based on the actual mean differences between the different types of sample provided.

5.4.8 Estimation of groundwater effective recharge

Groundwater in Amargosa Desert is recharged in part by infiltration of precipitation within the tributary drainage area, but the most is supplied by groundwater underflow through the bed rocks (Walker and Eakin, 1963). Many researchers (Winograd and Thordarson, 1975; Winograd 1981; Scott et al., 1983, Montazer and Wilson, 1984; CRWMS M&O, 2000; Flint et al., 2001a, 2001b, 2002; Bagtzoglou, 2003; Bechtel SAIC Company LLC, 2004; Woolhiser et al., 2000; USGS, 2004; Liu et al., 2003; SNL, 2008) have studied the groundwater net infiltration from the precipitation (as a percent of average annual precipitation) by using various approaches that could lead to estimate of net infiltration, including water-balance techniques, calculations using Darcy's law, a soil physics method applied to neutron-hole water-content data, inverse modeling of thermal profiles, atmospheric radionuclides, perched water chemistry, based on the presence of Carbon-14 found in perched water, calcite abundance studies of calcite mineral coatings on rock fractures, and empirical approaches. They found that net infiltration at Amargosa Desert is a small fraction of average annual precipitation, representing between about 1 percent and about 14 percent by an average annual of 7 percent, meaning that, on average, between 1 and 20 mm/yr of average annual precipitation (which is estimated on the order of 170 mm/yr) infiltrates into Amargosa Desert. In addition, precipitation estimates for a single area can vary by a factor of 2 and as much as 4; recharge estimates for a single area can vary by as much as a factor of 5.

In this study chloride balance approach is used to estimate the groundwater recharge that come from the precipitation part. Chloride ion is highly soluble, conservative, and not substantially taken up by vegetation, and because of that is considered a suitable tracer for

determining the movement of water. In this case the groundwater recharge is given by (Kumar, 1977; Chandra, 1979):

$$\boldsymbol{R = D/C} \qquad \boldsymbol{Eq.5.1}$$

where,

R: groundwater recharges (mm/yr)

D: wet and dry chloride deposition (mg/m^2/yr), and

C: concentration of chloride in groundwater (mg/l)

This method is convenient, fast and cheap. The chief drawback is the uncertainty in the determination of the wet and dry deposition. The principle source of chloride in ground water is from the atmosphere. In this case the recharge can be expressed as (Kumar, 1977; Chandra, 1979):

$$\boldsymbol{R = P \times \left(\frac{Cl\ of\ precipitation}{Cl\ of\ groundwater}\right)} \qquad \boldsymbol{Eq.5.2}$$

where,

R: groundwater recharges (mm/yr) and

P: average precipitation rate (mm/yr)

The chloride method must be treated with caution. Recharge under conditions of extremely high rainfall with a long recurrence period, is likely to influence the chloride concentration of ground water to a high degree resulting in an over estimate of the mean annual recharge.

5.5 RESULTS AND DISCUSSION

5.5.1 Surface runoff and precipitation sampling

Table 5.2 below shows the elevation of site locations, in addition to the measured amount of water accumulated in the rain gauges, WSBs, and NABs in each site location after four storm events occurred in the study area during February, 2009; September, 2009; and January, 2010; and December 2010.

The rain gauges are simple collectors that are open to the atmosphere. The simplicity of the samplers (low cost rain gauges) was dictated by costs and logistics (potential for vandalism). Rain gauge readings and chemistry were subject to unknown amounts of evaporation prior to collection so the readings should not be equated with precipitation amount or initial chemistry. Because of the dilute nature of the solutions, even subsequent to evaporation, the precipitation water chemistry should provide accurate measurements of a) relative abundance of different elements (e.g., when normalized relative to chloride) and b) an estimate of total mass loading of the elements.

The rain gauges included both wet-fall and dry-fall since the last time they were emptied and rinsed. All rain gauges collected precipitation during the storm events. The distribution of precipitation is related to the altitude and latitude of the land surface (Table 5.2), the higher mountains in the Northern part of the Amargosa Desert are receive the largest amounts of precipitation, and the valley the least, most of the precipitation falls in the winter, but some precipitation occurs in the summer as thunderstorms, and this is not true for surface runoff samplers, and maybe it is because the variation in the soil physical properties Also, the amount of precipitation cumulated in the rain gauges increases as December, 2010 storm > January, 2010 storm > February, 2009 storm > September, 2009 storm. Amargosa River's rain gauges produced

the least amount of water in February 2009 and January 2010 storms, by the amount of 22.9 mm at SRS-21 in February 2009, and 31.7 mm at SRS-31 in January 2010. In the other hand, western side of Yucca Mountain's rain gauges produced the greatest amount of water in the same storm events, by the amount of 53.3 mm at SRS-19 in February 2009, and 72.4 mm at SRS-14C in January 2010.

Table 5.2: The Measured Amount of Water Cumulated in the Rain Gauges, WSB, and NAB in each Site Location during February, 2009; September, 2009; January, 2010; and December, 2010.

		Storm event, Feb. 2009			Storm event, Sep. 2009			Storm event, Jan. 2010			Storm event, Dec. 2010		
Location	Elevation (m)	RG [g] (mm)	WSB (l)	NAB (l)	RG (mm)	WSB (l)	NAB (l)	RG (mm)	WSB (l)	NAB (l)	RG (mm)	WSB (l)	NAB (l)
SAD [a]													
SRS-23[b]	621.7	N/A	N/A	N/A	0	0.1	0	34.3	3.1	3.1	10.7	1.8	1.8
SRS-22	705.3	N/A	N/A	N/A	0	0.1	0	47	1.8	0	73.7	1.3	0.8
FMW [c]													
SRS-8A1	760.6	26.7	0.6	0				40.6	0.1	0			
SRS-8A2	762.6	27.2	1	0				43.2	2.3	0	57.1	1.8	0.8
SRS-8B	764.5	30.5	1.3	0				39.4	0.4	0			
SRS-7B	797.8	29.2	1.8	0				41.9	1.9	0	53.3	1.8	0
SRS-7A	802.3	26.7	1.5	0				39.8	0.9	0			
SRS-29	806.6	N/A	N/A	N/A				44.4	1.5	0			
SRS-15	814.2	31.7	2.1	0				40.6	0.3	0			
SRS-6B	817.3	29.8	2	0				40.6	2	0			
SRS-6B-2	818.3	N/A	N/A	N/A				47	0.8	0			
SRS-6A	819.6	33	1.4	0				44.4	0.6	0.3			
SRS-6A-2	821.7	N/A	N/A	N/A				47	0.9	0			
SRS-16ALT	838.7	N/A	N/A	N/A				43.2	0.8	0			
AR [d]													
SRS-31	763.1	N/A	N/A	N/A				31.7	0.3	0			
SRS-20	782.3	31.7	1.2	0	0	1.3	0	38.1	0	0.1			
SRS-25	807	N/A	N/A	N/A	0	0.3	0	39.4	0.9	0.3			
SRS-30	886.3	N/A	N/A	N/A				49.5	0.3	0			
RV [e]													
SRS-24	874.5	N/A	N/A	N/A				43.2	0.5	0			
SRS-21	912.8	22.9	0.8	0				48.3	0	0			
YMW [f]													
SRS-26	810.5	N/A	N/A	N/A				39.4	0.3	0			
SRS-10	898.7	36.8	1	0				40.6	1	0			
SRS-9	903.9	36.8	0.8	0				40.6	0	0			
SRS-18	960.4	41.9	1.3	0				47	1.9	0			
SRS-17	966.2	40.6	0.7	0				35.6	1.9	0			
SRS-14A	1094.3	45.7	2	0				48.3	0	0			
SRS-14B	1114.5	48.3	1.8	0				50.8	3.1	0.9			
SRS-14C	1148.4	49.5	1.5	0				72.4	1.9	0			
SRS-19	1153.8	53.3	2.1	0				63.5	1.9	0.3			
SRS-11	1210.8	N/A	N/A	N/A				66	2.2	0			

[a] southern Amargosa Desert; [b] surface runoff sampler; [c] Fortymile Wash; [d] Amargosa River; [e]Rock Valley; [f] western side of Yucca Mountain; [g] rain gauge.

In February 2009, 18 locations were provided runoff water from WSBs, and the sample volumes vary between 600 ml from site SRS-8A1 (Fortymaile Wash) with rain gauge reading 27.6 mm and 2100 ml from sites SRS-15 (Fortymile Wash) and SRS-19 (western side of Yucca Mountain) with rain gauge readings 31.7 and 53.3 mm respectively. The NABs did not produce any sample during this period. In September 2009, the rain gauges were empty (dried by evaporation), but 100, 100, 1300, and 300 ml samples were collected from southern Amargosa Desert WSBs (sites SRS-23 and SRS-22) and Amargosa River WSBs (sites SRS-20 and SRS-25) respectively; the NABs did not yield any samples. In January 2010, runoff samples were collected from 26 location's WSBs; SRS-14B (western side of Yucca Mountain) and SRS-23 (southern Amargosa Desert) WSBs produced the greatest amount of water (3100 ml) and SRS-8A1 (Fortymile Wash) WSB produced the least amount of water (100ml). In the same time, the NABs produced water in six locations with greatest amount of 3100 ml at SRS-23 and the least amount of 100 ml at SRS-20 (Amargosa River). In December 2010, SRS-23, SRS-22, SRS-8A2, and SRS-7B WSBs produced water by amount of 1800, 1300, 1800, and 1800 ml respectively; SRS-23, SRS-22, and SRS-7B NABs produced water by amount of 1800, 800, and 800 ml respectively; the rain gauges in SRS-23, SRS-22, SRS-8A2, and SRS-7B measured 10.7, 73.7, 57.1, and 53.3 mm of rain water.

Table 5.2 shows the relation between the amount water cumulated in the rain gauges and the amount of water accumulated in the surface runoff samplers for the same location in four different patterns. SRS-8B, SRS-18, and SRS-14C present the first pattern, where the measured rain gauges increased from February, 2009 to January, 2010 and the volume of water accumulated in the WSBs increased for the same events, whereas the NABs failed to produce water. SRS-7B, SRS-6B, and SRS-10 present the second pattern, where the measured rain

gauges increased, but the WSBs captured the same amount of water, and NABs didn't yield any sample. The third pattern presented in SRS-22, 8A1, 8B, 20, 7A, 15, 6A, 9, 21, 17, 14A, 14B, and SRS-19, where the precipitation accumulated increased, the runoff water captured by WSBs decreases or didn't form, and some of the NABs have captured runoff water in the locations with significant increase in precipitation. SRS-8A2 shows the last pattern, where precipitation accumulated in the rain gauge increased through February 2009, January 2010, and December 2010 storms, runoff accumulated in the WSB increased from February 2009 to January 2010, then decreased in December 2010, in the same time, NAB couldn't produce samples in February 2009 and January 2010, but it produced in December 2010. The general pattern can be summarized as NABs may capture runoff water if precipitation rate exceeded certain limit as shown in SRS-8A2, and it is not clear why the produced water from WSBs decreases, or vanished while the precipitation rate increases. At the time of sampling, type of sediment and thickness of the sediment layer above each bucket indicated the presence of surface water runoff in the study area (Figures 5.2, 5.3).

Figure 5.2: Amargosa River (site SRS-20) after December 2010 storm event.

Figure 5.3: Rock Valley (site SRS-21) after January 2010 storm event.

5.5.2 Sediment sampling

In order to understand the characteristics of location sediments that could control the infiltration of runoff, sediment samples from each location were analyzed based on ASTM standards (D422-63-07; D854-06; D1140-06; D2216-05, D4542-95) for the following physical properties: gravimetric water contents, hygroscopic water contents, bulk density, solid density, porosity, particle size distribution, uniformity coefficient, and the soil textural term (Table 5.3).

Table 5.3: Site Locations Soil Physical Properties.

Location	Gravimetric water content %	Bulk density (g/ml)	Hygroscopic water content %	Solid density (g/ml)	Porosity	Gravel total %	Sand total %	Silt %	Clay %	Uniformity. Coefficient (Cu=d60/d10)	Soil textural term
SAD [a]											
SRS-22 [b]	0.01	1.42	0.46	2.6	0.45	12.48	84.25	3.13	0.13	5.28	Sand
SRS-23	0.2	1.22	0.28	2.6	0.53	24.26	56.59	18.68	0.47	40	Silty Sand (Loamy sand)
FMW [c]											
SRS-15	2.25	1.4	0.35	2.65	0.47	13.29	83.74	2.91	0.06	7.65	Sand
SRS-7B	2.77	1.17	1.31	2.6	0.55	0	8.9	67.02	24.1	17.5	Clay-Silt (Silt loam)
SRS-7A	6.84	1.2	1.14	2.5	0.52	0	38.19	48.9	12.9	37.5	Sandy-Silt (Loam)
SRS-8B	1.01	1.41	0.46	2.55	0.45	21.21	71.12	7.33	0.33	5.83	Sand
SRS-8A1	1.59	1.37	0.45	2.5	0.45	28.54	62.42	8.72	0.32	23.89	Sand
SRS-8A2	1.33	1.42	0.51	2.55	0.44	38.81	58.98	2.16	0.06	9.4	Sand
SRS-6A	2.84	1.41	0.48	2.55	0.45	15.39	82.14	2.42	0.05	8	Sand
SRS-6B	1.85	1.37	0.5	2.55	0.46	37.52	57.97	4.38	0.12	18.42	Sand
SRS-6A-2	0.54	1.4	0.55	2.6	0.46	34.5	61.5	3.9	0.15	13.2	Sand
SRS-16ALT	0.02	1.43	0.4	2.65	0.46	19.31	77.73	2.85	0.11	8.46	Sand
SRS-6B-2	9.3	1.41	0.55	2.6	0.46	34.5	61.46	3.88	0.15	13.17	Sand
SRS-29	5.07	1.31	0.65	2.65	0.5	17.68	70.09	11.21	1.02	52	Sand (to Loamy sand)
AR [d]											
SRS-30	7.77	1.41	0.58	2.55	0.44	13.42	83.1	3.42	0.06	5.36	Sand
SRS-31	8.84	1.43	0.5	2.55	0.44	27.85	67.91	4.13	0.1	11	Sand
SRS-25	0.01	1.38	0.61	2.6	0.47	27.35	67.66	4.83	0.16	11.36	Sand
SRS-20	0.92	1.21	0.5	2.6	0.53	41.48	40.55	17.1	0.87	90.91	Silty Sand (Loamy sand)
RV [e]											
SRS-21	3.26	1.39	0.4	2.65	0.48	24.91	71.87	3.12	0.11	11.05	Sand
SRS-24	0.45	1.39	0.45	2.65	0.47	16.02	74.82	8.86	0.31	81.25	Sand
YMW [f]											
SRS-10	2.04	1.42	0.48	2.55	0.44	31.27	63.83	4.75	0.15	15	Sand
SRS-9	1.68	1.41	0.38	2.6	0.46	29.1	66.88	3.94	0.09	11.11	Sand
SRS-17	2.35	1.41	0.33	2.55	0.45	10.8	84.32	4.79	0.09	10	Sand
SRS-18	3.34	1.41	0.35	2.55	0.45	43.89	53.64	2.4	0.06	18.57	Sand
SRS-14A	2.92	1.41	0.44	2.55	0.45	51.89	40.78	7.08	0.25	105.26	Sand
SRS-14B	2.74	1.42	0.26	2.55	0.44	47.4	50.3	2.22	0.08	17.14	Sand
SRS-14C	3.07	1.39	0.48	2.6	0.47	53.23	42.55	4.09	0.13	43.33	Sand
SRS-11	1.13	1.38	0.38	2.55	0.46	42.23	52.18	5.37	0.22	35.71	Sand
SRS-19	2.03	1.41	0.3	2.55	0.45	36.89	59.42	3.58	0.12	26.67	Sand
SRS-22	0.01	1.42	0.46	2.6	0.45	12.48	84.25	3.13	0.13	5.28	Sand
SRS-23	0.2	1.22	0.28	2.6	0.53	24.26	56.59	18.68	0.47	40	Silty Sand (Loamy sand)
SRS-26	0.65	1.42	0.41	2.6	0.45	29.18	67.97	2.77	0.09	12	Sand

[a] southern Amargosa Desert; [b] surface runoff sampler; [c] Fortymile Wash; [d] Amargosa River; [e]Rock Valley; [f] western side of Yucca Mountain.

The gravimetric water contents ranged between 0.01% (at SRS-22 and SRS-25) and 9.30% (at SRS-6B-2) by an average of 2.6%; hygroscopic water contents ranged between 0.26% (at SRS-14B) and 1.31% (at SRS-7B) by an average of 0.5%, and this mean that the southern Amargosa Desert, Amargosa River, and western side of Yucca Mountain have the least water contents percent, whereas Fortymile Wash has the greatest water contents percent. The least value of soil bulk density exists in Fortymile Wash at sites SRS-7B and SRS-7A by a value of 1.17 g/ml, and the greatest value exists in Fortymile Wash at site SRS-16ALT and Amargosa River at site SRS-31 by a value of 1.43 g/ml, and the average of bulk density is 1.37 g/ml; the solid density ranged between 2.50 and 2.65% by an average of 2.58 g/ml, the least value exists in Fortymile Wash at sites SRS-7A and SRS-8A1, and the greatest value exists in Fortymile Wash at sites SRS-15, SRS-16ALT, and SRS-29; and Rock Valley at sites SRS-21 and SRS-24.

It was found by (Woolhiser et al., 2006; Woolhiser et al., 2000) that the porosity of the Amargosa Desert's sediment ranged between 0.34 and 0.39, whereas kilroy and Savard (1997) found it in the range of 0.41 and 0.42, but herein in this study (Table 5.3), the porosity ranged between 0.44 in Fortymile Wash (at SRS-8A2), western side of Yucca Mountain (at SRS-10 and 14B), and Amargosa River (at SRS-30 and 31), and 0.55 in Fortymile Wash (at SRS-7B) by an average of 0.47. Furthermore (Woolhiser et al., 2006; Woolhiser et al., 2000) studied the soil particle size distribution in the Amargosa Desert and found that 60 percent of the soil is sand, 20 percent is silt, 10 percent is gravel, and 10 percent is Clay.

The analysis of sediment samples from the Amargosa Desert region shows that soil sand ranged between 9% in the Fortymile Wash (at SRS-7B) and 84% in the western side of Yucca Mountain (at SRS-17) and southern Amargosa Desert (at SRS-22) by an average of 62%, gravel distributed from nil in the Fortymile Wash (at SRS-7B and 7A) to 53% in the western side of

Yucca Mountain (at SRS-14C) by an average of 27%, silt soil distributed from 2.2%, in Fortymile Wash (at SRS-8A2) and western side of Yucca Mountain (at SRS-14B), to 67% in Fortymile Wash (at SRS-7B), by an average of 9%, whereas clay soil distributed from 0.05%, in Fortymile Wash (at SRS-15, 8A2, and 6A), western side of Yucca Mountain (at SRS-18), and Amargosa River (at SRS-30), to 24% in Fortymile Wash (at SRS-7B) by an average of 2%. Table 5.4 below shows the main soil characteristics as distributed per each location.

Table 5.4: The Main Soil Characteristics as Distributed per each Location

Location	Surface runoff sampler site name	Site description
Fortymile Wash	SRS-15	Greatest solid density; Least clay contents; Sandy soil textural.
	SRS-7B	Greatest hygroscopic water contents; Least bulk density; Nil gravel contents; Least sand contents; Greatest silt contents; Greatest clay contents; Greatest porosity; Clay-silt (silt loam) textural.
	SRS-7A	Least bulk density; Least solid density; Nil gavel contents; Sandy-silt (silt loam) textural.
	SRS-8A1	Least solid density; Sand textural
	SRS-8A2	Least sand contents; Least silt contents; Least clay contents; Least porosity; Sand textural.
	SRS-6A	Least clay contents; Sand textural.
	SRS-6B-2	Greatest gravimetric water contents; Sand textural.
	SRS-16ALT	Greatest bulk density; Greatest solid density; Sand textural.
	SRS-29	Greatest solid density; Sand to loamy sand textural.
	SRS-6A-2, SRS-6B, SRS-8B.	Sand textural.
Western Side of Yucca Mountain	SRS-17	Greatest sand contents; Sand textural.
	SRS-18	Least clay contents; Sand textural.
	SRS-14A	Greatest uniformity coefficient; Sand textural.
	SRS-14B	Least hygroscopic water contents; least silt contents; least porosity; Sand textural.
	SRS-14C	Greatest gravel contents; Sand textural.
	SRS-10	Least porosity; Sand textural.
	SRS-19, SRS-11, SRS-9, SRS-26	Sand textural.
Amargosa River	SRS-25	Least Gravimetric water contents; Sand textural.
	SRS-30	Least clay contents, least uniformity coefficient; least porosity; Sand textural.
	SRS-31	Greatest bulk density; least porosity; Sand textural.
	SRS-20	Silty-sand (loamy sand).
Southern Amargosa Desert	SRS-22	Least Gravimetric water contents; greatest sand contents; least uniformity coefficient; Sand textural.
	SRS-23	Silty-sand (loamy sand).
Rock Valley	SRS-21	Greatest solid density. Sand textural.
	SRS-24	Greatest solid density. Sand textural.

Sandy soil presents the main textural for twenty-five site locations, the advantages for this type of soil are: very rapid infiltration, usually oxidized and dry, and low runoff potential; whereas the disadvantages are: very low cation exchange capacity, very high hydraulic conductivity rate, low available water, and little soil structure. Silty-sand (loamy sand) presents three site locations, the advantages for this type of soil are: high infiltration and low to medium runoff; the disadvantages are: low cation exchange capacity, moderate to high hydraulic conductivity rate, low to medium available water. Clay-silt (silt loam) presents one site location with the following advantages: Moderate infiltration, fair oxidation, moderate runoff potential, generally accessible, and good cation exchange capacity; and the disadvantages are: some crusting and fair to poor structure. Sandy-silt (loam) presents one site location with the advantages: moderate infiltration, fair oxidation, moderate runoff potential, generally accessible, good cation exchange capacity; and the disadvantage is: fair structure.

5.5.3 Statistical analysis

5.5.3.1 Descriptive statistics

A summary of the precipitation, sediment, runoff, and groundwater chemical constituent's descriptive statistics, and it is distribution within the site locations are given in Tables 5.5, 5.7, 5.8, and 5.9.

Table 5.5 shows the descriptive statistics of the chemical constituents for 45 precipitation samples. The least values of precipitation's TDS and chloride are 6.83 and 0.62 ppm originated in Amargosa River and Fortymile Wash; whereas the greatest values are 323.6 and 6.82 ppm originated in Rock Valley and southern Amargosa Desert, respectively. The precipitation's TDS and chloride means and standard deviations respectively are: 48.6 ppm and 65.7, 2.7 ppm and 1.7. Stetzenbach (1994) studied the precipitation chemistry in the vicinity of Yucca Mountain

from December, 1992 through March, 1993; Table 5.6 summarized Stetzenbach's (1994) results. Comparing the chemical constituents concentration of the precipitation in Table 5.5 (results obtained by the current study) and Table 5.6 (results obtained by Stetzenbach), it is clear that Stetzenbach samples more diluted, and it seems that it was collected directly after the storm events. Moreover, chloride concentrations in precipitation (Tables 5.5, 5.6) indicate that the precipitation samples of this research have been evaporated by a factor of 11.

Table 5.5: Summary of Precipitation Chemical Constituents (in mg/l, except otherwise indicated), and it is Distribution within the Site Locations.

Precipitation, 45 samples						
Element	Mean	Median	Minimum	Maximum	Std.Dev.	Element distribution per location
TDS	48.59	28.68	6.83	323.61	65.74	RV [c] >YMW [d] >FMW [e] >SAD [f] >AR [g]
T. Alk as $CaCO_3$ [a]	13.63	12.20	3.00	25.00	6.76	SAD>RV>YMW>AR>FMW
Non car. Alk [b] %	57.45	59.09	26.63	75.16	10.37	AR>YMW>SAD>FMW>RV
Cl^-	2.71	2.13	0.62	6.82	1.68	SAD>YMW>RV>AR>FMW
SO_4^{2-}	4.46	3.70	0.09	11.52	3.26	RV>YMW>FMW>SAD>AR
Ca^{2+}	5.12	4.36	0.60	11.95	2.61	RV>SAD>YMW>FMW>AR
Mg^{2+}	0.62	0.61	0.15	1.82	0.41	RV>YMW>FMW>SAD>AR
K^+	0.78	0.70	0.04	1.91	0.46	RV>AR>SAD>YMW>FMW
Na^+	1.61	1.27	0.40	3.90	0.96	SAD>YMW>RV>AR>FMW
F^-	0.34	0.18	0.05	1.30	0.34	SAD>YMW>FMW>AR>RV
Br^-	0.21	0.20	0.20	0.56	0.07	YMW>FMW>AR=RV=SAD
Total B	0.01	0.01	0.01	0.09	0.02	FMW>YMW=AR=RV=SAD
PO_4^{3-}	0.70	0.30	0.10	2.00	0.66	YMW>RV>FMW>AR>SAD
Total N	0.46	0.35	0.03	1.40	0.41	RV>SAD>AR>YMW>FMW
NO_3^-	2.04	1.56	0.13	6.16	1.79	RV>SAD>AR>YMW>FMW
NH_3	0.56	0.43	0.03	1.70	0.49	RV>SAD>AR>YMW>FMW
Al^{3+}	0.02	0.01	0.004	0.05	0.01	RV>SAD>FMW>YMW>AR
As^{3-}	0.01	0.01	0.0002	0.02	0.005	RV>AR>FMW>YMW>SAD
Total Fe	0.01	0.003	0.0003	0.06	0.01	RV>FMW>SAD>YMW>AR
Total Cu	0.003	0.004	0.00008	0.01	0.003	YMW>FMW>RV>SAD=AR
Ba^{2+}	0.01	0.01	0.003	0.03	0.01	YMW>SAD>RV>FMW>AR
Cs^+	0.01	0.01	0.001	0.03	0.01	YMW>RV>SAD>FMW>AR
Li^+	0.004	0.003	0.000003	0.03	0.01	AR>SAD>RV>YMW>FMW
Total Mo	0.001	0.001	0.00001	0.01	0.002	RV>SAD>FMW=YMW=AR
Sr^{2+}	0.04	0.04	0.01	0.15	0.03	RV>YMW>SAD>FMW>AR
Rb^+	0.001	0.001	0.001	0.004	0.001	RV>YMW>FMW=AR=SAD
Total U	0.001	0.0004	0.0001	0.005	0.001	AR>RV>SAD>YMW>FMW
Total V	0.001	0.001	0.0002	0.01	0.001	RV>AR>YMW>FMW>SAD
Zn^{2+}	0.01	0.01	0.001	0.05	0.01	RV>AR>FMW>SAD>YMW
Total Mn	0.01	0.01	0.00005	0.05	0.01	RV>AR>FMW>YMW>SAD
Ni^{2+}	0.0004	0.0004	0.00001	0.001	0.0002	RV>FMW>AR>SAD>YMW

[a] Total alkalinity as $CaCO_3$; [b] non carbonate alkalinity; [c] Rock Valley; [d] western side of Yucca Mountain; [e] Fortymile Wash; [f] southern Amargosa Desert; [g] Amargosa River.

Table 5.6: Chemical Constituents of Precipitation in the Vicinity of Yucca Mountain during the period December, 1992 through March, 2010; Results obtained from Stetzenbach (1994).

Element	Mean	Minimum	Maximum	Std.Dev.
Mg^{2+} (ppm)	0.0225	0.003	0.073	0.01775
Ca^{2+} (ppm)	0.22275	0.056	0.795	0.17025
Na^{+} (ppm)	0.126	0.039	0.308	0.06475
K^{+} (ppm)	0.046	0.012	0.203	0.0405
F^{-} (ppm)	0.069	0	0.398	0.06775
Cl^{-} (ppm)	0.25725	0.042	1.645	0.2525
NO_3^{-} (ppm)	2.203	0.326	23.624	3.42675
SO_4^{2-} (ppm)	0.6545	0.122	2.333	0.4285
Li^{+} (ppb)	0.14	0	0.6	0.3
Total V (ppb)	0.1385	0.085	0.191	0.0305
Total Mn (ppb)	1.36825	0.236	8.384	1.26875
Ni^{2+} (ppb)	0.28525	0.007	0.948	0.15325
As^{3-} (ppb)	0.30925	0	0.886	0.31225
Rb^{+} (ppb)	0.13	0	0.43	0.21
Sr^{2+} (ppb)	1.5535	0.423	6.986	1.5305
Cs^{+} (ppb)	0.019	0	0.072	0.0313333
Ba^{2+} (ppb)	2.1335	0.633	5.326	1.01975
Total Pb (ppb)	0.94275	0.259	2.056	0.55325
Total U (ppb)	0.006	0	0.017	0.0076667
Total Ti (ppb)	0.3375	0.16	1.54	0.2075
Zn^{2+} (ppb)	0.07075	0.009	0.87	0.1005
Total Mo (ppb)	0.064	0.02	0.15	0.02775

In Table 5.7, the descriptive statistics of the chemical constituents for 182 sediment samples is presented. The least values of sediment's TDS and chloride are 47.7 and 0.35 ppm originated in western side of Yucca Mountain and Fortymile Wash; whereas the greatest values are 1017.7 and 45 ppm originated in southern Amargosa Desert, the TDS and chloride means and standard deviations respectively are: 161.1ppm and 123.3, 1.98 ppm and 4.23.

Table 5.7: Summary of Sediment Chemical Constituents (in mg/l, except otherwise indicated), and it is Distribution within the Site Locations.

Sediment, 182 samples						
Element	Mean	Median	Minimum	Maximum	Std.Dev.	Element distribution per location
TDS	161.44	125.69	47.72	1017.70	123.31	SAD [f] >FMW [e] >RV [c] >AR [g] >YMW [d]
T. Alk as $CaCO_3$ [a]	156.31	136.14	35.46	892.18	100.12	SAD>FMW>AR>YMW>RV
Non car. Alk [b] %	78.19	78.30	46.87	95.52	8.98	AR>FMW>SAD>RV>YMW
Cl^-	1.98	0.91	0.35	45.00	4.23	SAD>AR>RV>YMW>FMW
SO_4^{2-}	6.25	2.46	0.21	88.67	11.65	SAD>AR>RV>FMW>YMW
Ca^{2+}	33.76	24.48	4.58	252.50	30.20	SAD>RV>FMW>YMW>AR
Mg^{2+}	2.19	1.69	0.18	25.16	2.65	SAD>FMW>YMW>RV>AR
K^+	8.42	7.04	1.74	30.46	5.23	AR>SAD>FMW>RV>YMW
Na^+	11.12	4.74	1.97	76.78	14.96	AR>SAD>FMW>YMW>RV
F^-	0.07	0.04	0.03	1.39	0.17	AR>SAD>RV>FMW>YMW
Br^-	1.66	0.14	0.14	35.78	5.76	AR>SAD>FMW>RV>YMW
Total B	1.49	1.22	0.003	4.42	1.13	AR>FMW>YMW>RV>SAD
PO_4^{3-}	0.77	0.08	0.07	9.11	1.33	AR>SAD>FMW>YMW>RV
Total N	1.34	0.90	0.09	13.82	1.73	AR>FMW>RV>SAD>YMW
NO_3^-	5.91	3.96	0.39	60.81	7.59	AR>FMW>RV>SAD>YMW
NH_3	1.64	1.10	0.11	16.86	2.11	AR>FMW>RV>SAD>YMW
Al^{3+}	0.13	0.06	0.01	5.76	0.48	AR>RV>SAD>FMW>YMW
As^{3-}	0.01	0.01	0.0002	0.03	0.01	SAD>FMW>YMW>RV>AR
Total Fe	0.12	0.05	0.0001	3.58	0.32	FMW>SAD>YMW>AR>RV
Total Cu	0.06	0.05	0.0001	0.20	0.05	YMW>FMW>RV>SAD>AR
Ba^{2+}	0.01	0.01	0.001	0.10	0.01	SAD>FMW>RV>YMW>AR
Cs^+	0.01	0.01	0.0002	0.09	0.01	SAD>RV>FMW>YMW>AR
Li^+	0.01	0.01	0.001	0.09	0.01	AR>SAD>FMW>YMW>RV
Total Mo	0.001	0.0004	0.0003	0.01	0.001	AR>SAD>FMW>RV>YMW
Sr^{2+}	0.12	0.09	0.01	0.92	0.11	SAD>RV>YMW>FMW>AR
Rb^+	0.01	0.002	0.0003	0.08	0.02	AR>FMW>YMW>SAD>RV
Total Ti	0.002	0.002	0.002	0.05	0.004	SAD>AR>RV>FMW>YMW
Total U	0.001	0.00004	0.00003	0.01	0.002	SAD>FMW>AR>RV>YMW
Total V	0.01	0.01	0.001	0.05	0.01	SAD>AR>FMW>RV>YMW
Zn^{2+}	0.01	0.004	0.0001	0.25	0.02	SAD>RV>AR>FMW>YMW
Total Mn	0.10	0.01	0.00001	3.95	0.39	YMW>SAD>FMW>AR>RV
Ni^{2+}	0.01	0.004	0.0002	0.05	0.01	SAD>AR>FMW>YMW>RV
Total Pb	0.002	0.0004	0.0003	0.02	0.003	AR>SAD>FMW>YMW>RV
Se^{2-}	0.00004	0.00004	0.00003	0.00004	0.000002	SAD>AR>RV>FMW>YMW

[a] Total alkalinity as $CaCO_3$; [b] non carbonate alkalinity; [c] Rock Valley; [d] western side of Yucca Mountain; [e] Fortymile Wash; [f] southern Amargosa Desert; [g] Amargosa River.

Tables 5.8 and 5.9 present the descriptive statistics of the chemical constituents for 167 runoff samples and 89 groundwater wells and bore holes. Runoff least TDS and chloride values are 12 and 1.5 ppm, and it is originated in western side of Yucca Mountain and Fortymile Wash, respectively. Groundwater least TDS and chloride are originated in Fortymile Wash and

Amargosa River by values of 196.7 and 5.1 ppm. Runoff greatest TDS and chloride are originated in Rock Valley and southern Amargosa Desert by values of 969 and 67.54 ppm respectively. Groundwater greatest TDS and chloride values are 1132.3 and 79.10 ppm, and it is originated in Amargosa River. Runoff's TDS and chloride means and standard deviations are: 246.3 ppm and 250.54, 11.25 ppm and 12.87; whereas for groundwater it is: 423.5 ppm and 222, 16.76 ppm and 15.8.

Table 5.8: Summary of Runoff Chemical Constituents (in mg/l, except otherwise indicated), and it is Distribution within the Site Locations.

Runoff, 167 samples						
Element	Mean	Median	Minimum	Maximum	Std.Dev.	Element distribution per location
TDS	246.35	110	12	969	250.54	RV [c] >SAD [f] >AR [g] >FMW [e] >YMW [d]
T. Alk as $CaCO_3$ [a]	126.34	73	30	451	105.22	RV>AR>SAD>FMW>YMW
Non car. Alk [b] %	63.90	66.96	23.33	89.03	17.77	AR>RV>FMW>SAD>YMW
Cl^-	11.25	8	1.50	67.54	12.87	SAD>AR>YMW>RV>FMW
SO_4^{2-}	19.95	9.50	1.50	154.34	29.91	SAD>RV>YMW>AR>FMW
Ca^{2+}	28.59	23.70	10.20	86.05	16.23	RV>AR>FMW>SAD>YMW
Mg^{2+}	7.24	3.49	1.10	58.65	10.63	RV>YMW>FMW>AR>SAD
K^+	11.65	6.30	3.10	41	10.66	RV>YMW>SAD>FMW>AR
Na^+	27.15	7.90	0.69	179	39.25	SAD>RV>YMW>FMW>AR
F^-	0.24	0.20	0.05	1.20	0.27	RV>AR>FMW>SAD>YMW
Br^-	0.38	0.20	0.20	2.07	0.49	YMW>RV>AR>FMW>SAD
Total B	0.25	0.13	0.005	3.92	0.69	SAD>RV>FMW>YMW>AR
PO_4^{3-}	1.38	0.20	0.10	17.48	3.54	RV>FMW>AR>YMW>SAD
Total N	12.59	0.90	0.01	146	32.16	YMW>FMW>AR>SAD>RV
NO_3^-	6.00	2.01	0.02	44.30	9.95	YMW>FMW>SAD>AR>RV
NH_3	8.17	0.57	0.04	103	20.38	YMW>FMW>AR>SAD>RV
Al^{3+}	0.38	0.07	0.02	8.23	1.47	RV>SAD>FMW>YMW>AR
As^{3-}	0.01	0.003	0.0002	0.08	0.01	RV>SAD>YMW>FMW>AR
Total Fe	0.19	0.02	0.005	4.17	0.75	RV>FMW>SAD>AR>YMW
Total Cu	0.01	0.003	0.0005	0.06	0.01	SAD>AR>FMW>YMW>RV
Ba^{2+}	0.06	0.05	0.002	0.22	0.05	YMW>FMW>AR>SAD>RV
Cs^+	0.06	0.04	0.0005	0.27	0.06	YMW>FMW>RV>AR>SAD
Li^+	0.02	0.02	0.0005	0.11	0.02	SAD>FMW>AR>RV>YMW
Total Mo	0.01	0.001	0.0005	0.17	0.03	RV>AR>YMW>FMW>SAD
Sr^{2+}	0.15	0.13	0.005	0.40	0.10	FMW>YMW>AR>SAD>RV
Rb^+	0.005	0.001	0.0005	0.03	0.01	RV>FMW>YMW>AR>SAD
Total Ti	0.01	0.003	0.003	0.02	0.01	YMW>SAD>RV>FMW>AR
Total U	0.003	0.001	0.00005	0.01	0.003	RV>FMW>SAD>AR>YMW
Total V	0.01	0.001	0.0005	0.18	0.03	RV>FMW>YMW>SAD>AR
Zn^{2+}	0.06	0.01	0.005	1.44	0.26	YMW>FMW>RV>SAD>AR
Total Mn	0.16	0.02	0.001	3.01	0.54	YMW>SAD>FMW>RV>AR
Ni^{2+}	0.01	0.001	0.0005	0.03	0.01	FMW>YMW>RV>SAD>AR
Total Pb	0.001	0.0001	0.00005	0.01	0.002	SAD>FMW>RV>YMW>AR
Se^{2-}	0.0004	0.0003	0.00005	0.002	0.0005	RV>YMW>FMW>SAD>AR

[a] Total alkalinity as $CaCO_3$; [b] non carbonate alkalinity; [c] Rock Valley; [d] western side of Yucca Mountain; [e] Fortymile Wash; [f] southern Amargosa Desert; [g] Amargosa River.

Table 5.9: Summary of Groundwater Chemical Constituents (in mg/l, except otherwise indicated), and it is Distribution within the Site Locations.

Groundwater, 89 samples						
Element (ppm)	Mean	Median	Minimum	Maximum	Std.Dev.	Element distribution per location
TDS	423.47	336.27	196.70	1132.30	221.89	AR [g] >SAD [f] >RV [c] >YMW [d] >FMW [e]
T. Alk as $CaCO_3$ [a]	183.39	152.55	81.19	790.62	100.41	AR>RV>SAD>YMW>FMW
Non car. Alk [b] %	82.95	82.96	24.39	99.82	11.36	YMW>FMW>RV>SAD>AR
Cl^-	16.76	9.90	5.10	79.10	15.80	AR>SAD>RV>YMW>FMW
SO_4^{2-}	71.76	34.70	5	644	81.66	AR>SAD>RV>FMW>YMW
Ca^{2+}	25.20	20.80	0.15	158	23.15	AR>RV>ASD>FMW>YMW
Mg^{2+}	7.90	2.70	0.01	86.90	12.16	AR>SAD>RV>FMW>YMW
K^+	8.11	5.93	1	63.40	8.15	SAD>AR>RV>FMW>YMW
Na^+	83.01	78.60	31.30	339	44.17	AR>SAD>RV>YMW>FMW
F^-	2.48	2.10	0.50	6.70	1.41	YMW>AR>SAD>RV>FMW
Total B	0.08	0.01	0.01	0.90	0.15	AR>FMW>YMW>SAD>RV
PO_4^{3-}	0.15	0.10	0.01	1.26	0.19	AR>FMW>SAD>YMW>RV
Total N	1.40	0.30	0.14	9.54	2.12	FMW>AR>YMW>SAD>RV
NO_3^-	0.62	0.50	0.05	2.17	0.34	FMW>SAD>YMW>RV>AR
NH_3	1.64	0.24	0.17	11.60	2.63	FMW>AR>YMW>SAD>RV
Al^{3+}	0.12	0.05	0.001	5.58	0.59	FMW>YMW>AR>SAD>RV
As^{3-}	0.004	0.001	0.001	0.03	0.01	FMW>AR>YMW>SAD>RV
Total Fe	0.32	0.01	0.01	19.74	2.11	AR>FMW>YMW>SAD>RV
Total Cu	0.01	0.01	0.0004	0.33	0.03	YMW>FMW>AR>SAD>RV
Ba^{2+}	0.01	0.002	0.002	0.26	0.03	FMW>AR>YMW>SAD>RV
Li^+	0.05	0.001	0.001	0.64	0.12	FMW>AR>YMW>SAD>RV
Total Mo	0.01	0.001	0.001	0.33	0.04	FMW>YMW>AR>SAD>RV
Sr^{2+}	0.18	0.02	0.001	2.29	0.39	RV>AR>FMW>YMW>SAD
Rb^+	0.01	0.001	0.001	0.20	0.02	AR>FMW>YMW>SAD>RV
Total Ti	0.02	0.003	0.001	0.70	0.08	YMW>FMW>AR>SAD>RV
Total U	0.001	0.0001	0.0001	0.01	0.002	AR>YMW>SAD>FMW>RV
Total V	0.01	0.001	0.001	0.34	0.04	YMW>FMW>AR>SAD>RV
Zn^{2+}	0.02	0.01	0.001	0.52	0.06	YMW>AR>FMW>SAD>RV
Total Mn	0.02	0.003	0.003	0.38	0.07	AR>YMW>FMW>SAD>RV
Ni^{2+}	0.01	0.001	0.001	0.51	0.05	YMW>AR>FMW>SAD>RV
Total Pb	0.001	0.0001	0.0001	0.05	0.01	AR>FMW>YMW>SAD>RV
Se^{2-}	0.001	0.0001	0.0001	0.03	0.003	AR>FMW>YMW>SAD>RV

[a] Total alkalinity as $CaCO_3$; [b] non-carbonate alkalinity; [c] Rock Valley; [d] western side of Yucca Mountain; [e] Fortymile Wash; [f] southern Amargosa Desert; [g] Amargosa River.

5.5.3.2 Box plots

Box plots (Figures 5.4 -5.30) are applied on the major ion concentrations, TDS, heavy metals, and nutrients after grouped by sample type (precipitation, sediment, runoff, and groundwater) and by site location (southern Amargosa Desert, Fortymile Wash, Amargosa River, Rock Valley, and western side of Yucca Mountain). Southern Amargosa Desert and Rock Valley have two site locations for each one, and the samples collected from these areas were not enough

to make successful comparison with other location. However, it is included with the box plot graphs below.

Box plots of the different sample types per location show three potential clusters of the sample's chemical constituents. First group presents the chemicals that have scavenged, where the chemical constituents concentrated in the precipitation is greater than that in runoff and sediment (i.e., precipitation > runoff > sediment). Second group presents the chemicals that have leached, and where the chemical constituents concentrated in the sediment is higher than that concentrated in the precipitation, whereas the concentrations in runoff is in the middle (i.e., sediment > runoff > precipitation). Finally, third group presents nutrients, where the chemical constituents that concentrated in the runoff samples is lower than that in sediment and precipitation samples (i.e., precipitation > sediment > runoff).

Figure 5.4, shows significant evaporative concentration occurs between precipitation and groundwater. Chloride is a conservative ion and thus tracks evaporative concentration of waters. Also, Chloride is highly soluble and has few geologic sources, making it an excellent tracer of evaporative concentration. Concentrations of chloride are approximately similar in the runoff and groundwater in Fortymile Wash, western side of Yucca Mountain, and southern Amargosa Desert even when the data shows that the groundwater has higher salinity (TDS). The chloride trend can be described as groundwater ≈ runoff > sediment > precipitation or groundwater ≈ runoff > precipitation > sediment, when the sediment leached the chloride during the storm events. This is consistent with the hypothesis that infiltration of surface runoff from storms has been a dominant source of groundwater in this area.

Figure (5.5) shows the box plots of uranium grouped by sample type and site location. Uranium presents group one (scavenged) in all locations.

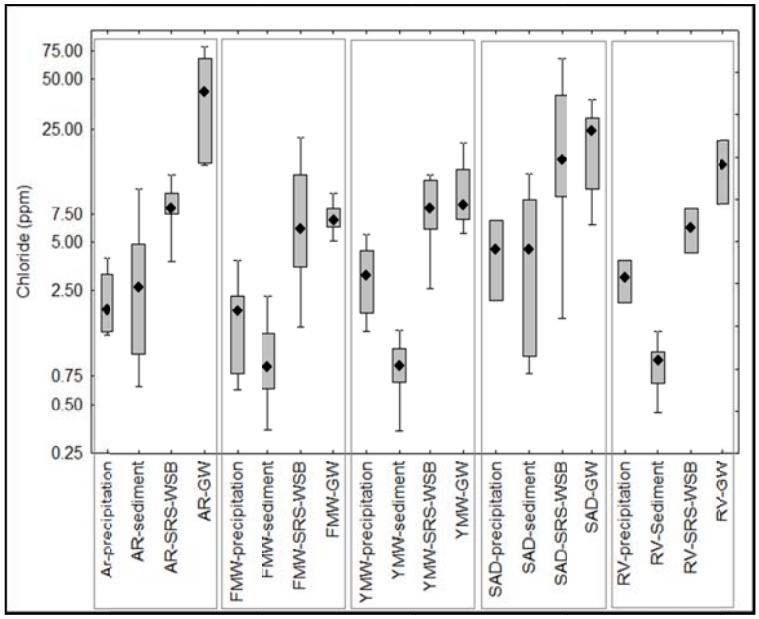

Figure 5.4: Box plots of chloride in the Amargosa Desert region grouped by sample type and site location.

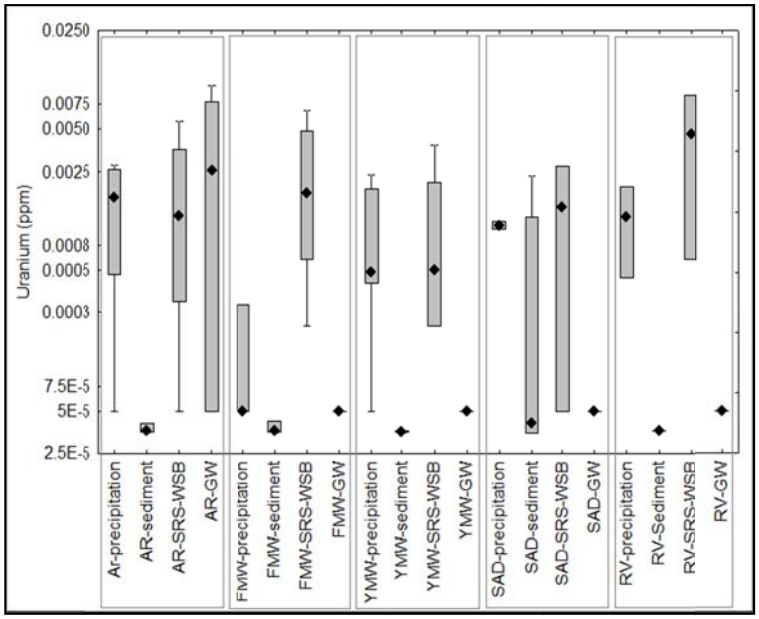

Figure 5.5: Box plots of uranium in the Amargosa Desert region grouped by sample type and site location.

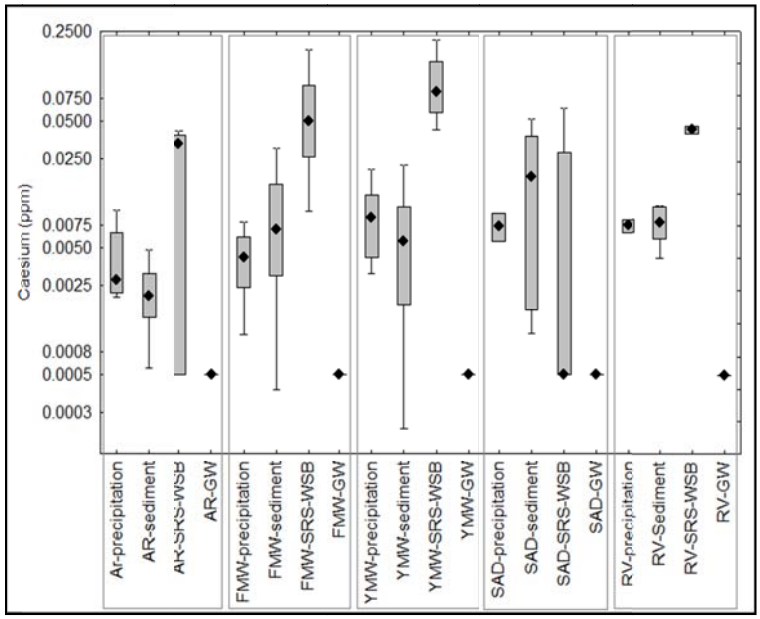

Figure 5.6: Box plots of cesium in the Amargosa Desert region grouped by sample type and site location.

Cesium (Figure 5.6) is scavenged in Amargosa River, western side of Yucca Mountain, and Rock Valley; it is strongly leached in Fortymile Wash, and it follows the nutrient group in the southern Amargosa Desert.

TDS, alkalinity, and non-carbonate alkalinity (Figures 5.7-5.9) follow the leached group in all locations. TDS and alkalinity increase greatly between precipitation and sediment, decreasing between sediment and runoff, and then increasing between runoff and groundwater. Alkalinity trend may be caused by precipitation and dissolution equilibrium of calcium carbonate, carbonate rocks, and from silicate mineral weathering reactions, which increase both sodium and alkalinity, and this matches with White (1979). The non-carbonate alkalinity forms (40-65%), (74-92%), (50-75%), and (75-95%) from the total alkalinity in the precipitation, sediment, runoff, and groundwater, respectively. Increasing of non-carbonate alkalinity in the groundwater may be caused by the Na/HCO3 aquifer. The H_2CO_3 contributes H^+, which attacks silicate minerals resulting in the release of cations (M^+) and the formation of bicarbonate by the reaction:

$$(\boldsymbol{Silicate\ rock})(\boldsymbol{M^+}) + \boldsymbol{H_2CO_3}) \rightarrow (\boldsymbol{Silicate\ rock})(\boldsymbol{H^+}) + \boldsymbol{M^+} + \boldsymbol{HCO_3^-} \quad \boldsymbol{Eq.\ 5.3}$$

Sodium (Figure 5.10) follows the leached group in the Amargosa River location, where, it increases in amount between precipitation and sediment, then decreases from sediment to runoff, and then increases again from runoff to groundwater. Sodium becomes strongly leached in the other locations, where it increases in amount between precipitation, sediment, runoff, and groundwater. Most of the alkalinity in the area's groundwater is non-carbonate (Na+K)-HCO_3, derived from weathering of silicate rocks rather than dissolution of carbonate rocks, and would account for this increase in sodium. Sodium also may originate as a result of ion exchange with calcium in infiltrating water.

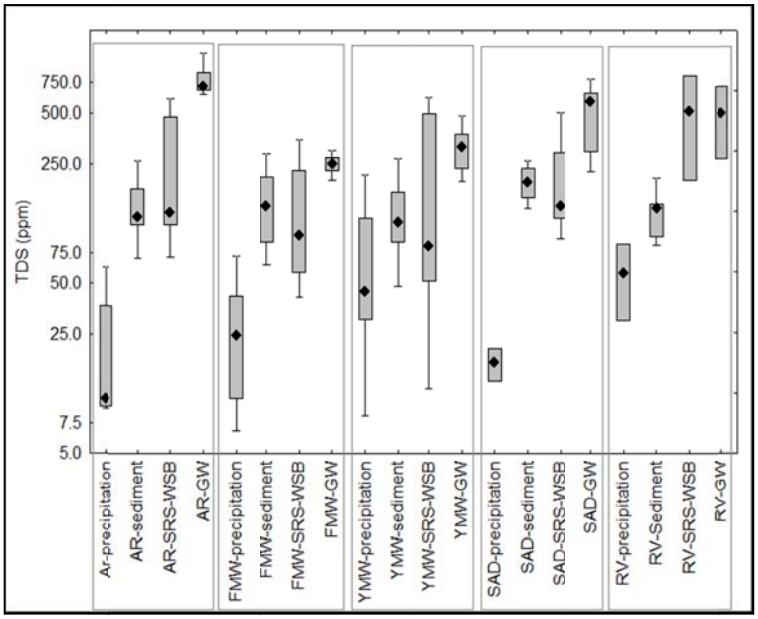

Figure 5.7: Box plots of TDS in the Amargosa Desert region grouped by sample type and site location.

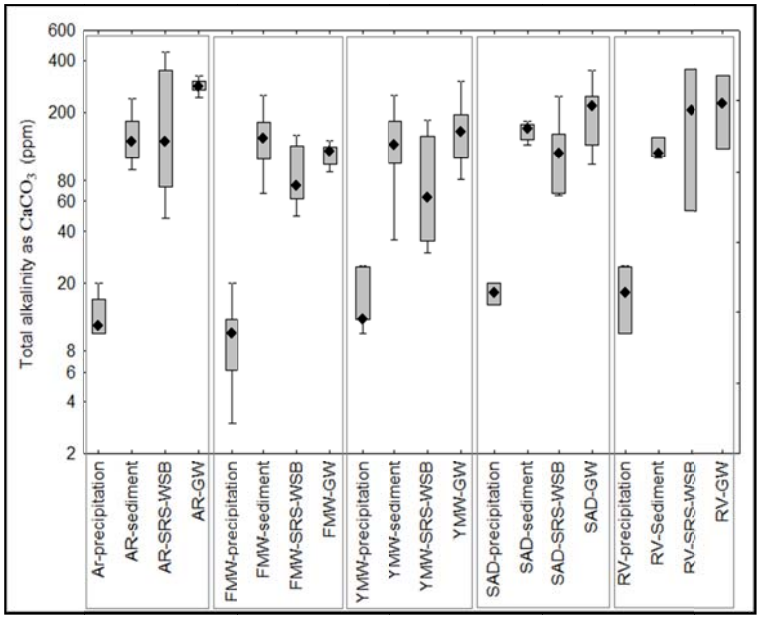

Figure 5.8: Box plots of total alkalinity in the Amargosa Desert region grouped by sample type and site location.

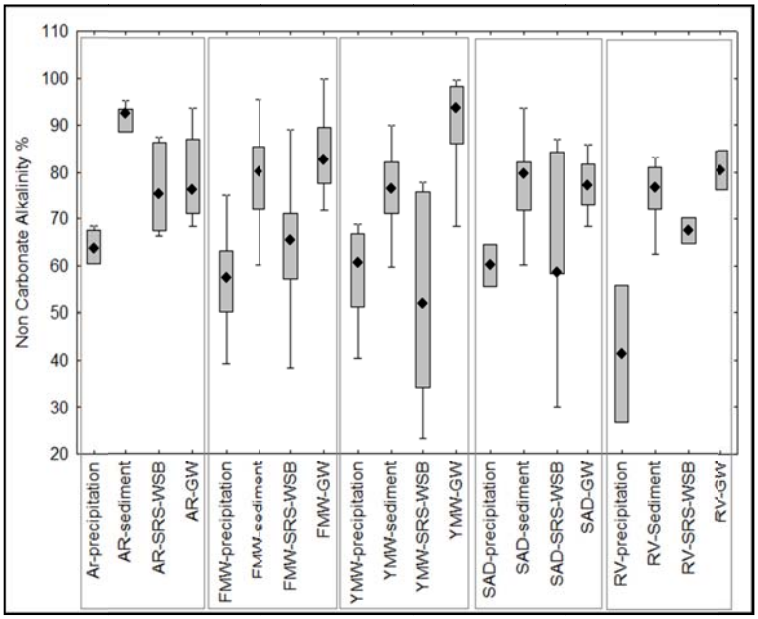

Figure 5.9: Box plots of non-carbonate alkalinity in the Amargosa Desert region grouped by sample type and site location.

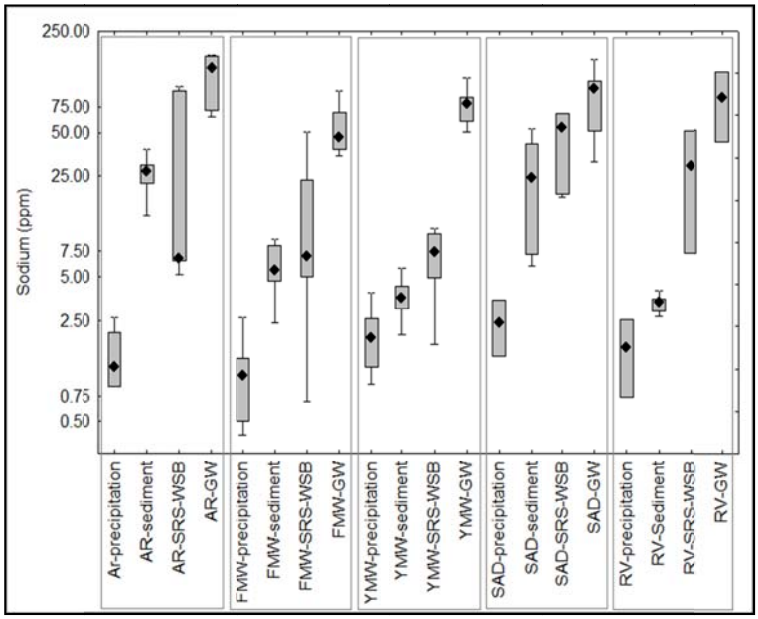

Figure 5.10: Box plots of sodium in the Amargosa Desert region grouped by sample type and site location.

Figure 5.11, shows the box plots of calcium concentrations grouped by sample type and site location. Calcium is increasing between precipitation and sediment in all locations; calcium is leached or strongly leached in all locations. It is increasing between sediment, runoff, and groundwater in the Amargosa River; increasing between sediment and runoff then decreasing between runoff and groundwater in Rock valley; it is almost the same in sediment and runoff, and then decreasing between sediment and groundwater in Fortymile Wash and western side of Yucca Mountain; decreasing between sediment and runoff and then increasing from runoff to groundwater in the southern Amargosa Desert. Weathering causes enrichment of calcium concentrations, in the form of $CaCO_3$ originally derived from carbonate rocks along the flow paths.

Figure 5.12, shows the box plots of magnesium in the different categories. Magnesium is strongly leached in all locations; it is increasing from precipitation to groundwater. Increasing of magnesium in the groundwater may be caused by the (Ca+Mg)-HCO3 carbonate aquifer.

Figure 5.13, shows the box plots of potassium concentrations in the different categories, with potassium increasing greatly between the precipitation and sediment in all locations, it is decreasing slightly between sediment and runoff, and then again increasing slightly from the runoff to groundwater in the southern Amargosa Desert and Amargosa River following leached group; it is increasing from sediment to runoff then decreasing from runoff to groundwater in the western side of Yucca Mountain and Rock Valley following the leached group; also, it is decreasing from sediment to groundwater in Fortymile Wash following the leached group.

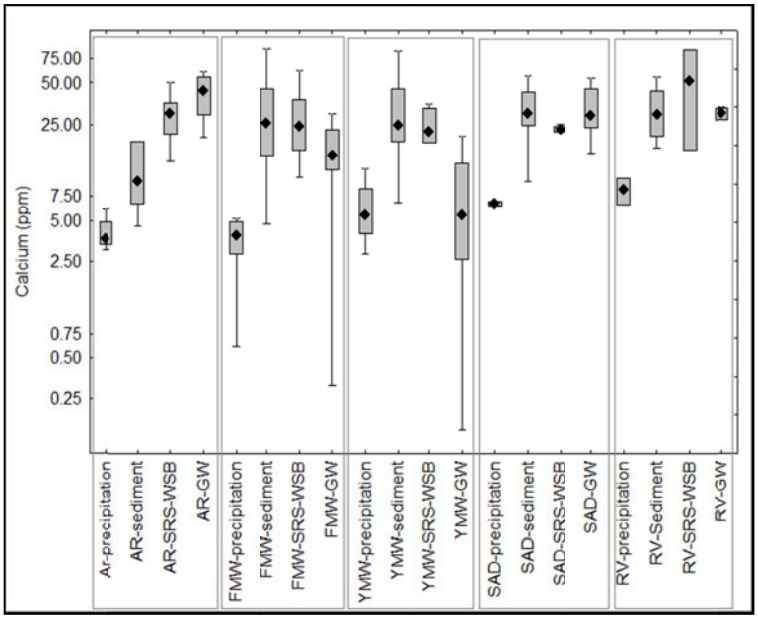

Figure 5.11: Box plots of calcium in the Amargosa Desert region grouped by sample type and site location.

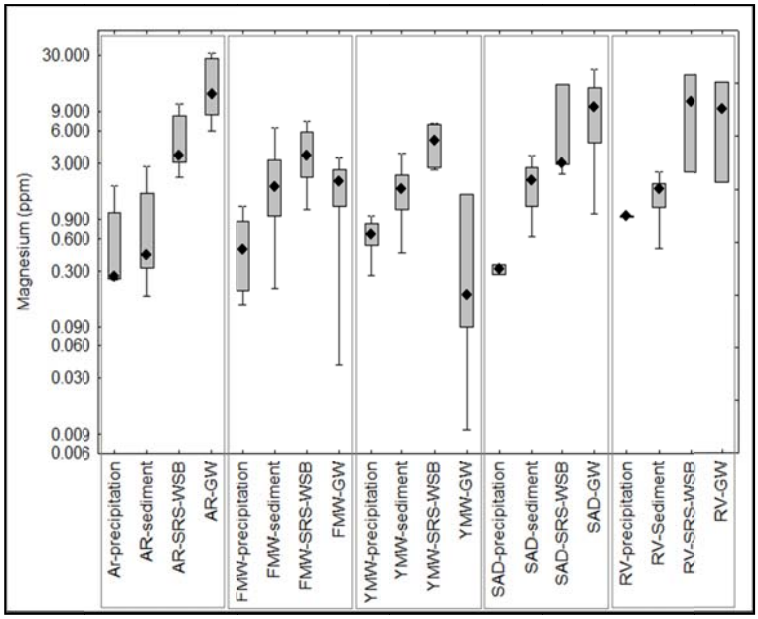

Figure 5.12: Box plots of magnesium in the Amargosa Desert region grouped by sample type and site location.

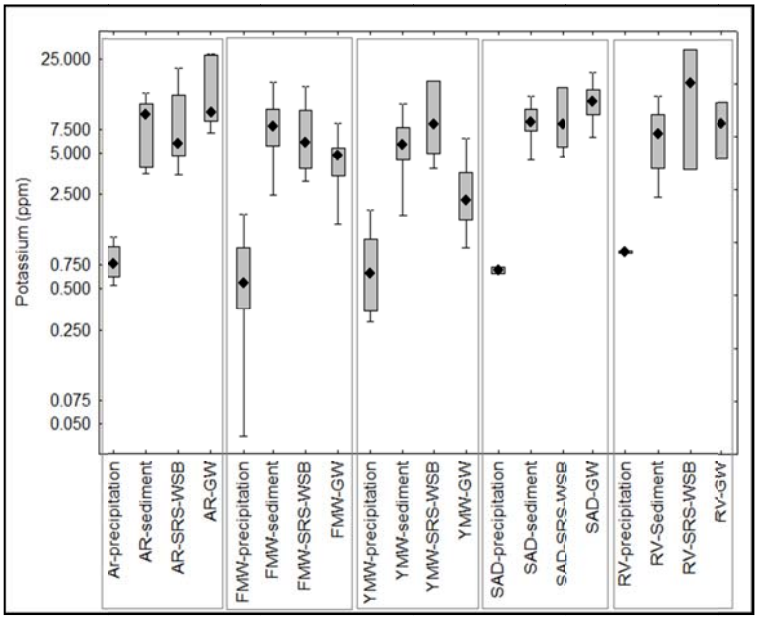

Figure 5.13: Box plots of potassium in the Amargosa Desert region grouped by sample type and site location.

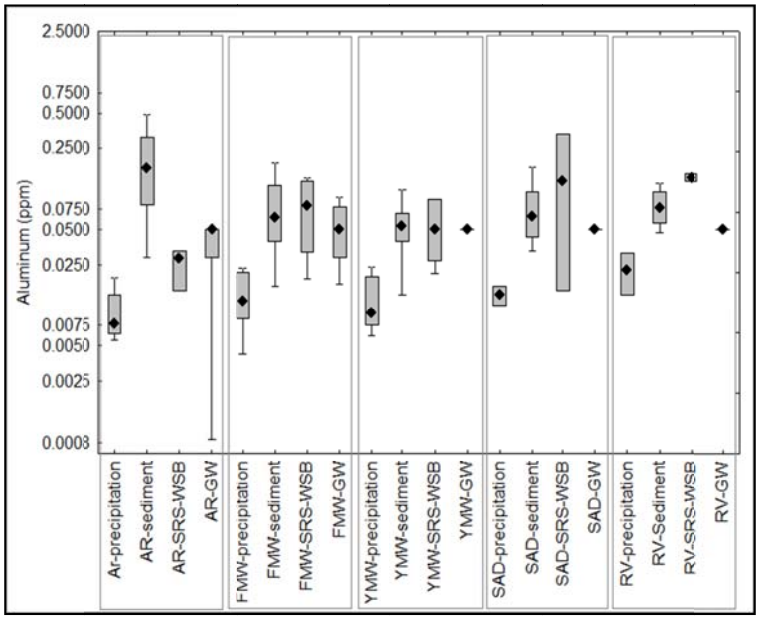

Figure 5.14: Box plots of aluminum in the Amargosa Desert region grouped by sample type and site location.

Aluminum (Figure 5.14) is increasing between precipitation and sediment in all locations, and then it is strongly leached in all locations. It is increasing between sediment and runoff in Fortymile Wash, southern Amargosa Desert, and Rock Valley, and decreases between runoff and groundwater in Fortymile Wash. In Amargosa River, aluminum decreases between sediment and runoff then increasing between runoff and groundwater following the leached group. Aluminum concentration in groundwater is not clear in western side of Yucca Mountain, southern Amargosa Desert, and Rock Valley because of the lake of data.

Figure 5.15, shows the box plots of iron concentrations in the different categories. Iron trend is not clear in groundwater in the western side of Yucca Mountain, southern Amargosa Desert, and Rock Valley because of the lake of data. Iron is increasing between precipitation and sediment in all locations; strongly leached in Rock Valley, and it is leached in the remaining locations; it is decreasing between runoff and groundwater in Fortymile Wash, and increasing between runoff and groundwater in the Amargosa River.

Figure 5.16, shows the box plots of lithium in the different categories. Lithium increases from precipitation to groundwater in all locations, and it is strongly leached in all locations.

Figure 5.17, shows the box plots of barium in the different categories. In western side of Yucca Mountain, barium decreases between precipitation and sediment, then increasing between sediment and runoff, and then decreases from runoff and groundwater following scavenged group. In the other locations, it is strongly leached.

Figure 5.18, shows the box plots of strontium in the different categories. Strontium is strongly leached in Amargosa River, Fortymile Wash, and western side of Yucca Mountain; it increases from precipitation to runoff, and then decreasing between runoff and groundwater in Fortymile Wash and western side of Yucca Mountain.

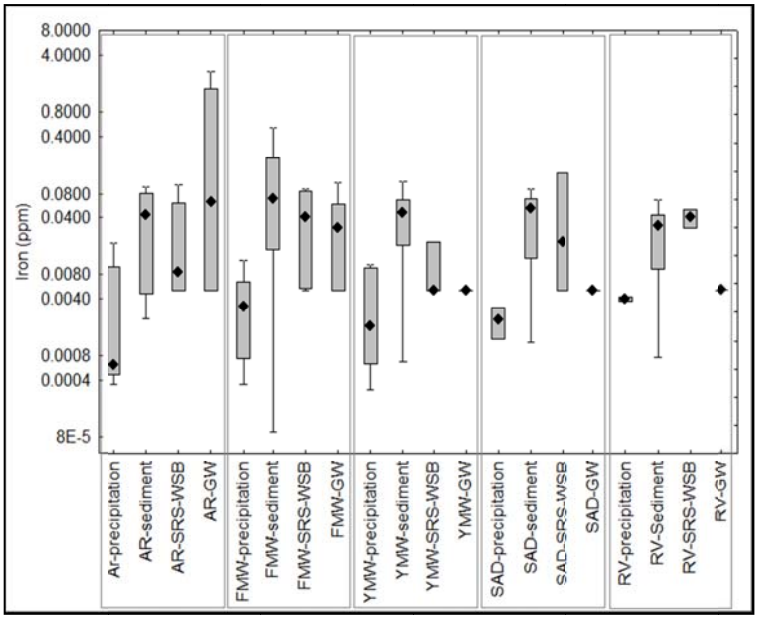

Figure 5.15: Box plots of iron in the Amargosa Desert region grouped by sample type and site location.

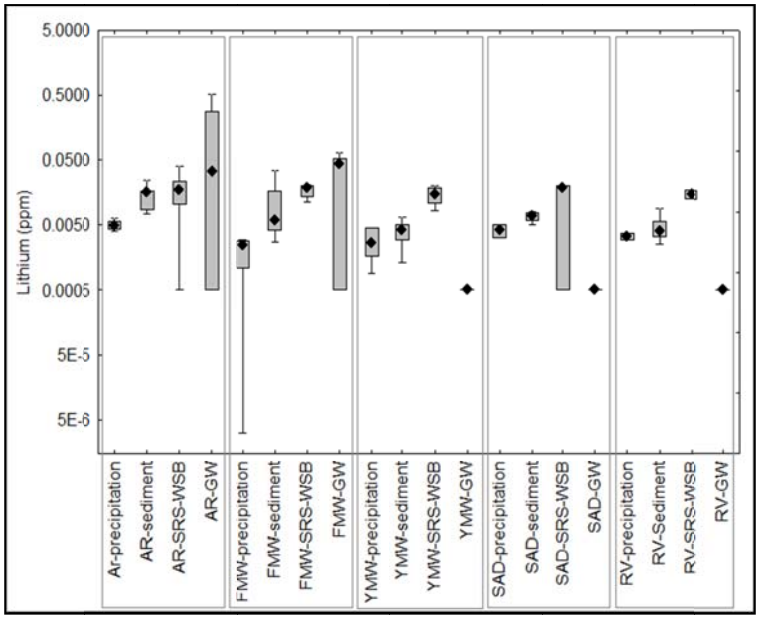

Figure 5.16: Box plots of lithium in the Amargosa Desert region grouped by sample type and site location.

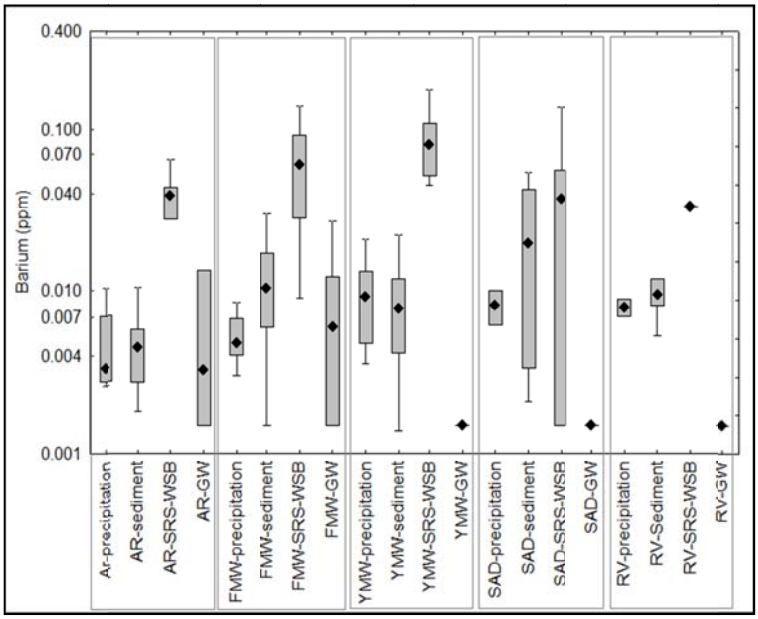

Figure 5.17: Box plots of barium in the Amargosa Desert region grouped by sample type and site location.

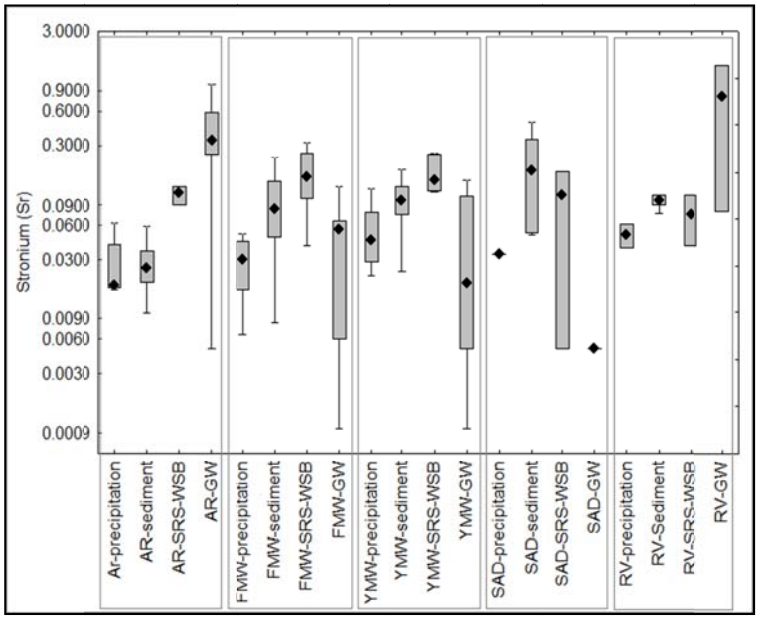

Figure 5.18: Box plots of strontium in the Amargosa Desert region grouped by sample type and site location.

Strontium is increasing between runoff and groundwater in the Amargosa River. In the southern Amargosa Desert and rock Valley, strontium increases between precipitation and sediment, then decreases from sediment to groundwater following leached group.

Total nitrogen (Figure 5.19) follows leached group in the Amargosa River and Fortymile Wash, where it is increasing between precipitation and sediment, and then decreasing between sediment and runoff; it is strongly leached in the western side of Yucca Mountain, where increasing from precipitation to runoff; and follows nutrient group in the southern Amargosa Desert and Rock Valley, where it is concentration in the runoff is lower than that in sediment and precipitation.

Figure 5.20, shows the box plots of nitrate in the different categories. Nitrate increases between precipitation and sediment in all locations, and it is strongly leached in western side of Yucca Mountain, and then follows nutrient group in the remaining locations.

Figure 5.21, shows the box plots of sulfate in the different categories. Groundwater contains the greatest amount of sulfate in all locations. The increase in sulfate moving from surface runoff to groundwater may be due to longer flow paths which allow more water/rock interaction and hydrothermal alteration of older volcanic rocks, i.e. secondary mineralization believed to have formed under closed conditions. Sulfate strongly leached in the Amargosa River and southern Amargosa Desert. In Fortymile Wash, western side of Yucca Mountain, and Rock Valley, sulfate decreases between precipitation and sediment, and then increases between sediment and runoff following the scavenged pattern.

Fluoride (Figure 5.22) follows the scavenged type in all locations, where decreases between precipitation and sediment, and then increases from sediment to groundwater. The greatest amount of fluoride concentrates in the groundwater in all locations.

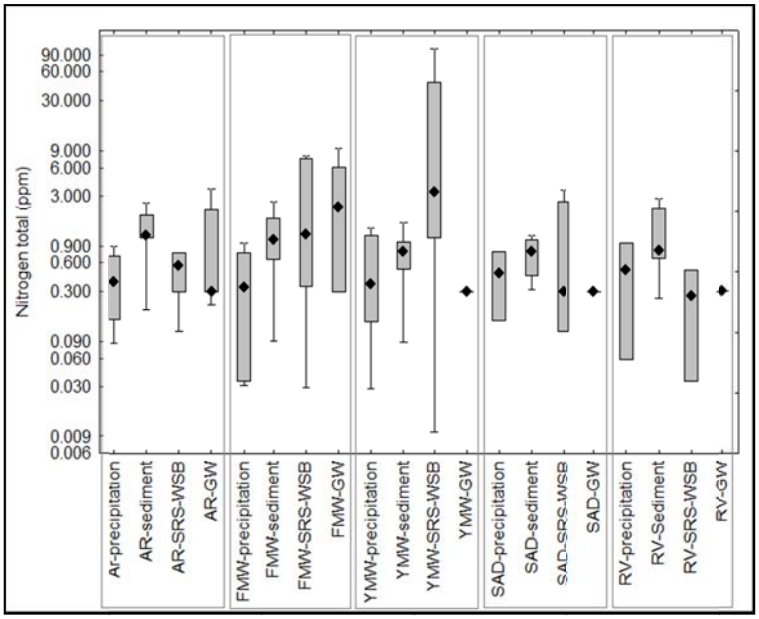

Figure 5.19: Box plots of nitrogen total in the Amargosa Desert region grouped by sample type and site location.

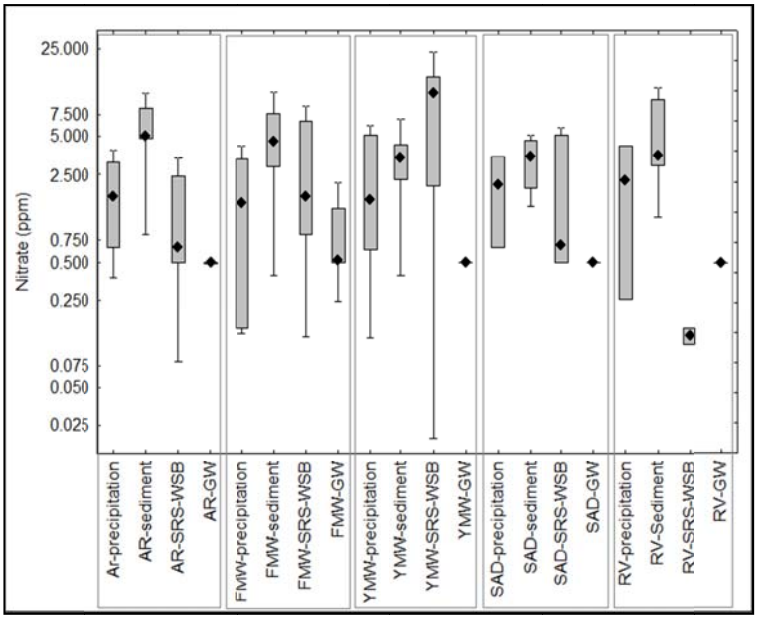

Figure 5.20: Box plots of nickel in the Amargosa Desert region grouped by sample type and site location.

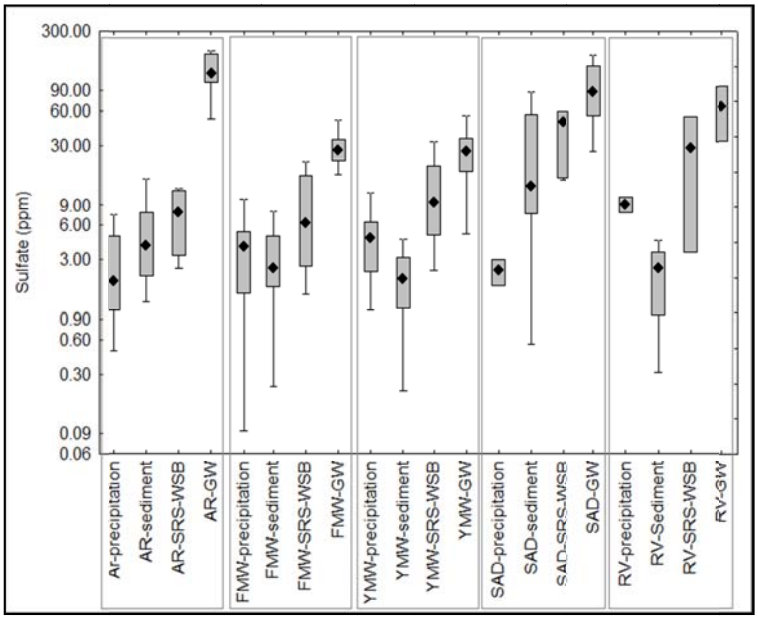

Figure 5.21: Box plots of sulfate in the Amargosa Desert region grouped by sample type and site location.

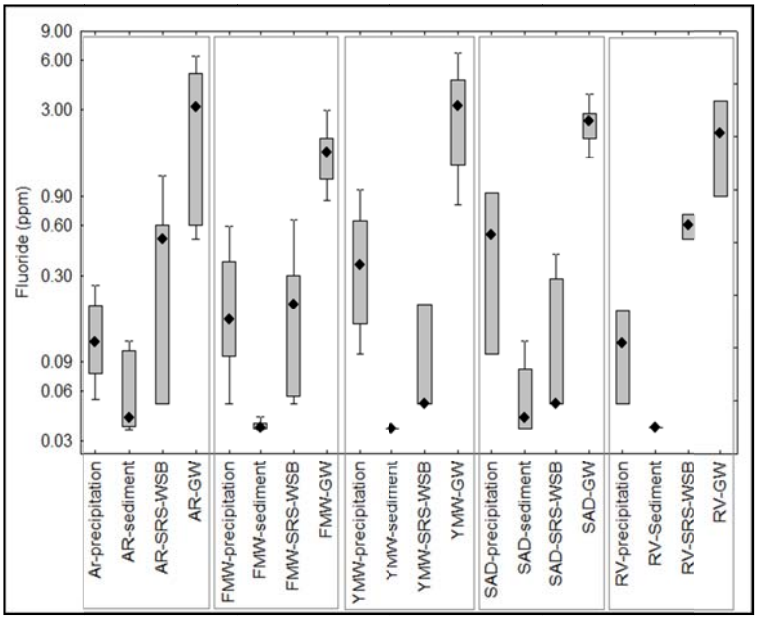

Figure 5.22: Box plots of fluoride in the Amargosa Desert region grouped by sample type and site location.

The general type of arsenic trend (Figure 5.23) in the Amargosa Desert area is nutrient. Arsenic increases between precipitation and sediment, and then decreases between sediment and runoff following the leached pattern in the southern Amargosa Desert; in the remaining locations it is decreasing from precipitation to groundwater following the nutrient pattern.

Phosphate (Figure 5.24) is scavenged in Fortymile Wash, western side of Yucca Mountain, and Rock Valley, and it is following the nutrient pattern in the southern Amargosa Desert and Amargosa River.

Copper (Figure 5.25) is following the nutrient pattern in the Amargosa River, and then is leached in the remaining locations.

Figure 5.26, shows the box plots of manganese in the different categories. Manganese is scavenged in Fortymile Wash and Rock Valley, strongly leached in the western side of Yucca Mountain and southern Amargosa Desert, and follows the nutrient pattern in the Amargosa Desert.

Figure 5.27, shows the box plots of molybdenum in the different categories. Molybdenum is scavenged in Fortymile Wash, western side of Yucca Mountain, and Rock Valley, strongly leached in the southern Amargosa Desert and Amargosa River.

Figure 5.28, shows the box plots of rubidium in the different categories. Rubidium is scavenged in the western side of Yucca Mountain, southern Amargosa Desert, and Rock Valley, leached in the Amargosa River and Fortymile Wash.

Figure 5.29, shows the box plots of vanadium in the different categories. Vanadium strongly leached in Rock Valley, and follows the nutrient group in the other locations.

Figure 5.30, shows the box plots of zinc in the different categories. Zink is leached in the Amargosa River, and scavenged in the other locations.

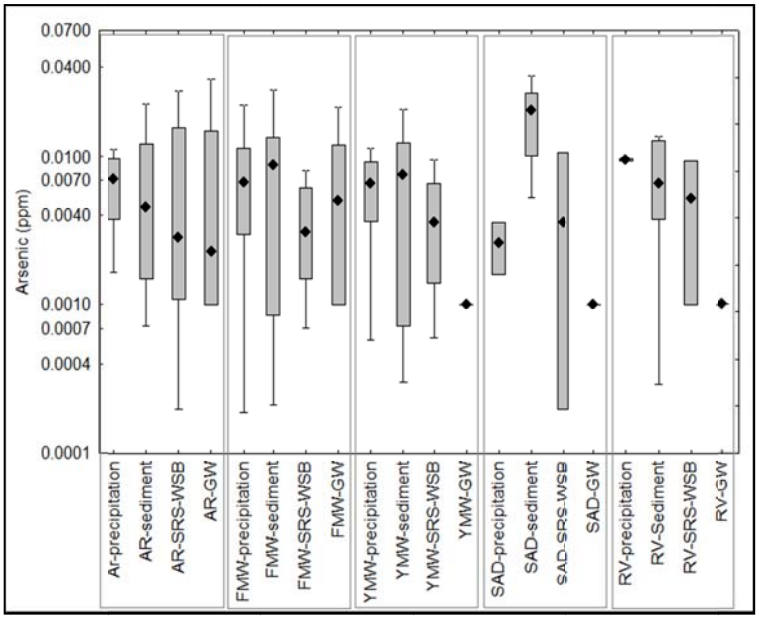

Figure 5.23: Box plots of arsenic in the Amargosa Desert region grouped by sample type and site location.

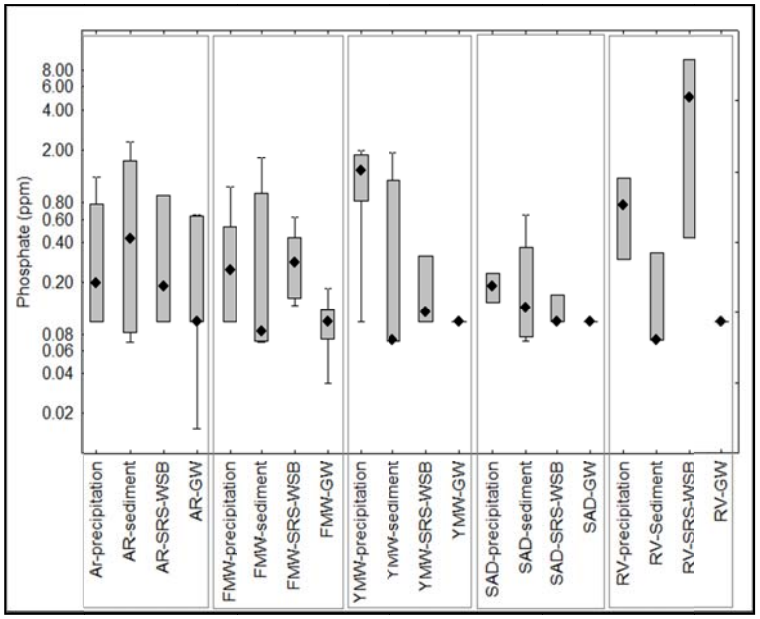

Figure 5.24: Box plots of phosphate in the Amargosa Desert region grouped by sample type and site location.

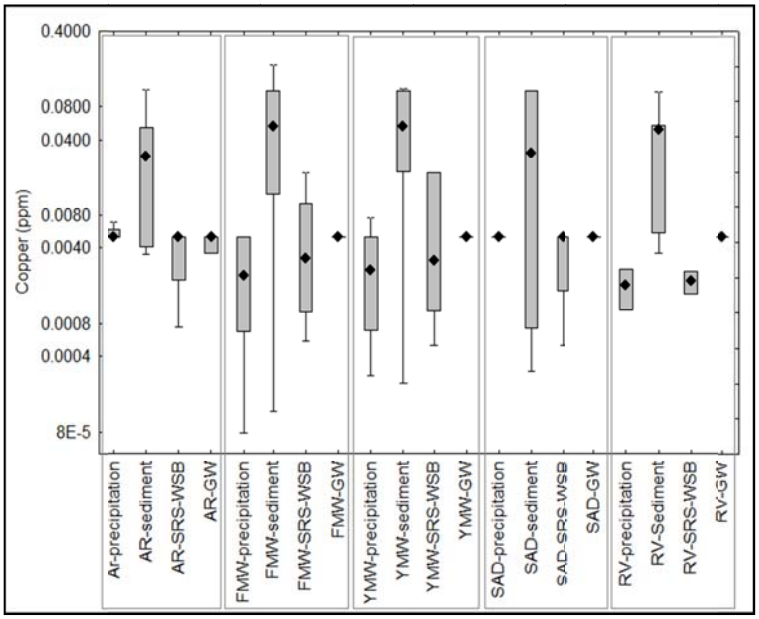

Figure 5.25: Box plots of copper in the Amargosa Desert region grouped by sample type and site location.

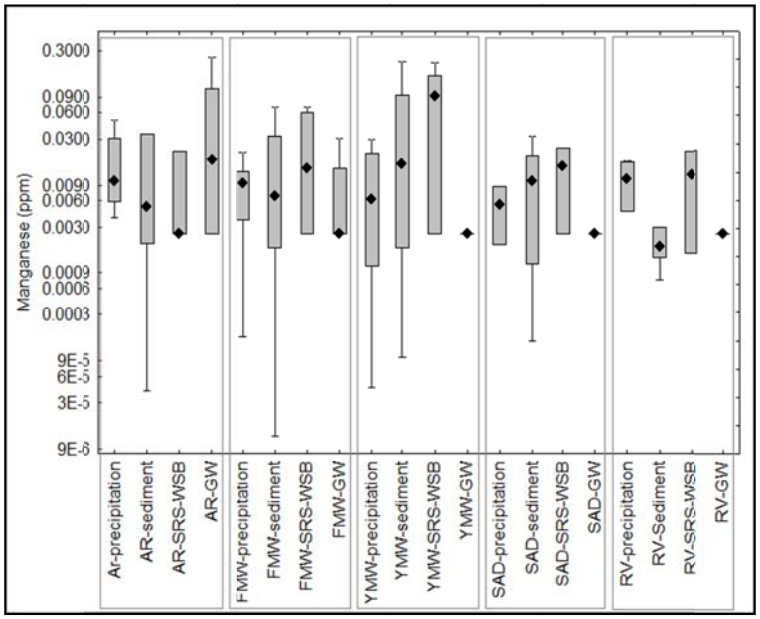

Figure 5.26: Box plots of manganese in the Amargosa Desert region grouped by sample type and site location.

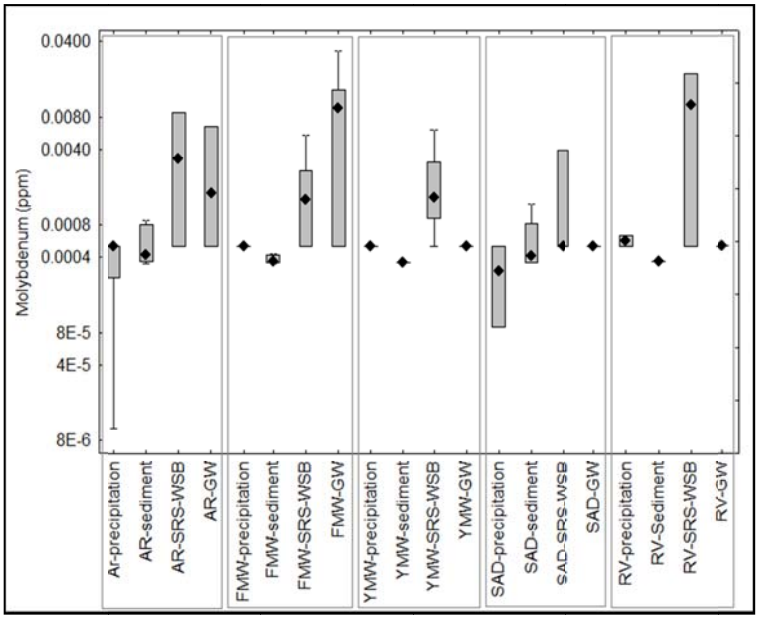

Figure 5.27: Box plots of molybdenum in the Amargosa Desert region grouped by sample type and site location.

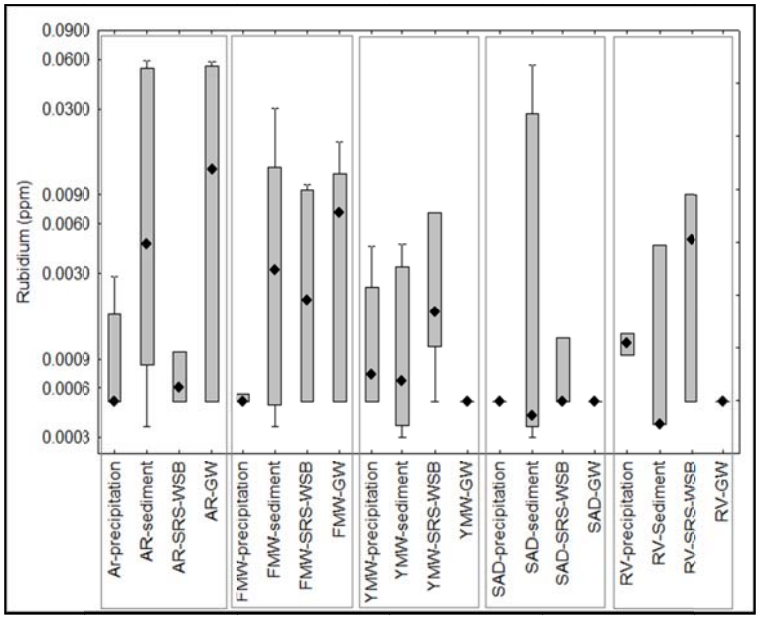

Figure 5.28: Box plots of rubidium in the Amargosa Desert region grouped by sample type and site location.

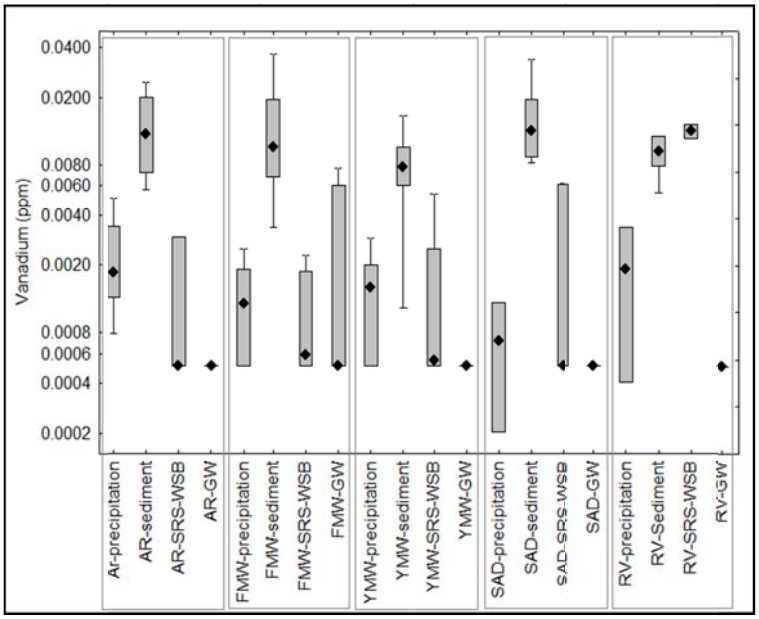

Figure 5.29: Box plots of vanadium in the Amargosa Desert region grouped by sample type and site location.

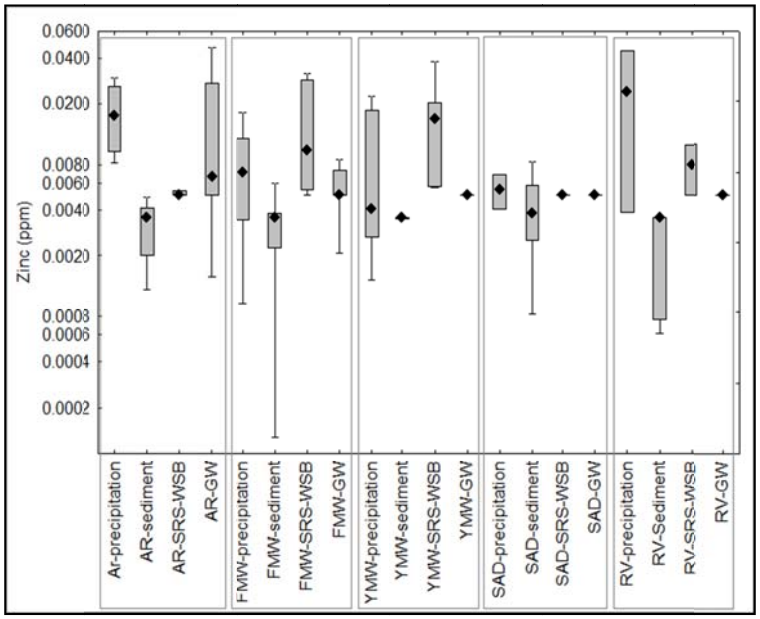

Figure 5.30: Box plots of zinc in the Amargosa Desert region grouped by sample type and site location.

5.5.3.3 Analysis of variance (ANOVA)

ANOVA is applied on the chemical constituents that grouped by all sample types with all locations (test 1 in Table 5.10), runoff and groundwater in all locations (test 2, Table 5.10), and runoff and groundwater in Fortymile Wash, Rock Valley, and western side of Yucca Mountain (test 3, Table 5.10). ANOVA indicates that some chemical constituents are statistically significant within different locations and sample types like sodium (in test 1, 2, 3), some of it significant within the locations but it is not within the sample types like calcium and magnesium (in test 2), and TDS (in test 3), some of it insignificant within the locations but it is within the sample types like calcium (in test 1), barium and cesium (in test 2), and sulfate (in test 3), and some of it insignificant within the locations and the sample types like aluminum, iron, and nickel (in test 1, 2, 3). ANOVA (in test 2, 3) indicates that chloride concentrations are statistically insignificant between runoff and groundwater, and this is consistent with the hypothesis that infiltration of surface runoff from storms has been a dominant source of groundwater in those locations.

5.5.4 Piper diagram

Figure 5.31 presents a Piper Plot showing precipitation, sediment, surface runoff, and groundwater in the Amargosa Desert Region. A number of evolutionary changes are evident between precipitation, runoff and incorporation into groundwater. The black arrows in the diamond-shaped area give an indication that the runoff is the major source for the groundwater chemistry evolution and then the groundwater recharge. The diagram shows that the precipitation plotting would be referred to as Ca/HCO_3-type water with some mixing. Sediment leached water plotting would be referred to as Ca/HCO_3 to Ca-(Na, K)/HCO_3-type water and no mixing. Runoff plotting would be referred as Ca/HCO_3 to Ca-(Na, K)/HCO_3-type water with some mixing.

Groundwater plotting would be referred as (Na, K)/HCO_3-type water with some mixing. Furthermore, the diagram shows mixed cation-mixed anion-types between precipitation, runoff, and groundwater.

Table 5.10: ANOVA Tests for Significant Differences between Means (Chemical Constituents in mg/l, except otherwise indicated)

	Test 1, all locations Vs all sample types		Test 2, all locations Vs R [c] & G [d]		Test 3, (FMW [e], RV [f], YMW [g]) Vs R & G	
Element	Location	Sample type	Location	Sample type	Location	Sample type
TDS	0.00	0.00	0.00	0.00	0.02	0.09
T. Alk as $CaCO_3$ [a]	0.02	0.00	0.00	0.00	0.01	0.01
Non car. Alk [b] %	0.01	0.00	0.20	0.00	0.84	0.00
Cl^-	0.00	0.00	0.00	0.07	0.14	0.42
SO_4^{2-}	0.00	0.00	0.00	0.00	0.26	0.00
Ca^{2+}	0.60	0.00	0.00	0.52	0.11	0.01
Mg^{2+}	0.00	0.00	0.00	0.84	0.08	0.50
K^+	0.00	0.00	0.00	0.03	0.29	0.00
Na^+	0.00	0.00	0.00	0.00	0.04	0.00
F^-	0.02	0.00	0.00	0.00	0.00	0.00
Br^-	0.90	0.04	0.02	0.00	0.03	0.00
Total B	0.50	0.00	0.71	0.03	0.12	0.44
PO_4^{3-}	0.50	0.00	0.21	0.00	0.15	0.02
Total N	0.40	0.00	0.51	0.00	0.63	0.00
NO_3^-	0.03	0.00	0.27	0.00	0.40	0.00
NH_3	0.06	0.00	0.23	0.01	0.38	0.01
Al^{3+}	0.50	0.16	0.72	0.14	0.59	0.76
As^{3-}	0.14	0.00	0.19	0.20	0.01	0.40
Total Fe	0.05	0.50	0.05	0.61	0.88	0.92
Total Cu	0.25	0.00	0.52	0.88	0.51	0.85
Ba^{2+}	0.34	0.00	0.30	0.00	0.32	0.00
Cs^+	0.04	0.00	0.10	0.00	0.41	0.00
Li^+	0.01	0.00	0.08	0.13	0.77	0.23
Total Mo	0.37	0.01	0.60	0.84	0.96	0.36
Sr^{2+}	0.14	0.02	0.00	0.45	0.05	0.75
Rb^+	0.00	0.00	0.00	0.34	0.04	0.29
Total Ti	0.27	0.00	0.48	0.23	0.92	0.23
Total U	0.29	0.00	0.03	0.00	0.73	0.00
Total V	0.99	0.05	0.82	0.59	0.67	0.64
Zn^{2+}	0.72	0.02	0.82	0.16	0.84	0.17
Total Pb	0.47	0.03	0.17	0.82	0.52	0.71
Total Mn	0.52	0.13	0.09	0.03	0.26	0.02
Ni^{2+}	0.62	0.50	0.66	0.84	0.61	0.95
Se^{2-}	0.16	0.05	0.25	0.51	0.32	0.86

[a] total alkalinity; [b] non-carbonate alkalinity; [c] runoff; [d] groundwater; [e] Fortymile Wash; [f] Rock Valley; [g] western side of Yucca Mountain. Red font means statistically significant.

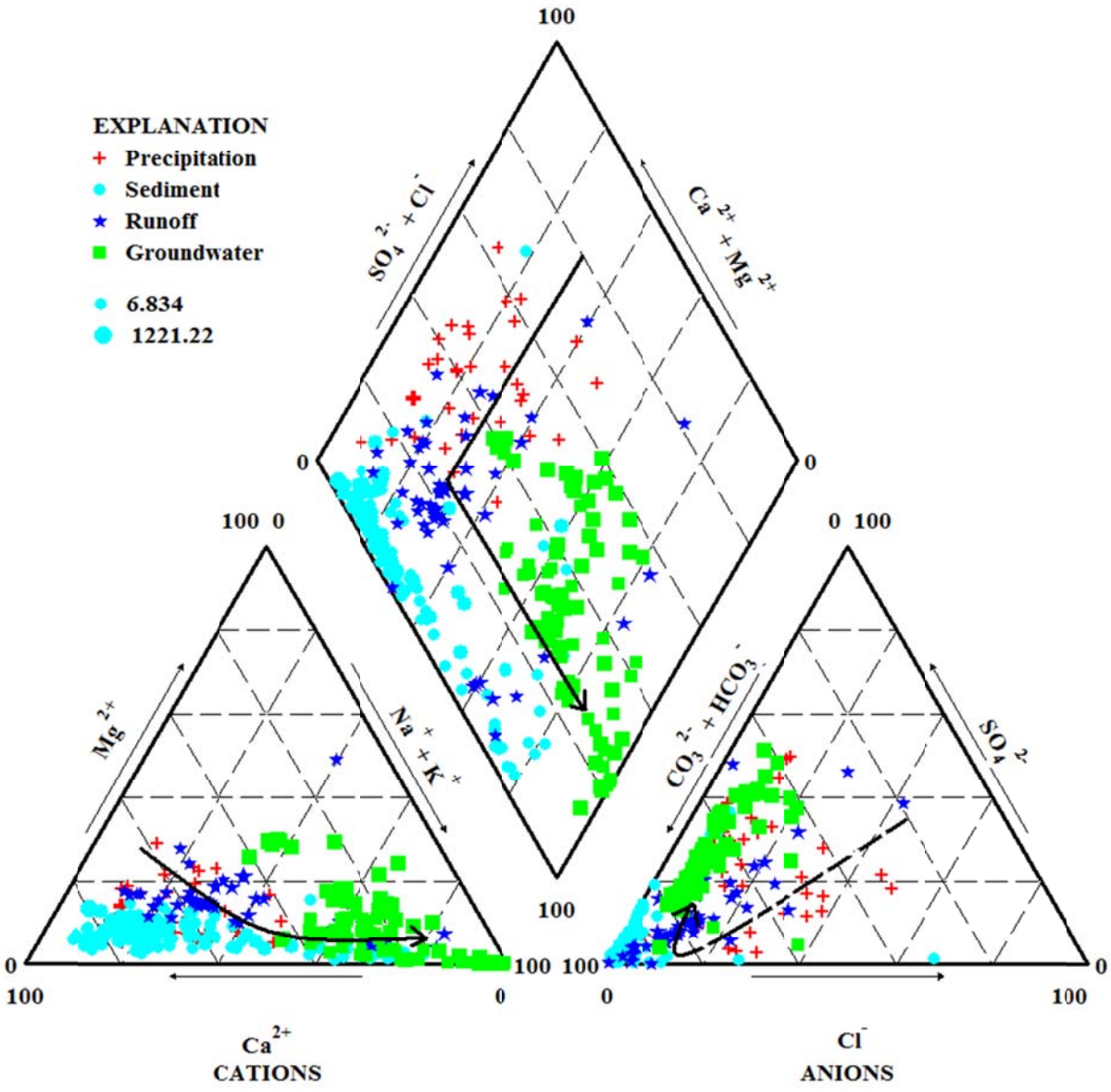

Figure 5.31: Piper diagram for definition of precipitation, sediment, surface runoff, and groundwater chemical types in the Amargosa Desert area. Cation percentages in meq/l plotted on the left triangle, and anion percentages in meq/l plotted on the right triangle; symbol size is proportional to TDS content, the bigger the symbol, the greater the TDS content.

5.5.5 Isotopic composition of water

The stable isotopes of water (^{18}O and ^{2}H) behave chemically conservatively at low temperature (i.e., below 60 °C), and this mean that their concentrations are not affected by geochemical reactions in normal aquifers (Mahlknecht et al., 2004). Therefore, groundwater

preserves its isotopic fingerprint reflecting the history and origin before infiltration, which makes it a useful tool to interpret recharge mechanisms (Mahlknecht et al., 2004). Because of the preferential rainout of heavy isotopes, large rain events are more depleted in isotopic composition than small rain events (Mahlknecht et al., 2004). Furthermore, because of the evaporation during minor rain events, ^{18}O and ^{2}H intensify will be effected by the enrichment of heavy isotopes (Mahlknecht et al., 2004). Evaporation process alters the original ^{18}O-^{2}H relationship of the rainfall resulting in deuterium excess (d-values) lower than eight, as reported in many arid regions (Mahlknecht et al., 2004). During the evaporation of water from the surface or soil water, enrichment of ^{18}O and ^{2}H occurs (Mahlknecht et al., 2004).

Classen (1985) found the $\delta^{2}H$ and $\delta^{18}O$ values of Amargosa Desert groundwater to be depleted compared to Yucca Mountain, this is attributed to colder climate conditions during recharge 10,000 to 15,000 years B.P. Using environmental isotopes, White and Chuma (1987) concluded that Oasis Valley groundwater is a mixture of underflow from Pahute Measa and recharge in the nearby Bulfrog Hills. Ingraham et al. (1989) studied five years of precipitation and spring $\delta^{2}H$ and $\delta^{18}O$ data from the Nevada test site (NTS) and suggested that the local meteoric water line was ($\delta^{2}H = 6.87\ \delta^{18}O - 6.5$), which was slightly $\delta^{18}O$ enriched from the global meteoric water line. Kerrisk (1987) and Matuska and Hess (1989) found that Yucca Mountain well waters were slightly $\delta^{2}H$ depleted from the Ingraham et al. (1989) proposed local meteoric line, and the global meteoric water line, in addition Matuska and Hess (1989) found that water samples in Fortymile Wash were slightly more enriched in terms of $\delta^{18}O$ and $\delta^{2}H$ than Yucca Mountain wells.

Figure 5.32 presents water stable isotope values of precipitation, surface runoff, and groundwater. The distance from the global meteoric water line which is indicative of the degree

of evaporation, is similar for surface runoff and groundwater. The surface runoff samples exhibit a broader spread parallel to the meteoric water line.

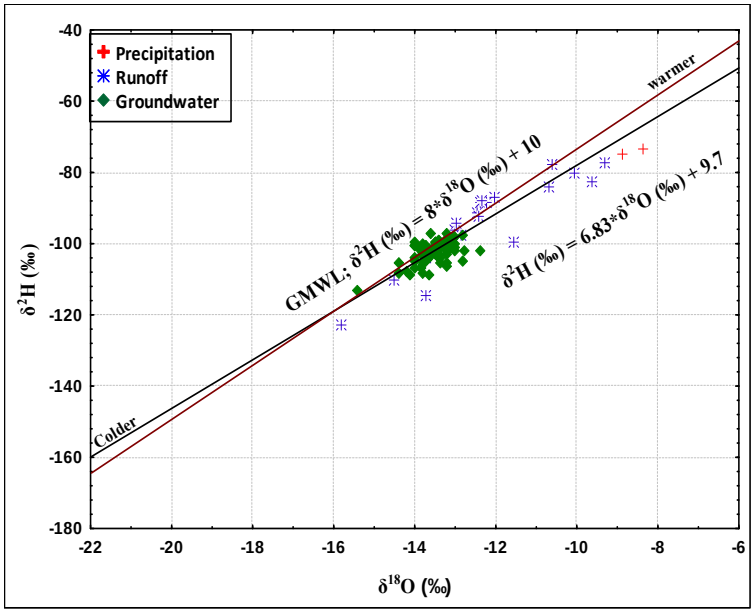

Figure 5.32: Relationship between the stable isotopes of water in precipitation, runoff, and groundwater of the independence catchment. GMWL means global mean water line.

Table 5.11: Mean Concentrations of the Stable Isotopes of Water Groped by Sample Type per each Site Location.

	Precipitation		Runoff		Groundwater	
Location	**δ^2H** ‰	**$\delta^{18}O$** ‰	**δ^2H** ‰	**$\delta^{18}O$** ‰	**δ^2H** ‰	**$\delta^{18}O$** ‰
AR [a]	N/A	N/A	-77.3	-9.3	-102.9	-13.8
YMW [b]	N/A	N/A	-86.2	-11.1	-102.6	-13.7
FMW [c]	-74	-8 6	-9 .3	-11.8	-101.6	-13.3
SAD [d]	N/A	N/A	-108.3	-13.5	-101.5	-13.2

[a] Amargosa River; [b] western side of Yucca Mountain; [c]Fortymile Wash; [d] southern Amargosa Desert.

The data presented in Figure 5.32 shows a new local meteoric line as (δ^2H = 6.83 $\delta^{18}O$ +9.7), which is slightly $\delta^{18}O$ enriched from the global meteoric water line. Precipitation is more enriched in terms of δ^2H and $\delta^{18}O$ than runoff and groundwater in the site locations, and this could indicate to a short rainfall event and high evaporation. Most of runoff samples are more enriched in terms of δ^2H and $\delta^{18}O$ than the groundwater from the same site location (Table 5.11), and per site location runoff's δ^2H and $\delta^{18}O$ depleted between Amargosa River, western side of Yucca Mountain, Fortymile Wash, and southern Amargosa Desert; whereas the groundwater's δ^2H and $\delta^{18}O$ follow an opposite direction per location, i.e. it is enriched between Amargosa River, western side of Yucca Mountain, Fortymile Wash, and southern Amargosa Desert (Table

5.11). This could mean that the southern Amargosa Desert location has highest infiltration rate, then Fortymile Wash, western side of Yucca Mountain, and Amargosa River. In addition, the most enriched groundwater could represent lower elevations and /or short rainfall events. Figures (5.A40-5.A42), in Appendix 5.A, show the relationship between the stable isotopes of water in runoff, and groundwater in Fortymile Wash, western side of Yucca Mountain, and southern Amargosa Desert, respectively.

5.5.6 Hydrochemical modeling

Mean saturation indices (SI) of different sample types are given in Table 5.12. In this study, if the SI is between (-0.5 and 0.5), water composition will be considered in equilibrium with respect to the mineral phase; a value greater than (0.5) will be considered as supersaturation; and a value less than (-0.5) will be considered as undersaturation. All water samples are undersaturated (SI <-0.5) with respect to alunite, anglesite, celestite, chrysotile, fluorite, gypsum, and melanterite. Precipitation, sediment leached, and runoff are undersaturated with respect to albite and sepiolite, whereas groundwater is in equilibrium. Precipitation, sediment leached, and groundwater are undersaturated with respect to anorthite, barite, and willemite, whereas runoff is in equilibrium. Precipitation and sediment leached are undersaturated with respect to Ca-montmorillonite, illite, K-feldspar, whereas runoff and groundwater are supersaturated. Runoff and groundwater are in equilibrium with respect to calcite and dolomite, whereas precipitation is undersaturated, and sediment leached is supersaturated. Runoff, groundwater, and sediment leached are supersaturated with respect to chlorite and hydroxyapatite, whereas precipitation is undersaturated. Precipitation and groundwater are undersaturated with respect to rhodochrosite, whereas runoff and sediment are

in equilibrium. Runoff and groundwater are supersaturated with respect to talc, whereas precipitation is undersaturated, and sediment is in equilibrium.

Table 5.12: Mean Saturation Indices (SI) of Different Sample Types Grouped by Site Locations.

Phase	Chemical formula	Precipitation SI	Sediment SI	Runoff SI	Groundwater SI
Albite	$NaAlSi_3O_8$	-8.46	-8.35	-1.77	0.53
Alunite	$KAl_3(SO_4)_2(OH)_6$	-8.37	-10.84	-4.33	-4.96
Anglesite	$PbSO_4$	-7.21	-7.61	-6.69	-6.31
Anorthite	$CaAl_2Si_2O_8$	-6.99	-3.28	-0.41	-0.56
Barite	$BaSO_4$	-1.68	-1.57	-0.37	-0.76
Ca-Montmorillonite	$Ca_{0.165}Al_{2.33}Si_{3.67}O_{10}(OH)_2$	-4.17	-1.9	4.22	4.77
Calcite	$CaCO_3$	-1.83	0.97	0.16	0.23
Celestite	$SrSO_4$	-4.13	-3.73	-3.13	-2.57
Chlorite(14A)	$Mg_5Al_2Si_3O_{10}(OH)_8$	-13.5	0.81	1.97	2.36
Chrysotile	$Mg_3Si_2O_5(OH)_4$	-10.89	-2.02	-2.48	-1.54
Dolomite	$CaMg(CO_3)_2$	-4.22	1.11	0.08	0.31
Fluorite	CaF_2	-2.88	-3.58	-2.56	-0.66
Gypsum	$CaSO_4{:}2H_2O$	-3.76	-3	-2.57	-2.14
Hydroxyapatite	$Ca_5(PO_4)_3OH$	-0.57	7.03	4.82	1.4
Illite	$K_{0.6}Mg_{0.25}Al_{2.3}Si_{3.5}O_{10}(OH)_2$	-5.15	-1.54	4.07	4.48
K-feldspar	$KAlSi_3O_8$	-5.77	-2.09	1.55	2.31
Melanterite	$FeSO_4{:}7H_2O$	-10.47	-12.32	-9.5	-8.77
Rhodochrosite	$MnCO_3$	-1.99	0.35	0.2	-0.56
Sepiolite	$Mg_2Si_3O_{7.5}OH{:}3H_2O$	-10.1	-3.22	-1.82	-0.4
Talc	$Mg_3Si_4O_{10}(OH)_2$	-10.35	-0.31	1.27	3.16
Willemite	Zn_2SiO_4	-3.89	-2.5	-0.35	-1.36

Simulations with the PHREEQC code indicate that the observed changes are consistent with a number of anticipated processes. Moving from precipitation to surface runoff, cations and anion increase, δ^2H and $\delta^{18}O$ depleted (Figure 5.33). Between surface runoff and groundwater sulfate, sodium, and alkalinity increase, whereas calcium, magnesium, potassium, and bromide decrease, δ^2H and $\delta^{18}O$ depleted. The evolution is clearest in the upper diamond of the Piper plot and in Figure 5.33 where an increase in alkalinity (precipitation to groundwater) is followed by an increase in sodium (precipitation to groundwater).

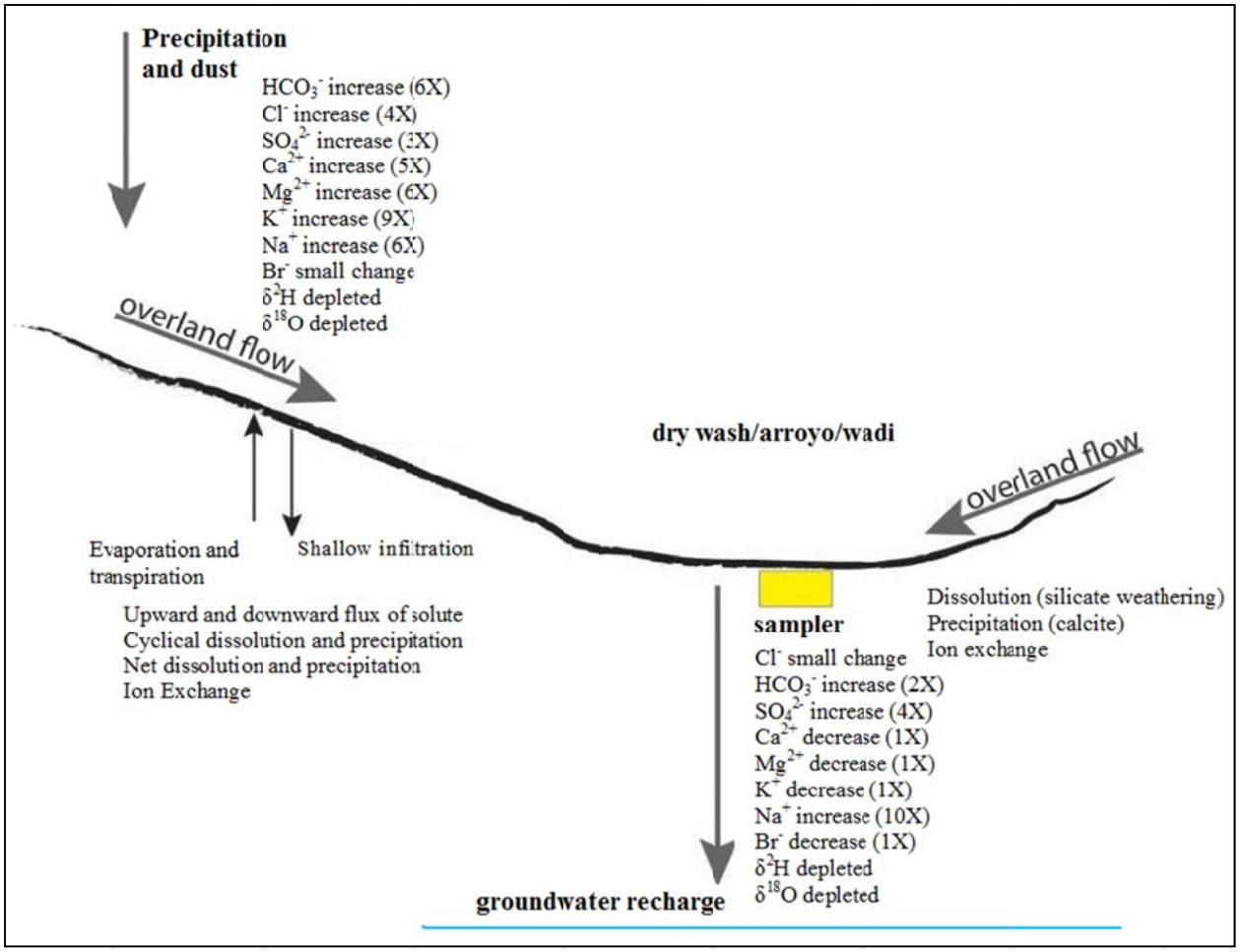

Figure 5.33: Schematic diagram for the observed changes in water chemistry from precipitation to groundwater.

5.5.7 Estimation of groundwater effective recharge

Equations 5.1 and 5.2 were used to estimate the groundwater recharge in the Amargosa Desert sub-regions; average chloride loading (wet and dry) is estimated by Fabryka-Martin et al. (2002) and Liu et al. (2003) on the order of 60 (lower loading) and 107 mg/m^2/yr (higher loading), respectively. Precipitation's chloride for each sub-region are taken from the results obtained by this study (Table 5.5) after considering the evaporative concentration occurred on the samples, based on Stetzenbach (1994) analysis (Table 5.6). Groundwater's chloride concentrations are taken as presented in Table 5.9. Average annual precipitation is taken as

estimated by many authors above as 170 mm/yr. The calculation results are presented in Table 5.13 below.

Table 5.13: Estimates Effective Recharge into the Amargosa Desert

Location	Precipitation Cl^- (mg/l), before correction	Precipitation Cl^- (mg/l), after correction	Groundwater Cl^- (mg/l)	Groundwater recharge (mm/yr), Eq. 5.1	Groundwater recharge (mm/yr), Eq. 5.2
SAD [a]	4.5	0.41	22.5	2.7-4.8	3.1
FMW [b]	2.14	0.2	7.8	7.7-13.7	4.35
AR [c]	2.3	0.21	42.2	1.4-2.5	0.85
RV [d]	3	0.273	14.75	4.1-7.25	3.15
YMW [e]	3.3	0.3	10.75	5.6-9.96	4.7
Total groundwater recharge in the Amargosa Desert				21.5-38.1	16.15

[a] Southern Anargosa Desert; [b] Fortymile Wash; [c] Amargosa River, [d] Rock Valley, [e] western side of Yucca Mountain

From Table (5.13), applying Equation 5.1 on the data indicates that the groundwater total recharge in the Amargosa Desert is ranged between 40,686 and 72,099 acre-feet/yr by an average of 56,392 acre-feet/yr (Amargosa Desert area is about 573440 acre (Lopes and Evetts, 2004)), which is 12.6-22.4 percent of precipitation with an average of 17.5 percent; whereas, Equation 5.2 estimates it on the order of 30,561 acre-feet/yr, which is 9.5 percent of precipitation, with the great contribution coming from western side of Yucca Mountain and Fortymile Wash.

Because of the uncertainty in estimation the chloride (wet and dry) deposits and the estimation that the all sub-regions have the same range, Equation 5.2 has accurate results, and this results matched the results that obtained from the literature as described in section 5.3, especially the results that obtained from (Walker and Eakin, 1963; Rush, 1970) which estimated the groundwater recharge in Amargosa Desert in the range 24,000-33,000 acre-feet/yr.

5.6 CONCLUSIONS

Five different sub-regions were selected in the Amargosa Desert region for runoff sampler emplacement to collect runoff water in order to measure the chemical characteristics of runoff water that has contacted and leached some of the top soil, which believed to be an

important source of groundwater recharge in the area. In total sixty runoff samplers were installed at thirty different locations in the major arroyos in the sub-regions as follows: 24 samplers in Fortymile Wash, 20 in western side of Yucca Mountain, 8 in the Amargosa River, 4 in Rock Valley, and 4 in the southern Amargosa Desert (Ash Meadows area). At each site location, rain gauge was installed to collect water precipitation, and sediment samples were sampled before and after the storm events that occurred during the research time period (January 2009 to January 2011). The runoff sampler design proved its ability to resist the arid weather conditions, capture runoff water, and provides unique data. In total, 167 runoff samples were collected from the washed sand filled sampler (WSB), 9 runoff samplers from natural alluvium filled sampler (NAB), in addition to 45 precipitation and 182 sediment samples, were collected during the period January 2009 and January 2011. Because of lack of data, runoff samples that were collected from the natural alluvium filled sampler were excluded from this research.

Because the degree of evaporation is unknown the changes in chemistry between precipitation and runoff samples is best viewed in terms of the changes in chemical signature rather than in terms of individual concentrations. In non-runoff producing storms the water has time to react with soil minerals prior to evaporation. When near complete evaporation of the water occurs the isotopic signature of the water will be lost, but any dissolved ions (and dry-fall) will remain in the shallow soil and sediments. When surface runoff occurs the new precipitation mixes with shallow soil moisture and dissolves some of the precipitated salts in the desiccated soil. The soil samples represent a leaching of the shallow sediment in the stream bottom, but the most soluble salts in these samples (e.g., chloride) may have been leached by a runoff event prior to sampling. The soil leaching process also provided less contact time between soil and water than the infiltration process.

Chemical analysis of precipitation, runoff, sediment, and groundwater show three potential clusters of the samples chemical constituents: leached, scavenged, and nutrients groups. Leached group is presented when constituent concentration in sediment is greater than that in precipitation and the concentration in runoff is in the middle like (TDS, total alkalinity, sodium, calcium, magnesium, potassium). Scavenged group is presented when the constituent concentration in precipitation and runoff is greater than that in sediment like (uranium). Nutrient cluster is presented when the chemical concentration in precipitation is greater than that in sediment which is greater than that in runoff, like (fluoride, sulfate, arsenic, copper, vanadium, bromide, and phosphate).

ANOVA tests indicate that most of chemical constituents are statistically significant between sample types and sample locations, and chloride is statistically insignificant between runoff and groundwater.

Piper diagram shows mixed cation-mixed anion-types between precipitation, runoff, and groundwater. In addition, it is show three hydrochemical faces, Ca/HCO_3-type water in precipitation, Ca/HCO_3 to Ca-(Na, K)/HCO_3-type water in runoff, and (Na, K)/HCO_3-type water in groundwater, and this could be because the dominance of hydrolysis reactions involving H_2CO_3 leaching of Na in the bed rocks.

Isotopes analysis shows that the distance from the meteoric water line which is indicative of the degree of evaporation, is similar for surface runoff and groundwater. The surface runoff samples exhibit a broader spread parallel to the meteoric water line. Isotopic data presents a local meteoric line as ($\delta^2H = 6.83\ \delta^{18}O+9.7$), which is slightly $\delta^{18}O$ enriched from the global meteoric water line. Precipitation is more enriched in terms of δ^2H and $\delta^{18}O$ than runoff and groundwater, and this is because the precipitation samples had evaporated between the time of precipitation

and the time of sampling. Most of runoff samples are more enriched in terms of δ^2H and $\delta^{18}O$ than the groundwater from the same site location, and per site location runoff's δ^2H and $\delta^{18}O$ depleted between Amargosa River, western side of Yucca Mountain, Fortymile Wash, and southern Amargosa Desert; whereas the groundwater's δ^2H and $\delta^{18}O$ follow an opposite direction per location, i.e. it is enriched between Amargosa River, western side of Yucca Mountain, Fortymile Wash, and southern Amargosa Desert. This could mean that the southern Amargosa Desert location has highest infiltration rate, then Fortymile Wash, western side of Yucca Mountain, and Amargosa River, in addition, the groundwater beneath southern Amargosa Desert and Fortymile Wash is younger than that in the other location, and the groundwater under Amargosa River is the oldest. The most enriched groundwater could represent lower elevations and /or short rainfall events.

PHREEQC results suggesting the precipitation of some type of calcium/magnesium carbonate (calcite and dolomite). Weathering of silicate minerals may release sodium and alkalinity with the increased alkalinity driving precipitation of carbonates. Illite, a potential sink for potassium, is supersaturated in groundwater. The increase in sulfate could be potentially from oxidation of small amounts of sulfide minerals in the volcanic rock sediments.

Groundwater total recharge in the Amargosa Desert is estimated on the order of 30,561 acre-feet/yr, which is 9.5 percent of average annual precipitation, with the great contribution coming from western side of Yucca Mountain and Fortymile Wash, this results matched with the results obtained from the literature, especially the results that obtained from (Walker and Eakin, 1963; Rush, 1970) which estimated the groundwater recharge in Amargosa Desert in the range 24,000-33,000 acre-feet/yr.

Together, the statistical analysis (descriptive statistics, box plots, and ANOVA), Piper diagram, stable isotopes analysis, and PHREEQC analysis for the precipitation, sediment, runoff and groundwater samples indicate that Chloride and the stable isotopes of water show substantial overlap of values with underlying groundwater, consistent with the concept that infiltration of surface runoff is a major contributor to groundwater recharge in the study area. Groundwater concentrations represent a larger collage of infiltration events than have been collected in the surface runoff sampling making an exact match unlikely, and the importance of surface runoff depends upon topography.

The dissolution and weathering of minerals during and subsequent to the infiltration process, but not with large amounts of additional evaporation prior to deep infiltration, cause the increasing of analyte concentrations in groundwater. The influence of transpiration on the chemistry of infiltrating water is more complicated than that of evaporation given that chloride uptake differs between plants; leading to a combination of evaporative concentration at depth and transport to the surface with eventual recycling in leaves and dead plant materials.

ACKNOWLEDGEMENTS

Funding for this research was provided by Nye County, NV through a grant from the US Department of Energy office of Civilian Radioactive Waste Management. John Klenke, Roger McRae, and the rest of the Nye County Staff for assistance with sampler construction, installation, and sampling. Dr. David Borrok (Geological Department, UTEP), Dr. Zhuping Sheng (Texas Agrilife Research Center), Dr. William Walker (Civil Engineering Department, UTEP) and their research groups for their help and support with chemical analysis. The Center for Environmental Resource Management of the University of Texas at El Paso for their funding and support.

REFERENCES

Al-Qudah, O.M., J.C. Walton, and A. Woocay (2010), Tracking the Chemical Footprint of Surface-Runoff Infiltration on Groundwater Recharge in an Arid Region, paper presented at 2010 Waste Management Symposium, Phoenix, AZ.

Al-Qudah, O.M., A. Woocay, and J.C. Walton (2008), Yucca Mountain Region Groundwater Geochemical Data Analyses, IHLRWMC, Las Vegas, Nevada. La Grange Park, Illinois: American Nuclear Society, p. 87-94. ISBN: 978-0-89448-062-1.

Al-Qudah, O.M., A. Woocay, and J.C. Walton (2011), Identification of Probable Groundwater Paths in the Amargosa Desert Vicinity, Journal of Applied Geochemistry, 26(4), pp. 565-574. DOI:10.1016/j.apgeochem.2011.01.014; ISSN 0883-2927.

ASTM D422-63 (2007), Standard Test Method for Particle-Size Analysis of Soils, ASTM international, west Conshohocken, Pennsylvania.

ASTM D854 (2006), Standard Test Method for Specific Gravity of Soil Solids by Water Pycnometer, ASTM international, west Conshohocken, Pennsylvania.

ASTM D1140 (2006), Standard Test Method for Laboratory Amount of Material in Soils Finer than No. 200 (75-μm) Sieve, ASTM international, west Conshohocken, Pennsylvania.

ASTM D2216 (2005), Standard Test Method for Laboratory Determination of Water (Moisture) Content of Soil and Rock by Mass, ASTM international, west Conshohocken, Pennsylvania.

ASTM D4542 (1995), Standard Test Method for Pore Water Extraction and Determination of the Soluble Salt Content of Soils by Refractometer, ASTM international, west Conshohocken, Pennsylvania.

Bagtzoglou, A.C. (2003), Perched Water Bodies in Arid Environments and their Role as Hydrologic Constraints for Recharge Rate Estimation: Part 2, the Case of Yucca Mountain, Environmental Forensics, 4:47-62.

Bechtel SAIC Company LLC, (2004), UZ Flow Models and Submodels, MDL-NBS-HS-000006 Rev. 02, RIS: DOC.20041101.0004.

Benson, L., and H. Klieforth (1989), Stable Isotopes in Precipitation and Groundwater in the Yucca Mountain Region, Southern Nevada – Paleoclimate Implications, in Peterson, D.H., ed., Aspects of Climate Variability in the Pacific and Western Americas, American Geophysical Union Geophysical Monograph, 55, pp. 41-59.

Bish, D. L. (1988), Smectite Dehydration and Stability: Applications to Radioactive Waste Isolation at Yucca Mountain, Nevada, Los Alamos National Laboratory, Report LA-11023-MS, 31 p.

Blankennagel, R.K., and J.E. Weir (1973), Geohydrology of the Eastern Part of Pahute Mesa Nevada Test Site, Nye County, Nevada, U.S. Geological Survey Professional Paper 712-B, 35 p.

Broxton, D.E., Bish, D. L., and R.G. Warren (1987), Distribution and Chemistry of Diagenetic Minerals at Yucca Mountain, Nye County, Nevada, Clays and Clay Minerals, 35(2), pp. 89-110.

Broxton, D.E., R.G. Warren, R.C. Hagan, and G. Luedemann, (1986), Chemistry of Diagenetically Altered Tufts at a Potential Nuclear Waste Repository, Yucca Mountain, Nye County, Nevada, Los Alamos National Laboratory, Report LA-10802-MS, 160 p.

Chandra, S. (1979), Estimation and Measurement of Recharge to Groundwater for Rainfall, Irrigation and Influent Seepage, International Seminar on Development and Management of Groundwater Resources.

Claassen, H.C. (1985), Sources and Mechanisms of Recharge for Groundwater in the West-Central Amargosa Desert, Nevada-A Geochemical Interpretation, U.S. Geological Survey Professional Paper 712-F, 31 p.

Clescerl, L.S. (Editor), A.E. Greenberg (Editor), A.D. Eaton (Editor) (2000), Standard Methods for the Examination of Water and Wastewater, (20th ed.), American Public Health Association, Washington, DC. ISBN 0-87553-235-7.

CRWMS M&O (Civilian Radioactive Waste Management System, Management & Operating Contractor), (2000), Geochemical and Isotopic Constraints on Ground-Water Flow Directions, Mixing, and Recharge at Yucca Mountain, Nevada, ANL-NBS-HS-000021, Rev. 00, August 2000. RIS: MOL.20000918.0287.

Drever, J.I. (1997), The Geochemistry of Natural Waters, 3rd ed. Prentice Hall, Upper Saddle River, New Jersey.

DOE-OCRWM (U.S. Department of Energy-Office of Civilian Radioactive Waste Management) (2006), Evaluation of Technical Impact on the Yucca Mountain Project Technical Basis Resulting From Issues Raised by E-Mails of Former Project Participants, DOE/RW-0583, 144 p.

Eberl, D.D., B.F. Jones, and H.N. Khoury (1982), Mixed-Layer Kerolite/Stevensite from the Amargosa Desert, Nevada, Clays and Clay Minerals, 30(5), pp. 321-326.

EPA (U.S. Environmental Protection Agency)-National Service Center for Environmental Publications (NSCEP) (2001), Public Health and Environmental Radiation Protection Standards for Yucca Mountain Neveda: Background Information Documant for 40 CFR 197", EPA 402-R-01-005.

Faunt, C.C., F.A. D'agnese, and G.M. O'brien (2004), Death Valley Regional Groundwater Flow System, Nevada and California-Hydrogeologic Framework and Transient Groundwater Flow Model, Rep. 2004-5205, U.S. Department of the Interior and U.S. Geological Survey.

Flint, A. L., L. E. Flint, G. S. Bodvarsson, E. M. Kwicklis, and J. T. Fabryka-Martin (2001a), Evolution of the Conceptual Model of Unsaturated Zone Hydrology at Yucca Mountain, Nevada, J. Hydrology, 247(2001), 1-30, pii: S0022-1694(01)00358-4.

Flint, A.L.; L.E. Flint; E.M. Kwicklis; G.S. Bodvarsson; and J.M. Fabryka-Martin (2001b), Hydrology of Yucca Mountain, Nevada, Reviews of Geophysics, American Geophysical Union, 39(4), pp. 447-470, TIC: 254424.

Flint, A.L., L.E. Flint, E.M. Kwicklis, J.T. Fabryka-Martin, and G.S. Bodvarsson (2002), Estimating Recharge at Yucca Mountain, Nevada, USA: Comparison of Methods, Hydrogeology Journal, 10(1), pp.180–204, doi:10.1007/s10040-001-0169-1.

Golden Software Inc. (2008), Surfer Version 8.09, Surface Mapping System, Golden, Colorado, <http://www.goldensoftware.com/>, (accessed 2008).

Ingraham, N.L., B.F. Lyles, R.L. Jacobson, and J.W. Hess (1989), Stable Isotope Study of Precipitation and Spring Discharge on the Nevada Test Site, Desert Research Institute, Las Vegas, Nevada, 31 pp.

Kerrisk, J.F. (1987), Groundwater Chemistry at Yucca Mountain, Nevada, and Vicinity, Los Alamos National Laboratory, Report LA-10929-MS, 118 p.

Khoury, H.N., D.D. Eberl, and B.F. Johnes (1982), Origin of Magnesium Clays from the Amargosa Desert, Nevada, Clays and Clay Minerals, 30(5), pp. 327-336.

Kilroy, K.C., and C.S. Savard (1997), Geohydrology of Pahute Mesa-3 Test Well, Nye County, Nevada: U.S. Department of the Interior, U.S. Geological Survey, Water-Resources Investigations Report-95-4239.

Kumar C.P. (1977), Estimation of Natural Ground Water Recharge, ISH Journal of Hydraulic Engineering, 3(1), pp. 61-74.

LANL (Los Alamos National Laboratory) (2007), Regional Groundwater Hydrochemical Data in the Yucca Mountain Area Used as Direct Input to ANLNBS-00021, Revision 01. LA0309RR831233.001.

Liu, J., E.L. Sonnenthal, and G.S. Bodvarson (2003), Calibration of Yucca Mountain Unsaturated Zone Flow and Transport Model Using Pore Water Chloride Data, J. Con. Hydrol,. 62-63(2003), 213-235, doi:10.1016/S0169-7722(02)00168-7.

Lopes, T.J., and D.M. Evetts (2004), Ground-Water Pumpage and Artificial Recharge Estimates for Calendar Year 2000 and Average Annual Natural Recharge and Interbasin Flow by Hydrographic Area, Nevada, U.S. Geological Survey Scientific Investigations Report 2004-5239, Carson City, Nevada, 87 pp.

Mahlknecht, J., J.F. Schneider, B.J. Merkel, I.N. de Leon, and S.M. Bernasconi (2004), Groundwater Recharge in a Sedimentry Basin in Semi-Arid Mexico, Hydrogeology Journal, 12:511-530. DOI 10.1007/s10040-004-0332-6.

Matuska, N.A., J.W. Hess (1989), The Relationship of the Yucca Mountain-Repository Block to the Regional Groundwater System: a Geochemical Model, NWPO-TR-011-89.

Moncure, G. K., Surdam, R. C., and McKague, H. L., 1981. "Zeolite diagenesis below Pahute Mesa, Nevada Test Site," Clay and Clay Minerals, v.29, n.5, p. 385-306.

Montazer, P., and W.E. Wilson (1984), Conceptual Hydrologic Model of Flow in the Unsaturated Zone, Yucca Mountain, NV, Rep. 84-4344, U.S. Geological Survey.

NWRPO (Nuclear Waste Repository Project Office) (2008), Geochemistry data files, Nye County, Nevada. < http://www.nyecounty.com> (accessed April 30, 2007).

Ogard, A.E. and J.F. Kerrisk (1984), Groundwater Chemistry Along Flow-paths Between a Proposed Repository Site and the Accessible Environment, Los Alamos National Laboratory, Report LA-10188-MS, 48 p.

Papke, K.G. (1972), A Sepiolite-Rich Playa Deposit in Southern Nevada, Clays and Clay Minerals, 20:211-215.

Parkhurst, D.L. (1995), User's Guide to PHREEQC: a Computer Program for Speciation, Reaction-Path, Advective-Transport, and Inverse Geochemical Calculations, U.S. Geol. Surv. Water-Resour. Invest. No. 95–4227.

Parkhurst, D.L., and C.A.J. Appelo (1999), User's Guide to PHREEQC (Version 2): a Computer Program for Speciation, Batch-Reaction, One-Dimensional Transport, and Inverse Geochemical Calculations: U.S. Geol. Surv. Water-Resour. Invest. Rep. 99–4259, 310 pp.

Parkhurst, D.L., L.N. Plummer, and D.C. Thorstenson (1982), Balance: a Computer Program for Calculating Mass Transfer for Geochemical Reactions in Groundwater. U.S. Geol. Surv. Water-Resour. Invest. No. 82–14.

Patterson, G.L., and T.A. Oliver (2004), Trace and Minor Elements in Saturated-Zone Water near Yucca Mountain, Nevada, paper presented at Geological Society of America annual meeting, 36(5), 297, Denver, CO.

Rush, F.E. (1970), Regional Groundwater Systems in the Nevada Test Site Area, Nye, Lincoln, and Clark Counties, Nevada, Water Resources-Reconnaissance Series-Report 54, State of Nevada-Department of Conservation and Natural Resources-Division of Water Resources.

Savard, C.S. (1994), Groundwater Recharge in Fortymile Wash Near Yucca Mountain, Nevada, 1992-93, IHLRWM Proceedings of the Fifth Annual International Conference, Las Vegas, Nevada, May 22-26, 1994. American Nuclear Society and American Society of Civil Engineers, p. 1805-1813.

Savard, C.S. (1995), Selected Hydrologic Data from Fortymile Wash in the Yucca Mountain Area, Nevada, Water Year 1992, Rep. 94-317, U.S. Geological Survey.

Savard, C.S. (1996), Selected Hydrologic Data from Fortymile Wash in the Yucca Mountain Area, Nevada, Water Years 1993-1994, Rep. 95-709, U.S. Geological Survey.

Savard, C.S. (1998), Estimated Groundwater Recharge From Streamflow in Fortymile Wash Near Yucca Mountain, Nevada, U.S. Geological Survey Water Resources Investigation Report 97-7273, pp. 1-30.

Savard, C.S., and D.A. Beck (1994), Transmission Losses in Fortymile Wash Near Yucca Mountain, Nevada, Eos, American Geophysical Union Transaction, 75(44), p. 283.

Scott, R.B., R.W. Spengler, S. Diehl,A.R. Lappin, and M.P. Chornack 1(983), Geologic character of tuffs in the unsaturated zone at Yucca Mountain, Southern Nevada, In: Mercer, J.W., Rao, P.S.C., and Marine, I.W. (eds.), Role of the Unsaturated Zone in Radioactive and Hazardous Waste Disposal, Ann Arbor Science, Ann Arbor, Michigan, 289-335. TIC: 222524.

SNL (Sandia National Laboratories) (2008), Total System Performance Assessment for the Yucca Mountain Site, DOC. 20080312.0001/ MDL-WIS-PA-000005 REV00.

StatSoft Inc. (1984–2010), Statistica Computer Program Manual for Windows, Tulsa, Oklahoma, <http://www.statsoft.com/>, (accessed September 22, 2010).

Stetzenbach, K. (1994), Fingerprinting of Groundwater by ICP-MS: Yucca Mountain Precipitation Sample Analysis Result Winter 1992/Spring 1993, Progress Report October

1, 1992 to December 31, 1992, Harry Reid Center for Environmental Studies, University of Nevada, Las Vegas, DOE Cooperative Agreement No. DE-FC 08-90NV10872.

USGS (U.S. Geological Survey) (2004), Yucca Mountain Research, Groundwater Chemistry, <http://www.usgs.gov/), (accessed 2011).

Walker, G.E., T.E. Eakin (1963), Geology and Groundwater of Amargosa Desert, Nevada-California, Groundwater Resources-Reconnaissance Series-Report 14, State of Nevada-Department of Conservation and Natural Resources.

White, A.F. (1979), Geochemistry of Groundwater Associated with Tuffaceous Rocks, Oasis Valley, Nevada, U.S. Geological Survey Professional Paper 712-E, 25 p.

White, A.F., and N.J. Chuma (1987), Carbon and Isotopic Mass Balance Models of Oasis Valley-Fortymile Canyon Groundwater Basin, Southern Nevada, Water Resources Research, 23(4), 571-582, paper number 6W4383, doi:0043-1397/87/006W-4383505.00

Wilson, M. L., P.N. Swift, J.A. McNeish, and S.D. Sevougian (2001), Total-System Performance Assessment for the Yucca Mountain Site, MOL.20020304.003 1.

Winograd, I.J., (1981), Radioactive Waste Disposal in Thick Unsaturated Zones, Science, American Association for the Advancement of Science, 212(5402), pp. 1457-1464. TIC: 217258.

Winograd, I.J., and W. Thordarson (1975), Hydrogeologic and Hydrochemical Framework, South-Central Great Basin, Nevada-California, with Special Reference to the Nevada Test Site, U.S. Geological Survey Professional Paper 712-C. 137 p. RIS: NNA.19870406.0201.

Winston, R.B. (2000), Graphical User Interface for MODFLOW, Version 4: U.S. Geological Survey Open-File Report 00-315, 27 p.

Woolhiser, D.A., R.W. Fedors, R.E. Smith, and S.A. Stothoff (2006), Estimating Infiltration in the Uper Split Wash Watershed, Yucca Mountain, Nevada, Journal of hydrologic Engineering, 11(2), pp. 123-133. DOI: 10.1061/ ASCE 1084-0699 2006 11:2 123

Woolhiser, D.A., S.A. Stothoff, , and G.W. Wittmeyer (2000), Channel Infiltration in Solitario Canyon, Yucca Mountain, Nevada, Journal of Hydrological Engineering, 5(3),pp. 240-249

APPENDIX 5.A

Table 5.A1: Median Concentrations of the Chemical Constituents of each Sample Type (Precipitation, Sediment, Runoff, and Groundwater) Normalized by Sample Chloride for all Site Locations together (Amargosa Desert Area) (in molar ratio, except otherwise indicated)

Chemical constituent	Precipitation	Sediment	Runoff	Groundwater
TDS/Cl	10.8717966	142.856	19.29	32.22365591
Total alkalinity (as CaCO3)/Cl	5.35810381	155.812	12.08	15.34575261
Non carbonate alkalinity as CaCO3 %	59.0877143	78.2953	66.96	82.95712911
Chloride (ppm)	2.127675	0.90621	8	9.9
Sulfate/Cl	1.49126641	3.00254	1.143	3.882352941
Calcium/Cl	2.23942272	29.7425	3.386	1.724137931
Magnesium/Cl	0.21868256	1.70495	0.579	0.2875
Potassium/Cl	0.28929599	8.13615	0.938	0.510638298
Sodium/Cl	0.625	5.19613	1.25	6.030150754
Fluoride/Cl	0.08734874	0.04103	0.014	0.166666667
Bromide/Cl	0.09838688	0.17274	0.029	0.02020202
Boron/Cl	0.00235006	1.25623	0.013	0.000684932
Phosphate/Cl	0.20536485	0.13683	0.035	0.01010101
Nitrogen total/Cl	0.16593885	0.88907	0.15	0.039473684
Nitrate/Cl	0.73013092	3.9119	0.242	0.052631579
Ammonia/Cl	0.20178164	1.08466	0.094	0.032105263
Aluminum/Cl	0.00608684	0.0624	0.008	0.004422642
Arsenic/Cl	0.00254492	0.00634	4E-04	0.000128205
Iron/Cl	0.00109201	0.04399	0.003	0.000684932
Copper/Cl	0.00112199	0.04861	5E-04	0.0005
Barium/Cl	0.00302554	0.00919	0.007	0.000197368
Caesium/Cl	0.00231205	0.0058	0.008	5.05051E-05
Lithium/Cl	0.00119591	0.00593	0.002	6.57895E-05
Molybdenum/Cl	0.00021593	0.00041	2E-04	6.57895E-05
Silica/Cl	0.15978525	0.18039	2.333	5.6
Strontium/Cl	0.01572956	0.09339	0.021	0.003448276
Rubidium/Cl	0.00031994	0.00146	3E-04	6.57895E-05
Titanium /Cl	0.00117503	0.00202	5E-04	0.000294118
Uranium/Cl	0.00020677	4.4E-05	2E-04	6.75676E-06
Vanadium/Cl	0.00058883	0.00927	2E-04	5.88235E-05
Zinc/Cl	0.00575152	0.00329	0.001	0.000595238
Lead/Cl	2.3501E-05	0.00054	2E-05	5.88235E-06
Manganese/Cl	0.0038318	0.00591	0.003	0.000320513
Nickel/Cl	0.00016243	0.00094	3E-04	0.0000625
Selenium/Cl	2.3501E-05	4E-05	4E-05	5.84795E-06

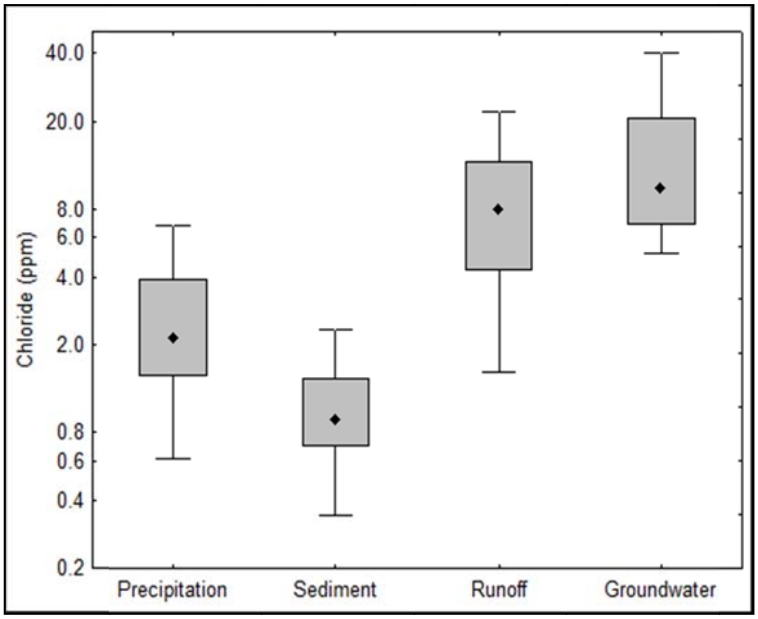

Figure 5.A1: Box plots of chloride in the Amargosa Desert region grouped by sample type.

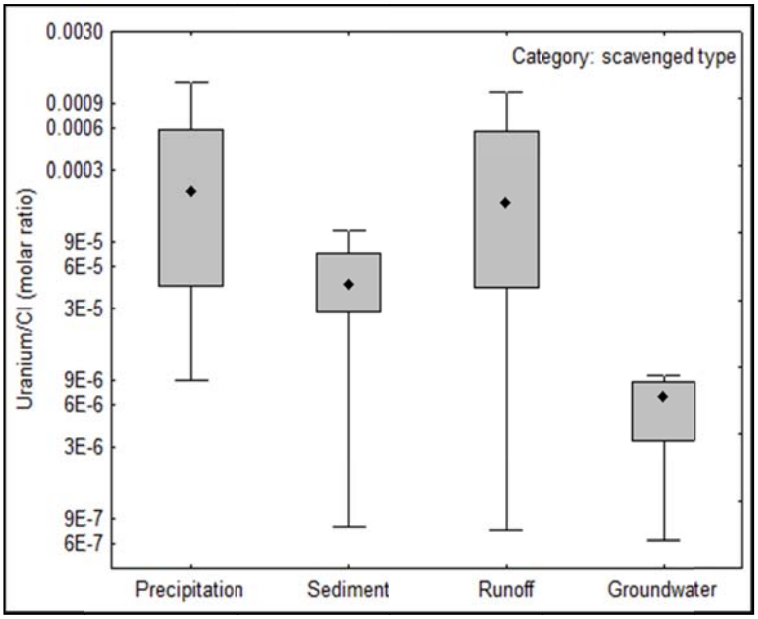

Figure 5.A2: Box plots of uranium in the Amargosa Desert normalized by sample chloride and grouped by sample type.

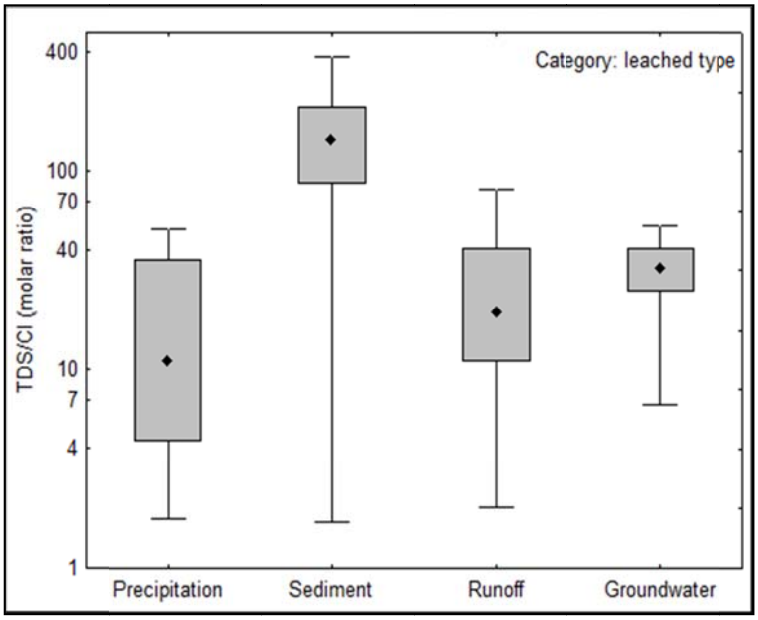

Figure 5.A3: Box plots of TDS in the Amargosa Desert region normalized by sample chloride and grouped by sample type.

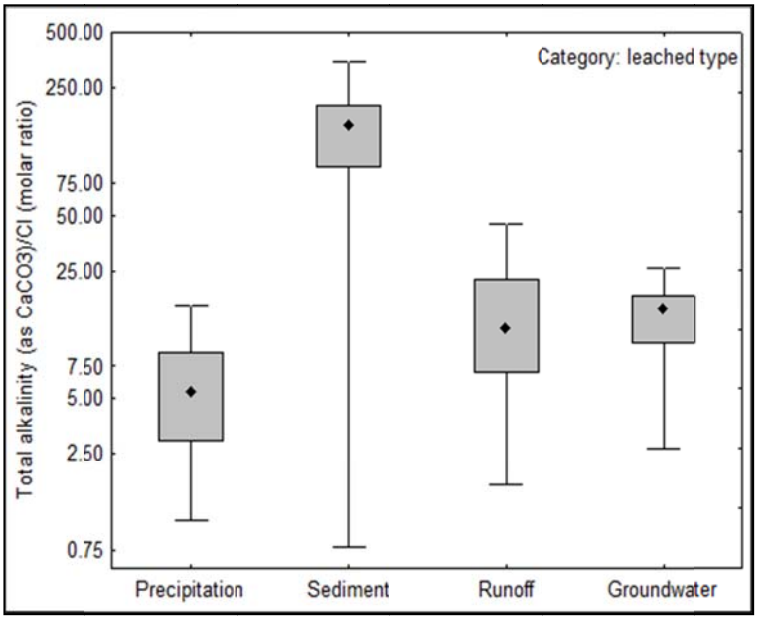

Figure 5.A4: Box plots of total alkalinity in the Amargosa Desert region normalized by sample chloride and grouped by sample type.

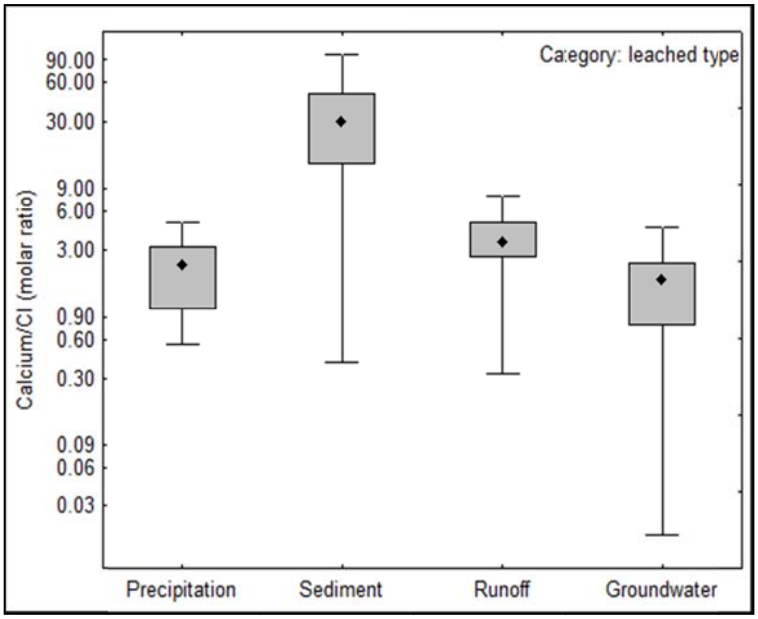

Figure 5.A5: Box plots of calcium in the Amargosa Desert region normalized by sample chloride and grouped by sample type.

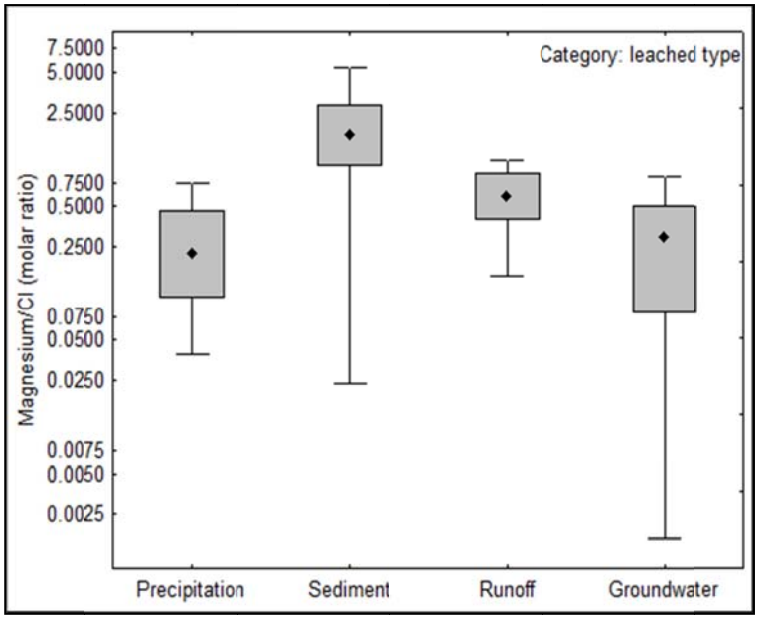

Figure 5.A6: Box plots of magnesium in the Amargosa Desert region normalized by sample chloride and grouped by sample type.

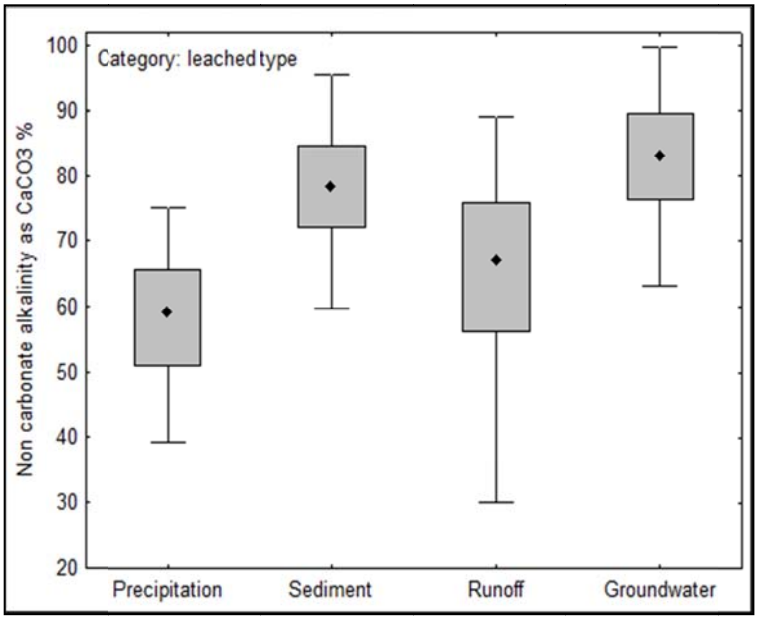

Figure 5.A7: Box plots of non-carbonate alkalinity in the Amargosa Desert region normalized by sample chloride and grouped by sample type.

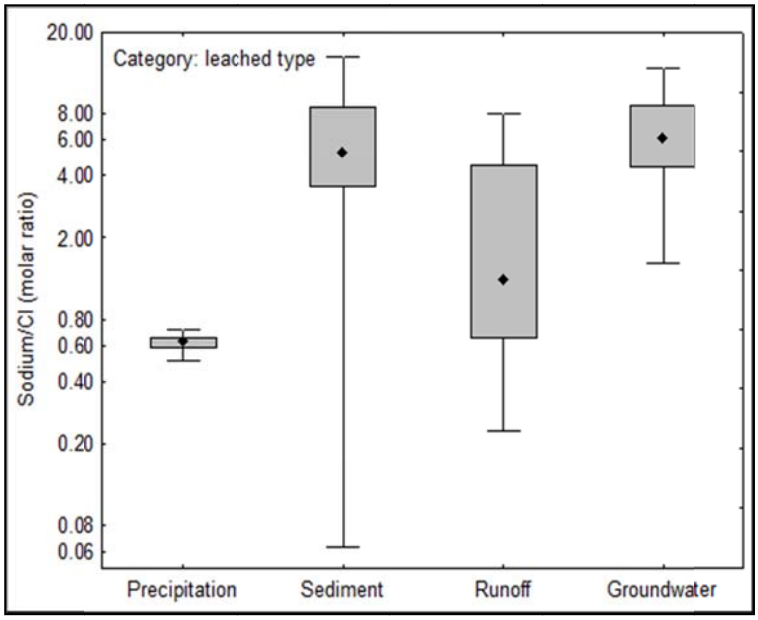

Figure 5.A8: Box plots of sodium in the Amargosa Desert region normalized by sample chloride and grouped by sample type.

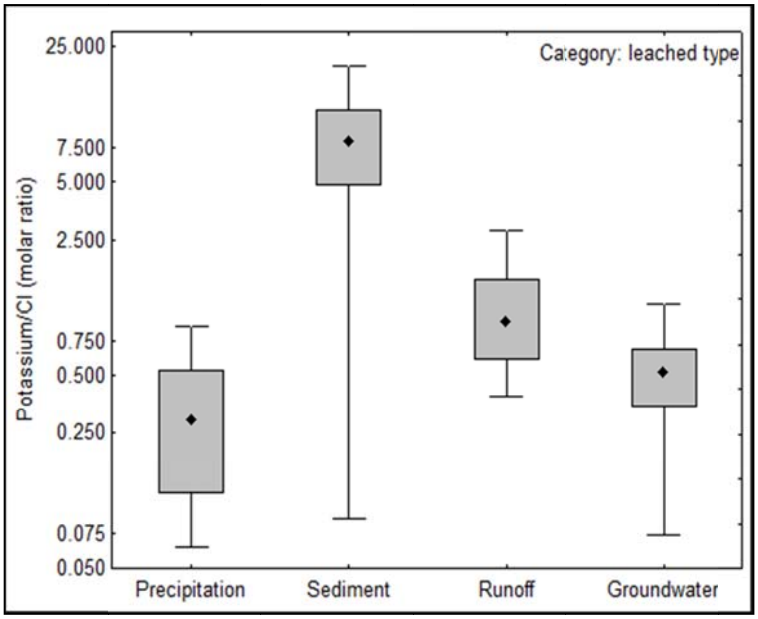

Figure 5.A9: Box plots of potassium in the Amargosa Desert region normalized by sample chloride and grouped by sample type.

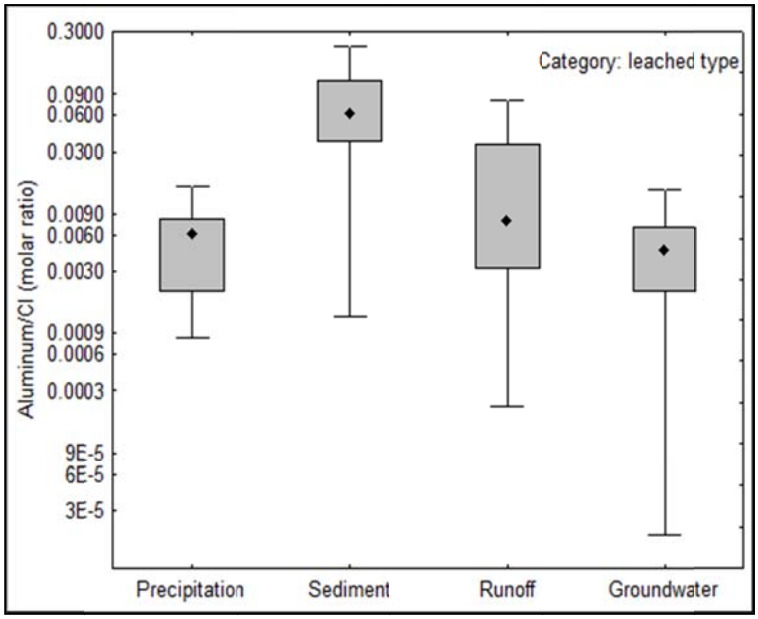

Figure 5.A10: Box plots of aluminum in the Amargosa Desert region normalized by sample chloride and grouped by sample type.

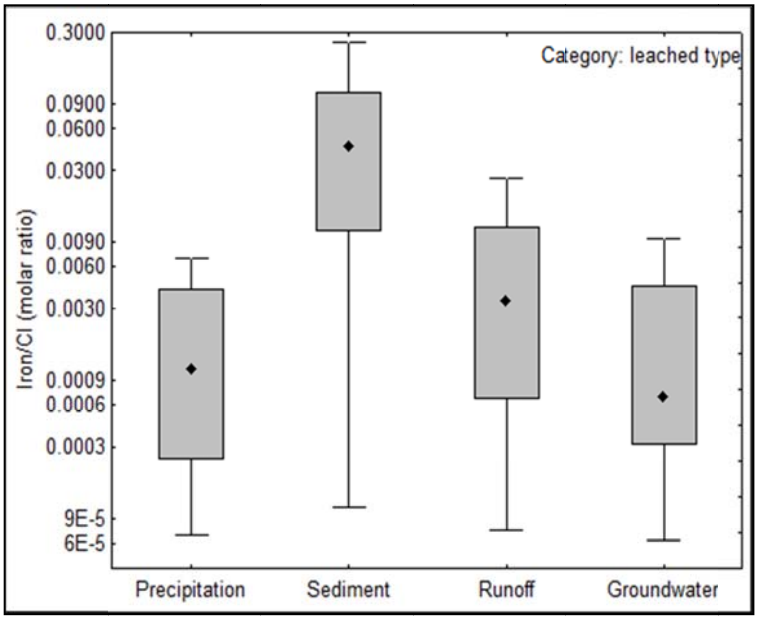

Figure 5.A11: Box plots of iron in the Amargosa Desert region normalized by sample chloride and grouped by sample type.

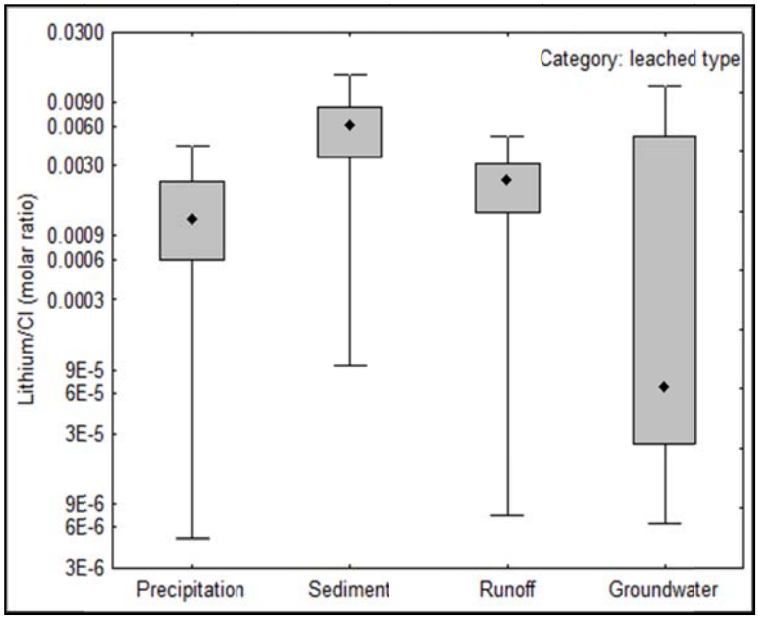

Figure 5.A12: Box plots of lithium in the Amargosa Desert region normalized by sample chloride and grouped by sample type.

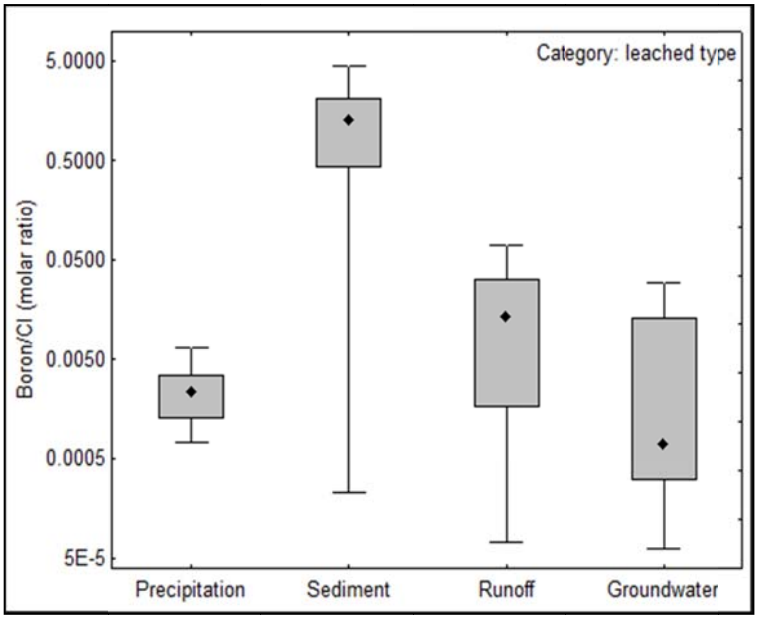

Figure 5.A13: Box plots of boron in the Amargosa Desert region normalized by sample chloride and grouped by sample type.

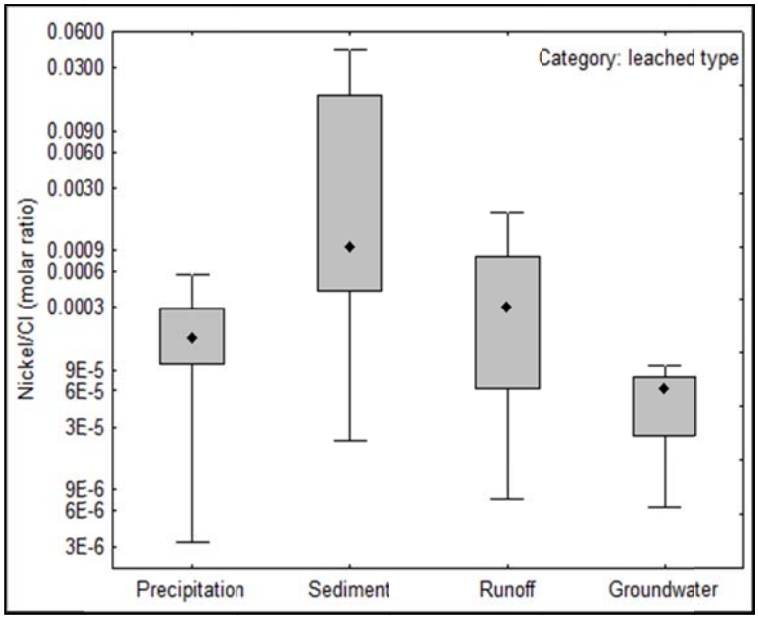

Figure 5.A14: Box plots of nickel in the Amargosa Desert region normalized by sample chloride and grouped by sample type.

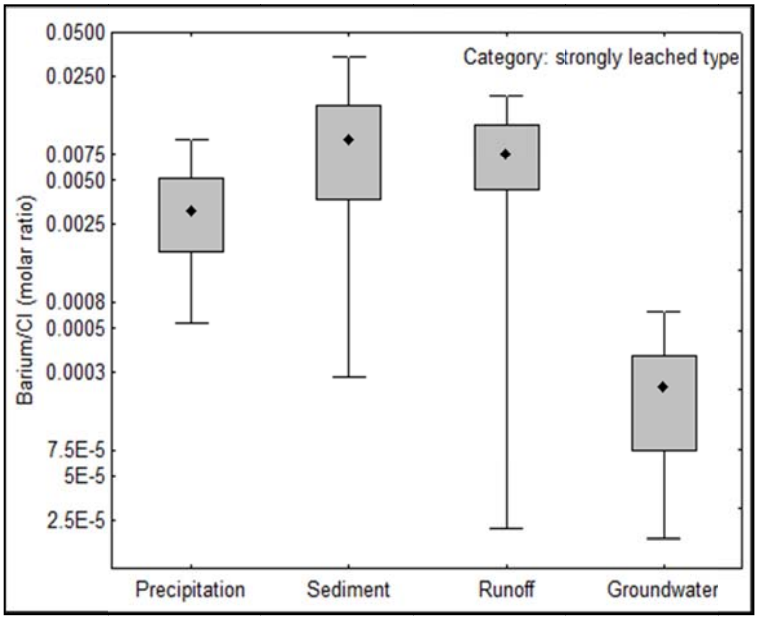

Figure 5.A15: Box plots of barium in the Amargosa Desert region normalized by sample chloride and grouped by sample type.

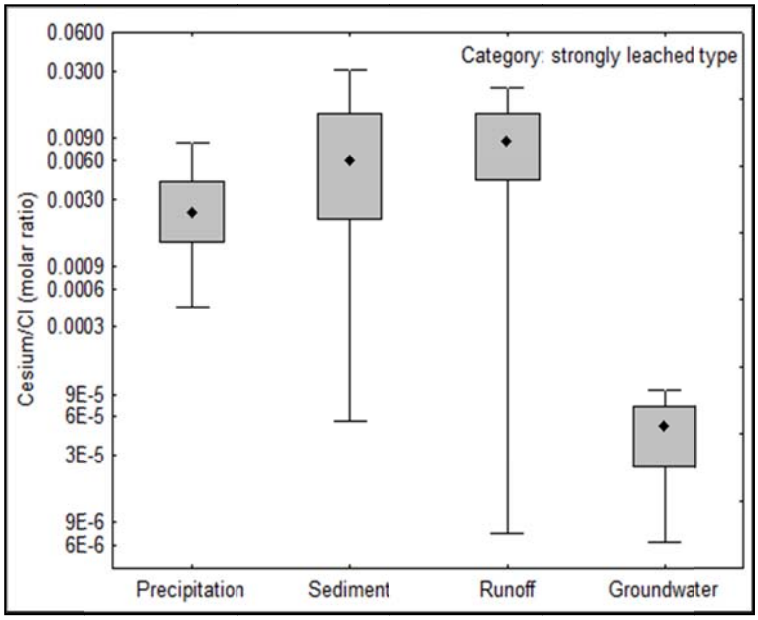

Figure 5.A16: Box plots of cesium in the Amargosa Desert region normalized by sample chloride and grouped by sample type.

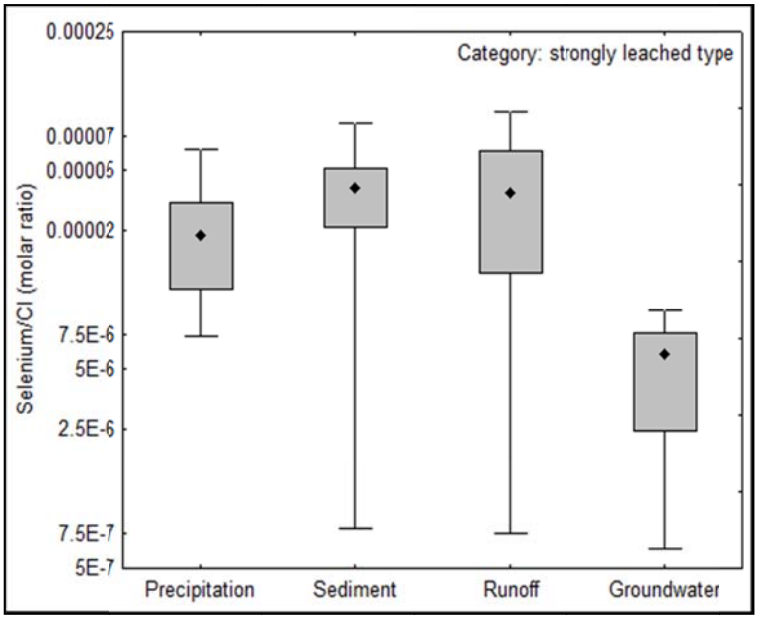

Figure 5.A17: Box plots of selenium in the Amargosa Desert region normalized by sample chloride and grouped by sample type.

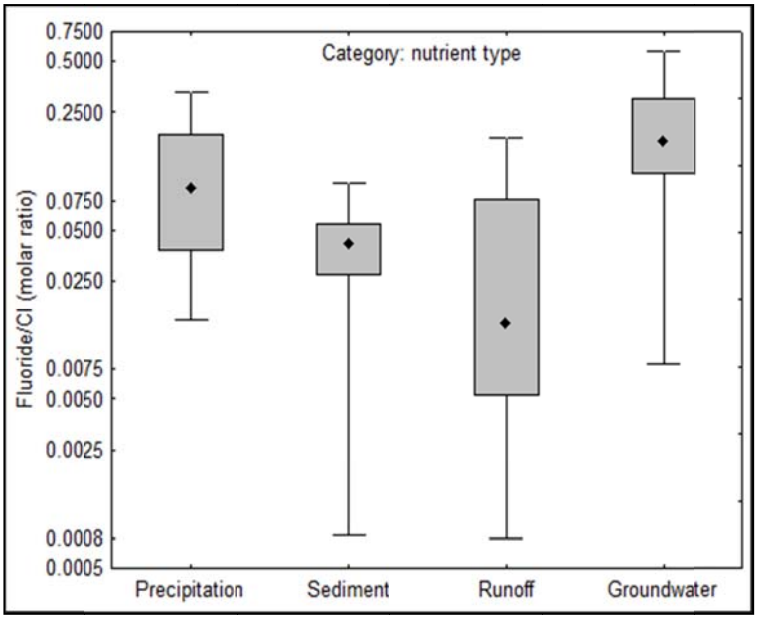

Figure 5.A18: Box plots of fluoride in the Amargosa Desert region normalized by sample chloride and grouped by sample type.

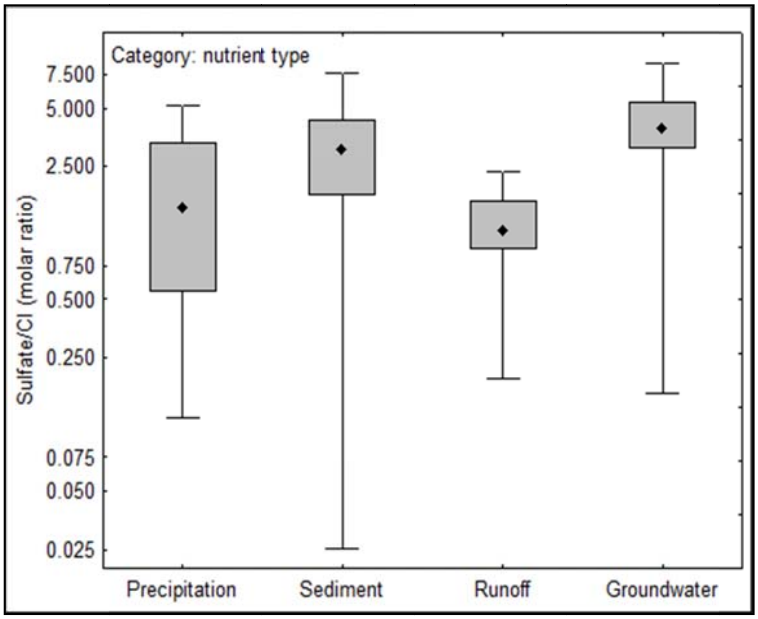

Figure 5.A19: Box plots of sulfate in the Amargosa Desert region normalized by sample chloride and grouped by sample type.

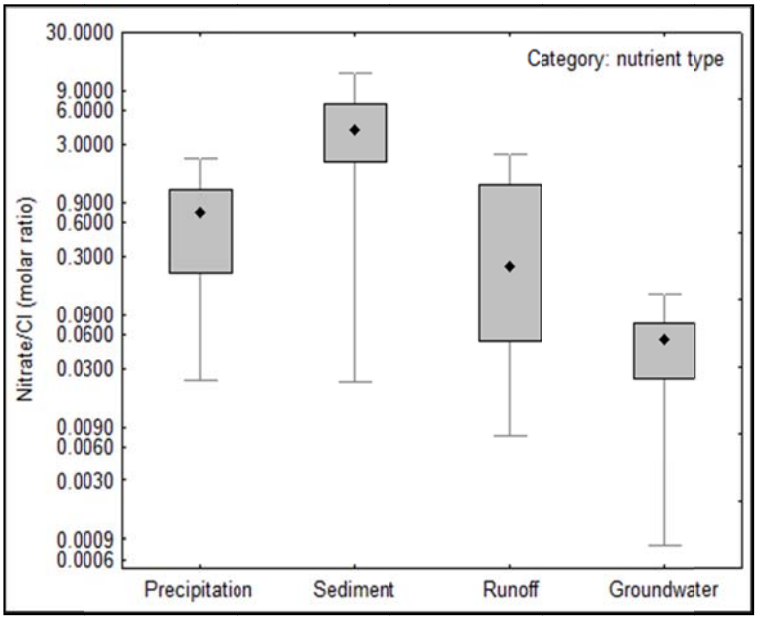

Figure 5.A20: Box plots of nitrate in the Amargosa Desert region normalized by sample chloride and grouped by sample type.

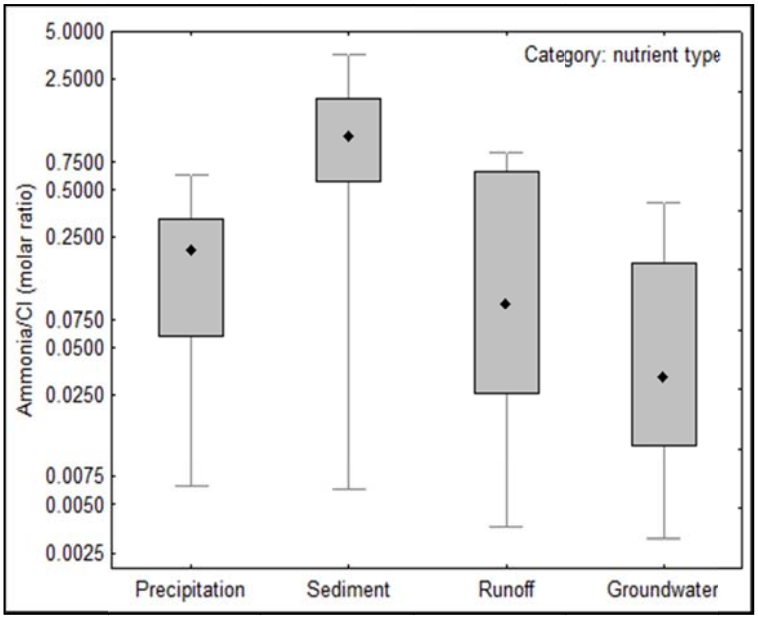

Figure 5.A21: Box plots of ammonium in the Amargosa Desert region normalized by sample chloride and grouped by sample type.

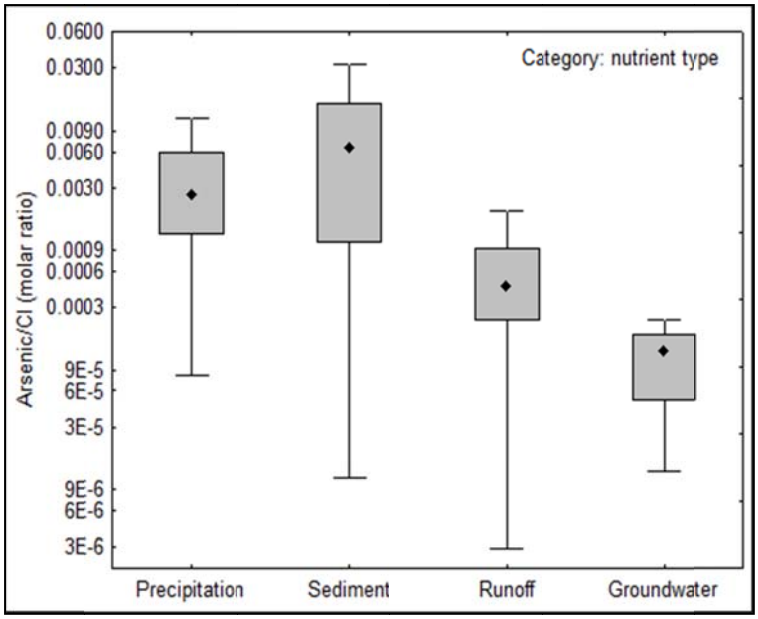

Figure 5.A22: Box plots of arsenic in the Amargosa Desert region normalized by sample chloride and grouped by sample type.

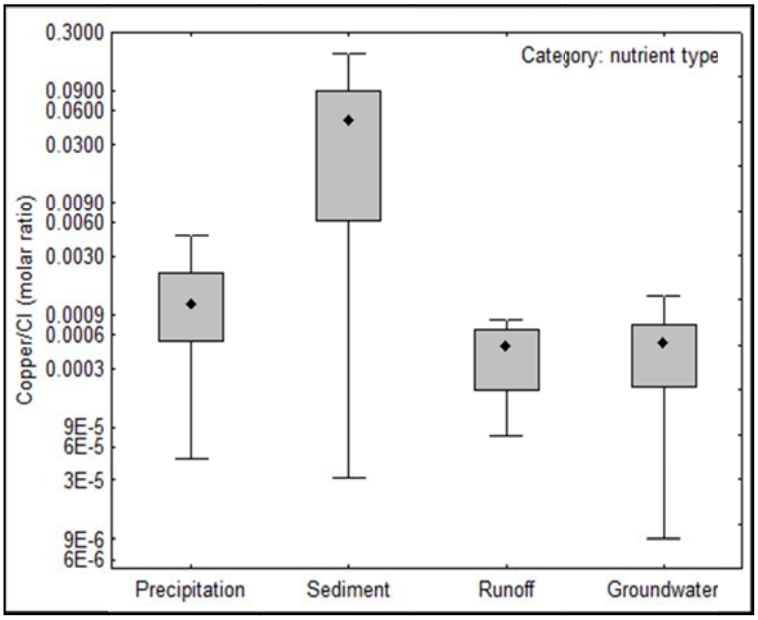

Figure 5.A23: Box plots of copper in the Amargosa Desert region normalized by sample chloride and grouped by sample type.

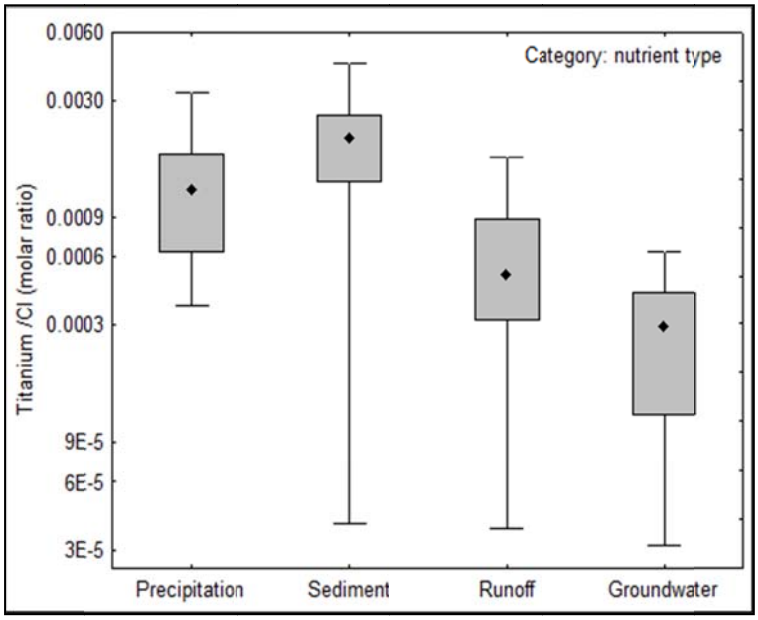

Figure 5.A24: Box plots of titanium in the Amargosa Desert region normalized by sample chloride and grouped by sample type.

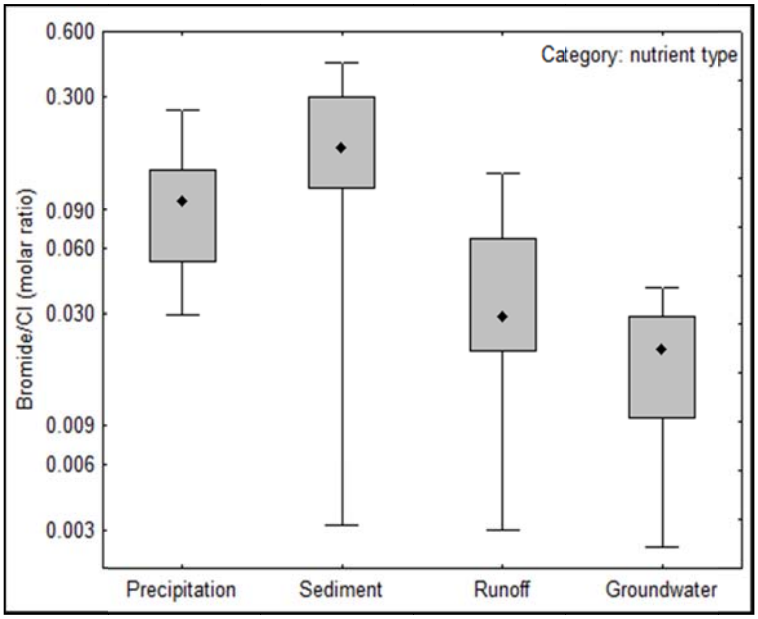

Figure 5.A25: Box plots of bromide in the Amargosa Desert region normalized by sample chloride and grouped by sample type.

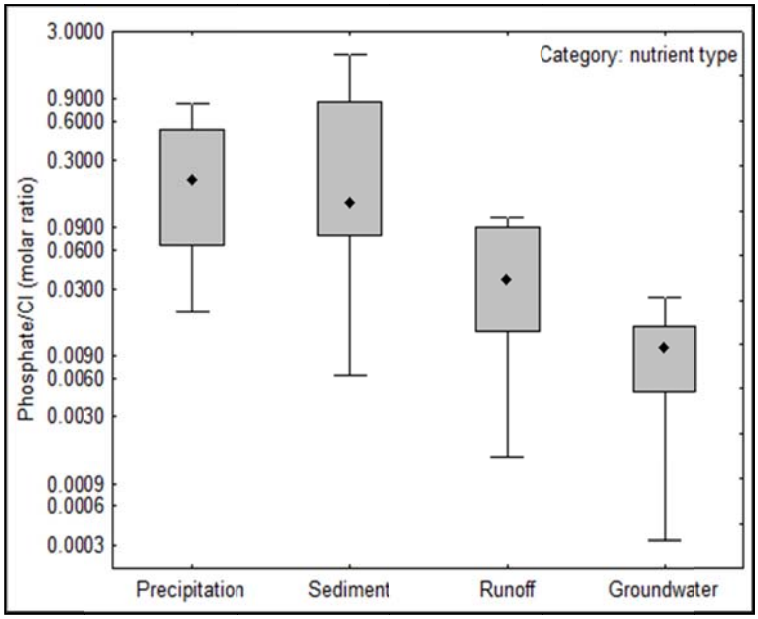

Figure 5.A26: Box plots of phosphate in the Amargosa Desert region normalized by sample chloride and grouped by sample type.

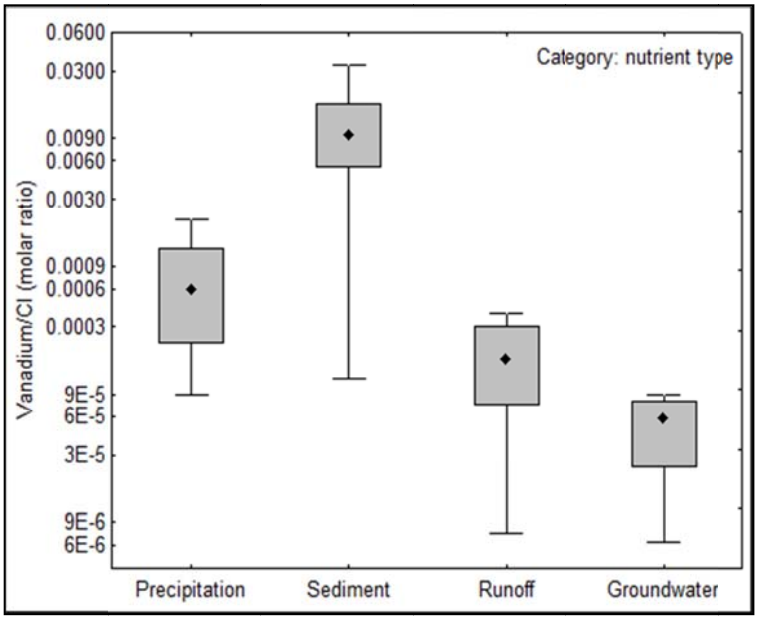

Figure 5.A27: Box plots of vanadium in the Amargosa Desert region normalized by sample chloride and grouped by sample type.

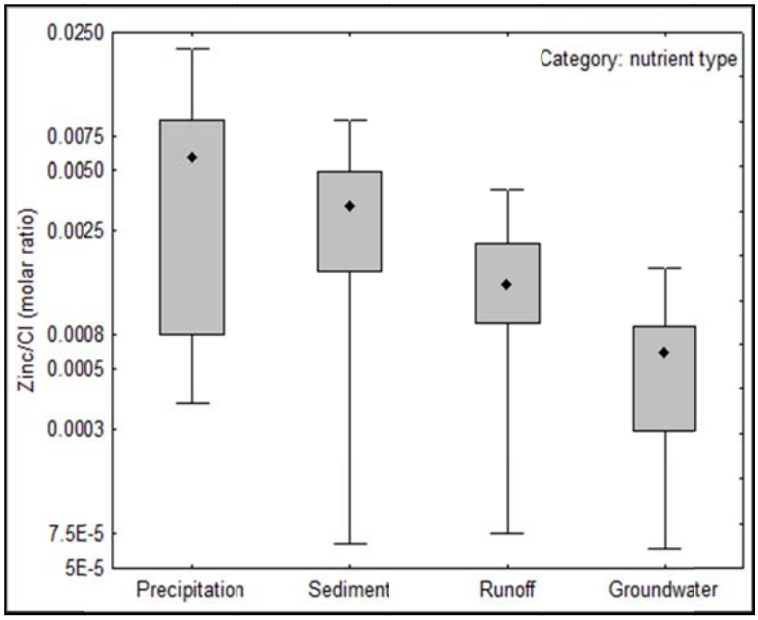

Figure 5.A28: Box plots of zinc in the Amargosa Desert region normalized by sample chloride and grouped by sample type.

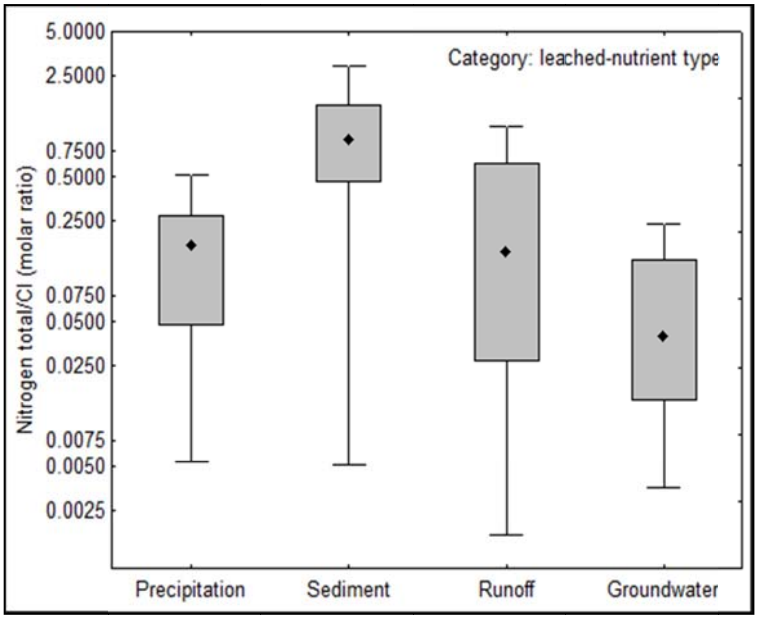

Figure 5.A29: Box plots of total nitrogen in the Amargosa Desert region normalized by sample chloride and grouped by sample type.

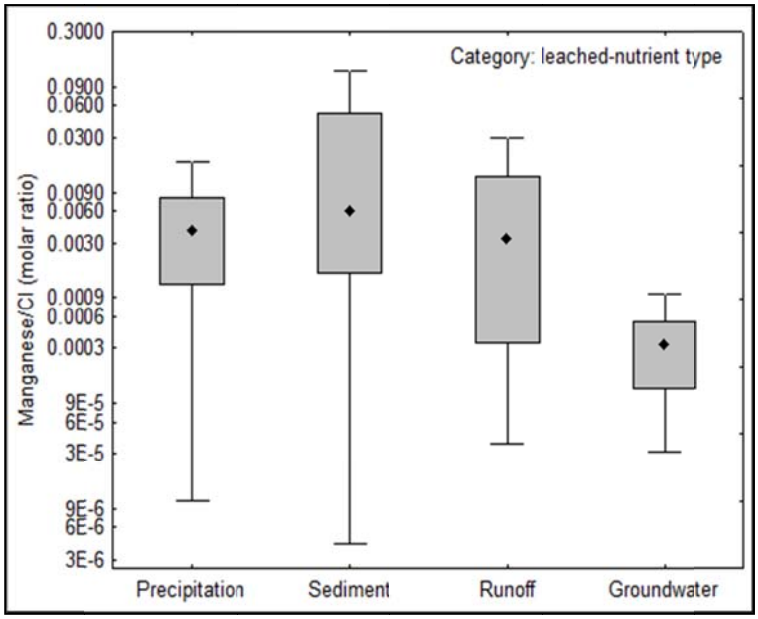

Figure 5.A30: Box plots of manganese in the Amargosa Desert region normalized by sample chloride and grouped by sample type.

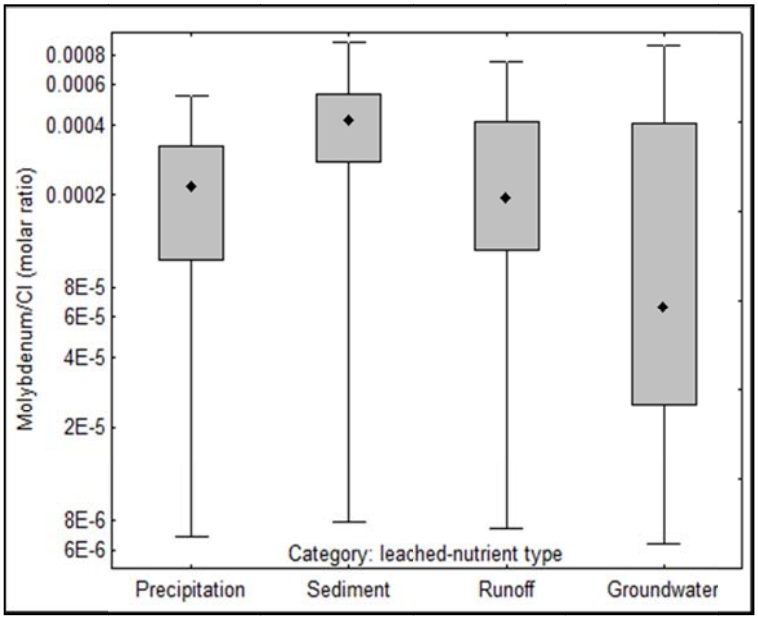

Figure 5.A31: Box plots of molybdenum in the Amargosa Desert region normalized by sample chloride and grouped by sample type.

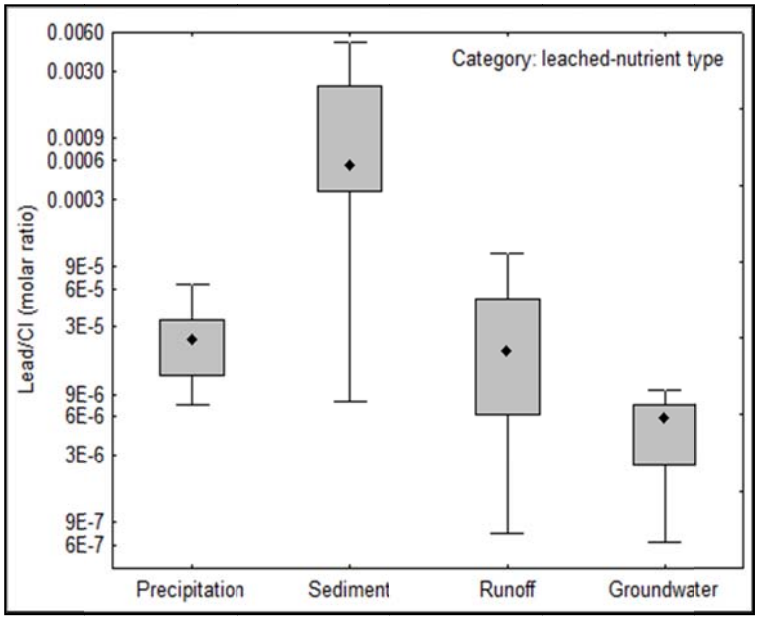

Figure 5.A32: Box plots of lead in the Amargosa Desert region normalized by sample chloride and grouped by sample type.

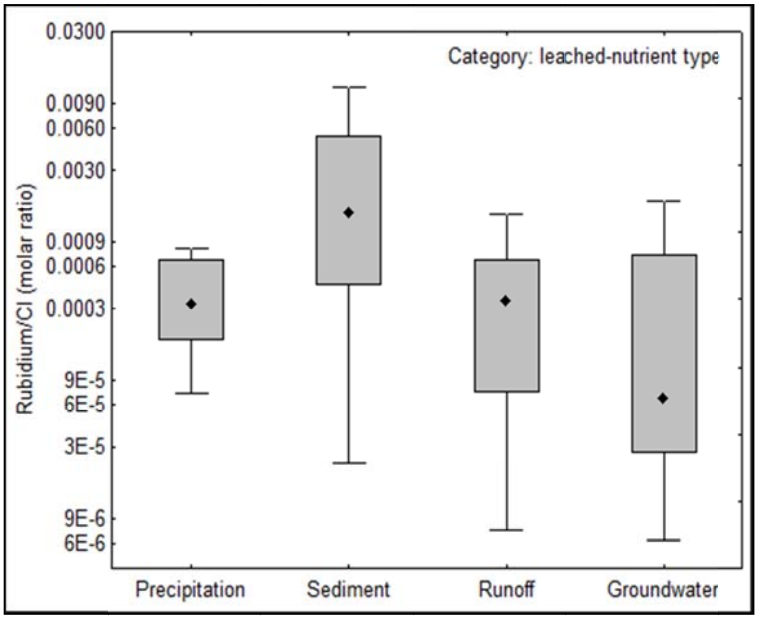

Figure 5.A33: Box plots of rubidium in the Amargosa Desert region normalized by sample chloride and grouped by sample type.

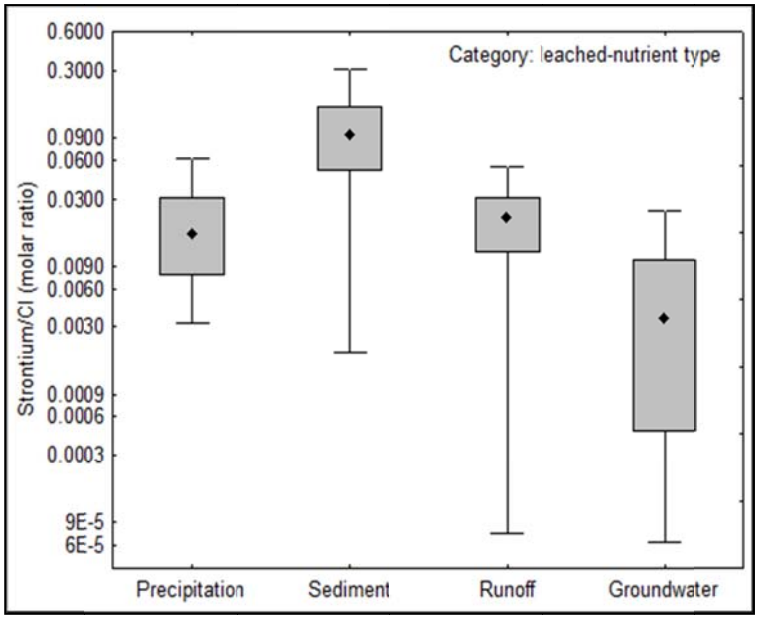

Figure 5.A34: Box plots of strontium in the Amargosa Desert region normalized by sample chloride and grouped by sample type.

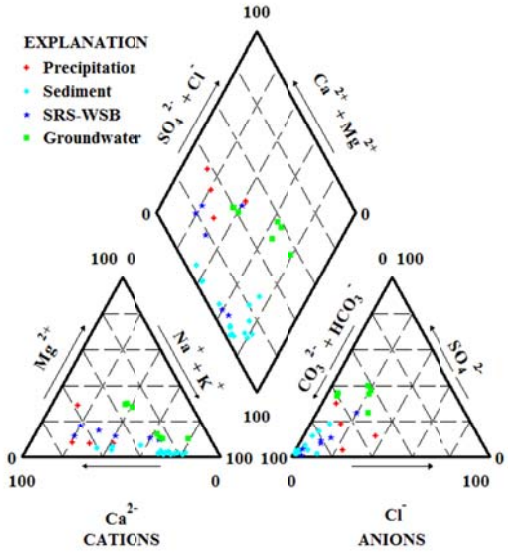

Figure 5.A35: Piper diagram for definition of precipitation, sediment, surface runoff, and groundwater chemical types in Amargosa River. Precipitation (Ca/HCO3)-type, Runoff (Ca/HCO3 to Ca-Na/HCO3)-type, groundwater (Na/HCO3)-type

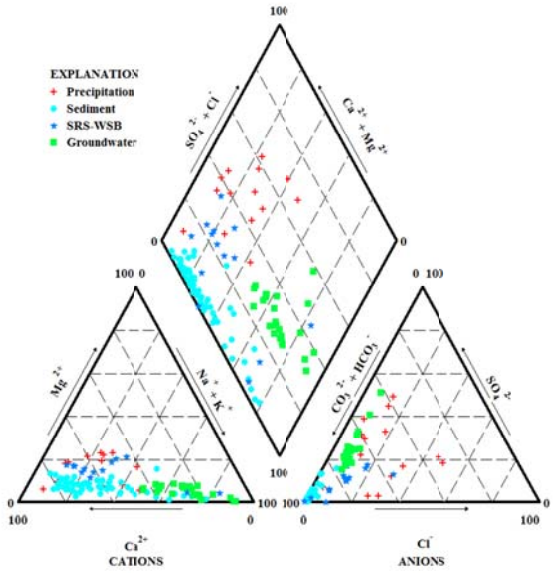

Figure 5.A36: Piper diagram for definition of precipitation, sediment, surface runoff, and groundwater chemical types in Fortymile Wash. Precipitation (Ca/HCO3)-type, runoff (Ca/HCO3 to Ca-Na/HCO3)-type, groundwater (Na/HCO3)-type.

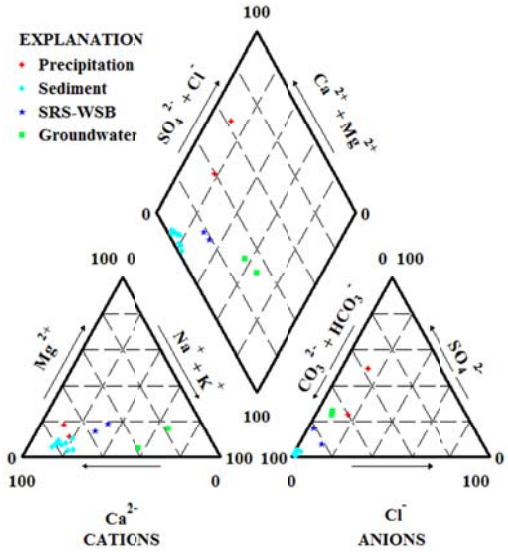

Figure 5.A37: Piper diagram for definition of precipitation, sediment, surface runoff, and groundwater chemical types in Rock Valley. Precipitation (Ca/HCO3)-type, runoff (Ca/HCO3)-type, groundwater (Na/HCO3)-type.

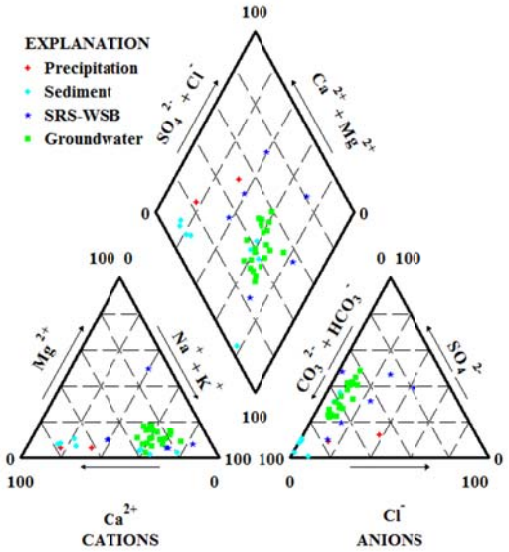

Figure 5.A38: Piper diagram for definition of precipitation, sediment, surface runoff, and groundwater chemical types in southern Amargosa Desert. Precipitation (Ca/HCO3)-type, runoff (Na/HCO3)-type, groundwater (Na/HCO3)-type.

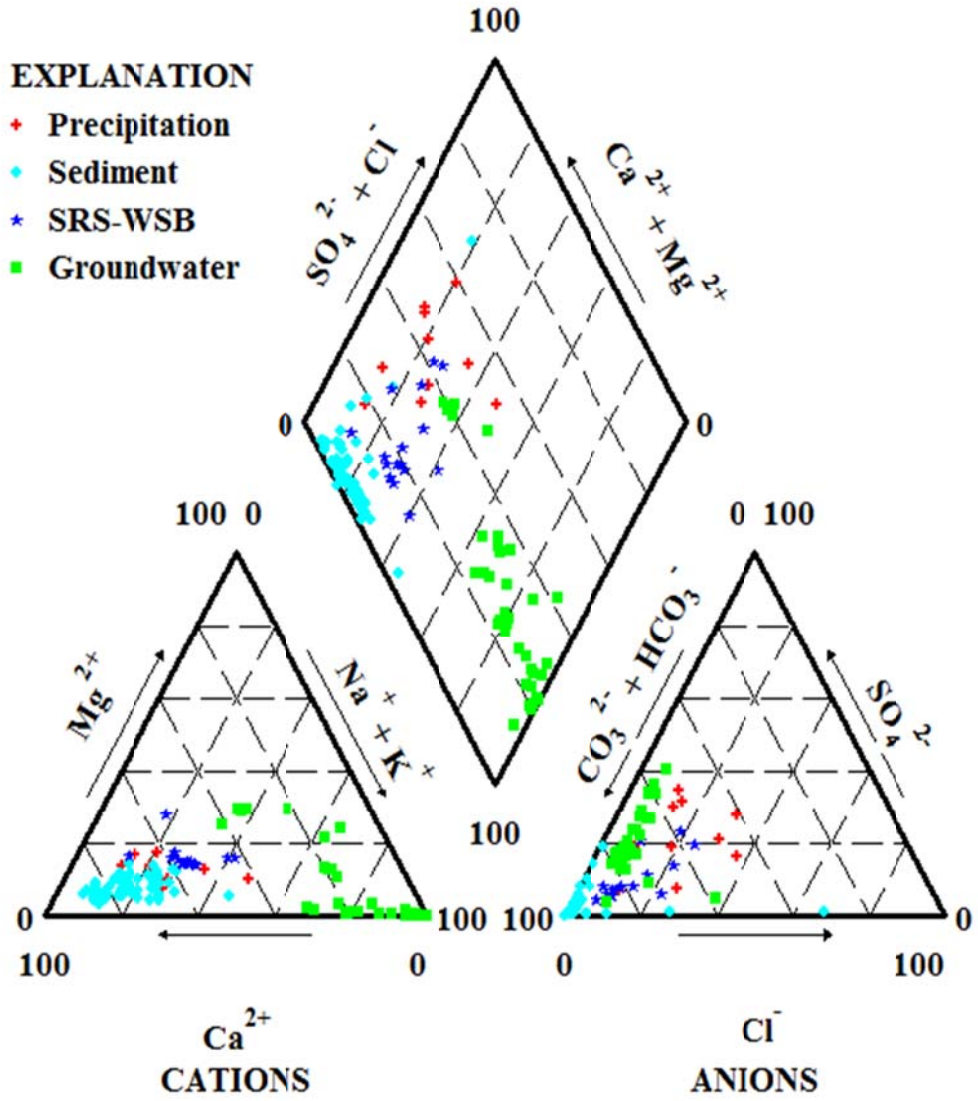

Figure 5.A.39: Piper diagram for definition of precipitation, sediment, surface runoff, and groundwater chemical types in western side of Yucca Mountain. Precipitation (Ca/HCO3)-type, runoff (Ca/HCO3)-type, groundwater (Na/HCO3)-type.

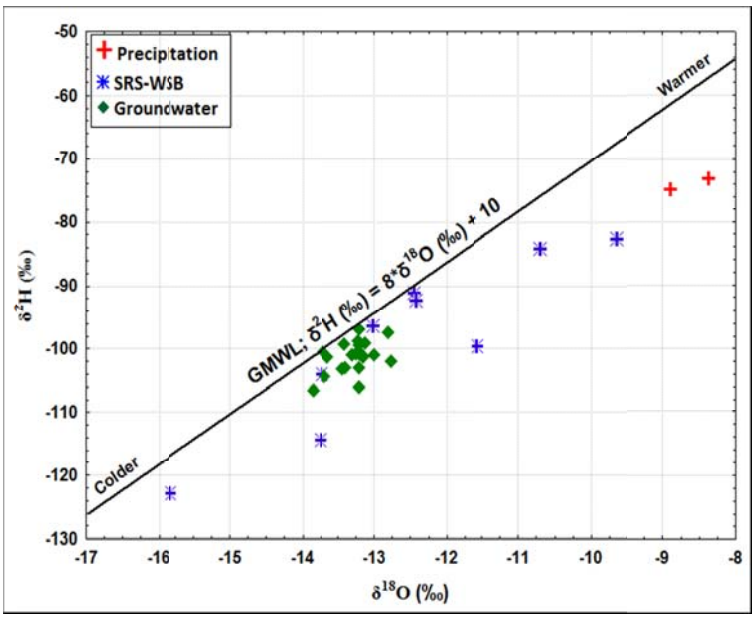

Figure 5.A40: Relationship between the stable isotopes of water in precipitation, runoff, and groundwater in Fortymile Wash.

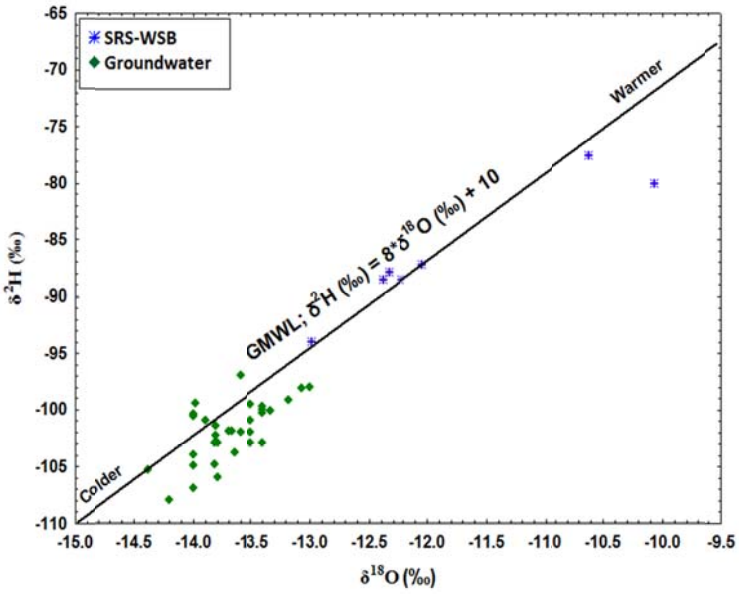

Figure 5.A41: Relationship between the stable isotopes of water in runoff and groundwater in western side of Yucca Mountain.

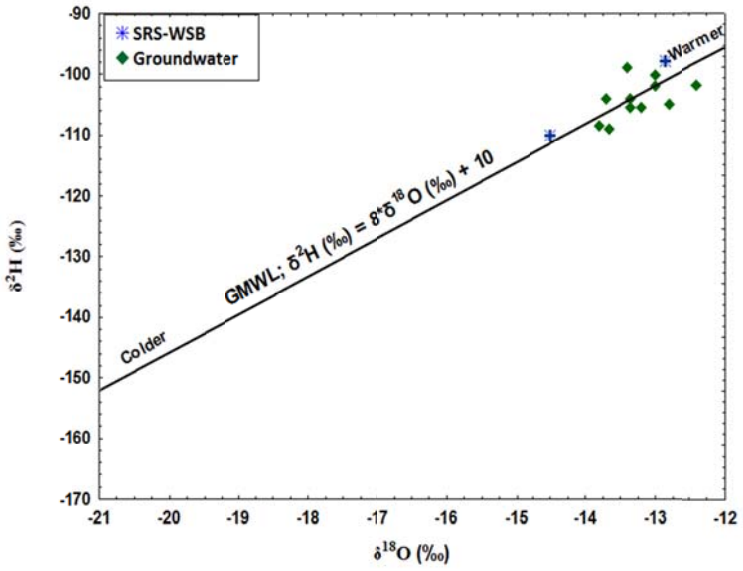

Figure 5.A42: Relationship between the stable isotopes of water in runoff and groundwater in southern Amargosa Desert.

Chapter 6

Groundwater Recharge in in the Amargosa Desert Region: Implications for Validity of Chloride Mass Balance

The material of this chapter is under review for publication in the Journal of Hydrology with a manuscript number: HYDROL11441

6. Groundwater Recharge in the Amargosa Desert Region: Implications for Validity of Chloride Mass Balance Calculations

Omar Al-Qudah [a,*], Arturo Woocay [a, b], and John Walton [a]

[a] *Civil Engineering Department-Environmental Science and Engineering Program, The University of Texas at El Paso, 500 W University Ave, El Paso, TX 79968, USA.*

[b] *División de Estudios de Posgrado e Investigación, Instituto Tecnológico de Ciudad Juárez, Ave. Tecnológico 1340, Ciudad Juárez, CHIH 32500, MX.*

[*] *Corresponding author: Tel.:+1 915 422 4260; fax: +1 915 747 8037; omal@miners.utep.edu.*

ABSTRACT

Groundwater infiltration through alluvium was investigated in the Amargosa Desert, Nevada using borehole drill cuttings, groundwater chemistry, and applying a novel method for collecting runoff water. Water chemistry and chloride concentrations collected from specially designed runoff samplers, placed in Fortymile Wash, an ephemeral arroyo, and its tributaries, closely match the chemistry of underlying groundwater where a plume of low chloride water underlies the wash until it connects with the Amargosa River. This evidence indicates that current and past infiltration of surface runoff (stormwater) is the primary source of the underlying groundwater plume. However, drill cuttings from wells near Fortymile Wash at an elevation of < 1,200 m analyzed using the chloride mass balance method (CMB) indicate that infiltration in the desert was negligible during at least the last 10,000 years, and that most chloride deposition during this time period accumulated in the upper alluvium. The collected data leads to a revised interpretation of semi-arid zone recharge and the CMB method. The results suggest that infiltration of surface runoff from large storm events in this region is a source of recharge more

important that previously realized and that CMB method is inaccurate when applied to surface runoff infiltration. CMB must be used with caution in these types of situations as most of the groundwater recharge occurs without including a significant fraction of watershed chloride.

KEYWORDS: Chloride Mass Balance, Groundwater, Surface Runoff, Fortymile Wash, Recharge.

6.1 INTRODUCTION

Quality, quantity and timing of recharge are primary factors for the sustainable use of groundwater, especially in semi-arid regions where water resources are limited. This study examines recharge characteristics by applying a novel method for collecting surface runoff consisting of specially designed samplers emplaced around Fortymile Wash, east of Yucca Mountain and north of the Amargosa Desert, Nevada. Yucca Mountain Site characterization activities associated with the concept of placing high level nuclear waste repository within the mountain provided a wealth of hydrological information that can be applied to estimating groundwater recharge and is used here to aid in the interpretation of data collected with surface runoff samples. In previous studies (Woocay and Walton, 2008a, 2008b), groundwater chemistry beneath the wash was found to be younger and fresher (lower chloride and total dissolved solids) than adjacent waters, for approximately 40 km, and this was taken as evidence of the large influence of surface runoff infiltration on recharge. In order to study and determine the effects of infiltration, surface runoff samplers were designed and emplaced at the wash and other ephemeral streams in the vicinity. Our research methodology included emplacement site determination and water analysis criteria establishment, along with surface runoff sampler design, construction, field emplacement and sampling as described in detail in Al-Qudah et al. (2010). This paper focuses on the chemical analysis results of collected precipitation, surface runoff, and groundwater in the Fortymile Wash region and their comparison to borehole chloride

profiles which lead to a revised interpretation of recharge in semi-arid regions and of limitations to the chloride mass balance method (CMB).

The chloride mass balance method (CMB) is one technique for estimating recharge to groundwater (Scanlon, 1991; Scanlon et al., 2002, 2006; Subyani, 2004; Flint et al., 2002; Hevesi et al., 2002; Russell, 2002; Wood and Sanford, 1995; Wood, 1999; Ginn, 1997; Bazuhair and Wood, 1996; Tyler et al., 1995). In CMB the aquifer's chloride concentration reflects the degree to which the water has been concentrated by evaporation. A major limitation of the CMB in arid regions is the presumption that chloride and water move together. When areal recharge is present (i.e., general net downward movement of water through the sediments and soil) chloride and water will move together and CMB can be applied, perhaps with corrections to reflect chloride transport in run-on and runoff waters (Wood and Sanford, 1995; Wood, 1999). When recharge is focused and net accumulation of chloride is occurring in soils and sediments, the mass balance becomes problematic.

Profiles of chloride concentrations in alluvium provide a qualitative estimate on downward water moisture fluxes over long periods. The CMB approach is based on several assumptions: (l) one-dimensional, vertical, downward, piston-type flow; (2) precipitation/deposition is the only source of chloride; (3) mean annual precipitation and chloride concentration of precipitation remains constant through time; (4) the steady-state chloride flux carried beneath the root zone by infiltrating water is equal to the chloride concentration in rainfall; (5) chloride behaves as a conservative tracer along the flow path and uptake by roots and anion exclusion are negligible (Scanlon, 1991; Bazuhair and Wood, 1996). In desert regions, chloride often accumulates in the soil while the associated water returns to the atmosphere by evaporation and evapotranspiration. This leads to a characteristic large bulge in soil chloride content at depths of usually less than 6

m in desert soil (Flint et al., 2002; Savard, 1996). In the study area there is evidence that the general behavior of chloride changes with elevation with areal recharge occurring at higher elevations and accumulation of chloride at lower elevations (Flint et al., 2002).

The Amargosa Desert (Figure 6.1) lays in southern Nevada, north east of Death Valley, between the Mojave Desert and the southern boundary of the Great Basin. Yucca Mountain is located on federal land north of the Amargosa Desert and approximately 160 km northwest of Las Vegas. The area is drained by the ephemeral Amargosa River drainage basin which is the major tributary drainage area to Death Valley. Fortymile Wash, also ephemeral, is a major tributary to the Amargosa River, originating between Timber Mountain and Shoshone Mountain and draining southward along the east side of Yucca Mountain. Near U.S. Highway 95, the Fortymile Wash channel changes from being moderately confined to fanning out into several distributary channels that are poorly confined and that drain through several small populated areas. This poorly-defined, distributary drainage pattern persists downstream to its confluence with the Amargosa River.

The present climate in the Amargosa Desert region is considered arid to semiarid, with average annual precipitation ranging from less than 130 millimeters (mm) at lower elevations to more than 280 mm at higher elevations (Flint et al., 2001). Between 2001 and 2005, average annual evapotransipiration rate, air temperature, soil temperature, and relative humidity were, respectively, 147.7-232.6 mm/year, 18-18.4 degrees centigrade (°C), 21.1-21.9 °C, and 21.7-33.3% (Johnson et al., 2007). In contrast, the climate at the end of the Pleistocene epoch at approximately 11,500 years before present (yr BP) marked in North America by the end of the Tioga glacial maximum of the Wisconsin glaciation, was colder and wetter than the present (Benson et al., 2002; Harvey et al., 1999). Evidence of a wetter transition from the Pleistocene to

the Holocene epoch is also found in black mats formed in the southern Great Basin by increased spring discharge, which extended from 11,800 to 6,300 yr BP, with the majority appearing at 10,000 yr BP (Quade et al., 1998). Other authors (Harvey et al., 1999) have noted the existence of large lakes in California and Nevada in the late Pleistocene to early Holocene epochs related to precipitation with temperatures 3 to 8 °C cooler and precipitation rates 60 to 300 percent greater than the current levels. These changes are attributed to a southward displacement of the jet stream, with resultant high winter precipitation (Harvey et al., 1999). Furthermore, of the early, middle, and late parts, into which the Holocene epoch is divided, the middle Holocene, approximately 8,000 to 3,000 yr BP, is considered the warmer and/or drier part of the three (Benson et al., 2002). From carbon, hydrogen, and oxygen isotope data, Claassen (1985) deduced that the major recharge in the area occurred during late Wisconsin glaciation, at the end of Pleistocene and through early Holocene time.

Contemporary recharge in the region is generally considered sparse and derived mostly from higher altitudes by infiltration of precipitation and ephemeral runoff (Flint et al., 2001), while some authors believe that infiltration occurs mainly in washes or by direct entry into fractures exposed at the surface (Claassen, 1985; Montazer and Wilson, 1984). Water may infiltrate from melting snowpack in the mountains primarily on volcanic or carbonate rocks or adjacent to the mountains from streams flowing over alluvium (fans and channels) (Faunt, 2004). White and Chuma (1987) investigated carbon and isotopic mass balances of the Oasis Valley-Fortymile Canyon groundwater basin and concluded that groundwater in Fortymile Canyon may be from local origin. Water quality studies of precipitation, surface water, and groundwater isotopic and common ion concentrations, in addition to computer simulation of the groundwater system in the vicinity of the Amargosa Desert (Claassen, 1985; White and Chuma, 1987; Benson and

Klieforth, 1989; Patterson and Oliver, 2004; USGS, 2004; Savard, 1995, 1996, 1998) have concluded that recharge water is entering the groundwater system north of Yucca Mountain and have determined that recharges from Fortymile Wash, Oasis Valley, and Amargosa River may be a significant source of groundwater.

Water moves along relatively shallow and localized flow paths that are superimposed on deeper, regional flow paths (Faunt, 2004). Regional groundwater flow is predominantly through conduits in the carbonate rocks. This flow field is influenced by complex geologic structures created by regional faulting and fracturing that can create conduits or barriers to flow. Infiltration of precipitation and runoff on high mountain ranges is thought to be the largest source of groundwater recharge. Savard (1995, 1996, 1998) found evidence of groundwater recharge from storm runoff events along the wash in the form of neutron logs, changes in water table elevation, and miscellaneous streamflow observations (such as velocity estimates, high water marks and the distance the streamflow traveled).

In general, hydraulic gradients north of the Amargosa Desert follow a northwest to southeast trend, followed by gradients in the Amargosa Desert that portray a leveling out and then a gradual turn southwest toward Death Valley (Woocay and Walton, 2008a, 2008b). Water levels are less than 850 m above sea level in most of the western side of the Amargosa Desert, Jackass Flats, and Amargosa Flat and decrease to 660 m at the foothills of the Funeral Mountains (Woocay and Walton, 2008a, 2008b). In contrast, topography in the same area changes from 1,050 m above sea level in the west and northeast to 700 m in the southeastern end of the Amargosa Desert near Ash Meadows (Woocay and Walton, 2008a, 2008b).

In this paper we present surface runoff chemistry and compare it to groundwater chemistry along with borehole chloride profiles to better understand the role of surface runoff as a source of groundwater recharge and the limitations of the CMB method.

6.2 METHODS

6.2.1 Surface runoff samplers

Runoff samplers were designed to collect surface runoff water in order to measure the chemical characteristics of runoff water that has contacted and leached some of the top soil. The construction started by threading flexible polyethylene tubing through a hole made 25 mm below the top edge of the 9.5-liter bucket, to provide access to the inside of the runoff sampler once it is buried. The inner edge of the tubing was fixed to the bucket bottom with an epoxy adhesive, and the outer end blocked with a plug to prevent tubing clogging. In total, twelve runoff samplers, filled with washed silica sand (WSB), were installed at twelve different locations around Fortymile Wash (Figure 6.1) to capture surface runoff water. The samplers were placed at locations in surface-runoff channels where water is likely to pool and where sufficient depth of sediment facilitates digging a hole for emplacement. To the extent possible, samplers were placed in low gradient (depositional) portions of the arroyo to minimize washing out during storms.

The runoff samplers are distributed in the study area in the following manner (Figure 6.1). Sampler-15 and Sampler-16-ALT are located in the Topopah Wash 122 m and 2.96 km upgradient from the Amargosa Valley Science and Technology Park, respectively. Sampler-29 is located in the west side of the Striped Hills, 0.43 km downgradient from U.S. highway 95. Sites

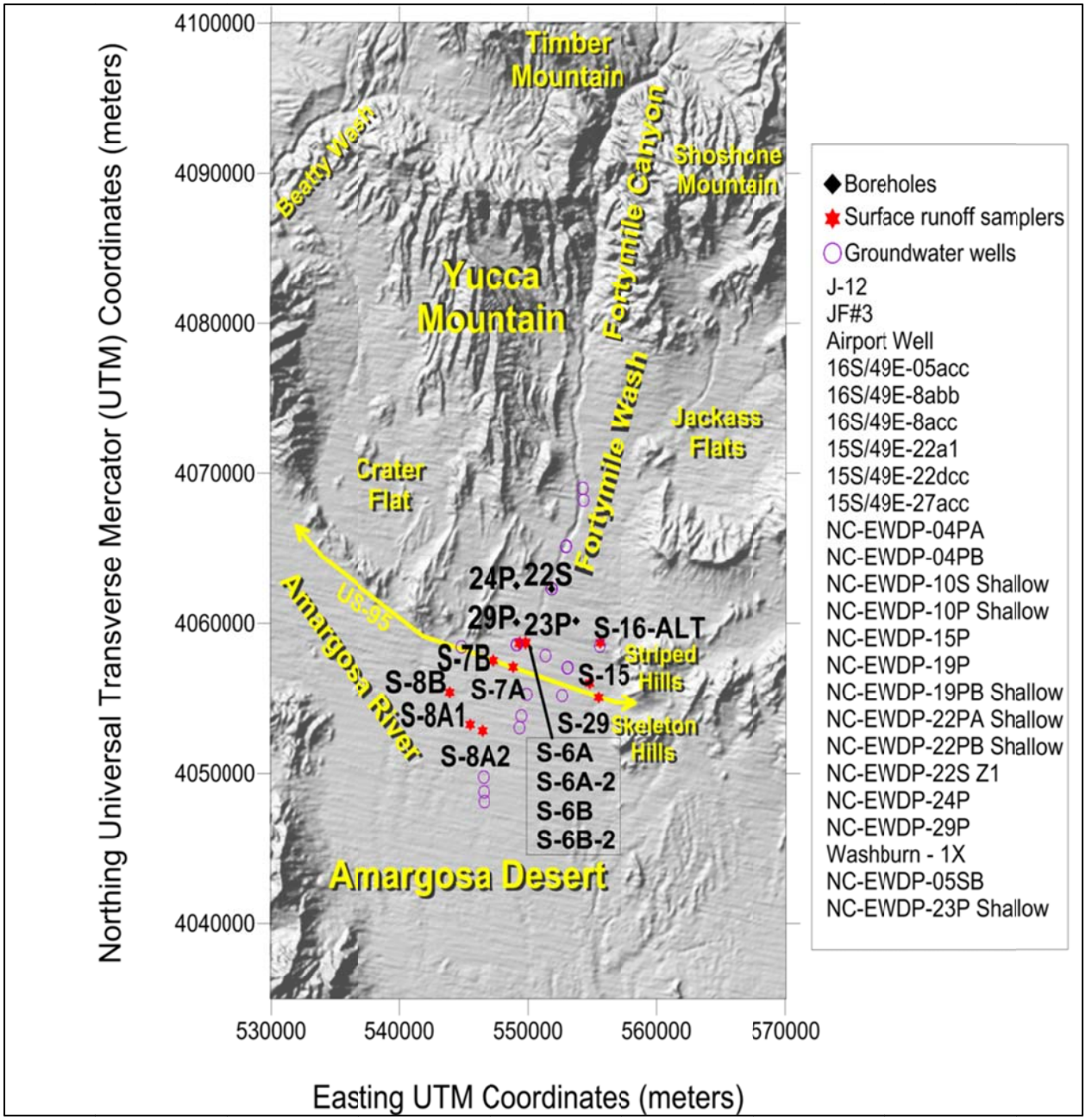

Figure 6.1: UTM coordinates map for the study area showing location of Fotymile Wash, Yucca Mountain, Amargosa Desert, and Amargosa River, Nye County, NV (modified from Woocay and Walton, 2008a). Stars represent surface runoff samplers, open circles represent groundwater wells, and diamonds represent boreholes.

for Sampler-6A and Sampler-6B-2 are located to the south of the pole line road, middle channel of Fortymile Wash. Sampler-6A-2 and Sampler-6B are located to the South of the pole line road, western channel of Fortymile Wash. Sampler-7A is located to the South of U.S. highway 95, eastern channel of Fortymile Wash. Sampler-7B is located to the South of U.S. highway 95, western channel of Fortymile Wash. Sampler-8A1 is located in the western branch of eastern channel of Fortymile Wash. Sampler-8A2 is located in the eastern branch of eastern channel of Fortymile Wash. Sampler-8B is located in the western channel of Fortymile Wash.

Samples collected at these sites included precipitation and surface runoff samples. Runoff samples were collected from the WSBs at each location shortly after three separate storm events occurring in: February, 2009; January, 2010; and December, 2010. Additionally, after the January, 2010, event, precipitation samples were collected from the rain gauges at each site. In total, twenty-two WSB samples and fourteen precipitation samples were collected during February, 2009, and December, 2010. Since the volume of water collected after storm events was variable, a decision criterion was established to evaluate if the amount of water stored in the samplers was enough to analyze all the required chemical parameters, and the laboratory used for analyses was contacted to determine minimum water sample volume requirements which then lead to determination of sampling priority based on data importance and volume requirements. The rain gauges used are simple (low cost) collectors that are open to the atmosphere. The water from rain gauges included both wet-fall and dry-fall since the last time each gauge was emptied and rinsed. Since readings and chemistry collected at rain gauges were subject to unknown amounts of evaporation prior to collection, the readings should not be equated with precipitation amount or initial chemistry.

Surface runoff and precipitation samples were collected, preserved, shipped, and analyzed based on the standards methods for the examination of water and wastewater (Clescerl, 2000) by using inductively coupled plasma mass spectrometry (ICP-MS) and ion-exchange chromatography (IEC) machines, in addition to the volumetric titration, for major cations and anion (Cl^-, HCO_3^-, SO_4^{2-}, Ca^{2+}, Mg^{2+}, K^+, and Na^+). Results generated by Statistica^{TM}9 (StatSoft Inc., 1984-2010) are presented on box plots to simplify data interpretation.

6.2.2 Geochemical modeling

PHREEQC (Parkhurst and Appelo, 1999) inverse modeling was used for simulating a variety of surface runoff and groundwater reactions and processes that can explain the water chemistry's evolution. Major anion and cation median concentrations of surface runoff and groundwater were used as an input for the PHREEQC inverse modeling taking into consideration the initial saturation indices, ion exchange reactions, and the potential dissolution and precipitation of common minerals in the study area that do not appear in the initial saturation indices. The PHREEQC output shows many potential models that explain the evolution, and the best model was chosen based on the actual median differences between the surface runoff and groundwater chemistry.

6.2.3 Nye County groundwater wells

Nye County has 24 wells in the region as shown on Figure 6.1. Groundwater chemistry data were obtained from the Nye County Nuclear Waste Repository Project Office (NWRPO) web site as of April 2008 (NWRPO, 2008) and a Los Alamos National Laboratory report (LANL, 2007). Data were compiled into a single database covering the Amargosa Desert region, and

giving preference to NWRPO (2008) data, due to data from newly developed wells and more resent analyses.

6.2.4 Borehole chloride analysis

Soil extracts were obtained from borehole cuttings samples that were previously collected by the Nye County Early Warning Drilling Program (NC-EWDP) from boreholes NC EWDP-22S, 23P, 24P and 29P which were drilled using air as the primary drilling fluid to preserve sample integrity. Table 6.1 presents a summary of borehole information. Borehole cutting samples were selected in an attempt to characterize the upper and lower drill cuttings and therefore are not evenly spaced. Drill cutting samples were separated into two subsamples; the first was oven dried to determine the sample's water percent content by weight, and the second one was used to obtain soil extracts. An extraction dilution of 1:1 (1 liter of deionized water per kg of soil) was used with a correction for the sample's original water content. Soil extracts were then analyzed for chloride concentrations following ASTM standards (ASTM D2216-98, D4542-95).

Table 6.1: Summary of Information for Boreholes Analyzed by Chloride Mass-Balance [a].

Borehole	NE-EWDP-22S	NE-EWDP-24P	NE-EWDP-29P	NE-EWDP-23P
Latitude (North)	36° 42' 15.132"	36° 42' 16.775"	36° 40' 57.297"	36° 41' 05.137"
Longitude (West)	116° 25' 06.636"	116° 26' 52.756"	116° 26' 52.884"	116° 23' 50.412"
Elevation (AMSL)	868.45 meters	850.45 meters	830.41 meters	868.58 meters
Depth to Water	144 meters	124 meters	106 meters	130 meters
Drilling Depth	142 meters	120 meters	96 meters	120 meters
Number of Extracts	93	12	11	12
Drilling Composition	0 to 109.7 meters: well-graded sand with silt and gravel (SW-SM) 109.7 to 338.3 meters: silty sand with gravel (SM)	0 to 18.3 meters interbedded well-graded sand with silt, clay and gravel (SW-SM/SC) and silty, clayey sand with gravel (SM/SC) 18.3 to 74.7 meters: well-graded sand with silt, clay and gravel (SW-SM/SC) 74.7 to 121.9 meters: silty, clayey sand with gravel (SM/SC)	0 to 38.1 meters: well-graded sand with silt, clay and gravel (SW-SM/SC) 38.1 to 80.8 meters: Interbedded silty, clayey sand with gravel (SM/SC) and well-graded sand with silt, clay and gravel (SW-SM/SC)	0 to 137.2 meters: well-graded sand with silt and gravel (SW-SM)

[a]Here SW, SM, and SC represent sand with silt, sand with gravel, and sand with clay

Boreholes 22S, 23P, 24P and 29P had, respectively, 93, 12, 12, and 11 available samples and plots of reported Cl mass at specific depth are presented in Figure 6.2.

A linear interpolation of chloride extract concentrations was performed through each borehole's sampling depth, and age-rates for both chloride loadings through depth at 1 m intervals were calculated as follows:

$$\frac{dt}{dz} = \frac{Cl_{concentration}\left[\frac{kg_{Cl}}{kg_{Soil}}\right] \times \rho_{Soil}\left[\frac{kg_{Soil}}{m^3}\right]}{Cl_{Loading}\left[\frac{kg_{Cl}}{m^2.year}\right]} \qquad Eq.6.1$$

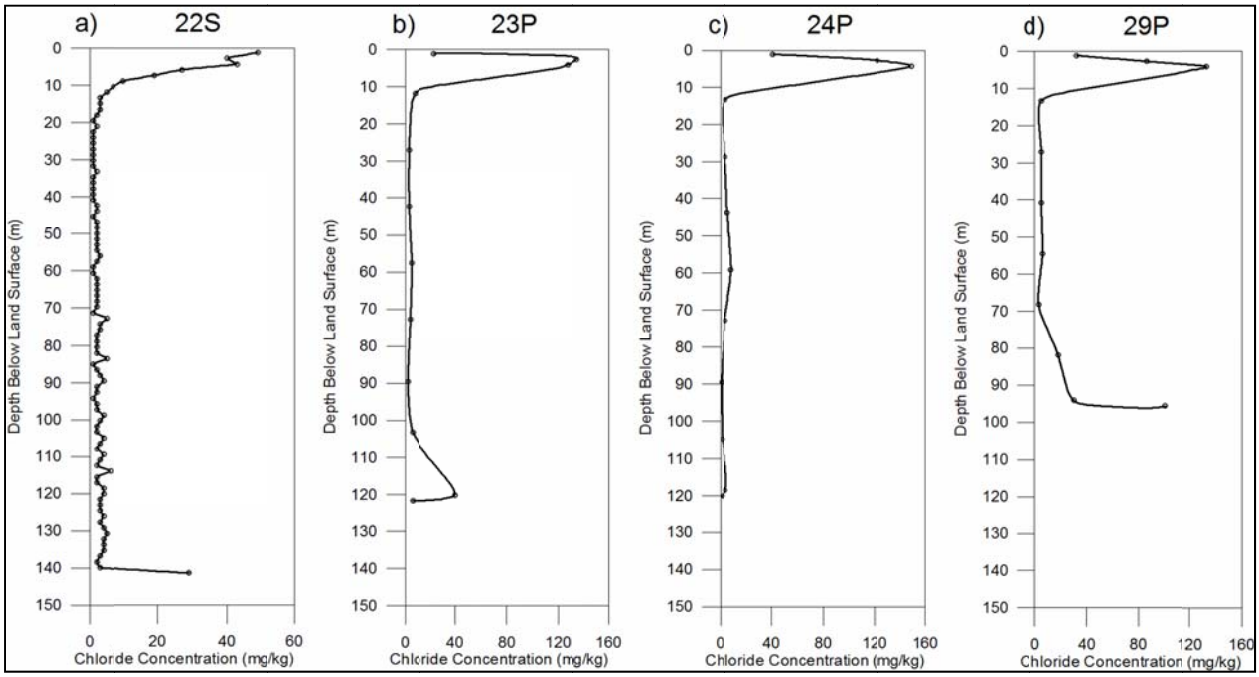

Figure 6.2: Interpolations of drill cutting chloride extracts from boreholes: (a) NC-EWDP-22S; (b) NC-EWDP-23P; (c) NC-EWDP-24P; and (d) NC-EWDP-29P.

In these calculations, t refers to age (years) and z is the depth from ground surface (meters), an average soil bulk density of 2,000 kg/m^3 is assumed. Two chloride deposition rates (loadings) obtained from literature were used to provide approximate upper and lower calculation limits, and these values are assumed constant throughout time in lieu of attempting to compensate for

specific fluctuations in chloride deposition and/or precipitation through time. With a lower chloride loading of 60 mg/m^2/year, corresponding to contemporary values (Fabryka-Martin et al., 2002), and considering a 170-mm average precipitation per year (Liu et al., 2003), an average chloride precipitation concentration of 0.35 mg/l is found, which is in agreement with values reported by Meijer (2002) for the Kawich Range sampling network some 150 km north of Yucca Mountain. With an upper chloride loading of 107 mg/m^2/year (Liu et al., 2003), an average chloride precipitation concentration of 0.62 mg/l is found, corresponding to an attempt to correct for either greater past chloride loading or a higher past precipitation with chloride concentration remaining constant. Integrating Equation 6.1 from the surface to the available data depths yields infiltrations dates before-present. Figure 6.3 presents the infiltration dates before present for borehole 22S which had the most available data points. Woocay and Walton (2008a, 2008b) present complete results for infiltration dates before present and pore velocities for all four boreholes, using upper and lower chloride loadings.

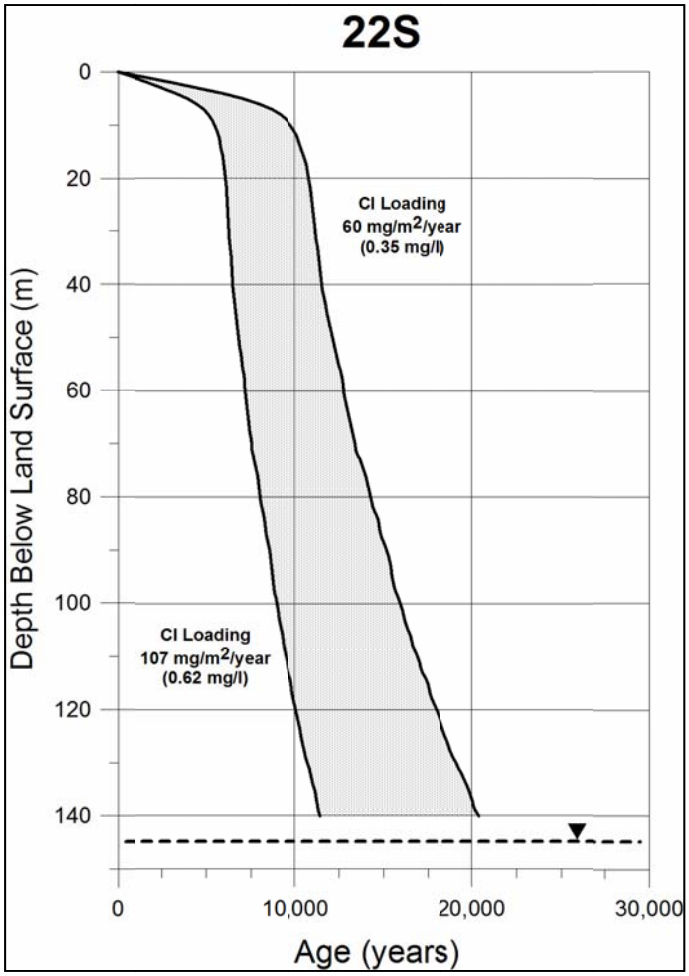

Figure 6.3: Integration of the chloride mass with depth and estimating ages from Borehole 22S, (Woocay and Walton, 2008a).

6.2.5 Effective recharge into Amargosa Valley

Chloride is a conservative tracer with no other sources other than precipitation and deposition. Average annual chloride loading in the region is considered invariable with respect to elevation and includes precipitation and dry deposition. Average chloride loading (L̇, wet and dry) is between 60 mg/m^2/year (lower loading) (Fabryka-Martin et al., 2002) and 107 mg/m^2/year (higher loading) (Liu et al., 2003).

The watershed is confined by the natural topological divides and the alluvium aquifer. Recharge and chloride do not infiltrate from the alluvium to the underlying carbonate aquifer nor does this aquifer upwell into the alluvium aquifers.

Enough time has elapsed for the watersheds under study to achieve steady state i.e. climate has been similar for the last 3,000 years, corresponding to the late Holocene, and warmer and/or drier between 8,000 to 3,000 years before present (YBP), corresponding to the middle Holocene (Benson et al., 2002).

Chloride concentration can be estimated as follows:

$$\mathbf{C} = \frac{\mathbf{M}}{\mathbf{V}} \qquad \boldsymbol{Eq.6.2}$$

Where:

M: chloride mass, mg

V: volume of water holding chloride, m^3

Chloride mass flux is chloride loading ($\dot{L}_{Cl}$ ($mg/m^2/year$)) times watershed area (A (m^2)).

$$\dot{\mathbf{M}} = \dot{\mathbf{L}}_{\mathbf{Cl}}\mathbf{A} \qquad \boldsymbol{Eq.6.3}$$

Noting that the mass flux of chloride entering the watershed is equal to mass flux exiting, and assuming a representative average chloride concentration for the groundwater exiting the watershed and entering the Amargosa Valley groundwater, the effective recharge from any given watershed is given by:

$$\dot{V}_{out} = \dot{M}_{Cl}/C_{out} = \dot{L}_{Cl}A/C_{out} \qquad \boldsymbol{Eq.6.4}$$

Equation 6.2 assumes that the entire watershed's area contributes chloride and water to the groundwater and this is not the case as some chloride is sequestered in thick soil at locations where not enough precipitation occurs to trigger percolation beyond the root zone that would

induce infiltration. An effective infiltration altitude of 1,200 meters above sea level (ASL) is assumed thus limiting the watershed area contributing to $\dot{M}_{Cl}$ and:

$$\dot{V}_{out} = \dot{L}_{Cl} A_{>1200} / C_{out} \qquad Eq. 6.5$$

Upper and lower bounds on recharge are estimated using: a range of average regional chloride loading found in literature (60 to 107 mg/m^2/year); Digital elevation model map is used to estimate watershed areas (total area and only area above 1,200 m ASL) (Figure 6.9); and average chloride concentrations in groundwater downgradient from each watershed at locations where a steady state can be assumed (corrected ^{14}C ages at or below 8,000 YBP) (Figures 6.4, 6.10). The lower bounds for each watershed are calculated using the lower Cl loading, and areas abode 1,200 m ALS; the upper bounds are calculated with the higher Cl loading and the total area of each watershed.

6.3 RESULTS AND DISCUSSION

6.3.1 Groundwater chloride concentration

Figure 6.4 shows the concentration of chloride in the groundwater. Well locations are marked and contours are drawn with Surfer™8 (Golden Software Inc., 2008) software using the software's existing Natural Neighbor gridding method. The most noticeable trend is that lower concentrations of chloride are present beneath and near Fortymile Wash and this trend extends down the Wash following its shape until its confluence with the Amargosa River.

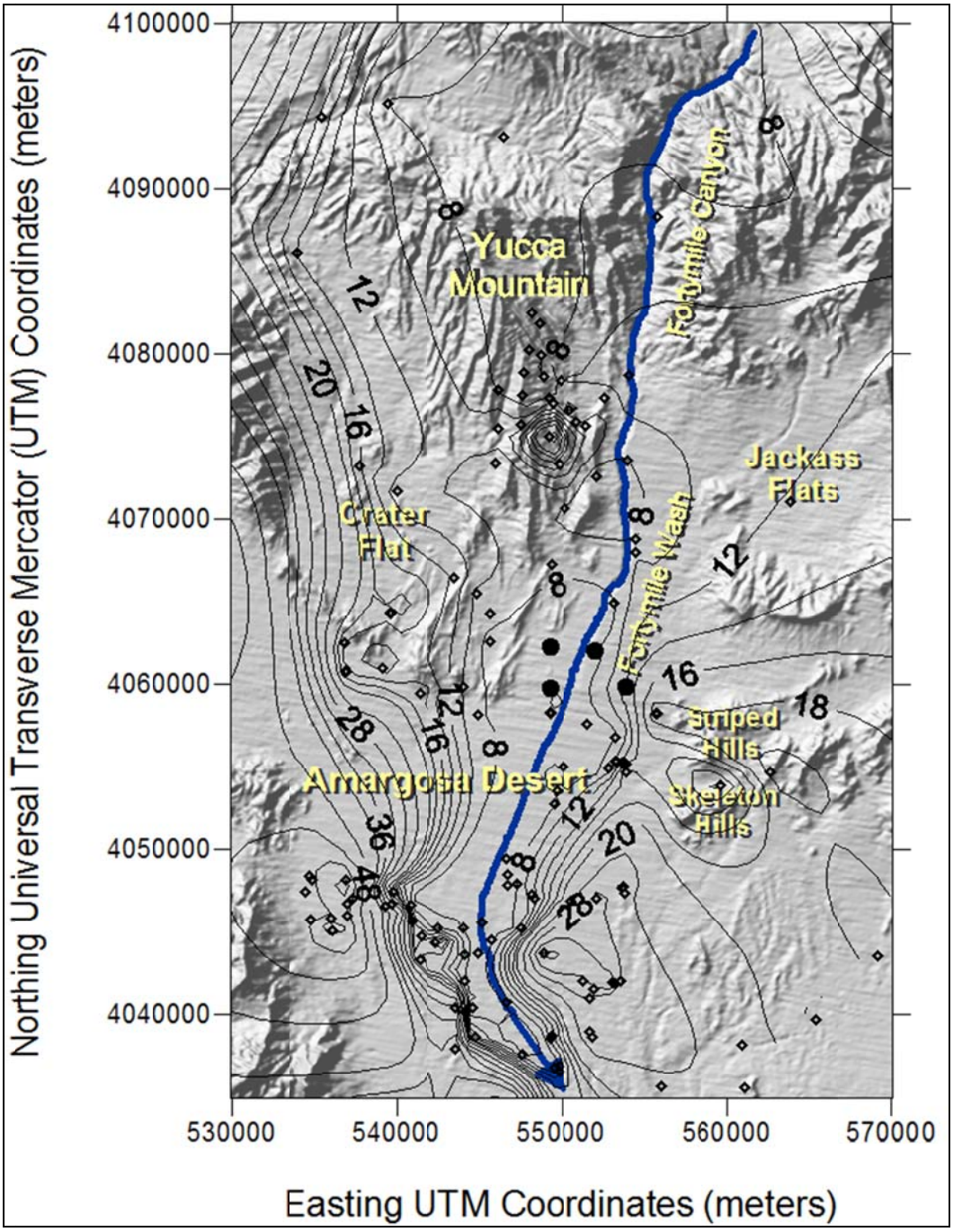

Figure 6.4: UTM coordinates map for the study area showing chloride contours in groundwater.

Groundwater in the study area is moving approximately north to south (Woocay and Walton, 2008b). In a flowpath, recharge is added to the surface of the groundwater. Given the apparent importance of sporadic surface runoff events and the winding/network spatial pattern of

ephemeral drainages, a high degree of variability would be anticipated, however, if recharge is occurring we should see younger water near the water table and older water at depth at the same location. Figure 6.5 presents carbon-14 (^{14}C) data from nearby Nye County wells where multiple sampling ports are available, although none of the sampling ports are precisely at the water table. With one exception, the wells indicate younger groundwater nearer the water table.

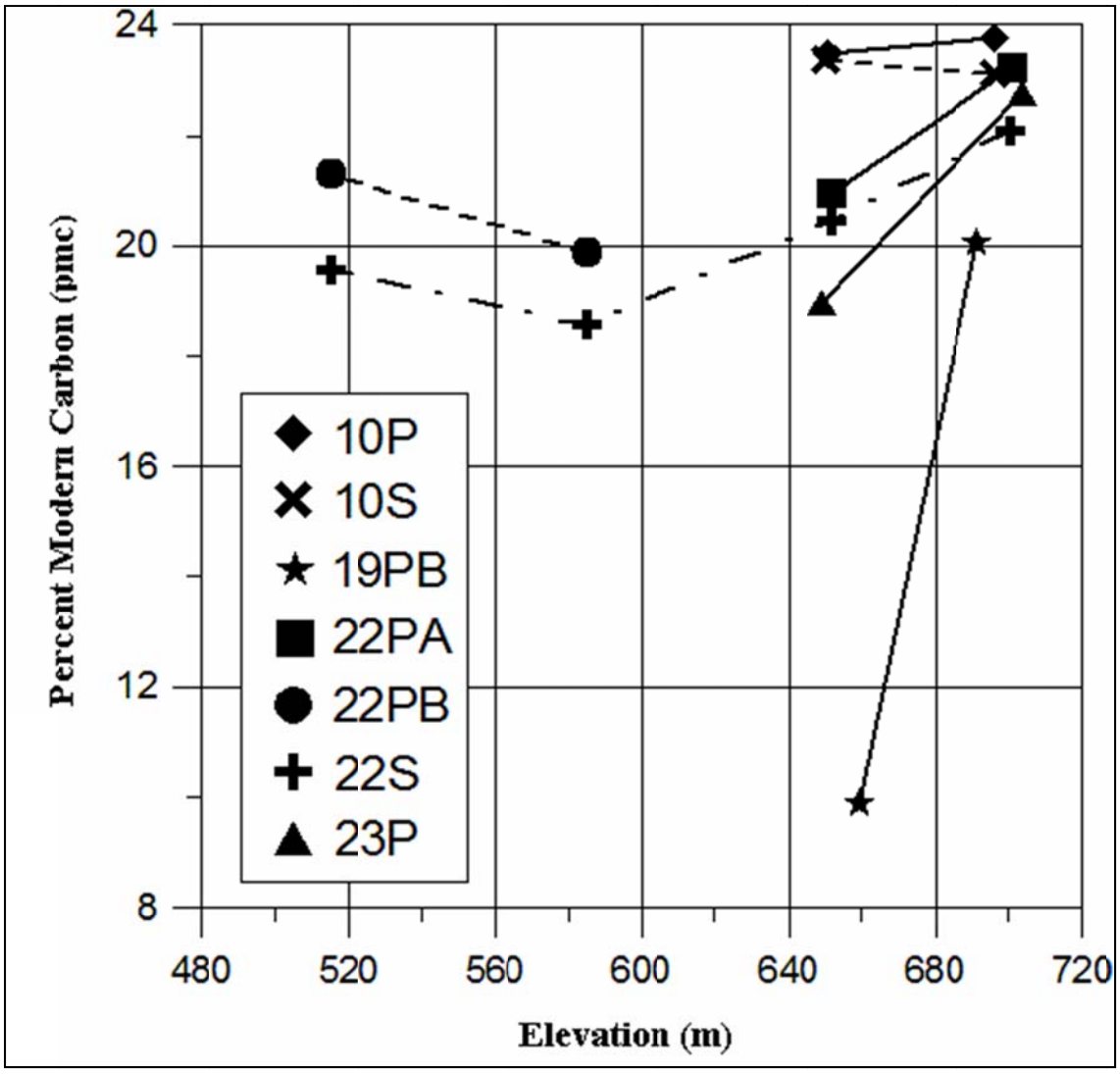

Figure 6.5: Carbon-14 (^{14}C) data from nearby Nye County groundwater wells at multiple sampling depths.

Furthermore, Flint et al. (2002) estimated areal recharge on Yucca Mountain just to the west of Fortymile Wash by using a Darcian approach, neutron logging of moisture profile (channel, terrace, side slope, and ridge top), borehole temperature profiles, Maxey and Eakin empirical method, and CMB (pore water, perched water, and groundwater). Flint et al. (2002) found evidence for net infiltration rates of 0.8 to 9.9 mm/yr on the ridge top (1400 m), with a mean chloride concentration of 33 ppm; and 1.0 to 1.5 mm/yr, with mean chloride concentration of 48 ppm on the lower side slopes of the mountain and terrace below (1200 m), beneath areas with negligible soil cover. This was associated with average pore water chloride concentrations of 48 ppm compared with chloride concentrations in the groundwater below of 7 ppm. The discrepancy in chloride concentrations between infiltration and groundwater mean that present day areal recharge from the mountaintop, sides, or terraces cannot be primarily responsible for current groundwater.

6.3.2 Borehole chloride mass balance (CMB)

Figure 6.2 shows the chloride concentrations from boreholes: (a) 22S; (b) 23P; (c) 24P; and (d) 29P. Each borehole's chloride profile exhibits a concentration bulge at the upper-most part of the profile (i.e., at relatively shallow depths) which is typically observed in arid regions and is attributed to large amounts of evapotranspiration at the surface. The increase in chloride concentration near the water table is evidence of upward migration of water from the water table driven by net evaporation in the vadose zone rather than infiltration. Tyler el al. (1995) examined three deep boreholes in Southern Nevada at an elevation of 1,000 m and also found a soil chloride surface bulge characteristic of the absence of areal recharge

Integration of the chloride mass with depth and dividing by assumed chloride loading (Woocay and Walton, 2008a) is shown in Figure 6.3 for 22S, the borehole with the most

complete data. The sites of all four boreholes indicate that significant areal infiltration has not occurred at these sites for the past ~10,000 years.

6.3.3 Water chemistry

Water chemistry for collected surface runoff, groundwater, and precipitation samples is summarized in Table 6.2. The ratios represent median normalization by the median chloride concentration for each category. Although precipitation samples underwent an unknown and variable amount of evaporation prior to sampling, relative ion concentrations should not change significantly in dilute waters with evaporation.

Table 6.2: Median Relative and Absolute Concentration of Measured Ions.

Measured Ion	Precipitation	Surface runoff	Groundwater
Cl^- median (meq/l)	0.05	0.18	0.2
(HCO_3^-; HCO_3^-/Cl^-) (median; median ratio)	(0.20; 3.78)	(1.82; 9.95)	(2.24; 11.06)
(SO_4^{2-}; SO_4^{2-}/Cl^-) (median; median ratio)	(0.08; 1.55)	(0.15; 0.83)	(0.58; 2.88)
(Ca^{2+}; Ca^{2+}/Cl^-) (median; median ratio)	(0.19; 3.66)	(1.20; 6.56)	(0.78; 3.85)
(Mg^{2+}; Mg^{2+}/Cl^-) (median; median ratio)	(0.04; 0.73)	(0.29; 1.60)	(0.18; 0.87)
(K^+; K^+/Cl^-) (median; median ratio)	(0.01; 0.27)	(0.16; 0.89)	(0.13; 0.64)
(Na^+; Na^+/Cl^-) (median; median ratio)	(0.04; 0.85)	(0.35; 1.93)	(1.92; 9.50)

A number of changes occur. Chloride increases between precipitation and surface runoff as previously deposited salts are partially removed from the soil. Most precipitation events do not lead to surface runoff and result in chloride accumulation in the shallow sediments as essentially all of the precipitation evaporates or is transpired. Between precipitation and runoff there are (relative to chloride) increases in bicarbonate, calcium, magnesium, sodium, and potassium, and

a slight decrease in sulfate. From surface runoff to groundwater, bicarbonate, sulfate and sodium increase while calcium, magnesium and potassium decrease.

Figure 6.6 presents box-plots of precipitation, surface runoff and groundwater chloride concentrations. The actual values for precipitation are less than or equal to the measured results given an unknown amount of evaporation occurred prior to sampling.

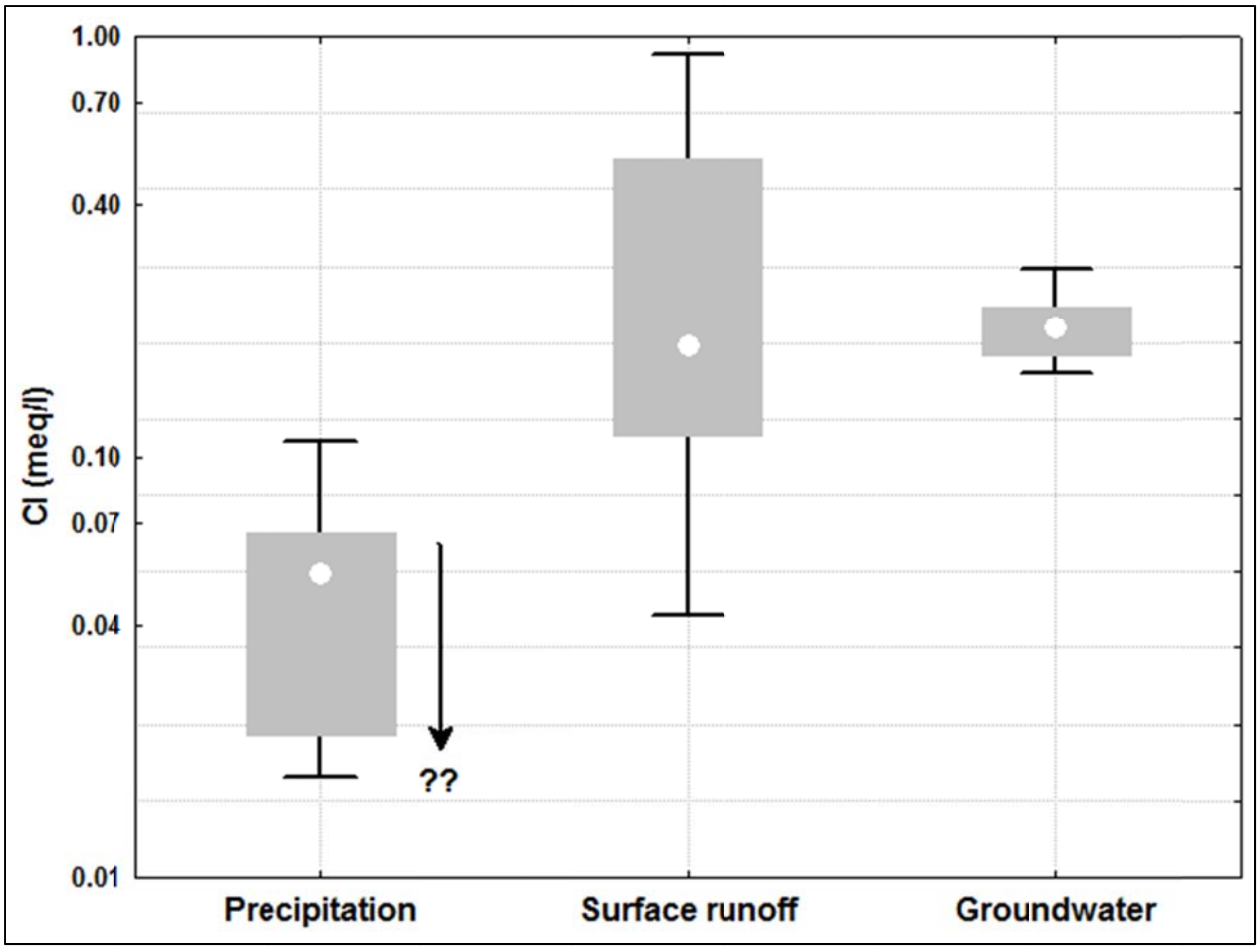

Figure 6.6: Box plot of measured chloride concentrations grouped by sample type.

The captured surface runoff has nearly the same median chloride concentration as the underlying groundwater corroborating other evidence that present day infiltration of surface runoff recharges underlying groundwater. Figure 6.7 presents water stable isotope values of surface runoff and groundwater. The distance from the meteoric water line which is indicative of

the degree of evaporation, is similar for surface runoff and groundwater. The surface runoff samples exhibit a broader spread parallel to the meteoric water line. Recharge occurring at any place in the aquifer would be younger than upgradient groundwater flow.

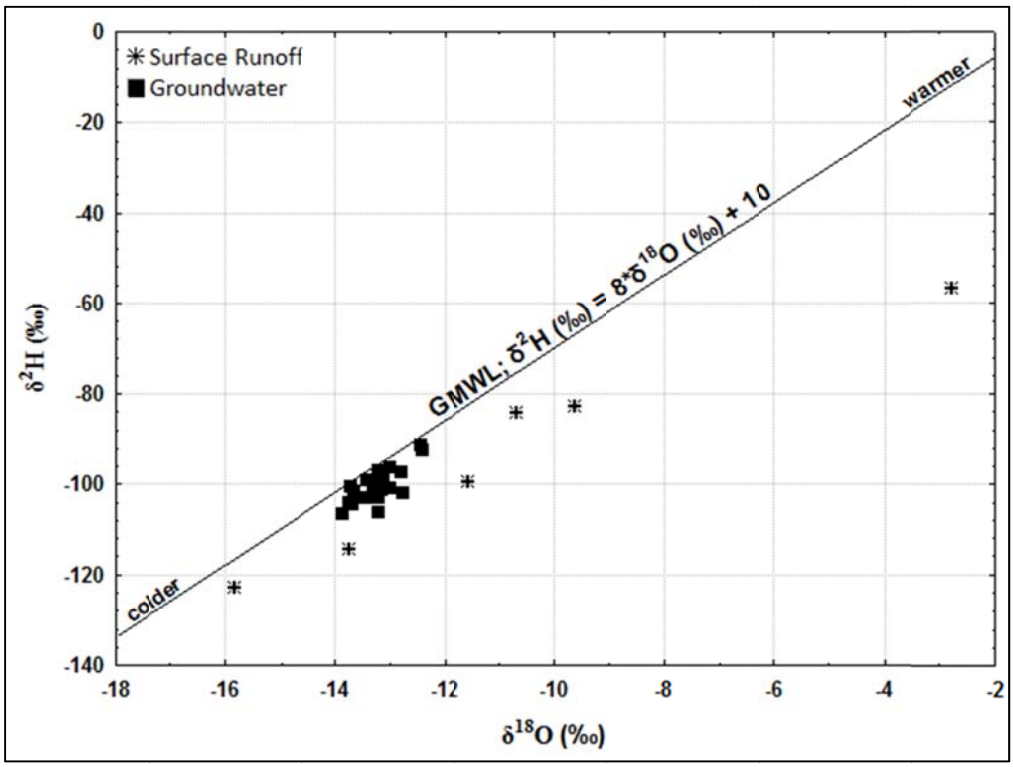

Figure 6.7: Relationship between the stable isotopes of water in surface runoff and groundwater of the independence catchment. GMWL: global mean water line.

Claassen (1985) used available groundwater quality data (major cations and anion, and carbon, hydrogen, and oxygen isotope data) in west-central Amargosa Desert, in addition to the geochemical reaction mechanisms, to develop a conceptual geochemical model of the hydrologic regime in order to determine the sources, mechanisms of recharge, and groundwater pathways in the area. Claassen (1985) concluded that the groundwater in the area was recharged primarily by overland flow in or near the present-day stream channels, rather than by subsurface flow from highland recharge areas to the north, and that the reasonable alternative is that surface runoff directly recharges the groundwater in the area.

Benson and Klieforth (1989) studied stable isotopes in precipitation and groundwater in the Yucca Mountain area and concluded groundwater recharge occurred by infiltration of cold-season precipitation, probably along the bottom of Fortymile Canyon. Savard (1995, 1996, 1998) found that neutron logging in some selected boreholes in Fortymile Wash showed increases in the volumetric water contents of the unsaturated alluvium indicating that water infiltrated to a depth of approximately five meters, and in subsequent visits to the wash, he identified evidence of the streamflow events.

Figure 6.8 presents a Piper Plot showing precipitation, surface runoff, and groundwater. A number of evolutionary changes are evident between precipitation, runoff and incorporation into groundwater. Simulations with the PHREEQC code indicate that the observed changes are consistent with a number of anticipated processes. Moving from precipitation to surface runoff, calcium, magnesium (and potassium) cations are replaced with sodium, whereas for anions, sulfate decreases and alkalinity increases. Between surface runoff and groundwater sulfate increases and alkalinity decreases slightly. The evolution is clearest in the upper diamond of the Piper Plot where an increase in alkalinity (precipitation to runoff) is followed by an increase in sodium (runoff to groundwater).

PHREEQC results indicate that the surface runoff and groundwater are both near saturation with calcite and dolomite suggesting the precipitation of some type of calcium/magnesium carbonate. Weathering of silicate minerals may release sodium and alkalinity with the increased alkalinity driving precipitation of carbonates. Illite, a potential sink for potassium, is supersaturated in surface runoff. The increase in sulfate could be potentially from oxidation of small amounts of sulfide minerals in the volcanic rock sediments.

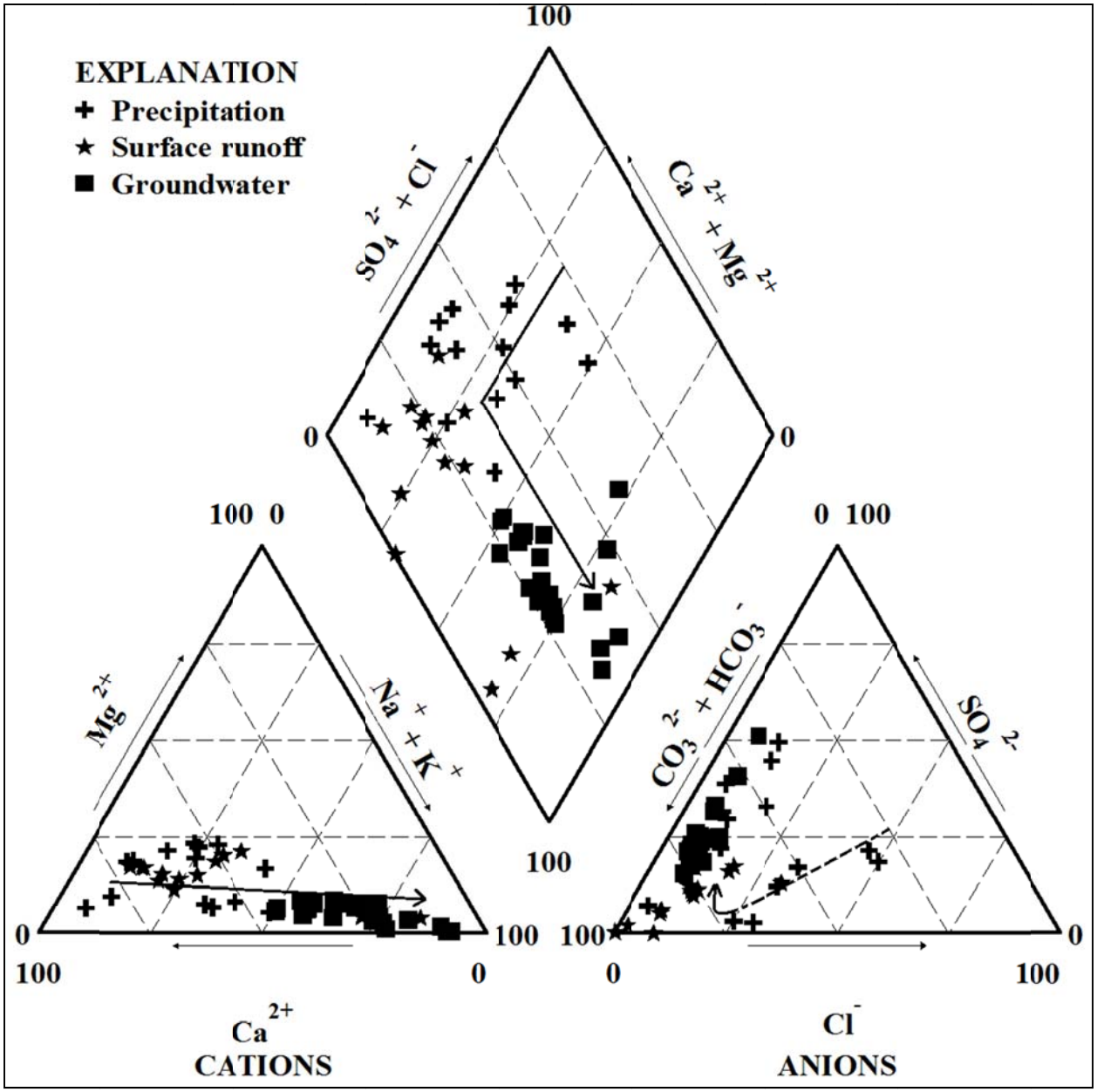

Figure 6.8: Piper diagram for precipitation, surface runoff, and groundwater chemical characteristics.

Figure 6.9 shows an overall schematic of chloride profiles. Along the mountain crest, vadose zone chloride concentrations are higher than in the groundwater beneath Fortymile Wash and higher than in the surface runoff. The data above 1,200 m elevation are consistent with areal based infiltration with evaporative concentration. In the lower desert areas with an elevation near

1,000 m borehole samples indicate accumulation of chloride in the shallow sediments and potentially net upward movement of water vapor (evaporation from the water table). The elevation of no areal recharge appears to be between 1,000 and 1,200 m. Given the relatively high chloride concentrations in the areal recharge from the study area, the low concentrations of chloride in the groundwater could result from a) older water representing a prior pluvial climate, b) areal recharge from higher elevation areas up gradient, and/or c) infiltration of surface runoff.

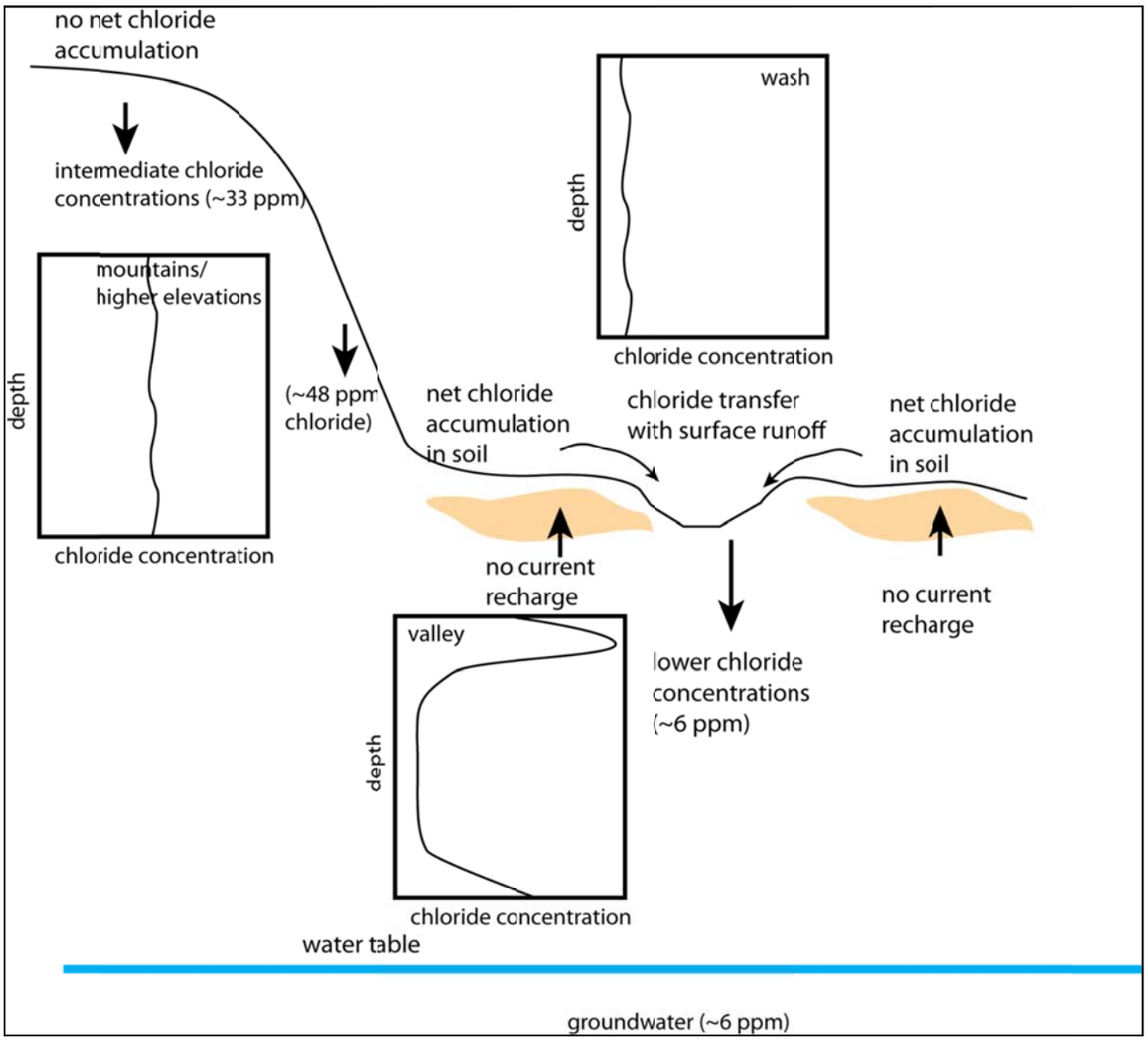

Figure 6.9: Schematic of chloride profiles at the edge of the Amargosa Desert, Nevada.

6.3.4 Effective recharge into Amargosa Valley

Watershed areas are estimated by using a regional DEM, which drawn by Surfer™8 (Golden Software Inc., 2008) as shown in Figure 6.10 below.

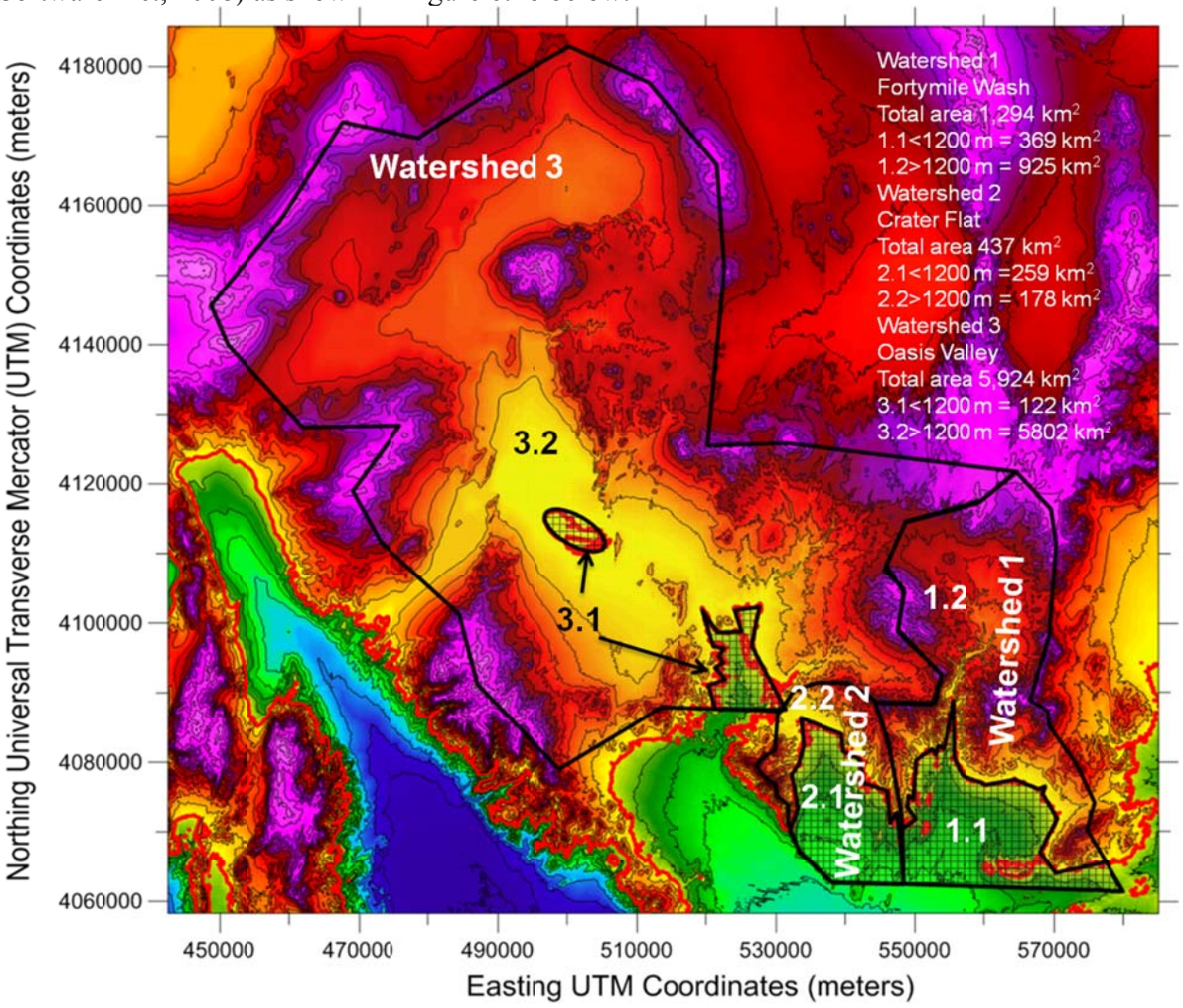

Figure 6.10: Digital Elevation Model of Region Showing Watersheds and Area within Watershed below 1,200 m ASL

C_{Out} values correspond to chloride concentration in the groundwater exiting each watershed and, to simplify calculation, the groundwater is considered well mixed and therefore each watershed presents a constant C_{Out}. Average groundwater chloride concentrations are estimated based on values observed down gradient of each watershed at locations with corrected ^{14}C ages

of approximately 8,000 years before present (YBP) or less, in order for the steady state assumption to hold. Figure 6.11 presents corrected ^{14}C ages and Figure 6.4 presents groundwater chloride concentrations.

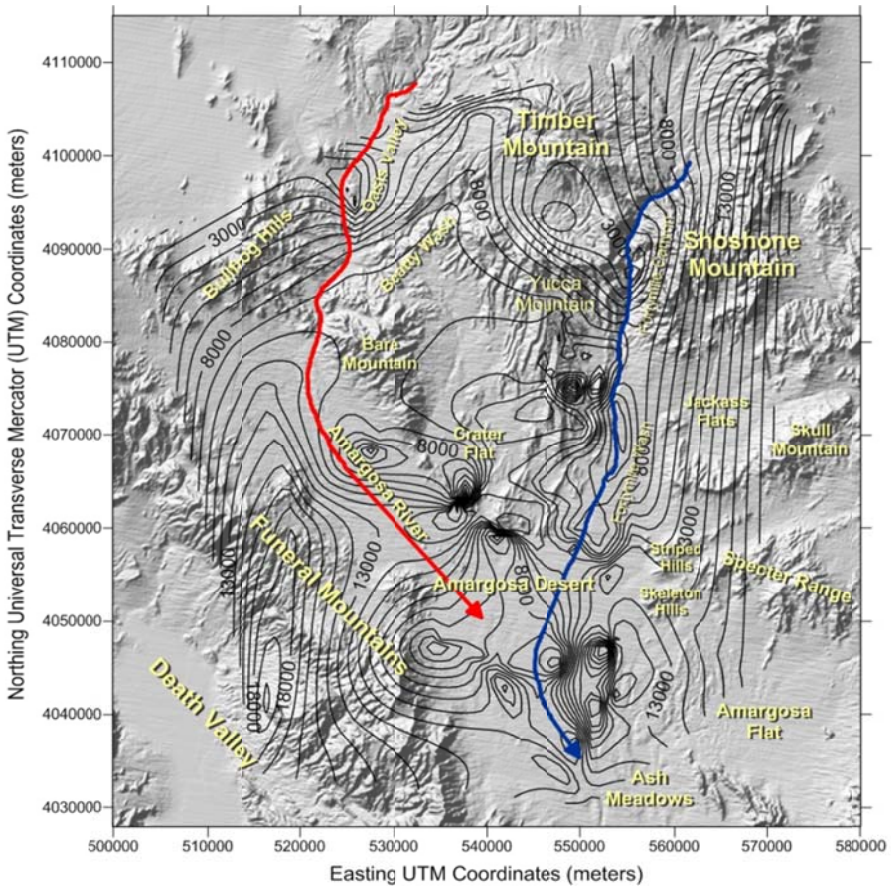

Figure 6.11: Groundwater corrected ^{14}C Dates (YBP).

Effective recharge into Amargosa Valley is projected using Equation 6.4 along with estimated watershed areas, chloride loading rates, and average groundwater chloride concentrations. Table 6.3 presents calculation results in conjunction with average groundwater Cl concentration values used.

Using the lower annual chloride loading of 60 mg/m^2/year and each watershed's area above 1,200 m ASL, along with the respective average chloride groundwater concentration for each watershed, a total minimum recharge of 10,600 acre-ft/yr is estimated, with the greatest

contribution (6,400 acre-ft/yr) coming from the Fortymile Wash watershed. Whereas, using the higher loading of 107 mg/m^2/year, each watershed's entire area and with respective average chloride concentration, a maximum recharge of 24,800 acre-ft/yr is estimated, with the greatest contribution (16,000 acre-ft/yr) again coming from the Fortymile Wash watershed.

Table 6.3: Estimates Effective Recharge into the Amargosa Valley

Recharge (Acre-ft/y)	Groundwater Average Cl (mg/L)	Area (km^2)		Chloride Loading (mg/m^2/year)			
				60		107	
Fortymile Wash	7	Watershed			8,992		16,036
		>1,200m	925	6,431		11,469	
Crater Flat	20	Watershed	437		1,063		1,896
		>1,200m	178	433		772	
Oasis Valley	75	Watershed	5,924		3,842		6,852
		>1,200m	5,802	3,763		6,711	
TOTAL		Watershed	7,655		13,898		**24,784**
		>1,200m	6,906	**10,627**		18,952	

Rush (1970) estimated average annual total recharge (from precipitation and underflow of groundwater) and discharge for the Amargosa Desert and Ash Meadows (southern Amargosa Desert) regional system on the order of 33,000 and 17,000 acre- feet, respectively. Walker and Eakin (1963) estimated the average annual total recharge to the groundwater of Amargosa Desert and Ash Meadows on the order of 24,000 acre-ft. of this amount 17,000 acre-feet are dicharged by the springes and evaporation, and 7000 acre-feet is potentially available for pumping from groundwater in Amargosa Desert.

6.4 CONCLUSIONS

The close agree with between chloride concentrations in the surface runoff with groundwater, combined with the distinct plume of low chloride concentrations beneath Fortymile Wash,

suggest that infiltration of surface runoff is the primary source of the low chloride plume. Upgradient sources of recharge water from Rainer Mesa to the north would be unlikely to follow the surface representation of the wash so precisely. Carbon-14, age dating, using dissolved organic carbon – which should give upper bounds on age – give age dates of 5,500 – 9,000 years (Thomas and others, 2004). Woocay and Walton (2008a) found slightly younger dates from corrected ^{14}C concentrations in dissolved inorganic carbon with younger waters moving north along Fortymile Wash. The source of the low chloride groundwater plume thus appears to be from a combination of past and present day infiltration of surface runoff in the form of focused infiltration along stream channels following large storm events. This study suggests that infiltration of surface runoff from large storm events in region is a source of recharge more important that previously realized. Additionally, recharge in semi-arid zones should be reevaluated to consider focused recharge at ephemeral arroyos which is not taken into account by the CMB method.

The observed mixture of slow areal recharge on ridge tops, no observable (or even negative) recharge in the desert, and focused recharge of high quality water along the ephemeral streams complicates estimating recharge rates. CMB appears to be a valid methodology for estimating higher elevation areal recharge. At lower elevations, the recharge of surface runoff occurs without taking all associated chloride (i.e., the liquid water and chloride no longer track each other). Without the ability to accurately separate the mass of chloride left in the shallow sediments from the mass of chloride in the infiltrating runoff, solving for the recharge volume from the CMB is not possible. The applicability of the CMB breaks down in moving from the climatic conditions on the ridge tops (1,400 m elevation) to the lower elevations (1,000 m elevation) when the elevation loss causes a shift from areal infiltration to chloride accumulation.

Net infiltration volume is estimated in the Amargosa Valley from 10,600 to 24, 800 acre-ft/yr by using annual chloride loading, average groundwater chloride concentrations, and DEM watershed estimation. It is clear from the calculations that the greatest contribution of this recharge is coming from Fortymile Wash, this results matched with the results obtained from the literature, especially the results that obtained from (Walker and Eakin, 1963) which estimated the groundwater recharge in Amargosa Desert on the order of 24,000 acre-feet/yr.

ACKNOWLEDGEMENTS

Funding for this research was provided by Nye County, NV through a grant from the US Department of Energy office of Civilian Radioactive Waste Management. John Klenke, Roger McRae, and the rest of the Nye County Staff for assistance with sampler construction, installation, and sampling. Dr. Dale Hammermeister for initiating chloride profile sampling at Nye County. Dr. David Borrok (Geological Department, UTEP) and Dr. Zhuping Sheng (Texas Agrilife Research Center) and their research groups for their help and support with chemical analysis. The Center for Environmental Resource Management of The University of Texas at El Paso for their funding and support.

REFERENCES

Al-Qudah, O.M., J.C. Walton, and A. Woocay (2010), Tracking the Chemical Footprint of Surface-Runoff Infiltration on Groundwater Recharge in an Arid Region, paper presented at 2010 Waste Management Symposium, Phoenix, AZ.

ASTM D2216 (1998), Standard Test Method for Laboratory Determination of Water (Moisture) Content of Soil and Rock by Mass, ASTM international, west Conshohocken, Pennsylvania.

ASTM D4542 (1995), Standard Test Method for Pore Water Extraction and Determination of the Soluble Salt Content of Soils by Refractometer, ASTM international, west Conshohocken, Pennsylvania.

Bazuhair, A.S., and W.W. Wood (1996), Chloride Mass-Balance for Estimating Groundwater Recharge in Arid Areas: Examples from Western Saudi Arabia, J. Hydrol., 186(1-4), 153-159, pii: S0022-1694(96)03028-4.

Benson, L., and H. Klieforth (1989), Stable Isotopes in Precipitation and Groundwater in the Yucca Mountain Region, Southern Nevada – Paleoclimate Implications, in Peterson, D.H., ed., Aspects of Climate Variability in the Pacific and Western Americas, American Geophysical Union Geophysical Monograph 55, 41-59.

Benson, L., M. Kashgarian, R. Rye, S. Lund, F. Paillet, J. Smoot, C. Kester, S. Mensing, D. Meko, and S. Lindstro'm (2002), Holocene Multidecadal and Multicentennial Droughts Affecting Northern California and Nevada, Quaternary Science Reviews 21(4–6), 455-733.

Claassen, H.C. (1985), Sources and Mechanisms of Recharge for Groundwater in the West-Central Amargosa Desert, Nevada-A Geochemical Interpretation, U.S. Geological Survey Professional Paper 712-F, 31 p.

Clescerl, L.S. (Editor), A.E. Greenberg (Editor), A.D. Eaton (Editor) (2000), Standard Methods for the Examination of Water and Wastewater, (20th ed.) American Public Health Association, Washington, DC. ISBN 0-87553-235-7.

Fabryka-Martin, J.T., A. Meijer, B. Marshall, L. Neymark, J. Paces, J. Whelan, and A. Yang (2002), Analysis of Geochemical Data for the Unsaturated Zone, Rep. ANL-NBS-HS-000017, OCRWM M&O, Las Vegas, Nevada.

Faunt, C.C., F.A. D'agnese, and G.M. O'brien (2004), Death Valley Regional Groundwater Flow System, Nevada and California-Hydrogeologic Framework and Transient Groundwater Flow Model, Rep. 2004-5205, U.S. Department of the Interior and U.S. Geological Survey.

Flint, A.L., L.E. Flint, E.M. Kwicklis, J.T. Fabryka-Martin, and G.S. Bodvarsson (2002), Estimating Recharge at Yucca Mountain, Nevada, USA: Comparison of Methods, Hydrogeology Journal 10, 180–204, doi:10.1007/s10040-001-0169-1.

Flint, A.L., L.E. Flint, G.S. Bodvarsson, E.M. Kwicklis, and J.T. Fabryka-Martin (2001), Evolution of the Conceptual Model of Unsaturated Zone Hydrology at Yucca Mountain, Nevada, J. Hydrology, 247(2001), 1-30, pii: S0022-1694(01)00358-4.

Ginn, T.R., and E.M. Murphy (1997), A Transient Flux Model for Convective Infiltration: Forward and Inverse Solutions for Chloride Mass Balance Studies, Water Resources Research, 33(9), 2065–2079, paper number 97WR01618.

Golden Software Inc. (2008), Surfer Version 8.09, Surface Mapping System, Golden, Colorado, <http://www.goldensoftware.com/>, (accessed 2008).

Harvey, A.M., P.E. Wigand, and S.G. Wells (1999), Response of Alluvial Fan Systems to the Late Pleistocene to Holocene Climatic Transitions: Contrasts Between the Margins of Pluvial Lakes Lahontan and Mojave, Nevada and California, USA, CATENA, 36(4), 255-281, doi:10.1016/S0341-8162(99)00049-1.

Hevesi, J.A., A.L. Flint, and, L.E. Flint (2002), Preliminary Estimates of Spatially Distributed Net Infiltration and Recharge for the Death Valley Region, Nevada–California, Rep. 02-4010, U.S. Geological Survey.

Johnson, M.J., C.J. Mayers, C.A. Garcia, and B.J. Andraski (2007), Selected Micrometeorological, Soil-Moisture, and Evapotranspiration Data at Amargosa Desert Research Site in Nye County Near Beatty, Nevada, 2001–05, Data Series 284, U.S. Department of the Interior, U.S. Geological Survey.

Liu, J., E.L. Sonnenthal, and G.S. Bodvarson (2003), Calibration of Yucca Mountain Unsaturated Zone Flow and Transport Model Using Pore Water Chloride Data, J. Con. Hydrol,. 62-63(2003), 213-235, doi:10.1016/S0169-7722(02)00168-7.

LANL (Los Alamos National Laboratory) (2007), Regional groundwater hydrochemical data in the Yucca Mountain area used as direct input to ANLNBS-0002, Revision 1, LA0309RR831233.001.

Meijer, A. (2002), Conceptual Model of the Controls on Natural Water Chemistry at Yucca Mountain, Nevada, J. Appl. Geo., 17(6), 793–805, pii: S0883-2927(02)00039-2.

Montazer, P., and W.E. Wilson (1984), Conceptual Hydrologic Model of Flow in the Unsaturated Zone, Yucca Mountain, NV, Rep. 84-4344, U.S. Geological Survey.

NWRPO (Nuclear Waste Repository Project Office) (2008), Geochemistry data files, Nye County, Nevada. < http://www.nyecounty.com> (accessed April 30, 2007).

Parkhurst, D.L., and C.A.J. Appelo (1999), User's Guide to PHREEQC (Version 2) - A Computer Program for Speciation, Batch-Reaction, One-Dimensional Transport, and Inverse Geochemical Calculations. Rep. 99-4259, U.S. Geological Survey.

Patterson, G.L., and T.A. Oliver (2004), Trace and Minor Elements in Saturated-Zone Water near Yucca Mountain, Nevada, paper presented at Geological Society of America annual meeting, 36(5), 297, Denver, CO.

Quade, J., R.M. Forester, W.L. Pratt, and C. Carter (1998), Black Mats, Spring-Fed Streams, and Late-Glacial-Age Recharge in the Southern Great Plains, J. Quat. Res., 49(2), 129-148, doi:10.1006/qres.1997.1959.

Rush, F.E. (1970), Regional Groundwater Systems in the Nevada Test Site Area, Nye, Lincoln, and Clark Counties, Nevada, Water Resources-Reconnaissance Series-Report 54, State of Nevada-Department of Conservation and Natural Resources-Division of Water Resources.

Russell, C.E., and T. Minor (2002), Reconnaissance Estimates of Recharge Based on an Elevation-Dependent Chloride Mass-Balance Approach, Rep. DOE/NV/11508-37, Publ. no. 45164, Nevada Operations Office National Nuclear Security Administration, U.S. DOE, Las Vegas, Nevada.

Savard, C.S. (1998), Estimated Groundwater Recharge From Streamflow in Fortymile Wash Near Yucca Mountain, Nevada, U.S. Geological Survey Water Resources Investigation Report 97-7273, pp. 1-30.

Savard, C.S. (1996), Selected Hydrologic Data from Fortymile Wash in the Yucca Mountain Area, Nevada, Water Years 1993-1994, Rep. 95-709, U.S. Geological Survey.

Savard, C.S. (1995), Selected Hydrologic Data from Fortymile Wash in the Yucca Mountain Area, Nevada, Water Year 1992, Rep. 94-317, U.S. Geological Survey.

Scanlon, B.R., K.E. Keese, A.L. Flint, L.E. Flint, C.B. Gaye, M.W. Edmunds, and I. Simmers (2006), Global Synthesis of Groundwater Recharge in Semiarid and Arid Regions, J. Hydrol. Process., 20(2006), 3335–3370, doi:10.1002/hyp.6335.

Scanlon, B.R., R.W. Healy, and P.G. Cook (2002), Choosing Appropriate Techniques for Quantifying Groundwater Recharge, J. Hydrogeology, 10(2002), 18–39, doi:10.1007/s10040-0010176-2.

Scanlon, B.R. (1991), Evaluation of Moisture Flux from Chloride Data in Desert Soils. J. Hydrol., 128(1-4), 137-156, doi:0022-1694/91/$03.50.

StatSoft Inc. (1984–2010), Statistica Computer Program Manual for Windows, Tulsa, Oklahoma, <http://www.statsoft.com/>, (accessed September 22, 2010).

Subyani, A.M. (2004), Use of Chloride-Mass Balance and Environmental Isotopes for Evaluation of Groundwater Recharge in the Alluvial Aquifer, Wadi Tharad, Western Saudi Arabia, Environmental Geology 46(2004), 741–749, doi:10.1007/s00254-004-1096-y.

Thomas, J., Z. Peterman, R. Hershey, D. Decker, T. Mihevc, G. Patterson, and J. Larsen (2004), Yucca Mountain Area Saturated Zone Dissolved Organic Carbon Isotopic Data, Rep. ORD-FY04-017.

Tyler, S., J. Chapman, S. Conrad, and D. Hammermeister (1995), Palaeoclimatic Response of Deep Vadose Zone in Southern Navada, USA, as Inferred from Soil Water Tracers, Applications of Tracers in Arid Zone Hydrology, IAHS Publ no. 232, 351-361, Proceedings of the Vienna Symposium.

U.S. Geological Survey, Yucca Mountain Research, Groundwater Chemistry <http://www.usgs.gov/>, (accessed 2004).

Walker, G.E., T.E. Eakin (1963), Geology and Groundwater of Amargosa Desert, Nevada-California, Groundwater Resources-Reconnaissance Series-Report 14, State of Nevada-Department of Conservation and Natural Resources.

White, A.F., and N.J. Chuma (1987), Carbon and Isotopic Mass Balance Models of Oasis Valley-Fortymile Canyon Groundwater Basin, Southern Nevada, Water Resources Research, 23(4), 571-582, paper number 6W4383, doi:0043-1397/87/006W-4383505.00

Woocay, A., and J.C. Walton (2008a), Infiltration History at Fortymile Wash, paper presented at 12th International High-Level Radioactive Waste Management Conference, 41-46, Las Vegas, Nevada. La Grange Park, Illinois: American Nuclear Society, ISBN: 978-0-89448-062-1

Woocay, A., and J. Walton (2008b), Multivariate Analyses of Water Chemistry: Surface and Groundwater Interactions, Groundwater, 46(3), 437-449, doi:10.1111/j.1745-6584.2007.00404.x.

Wood, W.W. (1999), Use and Misuse of the Chloride-Mass Balance Method in Estimating Groundwater Recharge, Groundwater, 37(1), 2-3, doi:10.1111/j.1745-6584.1999.tb00949.x.

Wood, W.W., and W.E. Sanford (1995), Chemical and Isotopic Methods for Quantifying Groundwater Recharge in a Regional, Semiarid Environment, Groundwater, 33(3), 458-468, doi:10.1111/j.1745-6584.1995.tb00302.x.

Chapter 7

7. General Conclusions

This study covers groundwater recharge from the surface runoff and infiltration in arid environments. The dissertation presented noval methods and results in identifying interaction of surface runoffs and infiltration with groundwater, groundwater flow patterns, groundwater recharge and geochemical evolution around Fortymile Wash near Yucca Mountain. Chapters 2 through 6 were covered specific issues: identification of probable groundwater paths in the Amargosa Desert Vicinity, groundwater recharge in the Amargosa Desert using surface-runoff chemistry, and groundwater recharge in southern Nevada.

The chemical speciation of the study area's groundwater indicates that free ion species represent more than 90% each of the elements Ca, Cl, F, K, Mg and Na in most of the analyzed groundwater samples. For the elements C, S and Si the dominant species are HCO_3^-; SO_4^{2-} and H_4SiO_4, respectively. Saturation indices indicate that the groundwater in the study area is undersaturated with respect to anhydrite, chrysotile, dolomite, fluorite, gypsum, halite, quartz and sepiolite, oversaturated with respect to talc, and near saturation with respect to amorphous silicate, aragonite, calcite and chalcedony. The oversaturated minerals may precipitate and adversely affect the aquifer properties. Similarly, the undersaturated minerals, if present, will dissolve from aquifer rock during groundwater flow, which will increase its porosity and permeability. The minerals near saturation reflect thermodynamic equilibrium between the groundwater and the specified solid phase.

Principal component factor analysis and k-means cluster analysis applied to Amargosa Desert's groundwater major ions, ion exchange, and SI describe the system through 4 factors,

identify six hydrogeochemical facies, and allow the visualization of the processes that govern their evolution. In the factor analysis, factor 1 (29% of the variance) is dominated by Mg, alkalinity and Ca, whereas factor 2 (26% of the variance) is primarily composed of Cl, Na and SO_4. The remaining two factors explain 31% of the variance, dominated by Ca/Na ion exchange in the third factor and F^- in the fourth factor. Factor 1 differentiates clusters 1, 3, and 6 (low Ca–Mg values) from clusters 2 and 4. Factor 2 separates cluster 3 with high Cl–Na values from the other clusters. Factor 3 separates Na-dominated waters (clusters 1 and 5) from the other clusters. Factor 4 differentiates the three Ca–Mg–HCO_3 groups from each other on the basis of F^-. The *k*-means cluster analysis produced six groups, which are presented on biplots to separate the samples into four basic factors.

The spatial plots of factor-score contours delineate areas influenced by particular hydrochemical processes and indicate the direction of change in that process (perpendicular to the contour); they allow the exposition of hydrochemical signatures indicating groundwater flow paths and their interaction with the geologic media. Together, factor-score contours and hydrochemical facies indicate the three potential groundwater flow paths or signatures presented in Figures 3.4–3.7. The hydrochemical and statistical analysis shows that the first major flow path of the study area's groundwater is beneath the Amargosa River, while the second one follows the trace of Fortymile Wash and its convergence with the Amargosa River. The third flow path is related to the trace of the Gravity Fault, Rock Valley and Death Valley. The signatures of major ion chemistry appear to be obtained near the region of infiltration, with little change along the flow paths. The high values of factor 1, which represent Mg^{2+} and Ca^{2+}, are located at Striped Hills, Skeleton Hills, and Crater Flat, which are downgradient of outcrops of the underlying carbonate aquifer. The high values of factor 2, which represent Cl^- and Na^+, are

found near the Funeral Mountains, around Oasis Valley, and SE of Fortymile Wash. The high values of factor 3, representing $Ca^{2+}/(Na^{+})^{2}$, are found at Ash Meadows, Crater Flat, Striped Hills, and Skeleton Hills, whereas low values are found at northern and southern Yucca Mountain and along its west face. Finally, the low values of factor 4, which correspond to low concentrations of F^{-} and low fluorite SI, are found encompassing Crater Flat, Striped Hills, and Skeleton Hills, whereas the high concentrations are found at Ash Meadows, Death Valley, and the west face of Yucca Mountain. The geochemical data support north-south flow along fractures that differs from the hydraulic gradient in the areas of clusters 1, 5 and 6. In the Ash Meadows area, which is near the edge of the study area, cluster 2 suggests a more east–west flow path. Based on the previous analysis, the study area's groundwater flows from north to south, following the traces of the Amargosa River and Fortymile Wash until they converge, and from east to west from Rock Valley (east of Skull Mountain), along the trace of Gravity Fault toward Death Valley.

Studies of Amargosa Desert regional groundwater indicate that infiltration of surface-runoff occurs in the valleys subsequent to runoff-producing storms and this infiltration represents a large portion of the groundwater recharge. Sampling of surface-runoff in a desert environment from ephemeral arroyos is complicated by a number of practical concerns. Surface-runoff events are uncommon, sometimes separated by gaps of more than a year, and difficult to forecast in advance.

This study presents a modification to the lysimeter called "Surface-Runoff Sampler (SRS)" designed to provide a stronger collection surface, more efficient connections for sample collection, and to measure particularly the first flush of runoff. In the absent of runoff a SRS acts

as lysimeter. SRS design has the advantages of low cost, low maintenance, and being long lived. Disadvantages are that it captures both precipitation and runoff and requires manual pumping.

Five different sub-regions were selected in the Amargosa Desert region for runoff sampler emplacement to collect runoff water in order to measure the chemical characteristics of runoff water that has contacted and leached some of the top soil, which believed to be an important source of groundwater recharge in the area. In total sixty runoff samplers were installed at thirty different locations in the major arroyos in the sub-regions as follows: 24 samplers in Fortymile Wash, 20 in western side of Yucca Mountain, 8 in the Amargosa River, 4 in Rock Valley, and 4 in the southern Amargosa Desert (Ash Meadows area). At each site location, a rain gauge was installed to collect water precipitation, and sediment samples were sampled before and after the storm events that occurred during the research time period (January 2009 to January 2011). The runoff sampler design proved its ability to resist the arid weather conditions, capture runoff water, and provides unique data. In total, 167 runoff samples were collected from the washed sand filled sampler (WSB), 9 runoff samplers from natural alluvium filled sampler (NAB), in addition to 45 precipitation and 182 sediment samples, were collected during the period January 2009 and January 2011. Because of lack of data, runoff samples that were collected from the natural alluvium filled sampler were excluded from this research.

Because the degree of evaporation is unknown the changes in chemistry between precipitation and runoff samples is best viewed in terms of the changes in chemical signature rather than in terms of individual concentrations. In non runoff producing storms the water has time to react with soil minerals prior to evaporation. When near complete evaporation of the water occurs the isotopic signature of the water will be lost, but any dissolved ions (and dry-fall) will remain in the shallow soil and sediments. When surface runoff occurs the new precipitation

mixes with shallow soil moisture and dissolves some of the precipitated salts in the desiccated soil. The soil samples represent a leaching of the shallow sediment in the stream bottom, but the most soluble salts in these samples (e.g., chloride) may have been leached by a runoff event prior to sampling. The soil leaching process also provided less contact time between soil and water than the infiltration process.

Chemical analysis of precipitation, runoff, sediment, and groundwater show three potential clusters of the samples chemical constituents: leached, scavenged, and nutrients groups. Leached group is presented when constituent concentration in sediment is greater than that in precipitation and the concentration in runoff is in the middle like (TDS, total alkalinity, sodium, calcium, magnesium, potassium). Scavenged group is presented when the constituent concentration in precipitation and runoff is greater than that in sediment like (uranium). Nutrient cluster is presented when the chemical concentration in precipitation is greater than that in sediment which is greater than that in runoff, like (fluoride, sulfate, arsenic, copper, vanadium, bromide, and phosphate).

ANOVA tests indicate that most of chemical constituents are statistically significant between sample types and sample locations, and chloride is statistically insignificant between runoff and groundwater.

Piper diagram shows mixed cation-mixed anion-types between precipitation, runoff, and groundwater. In addition, it is show three hydrochemical faces, Ca/HCO_3-type water in precipitation, Ca/HCO_3 to Ca-(Na, K)/HCO_3-type water in runoff, and (Na, K)/HCO_3-type water in groundwater, and this could be because the dominance of hydrolysis reactions involving H_2CO_3 leaching of Na in the bed rocks.

Isotopes analysis shows that the distance from the meteoric water line which is indicative of the degree of evaporation, is similar for surface runoff and groundwater. The surface runoff samples exhibit a broader spread parallel to the meteoric water line. Isotopic data presents a local meteoric line as (δ^2H= 6.83 $\delta^{18}O$+9.7), which is slightly $\delta^{18}O$ enriched from the global meteoric water line. Precipitation is more enriched in terms of δ^2H and $\delta^{18}O$ than runoff and groundwater, and this is because the precipitation samples had evaporated between the time of precipitation and the time of sampling. Most of runoff samples are more enriched in terms of δ^2H and $\delta^{18}O$ than the groundwater from the same site location, and per site location runoff's δ^2H and $\delta^{18}O$ depleted between Amargosa River, western side of Yucca Mountain, Fortymile Wash, and southern Amargosa Desert; whereas the groundwater's δ^2H and $\delta^{18}O$ follow an opposite direction per location, i.e. it is enriched between Amargosa River, western side of Yucca Mountain, Fortymile Wash, and southern Amargosa Desert. This could mean that the southern Amargosa Desert location has highest infiltration rate, then Fortymile Wash, western side of Yucca Mountain, and Amargosa River, in addition, the groundwater beneath southern Amargosa Desert and Fortymile Wash is younger than that in the other location, and the groundwater under Amargosa River is the oldest. The most enriched groundwater could represent lower elevations and /or short rainfall events.

PHREEQC results suggesting the precipitation of some type of calcium/magnesium carbonate (calcite and dolomite). Weathering of silicate minerals may release sodium and alkalinity with the increased alkalinity driving precipitation of carbonates. Illite, a potential sink for potassium, is supersaturated in groundwater. The increase in sulfate could be potentially from oxidation of small amounts of sulfide minerals in the volcanic rock sediments.

Together, the statistical analysis (descriptive statistics, box plots, and ANOVA), Piper diagram, stable isotopes analysis, and PHREEQC analysis for the precipitation, sediment, runoff and groundwater samples indicate that chloride and the stable isotopes of water show substantial overlap of values with underlying groundwater, consistent with the concept that infiltration of surface runoff is a major contributor to groundwater recharge in the study area. Groundwater concentrations represent a larger collage of infiltration events than have been collected in the surface runoff sampling making an exact match unlikely, and the importance of surface runoff depends upon topography.

The dissolution and weathering of minerals during and subsequent to the infiltration process, but not with large amounts of additional evaporation prior to deep infiltration, cause the increasing of analyte concentrations in groundwater. The influence of transpiration on the chemistry of infiltrating water is more complicated than that of evaporation given that chloride uptake differs between plants; leading to a combination of evaporative concentration at depth and transport to the surface with eventual recycling in leaves and dead plant materials.

Groundwater total recharge in the Amargosa Desert is estimated by using the average annual precipitation rate, precipitation's chloride concentrations, and groundwater's chloride concentrations' the results indicate that the groundwater recharge is on the order of 30,561 acre-feet/yr, which is 9.5 percent of average annual precipitation, with the great contribution coming from western side of Yucca Mountain and Fortymile Wash. Moreover, another estimate for the groundwater net infiltration volume is provided by this study using average annual chloride loading (wet and dry), average groundwater chloride concentrations, and DEM watershed area estimation; the results indicate that groundwater in the Amargosa Valley is recharged in the range 10,600-24,800 acre-feet/yr. in both methods, the greatest contribution of the groundwater

recharge in the Amargosa Desert is coming from Fortymile Wash, these results matched with the results obtained from the literature, especially the results that obtained from Walker and Eakin, (1963) and Rush (1970) which estimated the groundwater recharge in Amargosa Desert on the order of 24,000 acre-feet/yr.

Along the mountain crest, vadose zone chloride concentrations are higher than in the groundwater beneath Fortymile Wash and higher than in the surface runoff. The data above 1,200 m elevation are consistent with areal based infiltration with evaporative concentration. In the lower desert areas with an elevation near 1,000 m borehole samples indicate accumulation of chloride in the shallow sediments and potentially net upward movement of water vapor (evaporation from the water table). The elevation of no areal recharge appears to be between 1,000 and 1,200 m. Given the relatively high chloride concentrations in the areal recharge from the study area, the low concentrations of chloride in the groundwater could result from a) older water representing a prior pluvial climate, b) areal recharge from higher elevation areas up gradient, and/or c) infiltration of surface runoff. Given the relatively high chloride concentrations in the areal recharge from the study area, the low concentrations of chloride in the groundwater could result from a) older water representing a prior pluvial climate, b) areal recharge from higher elevation areas up gradient, and/or c) infiltration of surface runoff. The close agree with between chloride concentrations in the surface runoff with groundwater, combined with the distinct plume of low chloride concentrations beneath Fortymile Wash, suggest that infiltration of surface runoff is the primary source of the low chloride plume. Upgradient sources of recharge water from Rainer Mesa to the north would be unlikely to follow the surface representation of the wash so precisely. Carbon-14, age dating, using dissolved organic carbon - which should give upper bounds on age - give age dates of 5,500-9,000 years (Thomas and others, 2004).

Woocay and Walton (2008a) found slightly younger dates from corrected ^{14}C concentrations in dissolved inorganic carbon with younger waters moving north along Fortymile Wash. The source of the low chloride groundwater plume thus appears to be from a combination of past and present day infiltration of surface runoff in the form of focused infiltration along stream channels following large storm events. This study suggests that infiltration of surface runoff from large storm events in region is a source of recharge more important that previously realized. Additionally, recharge in semi-arid zones should be reevaluated to consider focused recharge at ephemeral arroyos which is not taken into account by the CMB method.

The observed mixture of slow areal recharge on ridge tops, no observable (or even negative) recharge in the desert, and focused recharge of high quality water along the ephemeral streams complicates estimating recharge rates. CMB appears to be a valid methodology for estimating higher elevation areal recharge. At lower elevations, the recharge of surface runoff occurs without taking all associated chloride (i.e., the liquid water and chloride no longer track each other). Without the ability to accurately separate the mass of chloride left in the shallow sediments from the mass of chloride in the infiltrating runoff, solving for the recharge volume from the CMB is not possible. The applicability of the CMB breaks down in moving from the climatic conditions on the ridge tops (1,400 m elevation) to the lower elevations (1,000 m elevation) when the elevation loss causes a shift from areal infiltration to chloride accumulation.

Further sample collection, statistical analysis, and infiltration modeling are required to gain a better understanding of hydrologic processes controlling groundwater recharge, and thus the sustainable yield of groundwater in arid environments.

Vita

Omar Mohammad Al-Qudah was born on the tenth of March, 1975, in Ajloun, Jordan. He holds a BSc in Chemical Engineering from Mutah University-Jordan, since 1997, and MSc in Chemical Engineering from Jordan University of Science and Technology University-Jordan, since 2000. He got his engineering training in Dortmund University-Germany, and his Master's thesis was about evaluation of medical waste disposal methods and their applications in Jordan. He worked during his Master studies as a teaching assistant, and after graduation, he worked as a researcher engineer in Queen Rania Al-Abdullah Center for Environmental Science and Technology, then he worked in the industry for one year as a quality control engineer before he returned to Jordan University of Science and Technology as a supervisor engineer in the Civil Engineering Department for about six years.

Omar came to the United States in August, 2007 to join the Environmental Science and Engineering PhD program at the University of Texas at El Paso. During his study at UTEP he participated as a speaker in several national and international conferences. While at UTEP, he authored and coauthored scientific publications in some of the most prestigious international journals in the fields of hydrology, Environment, Energy, and Geological Engineering. Omar received the Roy G., Post Foundation Scholarship for the year 2009-2010, and he recognized as a Miner Hero in the field of research in 2011. Below are enlisted his recent publications and presentations.

Publications

Peer-Reviewed Journal Papers (in press)

Al-Qudah, O., A. Woocay, and J. Walton (2011), Groundwater Recharge in Southern Nevada: Implications for Validity of Chloride Mass Balance Calculations, *Journal of Hydrology*.

Peer-Reviewed Journal Papers (published)

Al-Qudah, O., A. Woocay, and J. Walton (2011), Identification of probable groundwater paths in the Amargosa Desert Vicinity, J. Applied Geochemistry, 26(4), 565-574, doi:10.1016/j.apgeochem.2011.01.014

Conference Papers (published)

Al-Qudah, O., J. Walton, A. Woocay, and J. Klenke (2011), Groundwater Recharge on the Western Side of Yucca Mountain Using Surface-Runoff Chemistry, paper presented at the 13th International High-Level Radioactive Waste Management Conference (IHLRWMC), paper number 3476, Albuquerque, NM. ISBN: 978-0-89448-085-0.

Al-Qudah, O. M, J.C. Walton, A. Woocay, and J. Klenke (2011), Groundwater Recharge in the Southern Amargosa Desert Using Surface-Runoff Chemistry, paper presented at the 37th Annual Radioactive Waste Management Symposium, paper number 11489, Phoenix, AZ. ISBN # 978-0-9836186-0-7.

Al-Qudah, O.M., I. Coronado, J. Walton, and E. Hamlyn (2010), Lessons from the Proposed Radioactive Waste Disposal Site at Yucca Mountain, NV, paper presented at the 5th International Conference on Environmental Science & Technology, paper number 754, section 15-3Houston, TX. American Science Press, vol. 2, p. 388-396, ISBN: 978-0976885337.

Al-Qudah, O. M, J.C. Walton, and A. Woocay (2010), Tracking the Chemical Footprint of Surface-Runoff Infiltration on Groundwater Recharge in an Arid Region, paper presented at the 36th Annual Radioactive Waste Management Symposium, paper number 10454, vol. 5, p. 3621-3637, Phoenix, AZ, ISBN: 978-1-61738-797-5.

Hamdan, L.K., J. C. Walton, A. Woocay, and **O. Al-Qudah** (2010), Oxidation/Reduction Status of Water Pooled in a Penetrated Nuclear Waste Container, paper presented at the 36th Annual Radioactive Waste Management Symposium, paper number 10265, vol. 5, p. 3672-3679, Phoenix, AZ, ISBN: 978-1-61738-797-5.

Al-Qudah, O., A. Woocay, and J.C. Walton (2008), Yucca Mountain region groundwater geochemical data analyses, paper presented at the 12th International High-Level Radioactive Waste Management Conference (IHLRWMC), p. 87-94, Las Vegas, NV. ISBN: 978-0-89448-062-1

Reports

Walton, J., A. Woocay, **O. Al-Qudah**, and L. Hamdan (2008), Conceptual Model and Controls on Radionuclide Release at Yucca Mountain and Multivariate Analyses of Water Chemistry: Surface and Groundwater Interactions, Annual Report: April 2007 - March 2008, NWRPO-2008-01.

Conference Presentations

Al-Qudah, O., J. C. Walton, A. Woocay, and J. Klenke (2011), Sustainability of Groundwater in Arid Regions, paper presented at Sustainability on the Border: Water, Climate, and Social Change in a Fragile Landscape, El Paso, TX.

Al-Qudah, O., J. Walton, A. Woocay, and J. Klenke (2011), Surface Runoff as a Potential Source of Groundwater Recharge in Arid Regions, paper presented at Devil's Hole Workshop, Furnace Creek, CA.

Al-Qudah, O. M., J.C. Walton, and A. Woocay (2010), Evolution of Groundwater Chemistry during Surface Runoff and Infiltration Processes, paper presented at 2010 New Mexico Water Research Symposium, abstract number C-5, Socorro, NM.

Al-Qudah, O. M., J.C. Walton, and A. Woocay (2010), Issues on Groundwater Recharge in the Amargosa Desert Region, paper presented at 2010 Ground Water Summit and 2010 Ground Water Protection Council Spring Meeting, abstract number 7295, Denver, CO.

Al-Qudah, O. M., J.C. Walton, and A. Woocay (2009), Processes Controlling Groundwater Recharge in the Amargosa Desert, paper presented at 65th Southwestern Regional Meeting of the American Chemical Society (ACS), abstract number 394, El Paso, TX. Internet access: http://acs.confex.com/acs/swrm09/webprogram/Paper77113.html

Al-Qudah, O. M., J.C. Walton, and A. Woocay (2009), Chemical Evolution of groundwater in the Amargosa Desert, paper presented at Geological Society of America annual meeting, Vol. 41, No. 7, p. 218, session No 77, paper 5, Portland, OR, ISSN: 0016-7592.

Al-Qudah, O. M., J.C. Walton, and A. Woocay (2009), Chemical Fingerprint of Surface-Runoff on Groundwater Recharge in the Arid Regions, paper presented at 2009 New Mexico Water Research Symposium, abstract number C-4, Socorro, NM.

Al-Qudah, O., J.C. Walton, and A. Woocay (2009), Investigation and Classification of Groundwater Redox Conditions in the Vicinity of Yucca Mountain, paper presented at World Environmental and Water Resources Congress 2009: Great Rivers, Kansas City, MO, publisher: ASCE, ISBN13: 9780784410363

Al-Qudah, O., J. Walton, and A. Woocay (2009), Surface Runoff Chemistry in the Amargosa Desert, paper presented at Devil's Hole Workshop, Furnace Creek, CA.

Conference Abstracts

Al-Qudah, O.M., J.C. Walton, A. Woocay, and J. Klenke (2011), Using Surface-Runoff Chemistry for Indicating the Groundwater Recharge in the Amargosa Desert Vicinity, Nevada, paper presented at the 37th Annual Radioactive Waste Management Symposium, abstract number 11649, Phoenix, AZ.

Freiwan, S., R. Chianelli, B. Benedict, and **O. Al-Qudah** (2011), Wastewater to Energy, paper presented at the 37th Annual Radioactive Waste Management Symposium, abstract number 11633, Phoenix, AZ.

Al-Qudah, O., J.C. Walton, A. Woocay, and J., Klenke (2011), Surface Water and Groundwater Interaction in the Amargosa Desert Vicinity, Nevada, paper presented at Nevada Water Resources Association (NWRA) Annual Conference, Reno, NV.

Al-Qudah, O., J.C. Walton, and A. Woocay (2010), Using Surface-Runoff Geochemical Data to Model Groundwater Recharge Potential in the Amargosa Desert, Nevada, paper presented at Devil's Hole Workshop, Furnace Creek, CA.

Al-Qudah, O.M., A. Woocay, and J.C. Walton (2010), Chemical Footprint of Surface-Runoff Infiltration in the Vicinity of Yucca Mountain, paper presented at the 36th Annual Radioactive Waste Management Symposium, abstract number 10290, Phoenix, AZ.

Al-Qudah, O.M., J.C. Walton, and A. Woocay (2009), Precipitation and Surface-Runoff Sampling in the Arid Regions – New Lysimeter Techniques, Eos Trans., AGU, 90(52) Fall Meet., Suppl., San Francisco, CA, Bib. Code 2009AGUFM.H11D0836A.

Al-Qudah, O.M., J. Walton (2009), Mineralogical Analysis of Groundwater in the Vicinity of Yucca Mountain, paper presented at XIV International Clay Conference, abstract number HE8.Thu.P16, Castellaneta Marina, Italy.

Al-Qudah, O.M., A. Woocay, and J.C. Walton (2008), Groundwater Oxidizing and Reducing Conditions Near Yucca Mountain, Eos Trans., AGU, 89(53) Fall Meet., Suppl., San Francisco, CA, Bib. Code 2008AGUFM.H51B0803A.

Al-Qudah, O., N. Kyger, and Z. Sheng (2008), Water Quality Assessment in the El Paso Valley, paper presented at New Mexico Water Research Symposium, abstract number E-33, Socorro, NM.

Al-Qudah, O., A. Woocay, and J.C. Walton (2008), Geochemical Characterization of Groundwater in Yucca Mountain Region, paper presented at Devil's Hole Workshop, Furnace Creek, CA.

Al-Qudah, O., M. Allowzi, and M. Hawari (2008), Evaluation of Medical Wastes Disposal Methods and their Applications in Jordan, paper presented at the 7th International Symposium on Advanced Environmental Monitoring, Honolulu, Hawaii.

Permanent address:

600 Belvidere St, Apt#12C

El Paso, TX, 79912

This dissertation was typed by Omar Mohammad Al-Qudah, June 25, 2011.